

Northumbria Research Link

Citation: Tingey, David (2007) Estimation and control of some classes of dynamical systems with application to biological wastewater treatment. Doctoral thesis, Northumbria University.

This version was downloaded from Northumbria Research Link:
<http://nrl.northumbria.ac.uk/1222/>

Northumbria University has developed Northumbria Research Link (NRL) to enable users to access the University's research output. Copyright © and moral rights for items on NRL are retained by the individual author(s) and/or other copyright owners. Single copies of full items can be reproduced, displayed or performed, and given to third parties in any format or medium for personal research or study, educational, or not-for-profit purposes without prior permission or charge, provided the authors, title and full bibliographic details are given, as well as a hyperlink and/or URL to the original metadata page. The content must not be changed in any way. Full items must not be sold commercially in any format or medium without formal permission of the copyright holder. The full policy is available online: <http://nrl.northumbria.ac.uk/policies.html>

www.northumbria.ac.uk/nrl



**Estimation and Control of Some Classes of
Dynamical Systems with Application to
Biological Wastewater Treatment**

David Tingey

PhD

2006

THESIS/SUBMISSION DECLARATION

Title of thesis/submission: ESTIMATION AND CONTROL OF SOME
CLASSES OF DYNAMICAL SYSTEMS
WITH APPLICATION TO BIOLOGICAL
WASTEWATER TREATMENT

Author: DAVID TINGEY

Research undertaken in collaboration with:

I, DAVID TINGEY, the undersigned, claim copyright of the above described thesis/submission and declare that no quotation from it or information from it may be published without my prior written consent.

Signed: 

Date: 9/7/07

Estimation and Control of Some Classes of Dynamical Systems with Application to Biological Wastewater Treatment

David Tingey

This thesis is submitted in partial fulfilment
of the requirements of the
University of Northumbria at Newcastle
for the degree of
Doctor of Philosophy

Research undertaken in the School of Computing,
Engineering and Information Sciences

November 2006

Abstract

It is well-known that there are no general approaches for observer and controller design for nonlinear systems. Instead, focus is placed upon design for classes of systems. On the other hand, a wide variety of dynamical systems belong to the class of state-affine systems. Amongst these are biological wastewater treatment processes, which are essential in order to prevent pollution in the environment and prevent disease in the consumption of recycled water. An interesting aspect found in biological wastewater treatment systems, and many typical industrial processes, are time-delays. In almost all systems there are time-delays and nonlinearities and it is not surprising that time-delay and nonlinear systems have received a great deal of attention in mathematics and control engineering.

This project introduces new methodologies for the design of controllers and observers for a class of state-affine systems and a class of linear time-delay systems.

Firstly, new observable and controllable canonical forms are introduced. These are then used to establish new controller and observer design methodologies for a class of state-affine systems. In particular, an adaptive observer design is established. The methodologies are simple since they are based upon linear techniques.

Secondly, a full-state controller and a separation principle are established for a class of single-input single-output linear time-delay systems. The designs are based on a new stability criterion and are derived from first principles.

Finally, the new observer design methodology for the class of state-affine systems is used to produce observers for the estimation of biomass concentration in a biological wastewater treatment bioreactor. The observers are applied in theory and in simulation, where a full and a partial knowledge of the kinetic rate of reaction of biomass are considered. In addition, the performances are shown both in the absence and in the presence of measurement noise for a variety of influent flow characteristics.

Acknowledgements

Firstly, I would like to offer my deepest thanks to Dr. Krishna Busawon, my principal supervisor, for all of his help throughout this project. He has supported me in so many ways, providing me with his invaluable wise guidance and relentless enthusiasm. Indeed, I could not have hoped for a better mentor. He has been an inspiration, who I now consider a good friend.

I would also like to thank Dr. Sean Danaher, my secondary supervisor, for his support and advice throughout the project.

For supporting the presentation of my research overseas, I give thanks to Professor Fary Ghassemlooy and the Royal Academy of Engineering.

I would also like to express my gratitude to the Engineering and Physical Sciences Research Council for funding and supporting this project.


My family has always given me all of the love, support and encouragement that I could ever possibly need. For this, I am, and always will be, eternally grateful.

Last, but by no means least, I would like to thank my adorable partner, Lorna, from the bottom of my heart, for her undying love and undeniable support.

Declaration

I declare that the work contained in this thesis has not been submitted for any other award and that it is all my own work.

Name: David Tingey

Signature: 

Date: 9/7/07

Contents

1	Introduction	1
1.1	Introduction	1
1.2	The aims of the thesis	4
1.3	The objectives of the thesis	4
1.4	Scope of the thesis and literature review	5
1.5	Contributions	11
1.6	Thesis structure	12
2	Control Design Approach and Classes of Systems Considered	14
2.1	Description of systems from a state-space point of view	16
2.1.1	Systems without delay	16
2.1.2	Systems with time-delays	19
2.2	Classes of systems considered	19
3	The Extended Jordan Canonical Forms	21
3.1	The Jordan and Brunovskii canonical forms	22
3.1.1	The Jordan controllable canonical form	22
3.1.2	The Jordan observable canonical form	24
3.1.3	The Brunovskii controllable canonical form	24

3.1.4	The Brunovskii observable canonical form	25
3.2	The Extended Jordan Canonical forms - Linear case	26
3.3	The Extended Jordan Canonical forms - Nonlinear case	28
3.4	Some special classes of systems in partial EJCC form	32
3.4.1	Algorithm for EJCC form transformation	36
3.4.2	Example 3.1	37
3.4.3	Example 3.2	38
3.5	Some special classes of systems in partial EJOC form	40
3.5.1	Algorithm for EJOC form transformation	44
3.6	Summary	46
4	Control Design using the Extended Jordan Controllable Canonical Form	47
4.1	Introduction	47
4.2	Control design for a class of nonlinear systems using Extended Jordan Controllable Canonical forms	51
4.2.1	Example 4.1	54
4.2.2	Example 4.2	56
4.3	Conclusions	58
5	Observer Design using the Extended Jordan Observable Canonical Form	59
5.1	Introduction	59
5.2	Observer 1 - Observer design for a sub-class of single-output systems in EJOC form	60
5.2.1	Example 5.1	66
5.2.2	Concluding remarks 1	71

5.3	Observer 2 - Adaptive observer design for a sub-class of systems in EJOE form	72
5.3.1	Example 5.2	76
5.3.2	Concluding remarks 2	82
5.4	Observer 3 - Observer design for a sub-class of single-output state-affine systems partially transformable into EJOE form	84
5.4.1	Example 5.3	88
5.4.2	Concluding remarks 3	91
5.5	Observer 4 - Adaptive observer design for a sub-class of systems in EJOE form in the case of partially known parameters	92
5.5.1	Concluding remarks 4	93
5.6	Summary	93
6	A Control Design Strategy for a Class of Linear Time-Delay Systems	95
6.1	A control design for a class of linear time-delay systems	96
6.1.1	Control gain design	99
6.1.2	Example 6.1	108
6.1.3	Concluding remarks 5	111
6.2	A separation principle for a class of linear time-delay systems	112
6.2.1	Preliminary results	113
6.2.2	Observer-based control	115
6.2.3	Example 6.2	120
6.2.4	Concluding remarks 6	122
7	Focus of Application: Biological Wastewater Treatment and Progress in the Determination of Biomass	124

7.1	The need for clean water	124
7.2	The development of clean water in the UK	126
7.3	Biological wastewater treatment	127
7.3.1	The aerobic bioprocess model considered	129
7.4	Main problems in the control of aerobic biological treatment	131
7.4.1	Specific growth rate of biomass	131
7.4.2	Determination of biomass concentration	131
7.5	Estimation of biomass using observers - a comparative literature study	134
7.6	Summary	143
8	Estimation of Biomass Concentration in a Bioreactor	145
8.1	Biomass estimation for known SGR - Observer 1	146
8.2	Adaptive biomass estimation for known SGR - Observer 2	148
8.3	Biomass estimation for known SGR using the EJOC transformation method - Observer 3	150
8.4	Simulations for known specific growth rate	151
8.4.1	Estimation under clean measurement - Parameter Set 1	153
8.4.2	Estimation under noisy measurement - Parameter Set 1	158
8.5	Adaptive biomass estimation for partially known specific growth rate - Observer 4	167
8.6	Simulations for partially known specific growth rate	168
8.6.1	Estimation under clean measurement - Parameter Set 1	170
8.6.2	Estimation under noisy measurement - Parameter Set 1	171
8.6.3	Concluding remarks 9	173
8.7	Biomass estimation for time-delayed bioprocesses	174

8.8	Summary of biomass estimation	175
9	Conclusions and Future Work	177
9.1	Conclusions	177
9.2	Future work	183
9.3	Publications generated by this research	184
	Appendix A Biomass Estimation Simulations	186
A.1	Estimation for known SGR - Parameter Set 2	186
A.1.1	Estimation under clean measurement	188
A.1.2	Estimation under 5% measurement noise	190
A.1.3	Estimation under 10% measurement noise	193
A.2	Estimation for known SGR - Parameter Set 3	195
A.2.1	Estimation under clean measurement	197
A.2.2	Estimation under 5% measurement noise	199
A.2.3	Estimation under 10% measurement noise	202
A.3	Estimation for known SGR - Parameter Set 4	204
A.3.1	Estimation under clean measurement	206
A.3.2	Estimation under 5% measurement noise	208
A.3.3	Estimation under 10% measurement noise	210
A.4	Estimation for partially known SGR - Parameter Set 2	212
A.4.1	Estimation under clean measurement	212
A.4.2	Estimation under noisy measurement	213
	Appendix B Bioprocess Background Information	214
B.1	Specific growth rate of biomass	214
B.1.1	Influence of the substrate concentration	214

B.1.2	Influence of the biomass concentration	215
B.1.3	Influence of pH level	216
B.1.4	Influence of temperature	216
B.2	Bioprocess model derivation	216
B.2.1	General model of component concentration	217
B.2.2	Microbial growth reaction	218
B.3	Measurement of substrate concentration	220
Appendix C Theoretical Concepts - Stability of Dynamical Systems		222
C.1	Stability of nonlinear systems	222
C.2	Stability of linear time-invariant systems	227
C.3	Linear time-varying systems	229
C.4	Stability of linear time-delay systems	229
References		231
Bibliography		242

Chapter 1

Introduction

1.1 Introduction

There have been many developments in modern control theory during the last few decades. There is no doubt that further significant progress will be made in this area in the future due to the rapid development of powerful computers, which will inevitably permit the implementation of sophisticated feedback control algorithms. In addition, modern control theory has generated a huge wealth of interesting research problems that have attracted the attention of not only control theoreticians and engineers, but also mathematicians, physicists and computer scientists. Some of the latest hot research topics in modern control theory include the analysis of chaotic systems and time-delay systems.

Reflecting upon the progress of feedback control theory, it is readily apparent that key historical events such as the Industrial Revolution, the Second World War and the beginning of the computer age, have largely influenced its development. The Industrial Revolution of the late 18th and early 19th century began in Britain with the advent of the steam engine. Inevitably, the use of steam-powered systems resulted in the development of regulation systems for the control of system variables such as speed, pressure, and temperature. The

Second World War also provided considerable advancements in control theory, which were characterised by developments in flight, ships and weapons guidance control. However, it is the computer age that has given birth to the term *modern control theory* and, as such, it is standard to categorise results from 1960 onwards as *modern control*. In contrast, results yielded prior to 1960 are referred to as *classical control*. The classical control theory is mainly characterised by the frequency-domain approach, which is only appropriate for linear time-invariant systems and is mostly adequate when dealing with single-input/single-output systems. Modern control theory, however, is mainly characterised by the use of time-domain approaches rather than frequency-domain approaches to describe and analyse a control system. In effect, it is not at all surprising that the appearance of the time-domain approach for control system design has coincided with the development of powerful digital computers, which have facilitated not only control design procedures, but also the implementation of control techniques for systems of increasing complexity in real time.

It is somewhat difficult to give a complete account of all of the developments in control theory in the last few decades due to the wide range of new concepts, approaches and results that have since been generated. However, a broad summary of the main achievements and progress is hereafter given.

From the beginning of the 1960's up to the 1970's, the foundations of linear time-invariant systems theory, using the state-space approach, were established. The concepts of observability and controllability were developed [1], [2] and linear feedback control and linear observers for time-invariant systems were constructed. In addition, the Kalman decomposition [1] and Kalman filter [3] were derived. In the 1980's, significant advancements were made in nonlinear control theory through the use of new mathematical tools such as differential geometry [4], Lie algebra [5], [6] and differential algebra [7]. Since then, a number of new concepts were introduced such as Lyapunov stability [8], class K functions [9], zero

dynamics, relative degree and so on [5], [10], [11]. In addition, many control analysis and design techniques were invented such as feedback linearisation [12], passivity-based control design [13], backstepping [14], sliding mode control [15], high-gain observers [16], [17], the extended Kalman filter [18], and many more. It has subsequently been shown that many results from the linear control theory cannot be readily extended to the nonlinear case. For example, unlike linear systems, nonlinear observability depends upon the inputs [19], and the so-called separation principle does not necessarily hold for nonlinear systems [20]. Indeed, such realisations have significantly marked this period.

In the last couple of decades, knowledge-based approaches appeared on the scene. Neural networks [21], fuzzy logic [22], artificial intelligence [23] and the genetic algorithms [24] are some of the techniques that are currently used to deal with uncertain systems or systems whose models are not perfectly known. While there is still a lot of ongoing research on the foregoing topics, a number of new research topics seem to dominate the scene, such as model-based fault detection [25], chaos control [26] and time-delay systems [27].

With regards to industrial control, it can also be observed that control systems have found new areas of applications during the last few decades. In effect, alongside traditional areas such as mechanical, electrical and electromechanical systems - for control of robots and electrical motor drive systems - feedback control has found applications in other areas including chemical processing, medical sciences, economics, and biotechnology. In such areas, feedback control can have a variety of uses including composition control of polymers, regulation of medication, regulation of inflation, and control of biological wastewater treatment.

Biological wastewater treatment is an interesting and very important process. In fact, it is essential for the prevention of pollution in the environment and prevention of disease in the consumers of recycled water. With around 70 *million* people added to the planet each year, it is predicted that feeding humanity will require an additional water volume of around

5600km³/year by 2050 [28]. Hence, with such a phenomenal global demand, it is easy to appreciate the need for organised use of water. This further affirms the need for contributions towards wastewater treatment techniques.

In this work, we focus our attention on biological wastewater treatment systems. We consider the problem of biomass estimation, which is useful for its control. In this respect, we consider the structure of biological system models, which turn out to be largely of the state-affine form. Therefore, to give a general framework of control of biological wastewater systems, we mainly consider the problem of control of state-affine systems that include the models of biological wastewater treatment systems. In addition, as with many industrial processes, biological wastewater treatment systems also contain time-delays. We therefore attempt to consider the problem of time-delays involved in biological wastewater treatment systems.

1.2 The aims of the thesis

With regards to the above, the main aims of the thesis are to:

- Develop controller and observer design methodologies for a class of state-affine systems.
- Establish new estimators of biomass concentration in an aerobic fermentation process.
- Derive a control design strategy for a class of time-delay systems.
- Design an observer-based controller for the class of time-delay systems considered.

1.3 The objectives of the thesis

The specific objectives of the thesis are to:

- Investigate and study the canonical structure of a bioprocess consisting of an aerobic fermentation process.
- Use the canonical structure to give new controller and observer design methodologies for a class of state-affine systems.
- Study and compare the performance of the controller and observer in simulation.
- Apply the observer design methodology developed to the estimation of biomass concentration in an aerobic fermentation process in theory and simulation.
- Study and compare the performance of the biomass observer under measurement noise and uncertainty in the model of the specific growth rate.
- Synthesise a control design strategy for a class of time-delay systems with delay in the state and the output with the intent to apply the results obtained to biological wastewater treatment systems.
- Establish a separation principle for the class of time-delay systems considered.

1.4 Scope of the thesis and literature review

It is well-known that controller and observer design methods for linear systems are well-established. However, most theories for linear systems cannot always be easily extended to the nonlinear case. For example, with regards to stability, the frequency-domain approaches used in the linear case, such as pole location, are not applicable to nonlinear systems. Instead, other techniques based upon the time-domain are considered, the most commonly used of which is based upon stability criterion introduced by A. M. Lyapunov in 1892 (see Appendix C for definitions of stability). Consequently, the mathematical tools required to study

nonlinear systems are quite elaborate, such as those previously mentioned. There are also further difficulties with regards to feedback control design in the sense of knowing whether or not it is, in fact, possible to do so. Indeed, if a linear system is stabilisable, then it is always possible to design a feedback controller that will stabilise the system. However, for nonlinear systems this is not always true [20].

It is well-known that there are no general approaches for controller and observer design for nonlinear systems. Therefore, focus is placed upon classes of systems upon which the type of controller or observer employed are specific to that class of systems. As a result, controllers and observers are subdivided into various classes for which a specific, yet not unique, theory seems to apply.

As previously mentioned, a number of recent nonlinear control techniques have been developed such as integrator backstepping approaches, sliding mode, passivity, input-state linearisation, and the very commonly used methods of feedback linearisation (see e.g. [5], [15], [29], [30], [31]). As far as observer design for nonlinear systems is concerned, techniques used include the Extended Luenberger Observer (ELO) [32], the Extended Kalman Observer (EKO) [32], and sliding mode observers [33]. Another popular method, mentioned previously, is that of high-gain observers, which were introduced in the 1980's [16] and have since spurred a number of works in this area [17], [34]. However, the main drawback of high-gain observers is that they are generally not suitable for applications where measurement noise is to be considered, since they tend to amplify the noise.

In the process of control design, it is customary to study the canonical forms a system possesses. Therefore, one important topic of research in control systems theory is the search for canonical forms of dynamical systems. The main reason for this is that canonical forms allow us to highlight essential properties and characteristics of systems by mere inspection and, in particular, allow the development of a unified theory for their analysis. They also

permit the classification of systems into various families. For instance, it is well-known that controllable and observable linear time-invariant (LTI) systems can be transformed, by a change of coordinates, into the so-called Brunovskii or Jordan controllable and observable forms, respectively. In fact, the latter has been further developed into a more generalised form [35]. In addition, the Kalman canonical decomposition provides a general framework for the controllability and observability analysis of linear systems [36]. With regards to non-linear systems, uniformly observable systems (or systems that are observable for all inputs) can be steered into a triangular form [37], [38].

In this work, we focus upon the development of new estimation and control methods for special classes of state-affine systems that are observable for all inputs. The attraction to this class of systems originates from the very interesting and important application of biological wastewater treatment systems. The control of an overall biological wastewater treatment system is generally very complex. However, in common industrial applications it can be reduced to the control of a simple nonlinear microbial growth reaction. The term "simple" here refers to a reduced model of order two, involving the control and monitoring of a biomass (micro-organisms) and a substrate (organic content) concentration, even though the reaction remains a very complex one. The complexity arises due to insufficient knowledge of the nonlinear kinetic rate of reaction and the lack of cheap and/or reliable monitoring equipment for the on-line measurement of biomass concentration. Several models of the specific growth rate (SGR) have been proposed, such as the Monod and the Haldane models (see Appendix B), but do not provide a complete description of the SGR. Consequently, one interesting problem would be to estimate the biomass concentration, for monitoring and control purposes, using either a partial knowledge of the kinetic rate of reaction or perhaps without the use of any *a priori* model of the kinetic rate. The development of observers for biomass concentration is aimed at providing reliable concentration values whilst saving on the expense of biomass

monitoring equipment (capital and running costs), which are not yet fully developed. It is also important to consider estimation in the presence of measurement noise and if, in the estimation, the noise can be attenuated.

Along with biological wastewater treatment, a variety of systems can be described in the state-affine form, and as such, a number of works have been done in the area of observer and controller design for classes of state-affine systems. Some are based upon transformation into a state-affine form [39], and many are based upon methods of linearisation [1], [10]. An observer for state-affine systems is given in [40], and classifies the inputs for which convergence can be achieved. On the other hand, an observer design is considered for unknown inputs in [41] and an exponential observer for continuous-discrete time state-affine systems is constructed in [42] where sufficient conditions on the inputs and sampling times are given. Indeed, as mentioned previously, in the design of observers for nonlinear systems, attention must be paid as to what inputs are applied such that the system remains observable. In fact, singular inputs have also been considered in [43], which proposes a persistent observer for bilinear systems such that the system observability is maintained.

The present work considers special classes of state-affine systems that can be expressed in, or transformed into, the so-called Extended Jordan Canonical form, which is a concept that is introduced in this work. The main reason for introducing these canonical forms is that linear design techniques can be applied to synthesise observers and controllers for a class of state-affine systems, which, as mentioned previously, the bioprocess considered in this research belongs to.

Over the past couple of decades, there have been a number of results on biomass estimation for the bioprocess considered in this work [32], [44], [45], [46], [47]. Extensive research in this area can be found in [44] who illustrate some classical estimation techniques such as the application of the Extended Luenberger Observer (ELO) and the Extended Kalman

Observer (EKO) and also asymptotic observers [32], [45]. Other main estimation methods presented in the literature are high-gain observers [45], adaptive observers [32], [45], and interval observers [32], [46]. However, there is little consideration for estimation in the presence of measurement noise, and for those works that do consider this [32], [45], [46], there is a need for considerable trade-offs with regards to noisy estimations and convergence times. Indeed, there is a requirement for the development of biomass estimation methods for the microbial growth bioprocess; which is one of the problems considered in this work.

Another interesting aspect found in biological wastewater treatment systems are time-delays, which are typically introduced in the dynamics of material transportation in pipes and vessels, and in the form of lags in measurement equipment. In fact, time-delays are natural occurrences in many physical, industrial and engineering systems. The analysis and control of time-delay systems (TDSs) are generally much more problematic than those of delay-free systems with regards to system response-time and stability. Clearly, the issues of control system stability and performance of systems containing delays are of theoretical and practical importance.

A number of approaches have been proposed to deal with the control and estimation design problem for time-delay systems. These include LMI-based delay-dependent stability [48], adaptive control [49]-[51], passification of LTI time-delay systems [52], the Smith predictor [53], adaptive Smith controllers [54], robust guaranteed cost control of uncertain systems [55] (based on Lyapunov-Krasovskii functional techniques) and sliding mode control [56], [57] (Lyapunov-based approaches). The TDSs considered in the literature include those with delays in the state, or with some combination with input [58] and/or output [59], [60]. There are a number of classes of systems that have been considered including LTI systems [61], linear autonomous systems [62], uncertain time-delay systems [63], control-affine systems [64], and stochastic chaotic systems [65]. There are also monographs on observer

design for time-delay systems that make use of Lyapunov functionals proposed for the stability analysis of time-delay systems. In particular, the most widely used functionals are those of the Lyapunov-Krasovskii and Lyapunov-Razumikhin types and derivations thereof (see e.g. [66] and [67]). Types of estimation include state estimation [68], parameter estimation [58], and estimations of decay rate of linear systems solutions [69]. For the linear time-delay case, a number of estimation approaches applicable to linear systems have been proposed [70]-[72]. In [70], a full-state observer design for LTI systems with a delay in the state has been proposed, taking on a completely original approach and introducing new stability criteria called (α, r) -stability. Another approach [72] for linear TDSs is based upon a technique of coordinate transformation such that, in the new coordinates, all of the delay terms are associated with the output only, and can be easily dealt with through the use of output injection.

In the branch of robust control, results can be roughly split into two classes: The first consists of systems with input or output delays, and the second in state delays. However, there are few results present in the literature for TDSs which consider both cases and it is clear that the awareness of multiple delays in the system necessitates more precise control.

Despite the attention received by TDSs, this difficult field of research remains very much an open problem since there is still no general method to deal with time-delays in dynamical systems. In fact, the question of a general methodology for observer design for linear time-delay systems is not yet established. Furthermore, one cannot be sure that a linear time-delay system will remain stable when controlled via an observer; assuming that both observer and controller are synthesised separately. This is true for the non-delayed case where it is shown that there is a separation of the poles of the observer and the controller, and is known as the separation principle.

In this thesis, a class of linear time-delay systems, with delay in the state and output, is

studied with the intention to propose a controller design methodology, as well as to establish a separation principle for the considered system. The present work is distinctive from other work in this area in that it exploits the features of the characteristic equation of the system to derive the controller gain. A controller design methodology is therefore proposed by assigning a particular structure to the characteristic equation. No *a priori* control design approach was set in advance; that is, the controller was designed based on first principles.

1.5 Contributions

The main contributions of this work are listed below:

1. The concept of Extended Jordan Controllable and Observable Canonical forms is introduced.
2. Algorithms for transforming a class of nonlinear systems into partial Extended Jordan Controllable Canonical (EJCC) and Extended Jordan Observable Canonical (EJOC) forms are given.
3. A controller design for a class of state-affine systems that can be partially transformed into the EJCC form is proposed.
4. A constant tuning parameter and an adaptive tuning parameter observer design methodology are given for a class of state-affine systems in the EJOC form. In addition, the robustness of the adaptive observer is also shown.
5. An observer design methodology for a class of state-affine systems that can be partially transformed into the EJOC form is given.
6. A control design methodology for a class of linear time-delay systems with delay in the state or delay in the state and output is proposed.

7. A separation principle for a class of linear time-delay systems with delay in the state or delay in the state and output is established.
8. The obtained observers are used for the estimation of biomass in a biological wastewater treatment process. The resulting observers are applied in theory and in simulation where performance is shown, both in the absence and in the presence of measurement noise. The adaptive-gain observer is also applied where only a partial knowledge of the kinetic growth rate of reaction is assumed, both in the absence and in the presence of measurement noise.

1.6 Thesis structure

The thesis is broken down into nine chapters: The present chapter gives a brief history of the general development of modern control. The scope of the thesis and a literature review are also given, which highlight important areas of work in the field of analysis, control and estimation of classes of dynamical systems.

Chapter 2 presents the control design approach used and the classes of systems considered in this work.

Chapter 3 introduces the concept of Extended Jordan Observable and Controllable Canonical forms (EJOC and EJCC, respectively) and their relation to the Brunovskii canonical forms. Such forms are intended to facilitate the design of observers and controllers, using only linear design methods, for the class of systems considered and constitute the 1st main contribution of this thesis. Algorithms for the transformation of a class of nonlinear systems into the EJCC and EJOC forms are also given and are the 2nd contribution of this thesis.

Chapter 4 presents a control design using the EJCC form for a class of state-affine systems. This is the 3rd main contribution of this thesis.

Chapter 5 presents three observer designs using the EJOc form for a class of state-affine systems. Observers 1 and 2 are used for systems that are already in the EJOc form. The former uses a constant tuning parameter and the latter uses an adaptive tuning parameter in its gain. Observer 3 is used for systems that are transformed partially into the EJOc form. Observers 1 and 2 constitute the 4th main contribution of this thesis whilst Observer 3 constitutes the 5th main contribution.

Chapter 6 gives a control design and a separation principle for a class of linear time-delay systems. The concept of (α, r) -stability is also introduced. These designs constitute the 6th and 7th main contributions of this thesis.

Chapter 7 provides background details on the importance of biological wastewater treatment, which is the application considered in this work. The main treatment processes involved are then outlined, and the dynamical model that is used to describe the simple microbial growth reaction that takes place in most wastewater treatment systems is given. Finally, monitoring and control difficulties in biological wastewater treatment are presented, along with details of work done to resolve these issues.

Chapter 8 focuses on the application of the observer designs given in Chapter 5 to biological wastewater treatment systems. The model given in Chapter 7 is used to design new estimators of the biomass concentration in bioreactors. The performance of each observer is analysed in simulation. Overall, this constitutes the 8th and last main contribution of this work.

Chapter 9 presents the final conclusions and discussions of all the theoretical and simulation work in the thesis. In addition, possible directions for further research work are suggested.

Chapter 2

Control Design Approach and Classes of Systems Considered

In this chapter, we shall describe the general background of the control design approach (mainly state-space) undertaken in this work and introduce the classes of systems considered for both the delayed and the delay-free cases.

The main purpose of a control system is to modify or alter the performance of a system such that it behaves in a desired way. Such an alteration in behaviour is mainly aimed at achieving either maximum production or at regulating a variable at a fixed set-point or within a reasonable bound. Common examples of control applications include temperature control of furnaces, altitude control of satellites, speed control of motors, voltage regulation of generators, and composition control of chemical processes, to mention a few. There has been a considerable amount of research contributions in the area of control systems design for both linear and nonlinear dynamical systems over the past four decades, especially since the introduction of the state-space approach to control design, which is in fact, the approach that is used throughout this thesis.

The state-space approach to control design consists of examining a system, not only from

the available measurements (inputs and outputs) of the system, but also from the independent internal variables (state variables) describing the system. Consequently, systems are described by a set of first-order differential equations characterising the system rather than using a single closed-form differential equation of a certain order. As a result, a linear system is described by a set of first-order linear differential equations and, likewise, a nonlinear system is described by a set of first-order nonlinear differential equations.

The theory of linear time-invariant systems (LTI) with no time-delay is well-established. In fact, a general approach to linear feedback control and observer design for the non-delayed case is readily available. However, the theory of time-delay systems is far from complete. Indeed, there is no general approach to linear feedback control and observer design for linear time-delay systems. As for nonlinear systems control, there is no general approach either, since most theories that are established in the linear case cannot always be easily extended to the nonlinear case. Indeed, there is no general control strategy that can be applied to every kind of system. Instead, we consider classes of nonlinear systems for which a specific control design strategy is employed. As a result, due to the various theories involved, nonlinear control systems design has become a highly mathematical discipline.

In what follows, a classification of dynamical systems from a state-space point of view is given. Firstly, systems free of time-delay are presented.

2.1 Description of systems from a state-space point of view

2.1.1 Systems without delay

General nonlinear systems

A general nonlinear system is usually described by

$$\begin{cases} \dot{x} = f(x, u) \\ y = h(x, u) \end{cases} \quad (2.1)$$

where $x \in \mathbb{R}^n$ is the n -dimensional state vector, $u \in \mathbb{R}^m$ is the m -dimensional input vector, and $y \in \mathbb{R}^p$ is the p -dimensional output vector and $f : \mathbb{R}^n \times \mathbb{R}^m \rightarrow \mathbb{R}^n$ and $h : \mathbb{R}^n \times \mathbb{R}^m \rightarrow \mathbb{R}^p$ are assumed to be smooth functions.

Sometimes we can obtain an even more general system by including a time dependency in the vector fields f and h ; that is

$$\begin{cases} \dot{x} = f(x, u, t) \\ y = h(x, u, t) \end{cases} \quad (2.2)$$

where $f : \mathbb{R}^n \times \mathbb{R}^m \times \mathbb{R}^+ \rightarrow \mathbb{R}^n$ and $h : \mathbb{R}^n \times \mathbb{R}^m \times \mathbb{R}^+ \rightarrow \mathbb{R}^p$. However, in this thesis, we shall mainly be concerned with the first class of systems; that is, with no time dependency. Note that in the above systems, when $u = 0$, the systems are then said to be *autonomous* or *free*.

All other classes of non-delayed systems are special cases of the above nonlinear system.

State-affine systems

State-affine systems are a special case of the general nonlinear system (2.1) where $f(x, u) = F(u, y)x + g(u, y)$ and $h(x, u) = H(u, y)x$. More precisely, a state-affine system is given by

$$\begin{cases} \dot{x} = F(u, y)x + g(u, y) \\ y = H(u, y)x \end{cases} \quad (2.3)$$

where F and H are matrices of appropriate dimensions, and g is a smooth nonlinear function in u and y .

Control-affine systems

Control-affine systems are the special case where $f(x, u) = f(x) + \sum_{i=1}^m g_i(x)u_i$ and $h(x, u) = h(x)$; that is

$$\begin{cases} \dot{x} = f(x) + \sum_{i=1}^m g_i(x)u_i \\ y = h(x) \end{cases} \quad (2.4)$$

Bilinear systems

The bilinear system is a special case of the state-affine system and is described by

$$\begin{cases} \dot{x} = Ax + Bu + \sum_{i=1}^m u_i Gx \\ y = Hx \end{cases} \quad (2.5)$$

where A , B , G , and H are system matrices of appropriate dimensions.

Linear time-invariant (LTI) systems

Linear time-invariant systems are special cases of bilinear systems and are given by

$$\begin{cases} \dot{x}(t) = Ax(t) + Bu(t) \\ y(t) = Cx(t) \end{cases} \quad (2.6)$$

where A , B , and C are system matrices of appropriate dimensions.

Linear time-varying systems

When the matrices of an LTI system are time-dependent, we obtain a linear time-varying (LTV) system; that is

$$\begin{cases} \dot{x}(t) = A(t)x(t) + B(t)u(t) \\ y(t) = C(t)x(t) \end{cases} \quad (2.7)$$

where A , B , and C are system matrices of appropriate dimensions. This is a special case of system (2.2).

Some properties of nonlinear systems

The behaviour of nonlinear systems is generally more complex than that of linear systems.

Some properties of nonlinear systems include:

- They often have more than one equilibrium point.
- They can display oscillations of fixed amplitude and fixed period without applying an external input.
- As parameters change, the stability of the equilibrium point can change (as in linear systems also) along with the number of equilibrium points. This is known as bifurcation; the quantitative change in parameters that leads to the qualitative change in system properties.
- They can display a behaviour known as chaos. This is simply that the output is extremely sensitive to initial conditions and can be unpredictable. If initial conditions or external inputs cause the system to operate in a highly nonlinear region, then the probability of chaos increases [10].

2.1.2 Systems with time-delays

Unlike ordinary differential equations, time-delay systems are infinite dimensional, and are described by Functional Differential Equations (FDEs). A general nonlinear time-delay system is described as

$$\begin{cases} \dot{x}(t) = f(x(t), x(t - \tau_1), u(t - \tau_2)) \\ y(t) = h(x(t - \tau_3)) \end{cases}$$

where $x \in \mathbb{R}^n$, $u \in \mathbb{R}^m$, $y \in \mathbb{R}^p$, and $f : \mathbb{R}^n \times \mathbb{R}^m \rightarrow \mathbb{R}^n$ and $h : \mathbb{R}^n \times \mathbb{R}^m \rightarrow \mathbb{R}^p$ are assumed to be smooth functions. The time-delays τ_1 , τ_2 and τ_3 are assumed to be bounded.

There are more general and precise descriptions of time-delay systems than that presented above. However, this description of TDSs is employed as a matter of consistency with the description of systems without delay given in the previous section. It is clear that various sub-classes of systems such as state-affine, control-affine, bilinear and linear can also be described in the delay case.

2.2 Classes of systems considered

In this work, we mainly consider some classes of nonlinear systems, and some classes of linear time-delay systems with some special structural properties.

Nonlinear systems considered

We consider the class of systems given in (2.3) and the following sub-class of control-affine systems:

$$\dot{x} = F(x)x + G(x)u. \quad (2.8)$$

Note that when $F(x) = F(y)$ and $G(x) = G(y)$, then system (2.8) is a sub-class of (2.3).

The matrices $F(x)$, $G(x)$, $F(u, y)$, and $H(u, y)$ have special structural properties as will

be detailed in Chapters 4 and 5.

Time-delay systems considered

In this thesis, we consider linear time-delay systems that are special cases of the following main class of linear time-delay systems:

$$\begin{cases} \dot{x}(t) = Ax(t - \tau_1) + \check{A}x(t) + Bu(t) \\ y(t) = Cx(t - \tau_2) \end{cases}$$

where $x \in \mathbb{R}^n$, $u \in \mathbb{R}$, $y \in \mathbb{R}$, and A , B , and C are of the Brunovskii observable or controllable form (detailed in Chapter 3) depending whether the problem of observer or controller design is considered, respectively. The time-delays τ_1 and τ_2 are bounded where $0 \leq \tau_2 \leq \tau_1$. The matrix \check{A} satisfies a matching condition that is detailed in Chapter 6.

Chapter 3

The Extended Jordan Canonical Forms

As mentioned in Chapter 1, one important topic of research in control systems theory is the search for canonical forms of dynamical systems. This is mainly because we can easily recognise essential properties and characteristics of a system by mere inspection when canonical forms are used. Furthermore, the use of canonical forms allows the development of a unified theory for the analysis of systems. It also permits the classification of systems into various families.

In this chapter, we shall recall the Jordan and Brunovskii canonical forms, which are commonly used in control systems analysis and design. We shall then introduce the concept of Extended Jordan Observable and Controllable Canonical forms. Indeed, we shall see that the Extended Jordan Canonical forms are extensions of the Jordan and Brunovskii canonical forms. We show how a class of nonlinear systems can be partially transformed into such a form. Furthermore, we show the importance of such canonical forms in observer and control design in the subsequent chapters. It is important to note that if systems are controllable and observable, then they should remain so, under a change of variable. Therefore, it is assumed throughout this chapter that the systems at hand are controllable when dealing with controllable canonical forms, and are observable when dealing with observable canonical

forms.

3.1 The Jordan and Brunovskii canonical forms

3.1.1 The Jordan controllable canonical form

Consider the following single-input linear time-invariant system:

$$\dot{x} = Fx + Gu \quad (3.1)$$

where $x \in \mathbb{R}^n$, $u \in \mathbb{R}$ and $F \in \mathbb{R}^{n \times n}$ and $G \in \mathbb{R}^{n \times 1}$ are constant matrices. It is well-known that any matrix $F \in \mathbb{R}^{n \times n}$ can be transformed into the Jordan form or at best be completely diagonalised if the eigenvalues of F are all distinct [73]. Suppose that F is diagonalisable, then there exists a similarity transformation $z = P_d x$ where the matrix P_d is composed of n linearly independent eigenvectors (modal matrix) such that

$$\dot{z} = Dz + Bu$$

where

$$D = P_d F P_d^{-1} = \begin{bmatrix} \lambda_1 & 0 & \cdots & 0 \\ 0 & \lambda_2 & \ddots & \vdots \\ \vdots & \ddots & \ddots & 0 \\ 0 & \cdots & 0 & \lambda_n \end{bmatrix} \quad \text{and } B = P_d G = \begin{bmatrix} b_1 \\ b_2 \\ \vdots \\ b_n \end{bmatrix}.$$

We then have a set of n decoupled first-order equations of the form

$$\dot{z}_i = \lambda_i z_i + b_i u.$$

It is clear that if $b_i = 0$, then the i th state variable or mode will not be controllable. Consequently, the above system will be completely controllable if the matrix B has no zero rows.

Therefore, as mentioned above, the controllability status of the system can be determined by

mere inspection.

Now, if the matrix F is not diagonalisable, it can still be transformed into a Jordan form. Here, again the controllability of the system can be determined by a simple inspection. Indeed, suppose that the matrix F has one eigenvalue, say λ_1 , of multiplicity order r , while the others are distinct. Then, there exists a similarity transformation $\xi = P_J x$ (P_J non-singular) such that

$$\dot{\xi} = \Lambda \xi + \bar{B} u$$

where

$$\Lambda = \left[\begin{array}{cccc|ccc} \lambda_1 & 1 & 0 & \cdots & \cdots & \cdots & 0 \\ 0 & \ddots & \ddots & 0 & & & \vdots \\ \vdots & 0 & \lambda_1 & 1 & \ddots & & \vdots \\ \vdots & \vdots & \ddots & \lambda_1 & 0 & \ddots & \vdots \\ \hline \vdots & \vdots & & \ddots & \lambda_2 & \ddots & 0 \\ 0 & \vdots & & & \ddots & \ddots & 0 \\ 0 & 0 & \cdots & \cdots & \cdots & 0 & \lambda_{n-(r+1)} \end{array} \right] \quad \text{and } \bar{B} = \begin{bmatrix} \bar{b}_1 \\ \bar{b}_2 \\ \vdots \\ \bar{b}_r \\ \vdots \\ \bar{b}_n \end{bmatrix}.$$

That is, we have one Jordan block of order r . It is clear that the input applied to the last row of the Jordan block will influence the chained mode above the matrix diagonal. More precisely, if $\bar{b}_r = 0$, then the state variables corresponding to the Jordan block are not controllable.

Therefore, one can conclude that a system in Jordan form that has only one Jordan block per eigenvalue is completely controllable if and only if the entry of the matrix \bar{B} corresponding to the bottom row of each Jordan block is non-zero.

Now, in the extreme case where the system has only one eigenvalue λ of multiplicity order n , we would have only one Jordan block of order n . In that case, the matrix Λ will be of the form

$$\Lambda = \begin{bmatrix} \lambda & 1 & 0 & \cdots & 0 \\ 0 & \lambda & \ddots & \ddots & \vdots \\ \vdots & \ddots & \ddots & \ddots & 0 \\ \vdots & & \ddots & \ddots & 1 \\ 0 & \cdots & \cdots & 0 & \lambda \end{bmatrix} \quad \text{and } \bar{B} = \begin{bmatrix} \bar{b}_1 \\ \bar{b}_2 \\ \vdots \\ \vdots \\ \bar{b}_n \end{bmatrix}$$

and we will require $\bar{b}_n \neq 0$ for the system to be completely controllable.

If $\lambda = 0$, we have a special case of the Brunovskii controllable canonical form. The general Brunovskii controllable canonical form is explained in a subsequent subsection.

3.1.2 The Jordan observable canonical form

Suppose that we have an output equation associated with the system (3.1):

$$y = Hx \tag{3.2}$$

where $y \in \mathbb{R}$ and H is a constant matrix. Assume that the pair (F, H) is observable. Then, by using the above transformation $\xi = P_J x$, the transformed output equation is given by

$$y = HP_J^{-1}\xi = \bar{C}\xi = \begin{bmatrix} \bar{c}_1 & \bar{c}_2 & \cdots & \bar{c}_r & \cdots & \bar{c}_n \end{bmatrix} \xi.$$

In that case, it is obvious that the system is completely observable if and only if the entry of the matrix \bar{C} , corresponding to the last column of each Jordan block, is non-zero. This result can be obtained by duality; that is, by replacing H by G^T and F by F^T [73].

3.1.3 The Brunovskii controllable canonical form

Consider again the single-input system (3.1). Assume that the pair (F, G) is controllable. Then, it can be shown that there exists a transformation $z = P_c x$ such that the above system can be transformed into

$$\dot{z} = A_c z + B u$$

where

$$A_c = P_c F P_c^{-1} = \begin{bmatrix} 0 & 1 & 0 & \cdots & 0 \\ \vdots & \ddots & 1 & \ddots & \vdots \\ 0 & & \ddots & \ddots & 0 \\ 0 & \cdots & \cdots & 0 & 1 \\ -a_n & -a_{n-1} & \cdots & \cdots & -a_1 \end{bmatrix} \quad \text{and } B = P_c G = \begin{bmatrix} 0 \\ 0 \\ \vdots \\ 0 \\ 1 \end{bmatrix}.$$

Furthermore, it can be shown that the a_i 's are the coefficients of the characteristic equation of F :

$$p(s) = s^n + a_1 s^{n-1} + a_2 s^{n-2} + \cdots + a_{n-2} s^2 + a_{n-1} s + a_n. \quad (3.3)$$

The above canonical form is called the Brunovskii controllable canonical form and the pair (A_c, B) is called the Brunovskii controllable pair [73]. Note that the coefficients are deliberately in reverse order with respect to the conventional expression to help us later.

3.1.4 The Brunovskii observable canonical form

Consider again the single-input system (3.1) with the output equation (3.2). Then, by duality, it can be shown that there exists a similarity transformation $z = P_o x$ such that

$$\begin{cases} \dot{z} = A_o z + B u \\ y = C z \end{cases}$$

where

$$A_o = \begin{bmatrix} -a_1 & 1 & 0 & \cdots & 0 \\ -a_2 & 0 & 1 & \ddots & \vdots \\ \vdots & 0 & \ddots & \ddots & 0 \\ \vdots & \vdots & & \ddots & 1 \\ -a_n & 0 & \cdots & \cdots & 0 \end{bmatrix} \quad \text{and } C = \begin{bmatrix} 1 & 0 & \cdots & 0 \end{bmatrix}. \quad (3.4)$$

Furthermore, it can be shown that the a_i 's are the coefficients of the characteristic equation of F :

$$p(s) = s^n + a_1s^{n-1} + a_2s^{n-2} + \dots + a_{n-2}s^2 + a_{n-1}s + a_n. \quad (3.5)$$

The above canonical form is called the Brunovskii observable canonical form and the pair (A_o, C) is known as the Brunovskii observable canonical pair [73].

3.2 The Extended Jordan Canonical forms - Linear case

From the Brunovskii canonical forms, one can observe that the matrices A_c and A_o can be decomposed as

$$\begin{aligned} A_c &= \begin{bmatrix} 0 & 1 & 0 & \dots & 0 \\ \vdots & \ddots & 1 & \ddots & \vdots \\ 0 & & \ddots & \ddots & 0 \\ 0 & \dots & \dots & 0 & 1 \\ 0 & 0 & \dots & \dots & 0 \end{bmatrix} + \begin{bmatrix} 0 \\ \vdots \\ \vdots \\ 0 \\ 1 \end{bmatrix} \begin{bmatrix} -a_n & -a_{n-1} & \dots & \dots & -a_1 \end{bmatrix} \\ &= \bar{A} + BL \end{aligned}$$

and

$$\begin{aligned} A_o &= \begin{bmatrix} 0 & 1 & 0 & \dots & 0 \\ \vdots & \ddots & 1 & \ddots & \vdots \\ 0 & & \ddots & \ddots & 0 \\ 0 & \dots & \dots & 0 & 1 \\ 0 & 0 & \dots & \dots & 0 \end{bmatrix} + \begin{bmatrix} -a_1 \\ -a_2 \\ \vdots \\ \vdots \\ -a_n \end{bmatrix} \begin{bmatrix} 1 & 0 & \dots & \dots & 0 \end{bmatrix} \\ &= \bar{A} + KC. \end{aligned}$$

Note that the matrix

$$\bar{A} = \begin{bmatrix} 0 & 1 & 0 & \cdots & 0 \\ \vdots & \ddots & 1 & \ddots & \vdots \\ 0 & & \ddots & \ddots & 0 \\ 0 & \cdots & \cdots & 0 & 1 \\ 0 & 0 & \cdots & \cdots & 0 \end{bmatrix}$$

is a Jordan block with a single eigenvalue 0 with multiplicity of order n .

In [35], the question to whether the matrix \bar{A} can be extended to a more general Jordan block of the form

$$J_{\alpha\beta} = \begin{bmatrix} \alpha & \beta & 0 & \cdots & 0 \\ 0 & \alpha & \beta & \ddots & \vdots \\ \vdots & \ddots & \ddots & \ddots & 0 \\ 0 & & \ddots & \alpha & \beta \\ 0 & \cdots & \cdots & 0 & \alpha \end{bmatrix}$$

where α and β are arbitrary numbers with $\beta \neq 0$, was considered. More precisely, the following question was asked: *Assuming that the pairs (F, G) and (F, H) are controllable and observable, respectively, do there exist similarity matrices P_c and P_o such that*

$$\Phi_{\alpha\beta} = P_c F P_c^{-1} = \begin{bmatrix} \alpha & \beta & 0 & \cdots & 0 \\ 0 & \alpha & \beta & \ddots & \vdots \\ \vdots & \ddots & \ddots & \ddots & 0 \\ 0 & \cdots & 0 & \alpha & \beta \\ l_n & l_{n-1} & \cdots & l_2 & \alpha + l_1 \end{bmatrix} \quad \text{and } B = P_c G = \begin{bmatrix} 0 \\ 0 \\ \vdots \\ 0 \\ 1 \end{bmatrix}$$

and

$$\Psi_{\alpha\beta} = P_o F P_o^{-1} = \begin{bmatrix} l_1 + \alpha & \beta & 0 & \cdots & 0 \\ l_2 & \alpha & \beta & \ddots & \vdots \\ \vdots & 0 & \ddots & \ddots & 0 \\ \vdots & \vdots & \ddots & \alpha & \beta \\ l_n & 0 & \cdots & 0 & \alpha \end{bmatrix} \text{ and } H P_o^{-1} = C = \begin{bmatrix} 1 & 0 & \cdots & 0 \end{bmatrix} ?$$

In fact, it was shown in [35], that such similarity matrices P_c and P_o do exist, and a procedure to compute the former was given. As a result, the following single-input linear system:

$$\dot{z} = \Phi_{\alpha\beta} z + B u$$

is said to be in the *Extended Jordan Controllable Canonical (EJCC)* form.

Similarly, the single-output system

$$\begin{cases} \dot{z} = \Psi_{\alpha\beta} z + \bar{B} u \\ y = C z \end{cases}$$

is said to be in the *Extended Jordan Observable Canonical (EJOC)* form.

3.3 The Extended Jordan Canonical forms - Nonlinear case

In this work, we investigate the possibility of extending the above notion of Extended Jordan Canonical forms to nonlinear systems. In effect, consider the following single-input nonlinear system:

$$\dot{x} = f(x, u). \quad (3.6)$$

Suppose that the above system is controllable. Assume that there exists a diffeomorphism $z = \zeta(x)$ such that the above system is transformed into

$$\dot{z} = \Phi_{\alpha\beta}(u, z) z + B u \quad (3.7)$$

where

$$\dot{z} = \frac{\partial \zeta(x)}{\partial x} f(x, u) \Big|_{x=\zeta^{-1}(z)} = \Phi_{\alpha\beta}(u, z)z + Bu$$

where

$$\Phi_{\alpha\beta}(u, z) = \begin{bmatrix} \alpha(u, z)\delta_1 & \beta(u, z) & 0 & \cdots & 0 \\ 0 & \alpha(u, z)\delta_2 & \beta(u, z) & \ddots & \vdots \\ \vdots & \ddots & \ddots & \ddots & 0 \\ 0 & \cdots & 0 & \alpha(u, z)\delta_{n-1} & \beta(u, z) \\ l_n(u, z) & l_{n-1}(u, z) & \cdots & l_2(u, z) & \alpha(u, z)\delta_n + l_1(u, z) \end{bmatrix}$$

and

$$B = \begin{bmatrix} 0 & \cdots & \cdots & 0 & 1 \end{bmatrix}^T$$

with constants $\delta_i \neq 0; i = 1, \dots, n$ and where $\alpha(u, z)$ and $\beta(u, z)$ are two functions such that $\beta(u, z) \neq 0$ for all $z \in \mathbb{R}^n$ and $u \in \mathcal{U}$ where $\mathcal{U} \subset \mathbb{R}$ is a set of admissible inputs.

If such a transformation $z = \zeta(x)$ exists, then we say that the above system is in the *Nonlinear Extended Jordan Controllable Canonical (NL-EJCC)* form. In addition, we call the pair of matrices $(\Phi_{\alpha\beta}(u, z), B)$ an *extended Jordan controllable pair*.

Note that matrix $\Phi_{\alpha\beta}(u, z)$ can be decomposed as

$$\Phi_{\alpha\beta}(u, z) = (\alpha(u, z)\Delta + \beta(u, z)\bar{A}) + BL(u, z)$$

where $\Delta = \text{diag}[\delta_1, \dots, \delta_n]$ and

$$L(u, z) = \begin{bmatrix} l_n(u, z) & l_{n-1}(u, z) & \cdots & l_1(u, z) \end{bmatrix}.$$

Under the above assumptions, the system (3.7) is controllable and the pair $(\Phi_{\alpha\beta}(u, z), B)$ is controllable. Indeed, by calculating the controllability matrix

$$\mathcal{C} = \begin{bmatrix} B & \Phi_{\alpha\beta}(u, z)B & \cdots & \Phi_{\alpha\beta}^{n-1}(u, z)B \end{bmatrix}$$

we can see that $\det \mathcal{C} = (-\beta)^{\frac{n(n-1)}{2}}(u, z)$. Since $\beta(u, z) \neq 0$ for all u and z , we conclude that the pair $(\Phi_{\alpha\beta}(u, z), B)$ is controllable.

Similarly, consider the above system with an output equation

$$y = h(x)$$

where $y \in \mathbb{R}$. Consider a transformation $z = \nu(x)$ such that the above system is transformed into

$$\begin{cases} \dot{z} = \Psi_{\alpha\beta}(u, z)z + g(u, z) \\ y = Cz \end{cases} \quad (3.8)$$

where

$$\dot{z} = \left. \frac{\partial \nu(x)}{\partial x} f(x, u) \right|_{x=\nu^{-1}(z)} = \Psi_{\alpha\beta}(u, z)z + g(u, z)$$

where

$$\Psi_{\alpha\beta}(u, z) = \begin{bmatrix} l_1(u, z) + \alpha(u, z)\delta_1 & \beta(u, z) & 0 & \cdots & 0 \\ l_2(u, z) & \alpha(u, z)\delta_2 & \beta(u, z) & \ddots & \vdots \\ \vdots & 0 & \ddots & \ddots & 0 \\ l_{n-1}(u, z) & \vdots & \ddots & \alpha(u, z)\delta_{n-1} & \beta(u, z) \\ l_n(u, z) & 0 & \cdots & 0 & \alpha(u, z)\delta_n \end{bmatrix}$$

and

$$Cz = h(x = \nu^{-1}(z)) = z_1 = \begin{bmatrix} 1 & 0 & \cdots & 0 \end{bmatrix} z$$

with constants $\delta_i \neq 0$; $i = 1, \dots, n$ and where $g(u, z) = (g_1(u, z), \dots, g_n(u, z))$ has a lower triangular structure; i.e. $g_i(u, z) = g(z_1, z_2, \dots, z_i, u)$.

If such a transformation, $z = \nu(x)$ exists, then we can say that the above system is in the *Nonlinear Extended (or generalised) Jordan Observable Canonical* (NL-EJOC) form. Furthermore, we call the pair of matrices $(\Psi_{\alpha\beta}(u, z), C)$ an *extended Jordan observable pair*.

Note that matrix $\Psi_{\alpha\beta}(u, z)$ can be decomposed as

$$\Psi_{\alpha\beta}(u, z) = (\alpha(u, z)\Delta + \beta(u, z)\bar{A}) + \bar{L}(u, z)C$$

where Δ is as given above and

$$\bar{L}(u, z) = \begin{bmatrix} l_1(u, z) & l_2(u, z) & \cdots & l_n(u, z) \end{bmatrix}^T.$$

Under the above assumptions, the system (3.8) is observable and the pair $(\Psi_{\alpha\beta}(u, z), C)$ is observable. Indeed, by calculating the observability matrix

$$\mathcal{O} = \begin{bmatrix} C \\ C\Psi_{\alpha\beta}(u, z) \\ \vdots \\ C\Psi_{\alpha\beta}^{n-1}(u, z) \end{bmatrix}$$

we can see that $\det \mathcal{O} = \beta^{\frac{n(n-1)}{2}}(u, z)$. Since $\beta(u, z) \neq 0$ for all u and z , we conclude that the pair $(\Psi_{\alpha\beta}(u, z), C)$ is observable.

Throughout this work, we mostly consider the matrix Δ either as the identity matrix for simplicity, or as $\Delta = \Omega = \text{diag}[1, 2, \dots, n]$. The particular choice of the latter form will help us in the design of adaptive observers, as we shall show in Chapter 5.

Remark 3.1

It is not obvious to derive the two transformations $z = \zeta(x)$ and $z = \nu(x)$ such that a general nonlinear system is transformed into the NL-EJCC and NL-EJOC forms. Such a problem is not tackled in this work. However, there exist some classes of systems that are naturally of the above canonical form such as biological reactors, as we shall see in the subsequent chapters.

On the other hand, it is possible to categorise some classes of systems that can be partially transformed into the above class of systems, as we shall show next.

Finally, since the acronyms NL-EJCC and NL-EJOC are quite lengthy, we shall use the acronyms EJCC and EJOC used in the linear case, when we refer to the nonlinear case as well.

3.4 Some special classes of systems in partial EJCC form

Consider the following special class of systems:

$$\dot{x} = F(x)x + G(x)u \quad (3.9)$$

where $x \in \mathbb{R}^n$, $u \in \mathbb{R}$ and the matrices $F(x)$ and $G(x)$ are dependent on the state and are given as

$$F(x) = \begin{bmatrix} f_{11}(x) & \cdots & f_{1n}(x) \\ \vdots & & \vdots \\ f_{n1}(x) & \cdots & f_{nn}(x) \end{bmatrix} \text{ and } G(x) = \begin{bmatrix} g_1(x) \\ \vdots \\ g_n(x) \end{bmatrix}. \quad (3.10)$$

Given some bounded real-valued functions $\alpha(x)$ and $\beta(x)$ with $0 < |\beta(x)| \leq \bar{\beta}$ for all $x \in \mathbb{R}^n$, we consider the problem of constructing a transformation $z = M_{\alpha\beta}(x)x = \varphi(x)$ such that

$$\dot{z} = \Phi_{\alpha\beta}(z)z + Bu + \eta(z)z \quad (3.11)$$

where

$$\begin{aligned} \Phi_{\alpha\beta}(z) &= M_{\alpha\beta}(x)F(x)M_{\alpha\beta}^{-1}(x)\Big|_{x=\varphi^{-1}(z)} \\ &= \begin{bmatrix} \alpha(x) & \beta(x) & 0 & \cdots & 0 \\ 0 & \alpha(x) & \beta(x) & \ddots & \vdots \\ \vdots & \ddots & \ddots & \ddots & 0 \\ 0 & \cdots & 0 & \alpha(x) & \beta(x) \\ l_n(x) & l_{n-1}(x) & \cdots & l_2(x) & \alpha(x) + l_1(x) \end{bmatrix} \Big|_{x=\varphi^{-1}(z)} \end{aligned} \quad (3.12)$$

$$\text{and } \eta(z) = \dot{M}_{\alpha\beta}(x)M_{\alpha\beta}^{-1}(x)\Big|_{x=\varphi^{-1}(z)} \text{ and } M_{\alpha\beta}(x)G(x) = B$$

with B of the form previously given. Note that we have assumed that the diagonal matrix mentioned above is the identity matrix.

In what follows, we shall show that such a transformation exists if the following assumptions are made:

A3.1) The rank of the controllability matrix

$$U(x) = \begin{bmatrix} G(x) & F(x)G(x) & \cdots & F^{n-1}(x)G(x) \end{bmatrix}$$

is equal to n for all $x \in \mathbb{R}^n$.

A3.2) The functions $f_{ij}(x)$ and $g_i(x)$; $i, j = 1, \dots, n$, and their respective time derivatives are continuous and bounded for all $x \in \mathbb{R}^n$.

Assumption A3.1) implies that system (3.9) is controllable in the rank sense for all $x \in \mathbb{R}^n$. In such a case, we say that the pair $(F(x), G(x))$ is controllable for all $x \in \mathbb{R}^n$.

The main procedure for the construction of the matrix $M_{\alpha\beta}(x)$ is summarised in the following lemma:

Lemma 3.1. *Let $(F(x), G(x))$; $F(x) \in \mathbb{R}^{n \times n}$, $G(x) \in \mathbb{R}^{n \times 1}$ be a controllable pair for all $x \in \mathbb{R}^n$. For some given bounded real-valued functions $\alpha(x)$ and $\beta(x)$ with $0 < |\beta(x)| \leq \bar{\beta}$ for all $x \in \mathbb{R}^n$, define the row vector $L_{\alpha\beta}(x) = [l_n(x), l_{n-1}(x), \dots, l_1(x)]$ such that*

$$l_k(x) = -\frac{1}{\beta^{k-1}(x)} \left[C_n^k \alpha^k(x) + \sum_{i=1}^k a_i(x) C_{n-i}^{k-i} \alpha^{k-i}(x) \right] \quad (3.13)$$

with $C_n^k = \frac{n!}{(n-k)!k!}$ and the $a_i(x)$'s are the coefficients of the characteristic equation of $F(x)$:

$$\det [\lambda I_n - F(x)] = \lambda^n + a_1(x)\lambda^{n-1} + \cdots + a_{n-1}(x)\lambda + a_n(x).$$

Then, the pair $(F(x), G(x))$ is equivalent to the pair $(J_{\alpha\beta}(x) + BL_{\alpha\beta}(x), B)$.

In addition, the similarity matrix $M_{\alpha\beta}(x)$ such that the following two equalities:

$$M_{\alpha\beta}(x)F(x)M_{\alpha\beta}^{-1}(x) = J_{\alpha\beta}(x) + BL_{\alpha\beta}(x) \text{ and } M_{\alpha\beta}(x)G(x) = B \quad (3.14)$$

are satisfied is given by

$$M_{\alpha\beta}(x) = Y_{\alpha\beta}(x)U^{-1}(x) \quad (3.15)$$

where

$$U(x) = [G(x), F(x)G(x), \dots, F^{n-1}(x)G(x)] \quad (3.16)$$

and

$$Y_{\alpha\beta}(x) = [B, (J_{\alpha\beta}(x) + BL_{\alpha\beta}(x))B, \dots, (J_{\alpha\beta}(x) + BL_{\alpha\beta}(x))^{n-1}B]. \quad (3.17)$$

Proof of Lemma 3.1:

The proof of this lemma follows along the same lines as given in [74].

First of all, it is easy to check that the pair $(J_{\alpha\beta}(x) + BL_{\alpha\beta}(x), B)$ is controllable for every vector $L_{\alpha\beta}(x) = [l_n(x), l_{n-1}(x), \dots, l_1(x)]$. It can be shown that $\det Y_{\alpha\beta}(x) = (-\beta)^{\frac{n(n-1)}{2}}(x)$. Hence, $Y_{\alpha\beta}(x)$ is non-singular and its determinant is independent of $L_{\alpha\beta}(x)$. We then study the characteristic equations of $F(x)$ and $J_{\alpha\beta}(x) + BL_{\alpha\beta}(x)$. Firstly, recall that $J_{\alpha\beta}(x) = \alpha(x)I_n + \beta(x)\bar{A}$. It can be verified for any $L_{\alpha\beta}(x) = [l_n(x), l_{n-1}(x), \dots, l_1(x)] \in \mathbb{R}^n$, that

$$\begin{aligned} \det [\lambda I_n - (\beta(x)\bar{A} + BL_{\alpha\beta}(x))] &= \lambda^n - l_1(x)\lambda^{n-1} - \beta(x)l_2(x)\lambda^{n-2} - \dots \\ &\quad \dots - \beta^{n-2}(x)l_{n-1}(x)\lambda - \beta^{n-1}(x)l_n(x). \end{aligned}$$

Consequently, since

$$\begin{aligned} \det [\lambda I_n - (J_{\alpha\beta}(x) + BL_{\alpha\beta}(x))] &= \det [\lambda I_n - (\alpha(x)I_n + \beta(x)\bar{A} + BL_{\alpha\beta}(x))] \\ &= \det [(\lambda - \alpha(x))I_n - (\beta(x)\bar{A} + BL_{\alpha\beta}(x))] \end{aligned}$$

it is clear that

$$\begin{aligned} \det [\lambda I_n - (J_{\alpha\beta}(x) + BL_{\alpha\beta}(x))] &= \bar{\lambda}^n - l_1(x)\bar{\lambda}^{n-1} - \beta(x)l_2(x)\bar{\lambda}^{n-2} - \dots \\ &\quad \dots - \beta^{n-2}(x)l_{n-1}(x)\bar{\lambda} - \beta^{n-1}(x)l_n(x) \end{aligned}$$

where $\bar{\lambda} = (\lambda - \alpha(x))$.

Now, assume that the characteristic equation of $F(x)$ is equal to

$$\det [\lambda I_n - F(x)] = \lambda^n + a_1(x)\lambda^{n-1} + \dots + a_{n-1}(x)\lambda + a_n(x).$$

For the pairs $(F(x), G(x))$ and $(J_{\alpha\beta}(x) + BL_{\alpha\beta}(x), B)$ to be equivalent, the characteristic equations of $F(x)$ and $J_{\alpha\beta}(x) + BL_{\alpha\beta}(x)$ should be equal. Hence,

$$\begin{aligned}
\det [\lambda I_n - F(x)] &= \det [\lambda I_n - (J_{\alpha\beta}(x) + BL_{\alpha\beta}(x))] \\
&= \lambda^n + a_1(x)\lambda^{n-1} + \cdots + a_{n-1}(x)\lambda + a_n(x) \\
&= (\bar{\lambda} + \alpha(x))^n + a_1(x) (\bar{\lambda} + \alpha(x))^{n-1} + \cdots \\
&\quad \cdots + a_{n-1}(x) (\bar{\lambda} + \alpha(x)) + a_n(x) \\
&= \bar{\lambda}^n - l_1(x)\bar{\lambda}^{n-1} - \beta(x) l_2(x)\bar{\lambda}^{n-2} - \cdots - \beta(x)^{n-1} l_n(x).
\end{aligned}$$

Using the binomial expansion of $(\bar{\lambda} + \alpha(x))^{n-i}$, one can show that

$$\det [\lambda I_n - F(x)] = \bar{\lambda}^n + r_1(x)\bar{\lambda}^{n-1} + \cdots + r_{n-1}(x)\bar{\lambda} + r_n(x)$$

where

$$\begin{aligned}
r_k(x) &= C_n^k \alpha^k(x) + a_1(x) C_{n-1}^{k-1} \alpha^{k-1}(x) + a_2(x) C_{n-2}^{k-2} \alpha^{k-2}(x) + \cdots \\
&\quad \cdots + a_{k-1}(x) C_{n-(k-1)}^{k-(k-1)} \alpha^{k-(k-1)}(x) + a_k(x) \\
&= C_n^k \alpha^k(x) + \sum_{i=1}^k a_i(x) C_{n-i}^{k-i} \alpha^{k-i}(x).
\end{aligned}$$

It is easy to see that $\det [\lambda I_n - F(x)] = \det [\lambda I_n - (J_{\alpha\beta}(x) + BL_{\alpha\beta}(x))]$ if the elements of $L_{\alpha\beta}(x)$ are given as in (3.13).

Note: The index of the vector $L_{\alpha\beta}(x)$ is deliberately indexed in the reverse order so as to simplify the formula (3.13).

This completes the proof of Lemma 3.1. □

The application of the formula (3.13) for the construction of the vector $L_{\alpha\beta}(x)$ can be, at times, tedious. As a result, an algorithm, involving only matrix manipulation, for the construction of the matrix $M_{\alpha\beta}(x)$ is given in the following subsection.

3.4.1 Algorithm for EJCC form transformation

- i) First, compute $V_{\alpha\beta} = [B, J_{\alpha\beta}B, \dots, J_{\alpha\beta}^{n-1}B]$.
- ii) Then, construct the matrix $U = [G, FG, \dots, F^{n-1}G]$.
- iii) Compute $Q_{\alpha\beta} = V_{\alpha\beta}U^{-1}FUV_{\alpha\beta}^{-1} - J_{\alpha\beta}$.
- iv) Then, calculate $N_{\alpha\beta} = SQ_{\alpha\beta}^T S$, where

$$S = [B, \bar{A}B, \dots, \bar{A}^{n-1}B]. \quad (3.18)$$

- v) Compute $Y_{\alpha\beta} = [B, \Phi_{\alpha\beta}B, \dots, \Phi_{\alpha\beta}^{n-1}B]$, where $\Phi_{\alpha\beta} = J_{\alpha\beta} + N_{\alpha\beta}$.
- vi) Finally, define $M_{\alpha\beta} = Y_{\alpha\beta}U^{-1}$, which is the desired similarity matrix.

The argument of the various matrices was dropped for clarity of notation.

Remark 3.2

- 1) It can be verified that the matrix $N_{\alpha\beta}(x)$ can be decomposed as $N_{\alpha\beta}(x) = BL_{\alpha\beta}(x)$ where $L_{\alpha\beta}(x)$ is the row vector whose components are given by formula (3.13). More precisely, $N_{\alpha\beta}(x)$ is an $n \times n$ matrix which is zero everywhere except the last row - which is, in fact, the vector $L_{\alpha\beta}(x)$. Consequently, the above algorithm provides an alternative method to compute the similarity matrix $M_{\alpha\beta}(x)$ without explicitly computing the vector $L_{\alpha\beta}(x)$ by using formula (3.13).
- 2) If $\alpha(x) = 0$ and $\beta(x) = 1$ in the matrix $J_{\alpha\beta}(x)$, then the matrix $M_{\alpha\beta}(x)$ will permit to obtain the usual Brunovskii controllable canonical form.
- 3) Finally, note that in the special case where $F(x) = (J_{\alpha\beta}(x) + BL_{\alpha\beta}(x))$ and $G(x) = B$, then $Y_{\alpha\beta}(x) = U(x)$ and in which case $M_{\alpha\beta}(x) = I_n$.

We now give some examples of systems which can be partially transformed into the EJCC form or which are already in the EJCC form. We begin with the latter case.

3.4.2 Example 3.1

Consider the system

$$\begin{bmatrix} \dot{x}_1 \\ \dot{x}_2 \end{bmatrix} = \begin{bmatrix} x_1 \cos x_1 + 2x_2 \\ x_1 \sin x_1 + x_2 \cos x_1 + u \end{bmatrix} \quad (3.19)$$

which can be written as

$$\begin{bmatrix} \dot{x}_1 \\ \dot{x}_2 \end{bmatrix} = \begin{bmatrix} \cos x_1 & 2 \\ \sin x_1 & \cos x_1 \end{bmatrix} \begin{bmatrix} x_1 \\ x_2 \end{bmatrix} + \begin{bmatrix} 0 \\ 1 \end{bmatrix} u. \quad (3.20)$$

It is clear that system (3.20) is of the form (3.9) with

$$F(x) = \begin{bmatrix} \cos x_1 & 2 \\ \sin x_1 & \cos x_1 \end{bmatrix} \text{ and } G(x) = \begin{bmatrix} 0 \\ 1 \end{bmatrix} = B.$$

The above system also satisfies the Assumptions A3.1)-A3.2). Indeed,

$$\begin{aligned} U(x) &= \begin{bmatrix} G(x), & F(x)G(x) \end{bmatrix} \\ &= \begin{bmatrix} 0 & 2 \\ 1 & \cos x_1 \end{bmatrix}. \end{aligned}$$

Therefore, $U(x)$ is of full rank for all $x \in \mathbb{R}^2$. Also, the entries of $F(x)$ and $G(x)$ and their respective time derivatives are continuous and bounded for all $x \in \mathbb{R}^2$.

In addition,

$$\begin{aligned} F(x) &= \begin{bmatrix} \cos x_1 & 2 \\ \sin x_1 & \cos x_1 \end{bmatrix} \\ &= \begin{bmatrix} \cos x_1 & 2 \\ 0 & \cos x_1 \end{bmatrix} + \begin{bmatrix} 0 \\ 1 \end{bmatrix} \begin{bmatrix} \sin x_1 & 0 \end{bmatrix}. \end{aligned}$$

Therefore, $F(x)$ is of the form $J_{\alpha\beta}(x) + BL_{\alpha\beta}(x)$ with $\alpha(x) = \cos x_1$, $\beta(x) = 2$ and $L_{\alpha\beta}(x) = \begin{bmatrix} \sin x_1 & 0 \end{bmatrix}$.

As a result, (see Remark 3.2) we have

$$M_{\alpha\beta}(x) = \begin{bmatrix} 1 & 0 \\ 0 & 1 \end{bmatrix}.$$

Therefore, this system is already in the EJCC form.

3.4.3 Example 3.2

Consider the system

$$\begin{bmatrix} \dot{x}_1 \\ \dot{x}_2 \end{bmatrix} = \begin{bmatrix} 2x_1 \cos x_1 + x_2 \\ x_1 \sin^2 x_1 + u \end{bmatrix} \quad (3.21)$$

which can be written as

$$\begin{bmatrix} \dot{x}_1 \\ \dot{x}_2 \end{bmatrix} = \begin{bmatrix} 2 \cos x_1 & 1 \\ \sin^2 x_1 & 0 \end{bmatrix} \begin{bmatrix} x_1 \\ x_2 \end{bmatrix} + \begin{bmatrix} 0 \\ 1 \end{bmatrix} u. \quad (3.22)$$

It is clear that system (3.22) is of the form (3.9) with

$$F(x) = \begin{bmatrix} 2 \cos x_1 & 1 \\ \sin^2 x_1 & 0 \end{bmatrix} \text{ and } G(x) = \begin{bmatrix} 0 \\ 1 \end{bmatrix} = B$$

and satisfies the Assumptions A3.1)-A3.2). Indeed,

$$U(x) = [G(x), F(x)G(x)] = \begin{bmatrix} 0 & 1 \\ 1 & 0 \end{bmatrix}.$$

Therefore, $U(x)$ is of full rank for all $x \in \mathbb{R}^2$. In addition, the entries of $F(x)$ and $G(x)$ and their respective time derivatives are continuous and bounded for all $x \in \mathbb{R}^2$.

We will now transform the above system into the EJCC form.

We first compute

$$\det [\lambda I_2 - F(x)] = \det \left[\begin{bmatrix} \lambda & 0 \\ 0 & \lambda \end{bmatrix} - \begin{bmatrix} 2 \cos x_1 & 1 \\ \sin^2 x_1 & 0 \end{bmatrix} \right]$$

$$\begin{aligned}
&= \det \begin{bmatrix} \lambda - 2 \cos x_1 & -1 \\ -\sin^2 x_1 & \lambda \end{bmatrix} \\
&= \lambda^2 - 2\lambda \cos x_1 - \sin^2 x_1 \\
&= \lambda^2 + a_1(x)\lambda + a_2(x)
\end{aligned}$$

where $a_1(x) = -2 \cos x_1$ and $a_2(x) = -\sin^2 x_1$.

By applying Lemma 3.1, we have

$$\begin{aligned}
l_1(x) &= -[2\alpha(x) + a_1(x)] \\
&= -2[\alpha(x) - \cos x_1]
\end{aligned}$$

and

$$\begin{aligned}
l_2(x) &= -\frac{1}{\beta(x)} [\alpha^2(x) + a_1(x)\alpha(x) + a_2(x)] \\
&= -\frac{1}{\beta(x)} [\alpha^2(x) - 2 \cos x_1 \alpha(x) - \sin^2 x_1].
\end{aligned}$$

If we choose $\alpha(x) = \cos x_1$ and $\beta(x) = \alpha(x) + c = \cos x_1 + c$ where $c > 1$ is a constant,

then

$$L_{\alpha\beta}(x) = [l_2(x), l_1(x)] = \begin{bmatrix} \frac{1}{\cos x_1 + c} & 0 \end{bmatrix}.$$

Therefore, the pair $(F(x), G(x))$ is equivalent to the pair $(J_{\alpha\beta}(x) + BL_{\alpha\beta}(x), B)$, where

$$\begin{aligned}
J_{\alpha\beta}(x) + BL_{\alpha\beta}(x) &= \begin{bmatrix} \cos x_1 & \beta(x) \\ 0 & \cos x_1 \end{bmatrix} + \begin{bmatrix} 0 \\ 1 \end{bmatrix} \begin{bmatrix} \frac{1}{\cos x_1 + c} & 0 \end{bmatrix} \\
&= \begin{bmatrix} \cos x_1 & \cos x_1 + c \\ \frac{1}{\cos x_1 + c} & \cos x_1 \end{bmatrix}
\end{aligned}$$

and

$$Y_{\alpha\beta}(x) = [B, (J_{\alpha\beta}(x) + BL_{\alpha\beta}(x))B] = \begin{bmatrix} 0 & \cos x_1 + c \\ 1 & \cos x_1 \end{bmatrix}.$$

Hence,

$$M_{\alpha\beta}(x) = Y_{\alpha\beta}(x)U^{-1}(x) = \begin{bmatrix} \cos x_1 + c & 0 \\ \cos x_1 & 1 \end{bmatrix}.$$

Consequently, if we define the transformation $z = M_{\alpha\beta}(x)x$, then the above system will transform into

$$\dot{z} = (J_{\alpha\beta}(x) + BL_{\alpha\beta}(x))z + Bu + \dot{M}_{\alpha\beta}(x)M_{\alpha\beta}^{-1}(x)z$$

where

$$\dot{M}_{\alpha\beta}(x)M_{\alpha\beta}^{-1}(x) = \begin{bmatrix} -\dot{x}_1 \frac{\sin x_1}{\cos x_1 + c} & 0 \\ -\dot{x}_1 \frac{\sin x_1}{\cos x_1 + c} & 0 \end{bmatrix}.$$

3.5 Some special classes of systems in partial EJOC form

Consider the following special class of systems:

$$\begin{cases} \dot{x} = F(x)x + G(x)u \\ y = H(x)x \end{cases}$$

where $x \in \mathbb{R}^n$, $u \in \mathbb{R}$ and the matrices $F(x)$, $G(x)$, and $H(x)$ are dependent on the state and are given as in (3.10). Assume that the pair $(F(x), H(x))$ is observable. Then, given some bounded real-valued functions $\alpha(x)$ and $\beta(x)$ with $0 < |\beta(x)| \leq \bar{\beta}$ for all $x \in \mathbb{R}^n$, we consider the problem of constructing a transformation $z = M_{\alpha\beta}(x)x = \varphi(x)$ such that

$$\begin{cases} \dot{z} = \Psi_{\alpha\beta}(z)z + b(z)u + \eta(z)z \\ y = Cz \end{cases}$$

where

$$\Psi_{\alpha\beta}(z) = M_{\alpha\beta}(x)F(x)M_{\alpha\beta}^{-1}(x)|_{x=\varphi^{-1}(z)}$$

$$\Psi_{\alpha\beta}(z) = \left[\begin{array}{cccccc} l_1(x) + \alpha(x) & \beta(x) & 0 & \cdots & 0 \\ l_2(x) & \alpha(x) & \beta(x) & \ddots & \vdots \\ \vdots & 0 & \ddots & \ddots & 0 \\ l_{n-1}(x) & \vdots & \ddots & \alpha(x) & \beta(x) \\ l_n(x) & 0 & \cdots & 0 & \alpha(x) \end{array} \right] \Big|_{x=\varphi^{-1}(z)},$$

$$b(z) = M_{\alpha\beta}(x)G(x)|_{x=\varphi^{-1}(z)}, \quad \eta(z) = \dot{M}_{\alpha\beta}(x)M_{\alpha\beta}^{-1}(x)|_{x=\varphi^{-1}(z)}, \quad \text{and } H(x)M_{\alpha\beta}^{-1}(x) = C$$

with C of the form previously given.

In what follows, we shall show that such a transformation exists if the following assumptions are made:

A3.3) The rank of the observability matrix

$$\Upsilon(x) = \left[\begin{array}{c} H(x) \\ H(x)F(x) \\ \vdots \\ H(x)F^{n-1}(x) \end{array} \right]$$

is equal to n for all $x \in \mathbb{R}^n$.

A3.4) The functions $f_{ij}(x)$ and $g_i(x)$; $i, j = 1, \dots, n$, and their respective time derivatives are continuous and bounded for all $x \in \mathbb{R}^n$.

Assumption A3.3) implies that system (3.9) is observable in the rank sense for all $x \in \mathbb{R}^n$.

In such a case, we say that the pair $(F(x), H(x))$ is observable for all $x \in \mathbb{R}^n$.

Here, again we have assumed that $\Delta = I$. It should be clear from the context that the matrix $M_{\alpha\beta}(x)$ is not the same as in the previous section even though the notations are the same.

The main procedure for the construction of the matrix $M_{\alpha\beta}(x)$ is summarised in the following lemma:

Lemma 3.2. *Let $(F(x), H(x)); F(x) \in \mathbb{R}^{n \times n}$, $H(x) \in \mathbb{R}^{1 \times n}$ be an observable pair for all $x \in \mathbb{R}^n$. For some given bounded real-valued functions $\alpha(x)$ and $\beta(x)$ with $0 < |\beta(x)| \leq \bar{\beta}$ for all $x \in \mathbb{R}^n$, define the column vector $L_{\alpha\beta}(x) = [l_1(x), l_2(x), \dots, l_n(x)]^T$ such that*

$$l_k(x) = -\frac{1}{\beta^{k-1}(x)} \left[C_n^k \alpha^k(x) + \sum_{i=1}^k a_i(x) C_{n-i}^{k-i} \alpha^{k-i}(x) \right] \quad (3.23)$$

with $C_n^k = \frac{n!}{(n-k)!k!}$ and the $a_i(x)$'s are the coefficients of the characteristic equation of $F(x)$:

$$\det[\lambda I_n - F(x)] = \lambda^n + a_1(x)\lambda^{n-1} + \dots + a_{n-1}(x)\lambda + a_n(x). \quad (3.24)$$

Then, the pair $(F(x), H(x))$ is equivalent to the pair $(J_{\alpha\beta}(x) + L_{\alpha\beta}(x)C, C)$.

In addition, the similarity matrix $M_{\alpha\beta}(x)$ such that the following two equalities:

$$M_{\alpha\beta}(x)F(x)M_{\alpha\beta}^{-1}(x) = J_{\alpha\beta}(x) + L_{\alpha\beta}(x)C \text{ and } H(x)M_{\alpha\beta}^{-1}(x) = C \quad (3.25)$$

are satisfied is given by

$$M_{\alpha\beta}(x) = W_{\alpha\beta}^{-1}(x)\Upsilon(x) \quad (3.26)$$

where

$$\Upsilon(x) = \begin{bmatrix} H(x) \\ H(x)F(x) \\ \vdots \\ H(x)F^{n-1}(x) \end{bmatrix}$$

and

$$W_{\alpha\beta}(x) = \begin{bmatrix} C \\ C(J_{\alpha\beta}(x) + L_{\alpha\beta}(x)C) \\ \vdots \\ C(J_{\alpha\beta}(x) + L_{\alpha\beta}(x)C)^{n-1} \end{bmatrix}. \quad (3.27)$$

Proof of Lemma 3.2:

The proof of this lemma is similar to that of Lemma 3.1. First of all, it is easy to check that the pair $(J_{\alpha\beta}(x) + L_{\alpha\beta}(x)C, C)$ is observable for every vector $L_{\alpha\beta}(x) = [l_1(x), l_2(x), \dots, l_n(x)]^T$. It can be shown that $\det W_{\alpha\beta}(x) = \beta^{\frac{n(n-1)}{2}}(x)$. Hence, $W_{\alpha\beta}(x)$ is non-singular and its determinant is independent of $L_{\alpha\beta}(x)$. We then study the characteristic equations of $F(x)$ and $J_{\alpha\beta}(x) + L_{\alpha\beta}(x)C$. Firstly, recall that $J_{\alpha\beta}(x) = \alpha(x)I_n + \beta(x)\bar{A}$. It can be verified for any $L_{\alpha\beta}(x) = [l_1(x), l_2(x), \dots, l_n(x)]^T \in \mathbb{R}$, that

$$\begin{aligned} \det [\lambda I_n - (\beta(x)\bar{A} + L_{\alpha\beta}(x)C)] &= \lambda^n - l_1(x)\lambda^{n-1} - \beta(x)l_2(x)\lambda^{n-2} - \dots \\ &\quad \dots - \beta(x)^{n-2}l_{n-1}(x)\lambda - \beta(x)^{n-1}l_n(x). \end{aligned}$$

Consequently, since

$$\begin{aligned} \det [\lambda I_n - (J_{\alpha\beta}(x) + L_{\alpha\beta}(x)C)] &= \det [\lambda I_n - (\alpha(x)I_n + \beta(x)\bar{A} + L_{\alpha\beta}(x)C)] \\ &= \det [(\lambda - \alpha(x))I_n - (\beta(x)\bar{A} + L_{\alpha\beta}(x)C)] \end{aligned}$$

it is clear that

$$\begin{aligned} \det [\lambda I_n - (J_{\alpha\beta}(x) + L_{\alpha\beta}(x)C)] &= \bar{\lambda}^n - l_1(x)\bar{\lambda}^{n-1} - \beta(x)l_2(x)\bar{\lambda}^{n-2} - \dots \\ &\quad \dots - \beta(x)^{n-2}l_{n-1}(x)\bar{\lambda} - \beta(x)^{n-1}l_n(x) \end{aligned}$$

where $\bar{\lambda} = (\lambda - \alpha(x))$.

We now assume that the characteristic equation of $F(x)$ is equal to

$$\det [\lambda I_n - F(x)] = \lambda^n + a_1(x)\lambda^{n-1} + \dots + a_{n-1}(x)\lambda + a_n(x).$$

For the pairs $(F(x), H(x))$ and $(J_{\alpha\beta}(x) + L_{\alpha\beta}(x)C, C)$ to be equivalent, the characteristic equations of $F(x)$ and $J_{\alpha\beta}(x) + L_{\alpha\beta}(x)C$ should be equal. Hence,

$$\begin{aligned} \det [\lambda I_n - F(x)] &= \det [\lambda I_n - (J_{\alpha\beta}(x) + L_{\alpha\beta}(x)C)] \\ &= \lambda^n + a_1(x)\lambda^{n-1} + \dots + a_{n-1}(x)\lambda + a_n(x) \end{aligned}$$

$$\begin{aligned}
&= (\bar{\lambda} + \alpha(x))^n + a_1(x) (\bar{\lambda} + \alpha(x))^{n-1} + \cdots + a_{n-1}(x) (\bar{\lambda} + \alpha(x)) + a_n(x) \\
&= \bar{\lambda}^n - l_1(x)\bar{\lambda}^{n-1} - \beta(x)l_2(x)\bar{\lambda}^{n-2} - \cdots - \beta(x)^{n-1}l_n(x).
\end{aligned}$$

Using the binomial expansion of $(\bar{\lambda} + \alpha(x))^{n-i}$, one can show that

$$\det[\lambda I_n - F(x)] = \bar{\lambda}^n + r_1(x)\bar{\lambda}^{n-1} + \cdots + r_{n-1}(x)\bar{\lambda} + r_n(x)$$

where

$$\begin{aligned}
r_k(x) &= C_n^k \alpha^k(x) + a_1(x) C_{n-1}^{k-1} \alpha^{k-1}(x) + a_2(x) C_{n-2}^{k-2} \alpha^{k-2}(x) + \cdots \\
&\quad \cdots + a_{k-1}(x) C_{n-(k-1)}^{k-(k-1)} \alpha^{k-(k-1)}(x) + a_k(x) \\
&= C_n^k \alpha^k(x) + \sum_{i=1}^k a_i(x) C_{n-i}^{k-i} \alpha^{k-i}(x).
\end{aligned}$$

Recall that if the characteristic equations of $F(x)$ and $J_{\alpha\beta}(x) + L_{\alpha\beta}(x)C$ are the same, then the pair $(F(x), H(x))$ is equivalent to the pair $(J_{\alpha\beta}(x) + L_{\alpha\beta}(x)C, C)$. Then, it is easy to see that $\det[\lambda I_n - F(x)] = \det[\lambda I_n - (J_{\alpha\beta}(x) + L_{\alpha\beta}(x)C)]$ if the elements of $L_{\alpha\beta}(x)$ are given as in (3.23).

This completes the proof of Lemma 3.2. □

The application of the formula (3.23) for the construction of the vector $L_{\alpha\beta}(x)$ can be, at times, tedious. As a result, an algorithm, involving only matrix manipulation, for the construction of the matrix $M_{\alpha\beta}(x)$ is given in the following subsection.

3.5.1 Algorithm for EJOc form transformation

i) Define $R_{\alpha\beta} = \begin{bmatrix} C \\ C J_{\alpha\beta} \\ \vdots \\ C J_{\alpha\beta}^{n-1} \end{bmatrix}$.

ii) Construct the matrix $\Upsilon = \begin{bmatrix} H \\ HF \\ \vdots \\ HF^{n-1} \end{bmatrix}$.

iii) Compute $X_{\alpha\beta} = R_{\alpha\beta}^{-1} \Upsilon F \Upsilon^{-1} R_{\alpha\beta} - J_{\alpha\beta}$.

iv) Then, calculate $E_{\alpha\beta} = T X_{\alpha\beta}^T T$, where

$$T = \begin{bmatrix} C\bar{A}^{n-1} \\ \vdots \\ C\bar{A} \\ C \end{bmatrix}. \quad (3.28)$$

v) Construct $\Psi_{\alpha\beta} = J_{\alpha\beta} + E_{\alpha\beta}$.

vi) Compute $W_{\alpha\beta} = \begin{bmatrix} C \\ C\Psi_{\alpha\beta} \\ \vdots \\ C\Psi_{\alpha\beta}^{n-1} \end{bmatrix}$.

vii) Finally, define $M_{\alpha\beta} = W_{\alpha\beta}^{-1} \Upsilon$, which is the desired similarity matrix.

The argument of the various matrices was dropped for clarity of notation.

Remark 3.3

- 1) It can be verified that the matrix $E_{\alpha\beta}(x)$ can be decomposed as $E_{\alpha\beta}(x) = L_{\alpha\beta}(x)C$ where $L_{\alpha\beta}(x)$ is the column vector whose components are given by formula (3.23). More precisely, $E_{\alpha\beta}(x)$ is an $n \times n$ matrix, which is zero everywhere except the first column - which is, in fact, the vector $L_{\alpha\beta}(x)$. Consequently, the above algorithm pro-

vides an alternative method to compute the similarity matrix $M_{\alpha\beta}(x)$ without explicitly computing the vector $L_{\alpha\beta}(x)$ by using formula (3.23).

- 2) If $\alpha(x) = 0$ and $\beta(x) = 1$ in the matrix $J_{\alpha\beta}(x)$, then the matrix $M_{\alpha\beta}(x)$ will permit to obtain the usual Brunovskii observable canonical form.
- 3) Note that in the special case where $F(x) = (J_{\alpha\beta}(x) + L_{\alpha\beta}(x)C)$ and $H(x) = C$, then $W_{\alpha\beta}(x) = \Upsilon(x)$ and in which case $M_{\alpha\beta}(x) = I_n$.

Finally, it should be noted that since the functions $\alpha(x)$ and $\beta(x) \neq 0$ are fairly arbitrary, one can always aim at choosing $\alpha(x)$ and $\beta(x)$ such that the matrix $M_{\alpha\beta}(x)$ is almost constant. It is this flexibility in choosing $\alpha(x)$ and $\beta(x)$ that helps in the design of observers and controllers for some classes of nonlinear systems. This is also the main motivation behind the search for the Extended Jordan Canonical form.

3.6 Summary

In this chapter, we have introduced the concept of the Extended Jordan Observable and Controllable Canonical forms. We have also shown how a class of nonlinear systems can be partially transformed into these forms. Moreover, we have provided algorithms to generate the required transformations. These new canonical forms were introduced in order to help facilitate the design of controllers and observers for some classes of nonlinear systems. This is demonstrated in the subsequent chapters. In particular, in the next chapter, we give a control design for a class of control-affine systems using the Extended Jordan Controllable Canonical form.

Chapter 4

Control Design using the Extended Jordan Controllable Canonical Form

4.1 Introduction

In the previous chapter, we have defined the notion of Extended Jordan Canonical forms. In this chapter, we shall exploit this canonical form to design controllers for a class of nonlinear systems. The main motivation for employing this canonical form is twofold:

- 1) It allows the design of nonlinear controllers using only linear design techniques.
- 2) The Extended Jordan Canonical forms allow some design flexibility due to the arbitrary choice of functions in the main diagonal and non-zero functions above the main diagonal in the Jordan block. This, in turn, allows the simplification of the control function.

To clarify the above two points, let us first consider a simple system of order two. Indeed, consider the following system:

$$\dot{x} = \begin{bmatrix} \dot{x}_1 \\ \dot{x}_2 \end{bmatrix} = \begin{bmatrix} -x_1 e^{-x_1} + x_2 \\ -x_2 e^{-x_1} + u \end{bmatrix} = f(x). \quad (4.1)$$

Suppose we wish to stabilise this system to the origin. Then, there are various ways one can achieve this objective. For example, recent nonlinear techniques can be applied such as integrator backstepping approaches, sliding mode, passivity, input-state linearisation, feedback linearisation and so on (see e.g. [5], [15], [29], [30], [31]).

The most commonly employed method is feedback linearisation. In effect, if we employ the feedback linearisation method, we first must make the following change of variable:

$$z = \begin{bmatrix} z_1 \\ z_2 \end{bmatrix} = \begin{bmatrix} x_1 \\ L_f x_1 \end{bmatrix} = \begin{bmatrix} x_1 \\ -x_1 e^{-x_1} + x_2 \end{bmatrix} = \varphi(x).$$

It is easy to check that the Jacobian matrix of $\varphi(x)$ is

$$\frac{\partial \varphi(x)}{\partial x} = \begin{bmatrix} 1 & 0 \\ x_1 e^{-x_1} - e^{-x_1} & 1 \end{bmatrix}$$

and the determinant of which is non-zero. Therefore, $z = \varphi(x)$ is indeed a diffeomorphism and under this change of variable, we have

$$\begin{bmatrix} \dot{z}_1 \\ \dot{z}_2 \end{bmatrix} = \begin{bmatrix} z_2 \\ z_2 z_1 e^{-z_1} - 2z_2 e^{-z_1} - z_1 e^{-2z_1} + u \end{bmatrix}.$$

Consequently, a feedback linearising control law would be

$$u(z) = - (z_2 z_1 e^{-z_1} - 2z_2 e^{-z_1} - z_1 e^{-2z_1}) + k_1 z_1 + k_2 z_2$$

where k_1 and k_2 are chosen such that the closed-loop system

$$\begin{bmatrix} \dot{z}_1 \\ \dot{z}_2 \end{bmatrix} = \begin{bmatrix} z_2 \\ k_1 z_1 + k_2 z_2 \end{bmatrix}$$

is stable. In terms of the original coordinates, we have

$$u(x) = (-x_1 e^{-x_1} + x_2) [-x_1 e^{-x_1} + 2e^{-x_1} + k_2] + x_1 e^{-2x_1} + k_1 x_1.$$

It is clear that the above feedback linearising control law is fairly complicated to implement.

However, a simple inspection of the above system (4.1) shows that it is already in the EJCC form. In effect, the above system can be written as

$$\begin{bmatrix} \dot{x}_1 \\ \dot{x}_2 \end{bmatrix} = \begin{bmatrix} -e^{-x_1} & 1 \\ 0 & -e^{-x_1} \end{bmatrix} \begin{bmatrix} x_1 \\ x_2 \end{bmatrix} + \begin{bmatrix} 0 \\ 1 \end{bmatrix} u$$

which is in the EJCC form (3.11) with $\alpha(x) = -e^{-x_1}$, $\beta(x) = 1$ and $L_{\alpha\beta} = \begin{bmatrix} 0 & 0 \end{bmatrix}$.

In compact form, the system is written as

$$\dot{x} = -e^{-x_1} I_2 x + \bar{A}x + Bu$$

where

$$\bar{A} = \begin{bmatrix} 0 & 1 \\ 0 & 0 \end{bmatrix}, \quad B = \begin{bmatrix} 0 \\ 1 \end{bmatrix}$$

and I_2 is the 2-dimensional identity matrix. We shall now show that a simple linear controller

$$u(x) = k_1 x_1 + k_2 x_2 = Kx \tag{4.2}$$

where K is a vector such that $(\bar{A} + BK)$ is stable, will suffice to stabilise the system at the origin. First note that under the feedback (4.2) the closed-loop system is given by

$$\dot{x} = -e^{-x_1} I_2 x + (\bar{A} + BK)x.$$

Let $V(x) = x^T P x$ be a candidate Lyapunov function where P is a symmetric positive definite (SPD) matrix such that

$$P(\bar{A} + BK) + (\bar{A} + BK)^T P = -Q$$

where Q is an SPD matrix. Then,

$$\begin{aligned}\dot{V}(x) &= x^T P \dot{x} + \dot{x}^T P x \\ &= -2e^{-x_1} x^T P x + x^T [P(\bar{A} + BK) + (\bar{A} + BK)^T P] x \\ &= -2e^{-x_1} x^T P x - x^T Q x \leq 0.\end{aligned}$$

Hence, the above linear controller (4.2) is sufficient to control the nonlinear system (4.1).

Figure 4-1 and Figure 4-2 show the behaviour of x_1 and x_2 , respectively, under the feedback linearising (FL) controller (solid line) and the simple linear controller (dotted line). In both controllers, the same gain was used: $k_1 = -1$ and $k_2 = -2$.

To summarise, we observe that the EJCC form allows the design of simple controllers for classes of nonlinear systems.

We are now going to generalise this design procedure for the class of systems which can be put into a partial EJCC form as mentioned in the previous chapter.

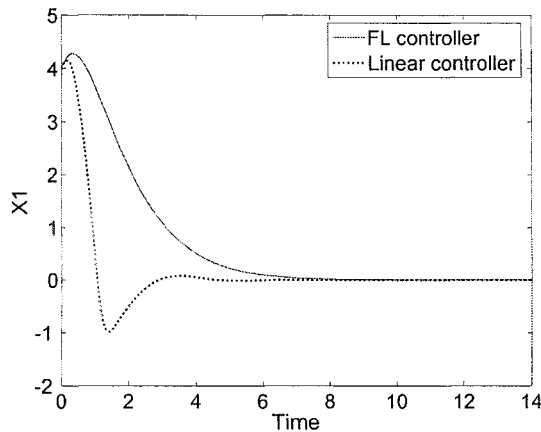


Figure 4-1: Profile of x_1 under the feedback linearising controller (solid line) and the simple linear controller (dotted line)

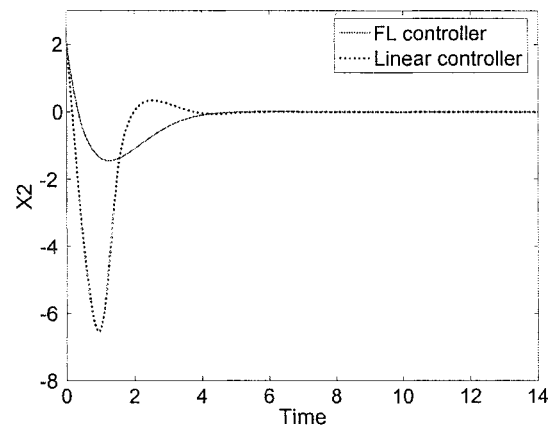


Figure 4-2: Profile of x_2 under the feedback linearising controller (solid line) and the simple linear controller (dotted line)

4.2 Control design for a class of nonlinear systems using Extended Jordan Controllable Canonical forms

We consider the problem of a controller design for the following special class of systems:

$$\dot{x} = F(x)x + G(x)u \quad (4.3)$$

where $x \in \mathbb{R}^n$, $u \in \mathbb{R}$ and the matrices $F(x)$ and $G(x)$, which are dependent upon the state, are given as

$$F(x) = \begin{bmatrix} f_{11}(x) & \cdots & f_{1n}(x) \\ \vdots & & \vdots \\ f_{n1}(x) & \cdots & f_{nn}(x) \end{bmatrix} \text{ and } G(x) = \begin{bmatrix} g_1(x) \\ \vdots \\ g_n(x) \end{bmatrix}. \quad (4.4)$$

We assume that:

A4.1) The rank of the controllability matrix

$$U(x) = \begin{bmatrix} G(x) & F(x)G(x) & \cdots & F^{n-1}(x)G(x) \end{bmatrix}$$

is equal to n for all $x \in \mathbb{R}^n$.

A4.2) The functions $f_{ij}(x)$ and $g_i(x)$; $i, j = 1, \dots, n$, and their respective time derivatives are continuous and bounded for all $x \in \mathbb{R}^n$.

A4.3) The origin is an equilibrium point for the autonomous system.

Now, since the pair $(F(x), G(x))$ is a controllable pair for all $x \in \mathbb{R}^n$, we can define a similarity matrix $M_{\alpha\beta}(x)$ given by (3.15) such that relation (3.14) is satisfied for some arbitrary bounded real-valued functions $\alpha(x)$ and $\beta(x)$ with $0 < |\beta(x)| \leq \beta_1$ for all $x \in \mathbb{R}^n$.

In particular, one can try to choose, if possible, the functions $\alpha(x)$ and $\beta(x)$ such that the upper bound of $\dot{M}_{\alpha\beta}(x)M_{\alpha\beta}^{-1}(x)$ does not exceed a certain desired value. In what follows, we shall make the following additional assumption:

A4.4) We assume that there exists a bounded real-valued function $\alpha(x)$ with $0 \leq |\alpha(x)| \leq \alpha_1$ and a strictly positive bounded real-valued function $\beta(x)$ with $0 < \beta_0 \leq \beta(x) \leq \beta_1$ such that $0 \leq \alpha_1 < \beta_0$ and $\left\| \dot{M}_{\alpha\beta}(x)M_{\alpha\beta}^{-1}(x) \right\| \leq c_0 < \beta_0 - \alpha_1$.

Now, consider the control law defined by

$$u(x) = -[L_{\alpha\beta}(x) + \beta(x)K]M_{\alpha\beta}(x)x \quad (4.5)$$

where

- i) K is a row vector chosen such that the matrix $\bar{A} - BK$ is Hurwitz.
- ii) $L_{\alpha\beta}(x)$ is as in (3.13) and $M_{\alpha\beta}(x)$ is as in (3.15).
- iii) $\alpha(x)$ and $\beta(x)$ are chosen such that Assumption A4.4) is satisfied.

We can now state the following:

Theorem 4.1. *Assume that system (4.3) satisfies Assumptions A4.1)-A4.4). Then, the origin of the following closed-loop system:*

$$\dot{x} = F(x)x + G(x)u(x) \quad (4.6)$$

where $u(x)$ is defined as in (4.5), is globally asymptotically stable.

Proof of Theorem 4.1:

Consider the closed-loop system (4.6). Let $z = M_{\alpha\beta}(x)x$.

Then,

$$\begin{aligned} \dot{z} &= M_{\alpha\beta}(x)\dot{x} + \dot{M}_{\alpha\beta}(x)x \\ &= M_{\alpha\beta}(x)F(x)M_{\alpha\beta}^{-1}(x)z + M_{\alpha\beta}(x)G(x)u(x) + \dot{M}_{\alpha\beta}(x)M_{\alpha\beta}^{-1}(x)z \\ &= [J_{\alpha\beta}(x) + BL_{\alpha\beta}(x)]z + Bu(x) + \dot{M}_{\alpha\beta}(x)M_{\alpha\beta}^{-1}(x)z \\ &= [\alpha(x)I_n + \beta(x)\bar{A} + BL_{\alpha\beta}(x)]z + Bu(x) + \dot{M}_{\alpha\beta}(x)M_{\alpha\beta}^{-1}(x)z. \end{aligned}$$

By replacing $u(x) = -[L_{\alpha\beta}(x) + \beta(x)K] M_{\alpha\beta}(x)x = -L_{\alpha\beta}(x)z - \beta(x)Kz$, we obtain

$$\dot{z} = \alpha(x)Iz + \beta(x) (\bar{A} - BK) z + \dot{M}_{\alpha\beta}(x)M_{\alpha\beta}^{-1}(x)z.$$

On the other hand, since $\bar{A} - BK$ is Hurwitz, there exists a symmetric positive definite matrix P such that

$$(\bar{A} - BK)^T P + P (\bar{A} - BK) = -I_n.$$

Let $V(z) = z^T Pz$ be a candidate Lyapunov function. Then,

$$\begin{aligned} \dot{V}(z) &= 2z^T P\dot{z} \\ &= 2\alpha(x)z^T Pz - \beta(x)\|z\|^2 + 2z^T P\dot{M}_{\alpha\beta}(x)M_{\alpha\beta}^{-1}(x)z \\ &\leq 2|\alpha(x)| \|P\| \|z\|^2 - \beta_0 \|z\|^2 + 2\|P\| \cdot \|\dot{M}_{\alpha\beta}(x)M_{\alpha\beta}^{-1}(x)\| \cdot \|z\|^2 \\ &\leq 2\alpha_1 \|P\| \|z\|^2 - \beta_0 \|z\|^2 + 2\|P\| \cdot \|\dot{M}_{\alpha\beta}(x)M_{\alpha\beta}^{-1}(x)\| \cdot \|z\|^2. \end{aligned}$$

By using Assumption A4.4), we obtain

$$\dot{V}(z) \leq 2\alpha_1 \|P\| \|z\|^2 - \beta_0 \|z\|^2 + 2c_0 \|P\| \cdot \|z\|^2.$$

Now, we can always choose K such that $\|P\| \leq \frac{1}{2}$ and in which case, we have

$$\begin{aligned} \dot{V}(z) &\leq \alpha_1 \|z\|^2 - \beta_0 \|z\|^2 + c_0 \|z\|^2 \\ &\leq -(\beta_0 - \alpha_1 - c_0) \|z\|^2 < 0 \end{aligned}$$

owing to Assumption A4.4).

This completes the proof of Theorem 4.1. □

Remark 4.1

- 1) If $F(x) = F$ and $G(x) = G$ where F and G are both constant matrices, then $M_{\alpha\beta}(x) = M_{\alpha\beta}$ is obviously constant and the $u(x)$ defined by (4.5) amounts to the classical state feedback control for linear time-invariant systems.
- 2) Assumption A4.4) is somewhat restrictive. It might not always be possible to find $\alpha(x)$

and $\beta(x)$ such that $0 < \beta_0 \leq \beta(x)$ and $\left\| \dot{M}_{\alpha\beta}(x)M_{\alpha\beta}^{-1}(x) \right\| < \beta_0 - \alpha_1$. This would naturally impose some particular structure on $F(x)$ and $G(x)$. In general, one should aim to choose $\alpha(x)$ and $\beta(x)$ such that the matrix $M_{\alpha\beta}(x)$ becomes a constant matrix or at least as close as to a constant matrix so that the term $\dot{M}_{\alpha\beta}(x)M_{\alpha\beta}^{-1}(x)$ will be almost zero. This can sometimes be done through the inclusion of some preliminary compensation as Example 4.2 given below shows.

3) Finally, it should be realised that the condition that $\beta_0 - \alpha_1 - c_0$ be positive is conservative.

If $\alpha(x) = -\gamma(x) + \nu(x)$ where $\gamma(x)$ is positive for all $x \in \mathbb{R}^n$, then $\beta_0 - |\nu(x)| - c_0 > 0$ would be a sufficient condition for $\dot{V}(z)$ to be negative.

4.2.1 Example 4.1

Consider the system

$$\begin{bmatrix} \dot{x}_1 \\ \dot{x}_2 \end{bmatrix} = \begin{bmatrix} x_1 \cos x_1 + 2x_2 \\ x_1 \sin x_1 + x_2 \cos x_1 + u \end{bmatrix} \quad (4.7)$$

which can be written as

$$\begin{bmatrix} \dot{x}_1 \\ \dot{x}_2 \end{bmatrix} = \begin{bmatrix} \cos x_1 & 2 \\ \sin x_1 & \cos x_1 \end{bmatrix} \begin{bmatrix} x_1 \\ x_2 \end{bmatrix} + \begin{bmatrix} 0 \\ 1 \end{bmatrix} u. \quad (4.8)$$

It is clear that system (4.8) is of the form (4.3) with

$$F(x) = \begin{bmatrix} \cos x_1 & 2 \\ \sin x_1 & \cos x_1 \end{bmatrix} \text{ and } G(x) = \begin{bmatrix} 0 \\ 1 \end{bmatrix} = B$$

and satisfies all the Assumptions A4.1)-A4.3). Indeed,

$$U(x) = [G(x), F(x)G(x)] = \begin{bmatrix} 0 & 2 \\ 1 & \cos x_1 \end{bmatrix}.$$

Therefore, $U(x)$ is of full rank for all $x \in \mathbb{R}^2$. The entries of $F(x)$ and $G(x)$ and their respective time derivatives are continuous and bounded for all $x \in \mathbb{R}^2$.

In addition,

$$\begin{aligned} F(x) &= \begin{bmatrix} \cos x_1 & 2 \\ \sin x_1 & \cos x_1 \end{bmatrix} \\ &= \begin{bmatrix} \cos x_1 & 2 \\ 0 & \cos x_1 \end{bmatrix} + \begin{bmatrix} 0 \\ 1 \end{bmatrix} \begin{bmatrix} \sin x_1 & 0 \end{bmatrix}. \end{aligned}$$

Therefore, $F(x)$ is of the form $J_{\alpha\beta}(x) + BL_{\alpha\beta}(x)$ with $\alpha(x) = \cos x_1$, $\beta(x) = 2$ and $L_{\alpha\beta}(x) = \begin{bmatrix} \sin x_1 & 0 \end{bmatrix}$. As a result, (see Remark 4.1), we have

$$M_{\alpha\beta}(x) = \begin{bmatrix} 1 & 0 \\ 0 & 1 \end{bmatrix}.$$

Since $\beta(x) - \alpha(x) = 2 - \cos x_1 > 0$ and $\dot{M}_{\alpha\beta}(x)M_{\alpha\beta}(x)^{-1} = 0$, we can design a controller of the form (4.5):

$$\begin{aligned} u(x) &= -[L_{\alpha\beta}(x) + \beta(x)K] M_{\alpha\beta}(x)x \\ &= -\left[\begin{pmatrix} \sin x_1 & 0 \end{pmatrix} + 2 \begin{pmatrix} k_1 & k_2 \end{pmatrix} \right] \begin{bmatrix} x_1 \\ x_2 \end{bmatrix} \\ &= -(\sin x_1 + 2k_1)x_1 - 2k_2x_2 \end{aligned}$$

where k_1 and k_2 are chosen such that the eigenvalues of the matrix

$$\bar{A} - BK = \begin{bmatrix} 0 & 1 \\ -k_1 & -k_2 \end{bmatrix}$$

lie in the left-half complex plane. For example, k_1 and k_2 can be chosen as $k_1 = 1$ and $k_2 = 1$.

4.2.2 Example 4.2

Consider the system

$$\begin{bmatrix} \dot{x}_1 \\ \dot{x}_2 \end{bmatrix} = \begin{bmatrix} -2x_1 + \sin x_1 + ax_2 \\ -x_2 \cos x_1 + u \cos 2x_1 \end{bmatrix}. \quad (4.9)$$

This example is borrowed from [10] where it is shown that the following control law:

$$u = \frac{1}{a \cos 2x_1} (-2ax_2 - 2 \sin x_1 - \cos x_1 \sin x_1 + 2x_1 \cos x_1) \quad (4.10)$$

is a feedback that stabilises the system at the equilibrium point $(0, 0)$ using the input-state linearising method. We shall apply the control design method given in the previous section and compare the results obtained.

First, let us apply the preliminary control

$$u = \frac{1}{\cos 2x_1} \left(-2x_2 + \left(\frac{\sin x_1}{x_1} \right) x_2 + x_2 \cos x_1 + v \right). \quad (4.11)$$

By applying (4.11) to (4.9), we obtain

$$\begin{bmatrix} \dot{x}_1 \\ \dot{x}_2 \end{bmatrix} = \begin{bmatrix} -2x_1 + \sin x_1 + ax_2 \\ -2x_2 + \frac{\sin x_1}{x_1} x_2 + v \end{bmatrix}$$

which can be written as

$$\begin{bmatrix} \dot{x}_1 \\ \dot{x}_2 \end{bmatrix} = \begin{bmatrix} -2 + \frac{\sin x_1}{x_1} & a \\ 0 & -2 + \frac{\sin x_1}{x_1} \end{bmatrix} \begin{bmatrix} x_1 \\ x_2 \end{bmatrix} + \begin{bmatrix} 0 \\ 1 \end{bmatrix} v. \quad (4.12)$$

It is clear that system (4.12) is of the form (4.3) with

$$F(x) = \begin{bmatrix} -2 + \frac{\sin x_1}{x_1} & a \\ 0 & -2 + \frac{\sin x_1}{x_1} \end{bmatrix} \text{ and } G(x) = \begin{bmatrix} 0 \\ 1 \end{bmatrix} = B$$

and satisfies all the Assumptions A4.1)-A4.3).

If we choose $\alpha(x) = -2 + \frac{\sin x_1}{x_1}$ and $\beta(x) = a$, it can readily be seen that system (4.12) is already of the extended Jordan controllable form with $L_{\alpha\beta}(x) = \begin{bmatrix} 0 & 0 \end{bmatrix}$. Consequently,

$$M_{\alpha\beta}(x) = \begin{bmatrix} 1 & 0 \\ 0 & 1 \end{bmatrix}. \text{ As a result,}$$

$$v(x) = -\beta(x)Kx = -ak_1x_1 - ak_2x_2$$

where k_1 and k_2 are chosen such that the eigenvalues of the matrix

$$\bar{A} - BK = \begin{bmatrix} 0 & 1 \\ -k_1 & -k_2 \end{bmatrix}$$

lie in the left-half complex plane. For example, k_1 and k_2 can be chosen as $k_1 = 1$ and $k_2 = 2$.

For this choice of k_1 and k_2 , the overall control law is given by

$$u = \frac{1}{\cos 2x_1} \left(-ax_1 - 2(1+a)x_2 + \left(\frac{\sin x_1}{x_1} \right) x_2 + x_2 \cos x_1 \right). \quad (4.13)$$

Since $\alpha(x) = -2 + \frac{\sin x_1}{x_1}$ and $\left| \frac{\sin x_1}{x_1} \right| \leq 1$, it is clear that the above controller will work if $\beta(x) - \left| \frac{\sin x_1}{x_1} \right| = a - 1 \geq 0$; that is $a \geq 1$.

Figure 4-3 and Figure 4-4 show the profiles of x_1 and x_2 obtained by applying controllers (4.10) and (4.13). The proposed method is shown in solid lines and the input-state linearising method is shown in dotted lines. The poles of the linearised system obtained by the input-state linearising method, and the poles of the matrix $\bar{A} - BK$ involved in the proposed method were both placed at -1 . Consequently, the comparison is justifiable. It can be seen that the controllers have similar performances.

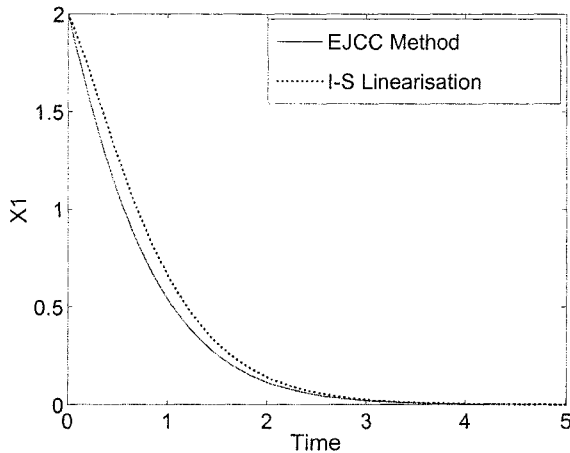


Figure 4-3: Profile of x_1 using the input-state linearising method (dotted line) and the proposed EJCC method (solid line)

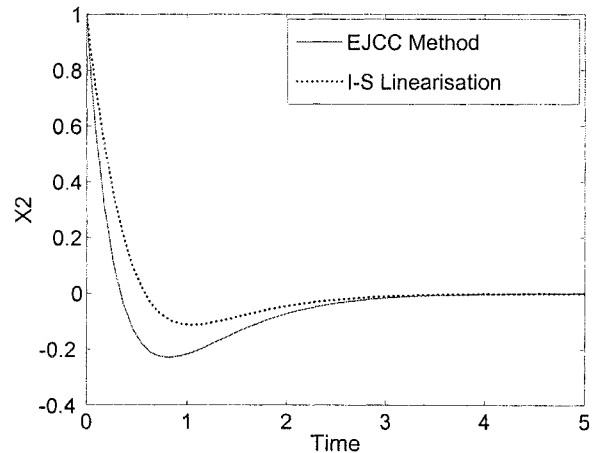


Figure 4-4: Profile of x_2 using the input-state linearising method (dotted line) and the proposed EJCC method (solid line)

4.3 Conclusions

In this chapter, we have proposed a controller design methodology for a class of single-input nonlinear systems which can be transformed, partially, into the Extended Jordan Controllable Canonical form. It is shown that such a canonical form facilitates the design of a controller since it provides additional degrees of freedom in tuning the controller parameters. In addition, only linear design techniques are used for the controller design, which has been shown to compare well with an input-state linearising controller.

In the next chapter, we shall tackle the issue of observer design for a sub-class of state-affine systems and highlight some difficulties associated with this.

Chapter 5

Observer Design using the Extended Jordan Observable Canonical Form

5.1 Introduction

In the previous chapter, we have proposed a controller design methodology for systems in EJCC form. In this present chapter, we shall attempt to propose a methodology for observer design for systems which can be put into a partial EJOC form. We shall see that this is not an easy matter, especially for systems in the general EJOC form (3.8) as described in Chapter 3. Indeed, consider the class of systems described by equation (3.8). Suppose that we wish to design an observer for the system (3.8) of the following form:

$$\dot{\hat{z}} = \Psi_{\alpha\beta}(u, \hat{z})\hat{z} + g(u, \hat{z}) + K(y - C\hat{z})$$

where K is the gain of the observer, possibly depending on the measured variables u and y .

By setting $e = z - \hat{z}$, we can see that the error dynamics are given by

$$\begin{aligned}\dot{e} &= \Psi_{\alpha\beta}(u, z)z - \Psi_{\alpha\beta}(u, \hat{z})\hat{z} - KCe + [g(u, z) - g(u, \hat{z})] \\ &= [\Psi_{\alpha\beta}(u, \hat{z})z - \Psi_{\alpha\beta}(u, \hat{z})\hat{z}] - KCe + [\Psi_{\alpha\beta}(u, z) - \Psi_{\alpha\beta}(u, \hat{z})]z + [g(u, z) - g(u, \hat{z})]\end{aligned}$$

$$\dot{e} = (\Psi_{\alpha\beta}(u, \hat{z}) - KC)e + [\Psi_{\alpha\beta}(u, z) - \Psi_{\alpha\beta}(u, \hat{z})]z + [g(u, z) - g(u, \hat{z})].$$

Firstly, it is important to realise that, in general, it is not easy to design a K such that the matrix $(\Psi_{\alpha\beta}(u, \hat{z}) - KC)$ is stable. Next, since z is not measured, some assumptions are needed for the compensation of the residual terms $[\Psi_{\alpha\beta}(u, z) - \Psi_{\alpha\beta}(u, \hat{z})]z$ and $[g(u, z) - g(u, \hat{z})]$. Some boundedness or Lipschitz continuity assumptions might be used for that purpose. However, these assumptions are too restrictive.

On the other hand, if we consider a sub-class of the above systems where the matrix $\Psi_{\alpha\beta}(u, z)$ depends only on the input and the output (i.e. $\Psi_{\alpha\beta}(u, z) = \Psi_{\alpha\beta}(u, y)$ and $g(u, z) = g(u, y)$), then the residual terms will become zero. Therefore, the only problem that remains to be solved is to find the appropriate gain K that will make the matrix $(\Psi_{\alpha\beta}(u, y) - KC)$ stable. Because of these observations, we shall, in this chapter, consider the problem of observer design for the above system in EJO form when $\Psi_{\alpha\beta}(u, z) = \Psi_{\alpha\beta}(u, y)$ and $g(u, z) = g(u, y)$. Then, we show how this observer can be adapted to design observers for a class of state-affine systems that can be partially transformed into the EJO form. As in the controller design case, we shall see that the interesting feature of the EJO form is that it provides additional degrees of freedom to tune the observer gain.

5.2 Observer 1 - Observer design for a sub-class of single-output systems in EJO form

Consider the following sub-class of systems in EJO form:

$$\begin{cases} \dot{z} = \Psi_{\alpha\beta}(u, y)z + g(u, y) \\ y = Cz \end{cases} \quad (5.1)$$

where $z \in \mathbb{R}^n$, $u \in \mathbb{R}^m$ and $y \in \mathbb{R}$. The matrices $\Psi_{\alpha\beta}(u, y)$ and C are given as

$$\Psi_{\alpha\beta}(u, y) = \begin{bmatrix} l_1(u, y) + \alpha(u, y)\delta_1 & \beta(u, y) & 0 & \cdots & 0 \\ l_2(u, y) & \alpha(u, y)\delta_2 & \beta(u, y) & \ddots & \vdots \\ \vdots & 0 & \ddots & \ddots & 0 \\ l_{n-1}(u, y) & \vdots & \ddots & \alpha(u, y)\delta_{n-1} & \beta(u, y) \\ l_n(u, y) & 0 & \cdots & 0 & \alpha(u, y)\delta_n \end{bmatrix} \text{ and}$$

$$C = \begin{bmatrix} 1 & 0 & \cdots & 0 \end{bmatrix}.$$

Note that matrix $\Psi_{\alpha\beta}(u, y)$ can be decomposed as

$$\Psi_{\alpha\beta}(u, y) = (\alpha(u, y)\Delta + \beta(u, y)\bar{A}) + L_{\alpha\beta}(u, y)C$$

where $\Delta = \text{diag}[\delta_1, \dots, \delta_n]$ and

$$L_{\alpha\beta}(u, y) = \begin{bmatrix} l_1(u, y) & l_2(u, y) & \cdots & l_n(u, y) \end{bmatrix}^T.$$

For the case of Observer 1, we have $\Delta = I_n$ where I_n is the n -dimensional identity matrix. It is assumed that $\beta(u, y) \neq 0$ for all u and y . As stated in the previous chapter, this assumption ensures that the above system is observable for all u ; i.e. the system is uniformly observable.

Since $\beta(u, y) \neq 0$ for all u and y , this means that $\beta(u, y)$ is either a strictly positive or a strictly negative function. Consequently, we shall make the following assumptions:

A5.1) There exists a set of admissible inputs \mathcal{U} such that for all $u \in \mathcal{U}$, the matrix

$$\Upsilon(u, y) = \begin{bmatrix} C \\ C\Psi_{\alpha\beta}(u, y) \\ \vdots \\ C\Psi_{\alpha\beta}^{n-1}(u, y) \end{bmatrix} \quad (5.2)$$

is of full rank for all $y \in \mathbb{R}$.

A5.2) We shall assume that the function $g(u, y)$ and the entries of the matrix $\Psi_{\alpha\beta}(u, y)$ are smooth and bounded.

A5.3) We assume that there exist $\beta_0 > 0$ and $\beta_1 > 0$ such that $\beta_0 < |\beta(u, y)| < \beta_1$.

Now, consider the following system:

$$\dot{\hat{z}} = \Psi_{\alpha\beta}(u, y)\hat{z} + g(u, y) + \hat{K}(u, y)(y - C\hat{z}) \quad (5.3)$$

where

- $\hat{K}(u, y) = \beta(u, y) D_{\theta_c}^{-1} K_0 + L_{\alpha\beta}(u, y)$, where
- $D_{\theta_c} = \text{diag} \left[\frac{1}{\theta_c} \quad \frac{1}{\theta_c^2} \quad \dots \quad \frac{1}{\theta_c^n} \right]$, and
- K_0 is a constant vector chosen such that the matrix $\bar{A} - K_0 C$ is stable.

We can now state the following:

Theorem 5.1. *Assume that system (5.1) satisfies Assumptions A5.1)-A5.3). Then, the system (5.3) is an exponential observer for system (5.1) if:*

- i)** $\theta_c > 0$ when $\alpha(u, y) \leq 0$ and $\beta(u, y) > 0$ for all u and y .
- ii)** $\theta_c < 0$ when $\alpha(u, y) \leq 0$ and $\beta(u, y) < 0$ for all u and y .
- iii)** $\theta_c > \bar{\theta}_0$ for some $\bar{\theta}_0 > 0$ when $\alpha(u, y) > 0$ and $\beta(u, y) > 0$ for all u and y .
- iv)** $\theta_c < \bar{\theta}_1$ for some $\bar{\theta}_1 < 0$ when $\alpha(u, y) > 0$ and $\beta(u, y) < 0$ for all u and y .

Proof of Theorem 5.1:

Defining the estimation error as $e = z - \hat{z}$, we have

$$\dot{e} = \Psi_{\alpha\beta} e - \hat{K} C e$$

$$\begin{aligned}
\dot{e} &= \Psi_{\alpha\beta}e - [\beta D_{\theta_c}^{-1}K_0 + L_{\alpha\beta}]Ce \\
&= (J_{\alpha\beta} + L_{\alpha\beta}C)e - \beta D_{\theta_c}^{-1}K_0Ce - L_{\alpha\beta}Ce \\
&= (J_{\alpha\beta} - \beta D_{\theta_c}^{-1}K_0C)e.
\end{aligned}$$

Note that the arguments of the various matrices have been dropped for the sake of simplicity.

Since $J_{\alpha\beta} = \alpha I_n + \beta \bar{A}$ and

$$\bar{A} = \begin{bmatrix} 0 & 1 & 0 & \cdots & 0 \\ 0 & 0 & 1 & \ddots & \vdots \\ \vdots & \ddots & \ddots & \ddots & 0 \\ \vdots & & \ddots & 0 & 1 \\ 0 & \cdots & \cdots & 0 & 0 \end{bmatrix} \quad (5.4)$$

we have

$$\dot{e} = \alpha I_n e + \beta (\bar{A} - D_{\theta_c}^{-1}K_0C) e.$$

Now, let $\varepsilon = D_{\theta_c}e$. Then,

$$\begin{aligned}
\dot{\varepsilon} &= D_{\theta_c}\dot{e} \\
&= \alpha D_{\theta_c}e + \beta D_{\theta_c}(\bar{A} - D_{\theta_c}^{-1}K_0C)e \\
&= \alpha D_{\theta_c}D_{\theta_c}^{-1}\varepsilon + \beta D_{\theta_c}(\bar{A} - D_{\theta_c}^{-1}K_0C)D_{\theta_c}^{-1}\varepsilon.
\end{aligned}$$

It can be verified that $D_{\theta_c}\bar{A}D_{\theta_c}^{-1} = \theta_c\bar{A}$ and $CD_{\theta_c}^{-1} = \theta_cC$. Consequently,

$$\dot{\varepsilon} = \alpha I_n \varepsilon + \beta \theta_c (\bar{A} - K_0C) \varepsilon.$$

Now, since the matrix $(\bar{A} - K_0C)$ is stable, there exists a symmetric positive definite matrix P such that

$$(\bar{A} - K_0C)^T P + P(\bar{A} - K_0C) = -I_n. \quad (5.5)$$

Consider the following candidate Lyapunov function $V(\varepsilon) = \varepsilon^T P \varepsilon$. Then, we have

$$\dot{V} = \dot{\varepsilon}^T P \varepsilon + \varepsilon^T P \dot{\varepsilon}.$$

Since $\dot{\varepsilon}^T P \varepsilon$ is of dimension 1×1 , i.e. a number, we can use its transpose and obtain

$$\begin{aligned}\dot{V} &= 2\varepsilon^T P \dot{\varepsilon} \\ &= 2\alpha \varepsilon^T P \varepsilon + 2\beta \theta_c \varepsilon^T P (\bar{A} - K_0 C) \varepsilon.\end{aligned}$$

It can be shown that a pre-multiplication of (5.5) with ε^T and a post-multiplication of (5.5) with ε yields terms of dimension 1×1 :

$$\varepsilon^T (\bar{A} - K_0 C)^T P \varepsilon + \varepsilon^T P (\bar{A} - K_0 C) \varepsilon = -\varepsilon^T I_n \varepsilon.$$

Therefore, we can use a transpose:

$$\varepsilon^T (\bar{A} - K_0 C)^T P \varepsilon = (\varepsilon^T (\bar{A} - K_0 C)^T P \varepsilon)^T = \varepsilon^T P (\bar{A} - K_0 C) \varepsilon$$

to obtain

$$\varepsilon^T (\bar{A} - K_0 C)^T P \varepsilon + \varepsilon^T P (\bar{A} - K_0 C) \varepsilon = 2\varepsilon^T P (\bar{A} - K_0 C) \varepsilon = -\varepsilon^T \varepsilon.$$

Hence,

$$\begin{aligned}\dot{V} &= 2\alpha \varepsilon^T P \varepsilon + 2\beta \theta_c \varepsilon^T P (\bar{A} - K_0 C) \varepsilon \\ &= 2\alpha \varepsilon^T P \varepsilon - \beta \theta_c \varepsilon^T \varepsilon.\end{aligned}$$

First note that $\varepsilon^T P \varepsilon$ and $\varepsilon^T \varepsilon$ are always positive. For $\varepsilon(t) \rightarrow 0$ as $t \rightarrow +\infty$, we require $\dot{V}(\varepsilon) < 0$. Therefore, if $\alpha(u, y) \leq 0$ and $\beta(u, y) > 0$, it suffices to choose $\theta_c > 0$ such that $\dot{V}(\varepsilon) < 0$. Similarly, if $\alpha(u, y) \leq 0$ and $\beta(u, y) < 0$, it suffices to choose $\theta_c < 0$ such that $\dot{V}(\varepsilon) < 0$. Therefore, the only two critical cases that are left are:

- Case 5.1: $\alpha(u, y) > 0$ and $\beta(u, y) > 0$.
- Case 5.2: $\alpha(u, y) > 0$ and $\beta(u, y) < 0$.

Case 5.1

In this case,

$$\dot{V}(\varepsilon) = 2\alpha \varepsilon^T P \varepsilon - \beta \theta_c \varepsilon^T \varepsilon \leq 2\alpha_{\max} \varepsilon^T P \varepsilon - \beta \theta_c \varepsilon^T \varepsilon$$

where α_{\max} is the upper bound of $\alpha(u, y)$. On the other hand, we know that there exists $c_1 > 0$ and $c_2 > 0$ such that

$$c_1 \varepsilon^T \varepsilon \leq \varepsilon^T P \varepsilon \leq c_2 \varepsilon^T \varepsilon.$$

In effect, c_1 and c_2 are the smallest and largest eigenvalues of P , respectively. Therefore,

$$\begin{aligned} \dot{V} &\leq 2\alpha_{\max} c_2 \varepsilon^T \varepsilon - \beta \theta_c \varepsilon^T \varepsilon \\ &\leq (2\alpha_{\max} c_2 - \beta_0 \theta_c) \varepsilon^T \varepsilon \end{aligned}$$

where β_0 is the lower bound of $\beta(u, y)$ as mentioned in Assumption A5.3). Hence, for $\dot{V}(\varepsilon) < 0$, we require

$$2\alpha_{\max} c_2 - \beta_0 \theta_c < 0.$$

Therefore, it suffices to choose

$$\theta_c > \frac{2\alpha_{\max} c_2}{\beta_0} = \bar{\theta}_0.$$

Case 5.2

In this case,

$$\begin{aligned} \dot{V} &= 2\alpha \varepsilon^T P \varepsilon - \beta \theta_c \varepsilon^T \varepsilon \\ &\leq 2\alpha_{\max} \varepsilon^T P \varepsilon - \beta \theta_c \varepsilon^T \varepsilon \\ &\leq 2\alpha_{\max} \varepsilon^T P \varepsilon + \beta_1 \theta_c \varepsilon^T \varepsilon \\ &\leq 2\alpha_{\max} c_2 \varepsilon^T \varepsilon + \beta_1 \theta_c \varepsilon^T \varepsilon \\ &\leq (2\alpha_{\max} c_2 + \beta_1 \theta_c) \varepsilon^T \varepsilon. \end{aligned}$$

Hence, in order for $\dot{V}(\varepsilon) < 0$, we require

$$2\alpha_{\max} c_2 + \beta_1 \theta_c < 0.$$

Therefore, it suffices to choose

$$\theta_c < \frac{-2\alpha_{\max} c_2}{\beta_1} = \bar{\theta}_1.$$

Note that the arguments of the functions were dropped for brevity.

This completes the proof of Theorem 5.1. □

5.2.1 Example 5.1

We now give a simulation example to illustrate the performance of the observer. Consider the 2nd-order system expressed in the EJOc form (5.1) as

$$\begin{aligned} \begin{bmatrix} \dot{x}_1 \\ \dot{x}_2 \end{bmatrix} &= \begin{bmatrix} \alpha(u, y) & \beta(u, y) \\ 0 & \alpha(u, y) \end{bmatrix} \begin{bmatrix} x_1 \\ x_2 \end{bmatrix} + \begin{bmatrix} 0 \\ x_1 u \end{bmatrix} \\ y &= \begin{bmatrix} 1 & 0 \end{bmatrix} \begin{bmatrix} x_1 \\ x_2 \end{bmatrix} = x_1 \end{aligned} \quad (5.6)$$

where u is a step input. Note that here, $\Delta = I_2$ and $L_{\alpha\beta}(u, y) = \begin{bmatrix} 0 & 0 \end{bmatrix}^T$.

We shall consider the following cases:

- Case 5.3: $\alpha(u, y) = -1; \beta(u, y) = \frac{1}{x_1^2+1}$.
- Case 5.4: $\alpha(u, y) = -1; \beta(u, y) = -\frac{1}{x_1^2+1}$.
- Case 5.5: $\alpha(u, y) = 1; \beta(u, y) = \frac{1}{x_1^2+1}$.
- Case 5.6: $\alpha(u, y) = 1; \beta(u, y) = -\frac{1}{x_1^2+1}$.

For each case considered, the gain is given by

$$\widehat{K} = \begin{bmatrix} \psi_1 \\ \psi_2 \end{bmatrix} = \beta(u, y) D_{\theta_c}^{-1} K_0 + L_{\alpha\beta}(u, y) \quad (5.7)$$

with

$$D_{\theta_c} = \text{diag} \left[\frac{1}{\theta_c} \quad \frac{1}{\theta_c^2} \right]$$

and K_0 is chosen as

$$K_0 = \begin{bmatrix} 2 & 1 \end{bmatrix}^T.$$

That is,

$$\hat{K} = \begin{bmatrix} 2\theta_c\beta(u, y) \\ \theta_c^2\beta(u, y) \end{bmatrix}.$$

To appreciate the magnitude of gain required to attain such performances, a selection of profiles of the observer gains ψ_1 and ψ_2 are also given.

Simulation results

Observer 1 - Case 5.3 In this case, as we have seen previously, any positive value of θ_c will work. The fixed simulation parameter values used are shown in Table 5.1.

$x_1(0) = 1$	$\hat{x}_1(0) = 1$
$x_2(0) = 2$	$\hat{x}_2(0) = 4$

Table 5.1: Observer 1 - Case 5.3 and Case 5.4 parameter values

Figure 5-1 and Figure 5-2 show the observer performance with a choice of $\theta_c = 1$ and $\theta_c = 5$, respectively. From these, it is clear that a larger magnitude of θ_c results in a faster convergence performance. Figure 5-3 shows a failure in convergence for a choice of $\theta_c = -0.2$.

Observer 1 - Case 5.4 In this case, as shown previously, any negative value of θ_c will work. The fixed simulation parameter values used for Case 5.4 are shown in Table 5.1. Figure 5-4 and Figure 5-5 show the observer performance with a choice of $\theta_c = -1$ and $\theta_c = -5$, respectively. From these, it is clear that a larger magnitude of θ_c results in a faster convergence performance. Figure 5-6 demonstrates the positive limit of $\theta_c = 0.76$ at which convergence can still be achieved.

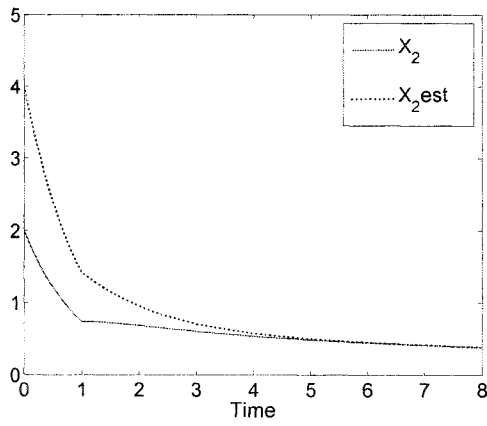


Figure 5-1: Estimation of x_2 where $\theta_c = 1$ for Case 5.3

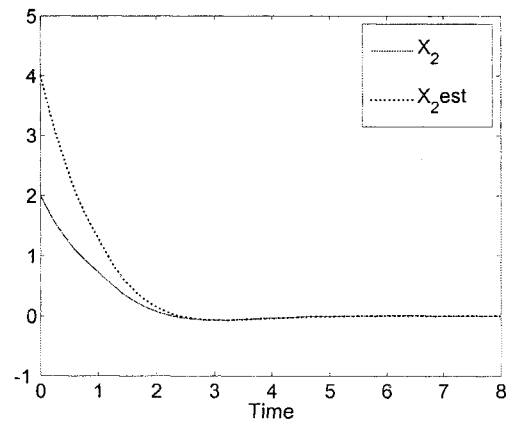


Figure 5-4: Estimation of x_2 where $\theta_c = -1$ for Case 5.4

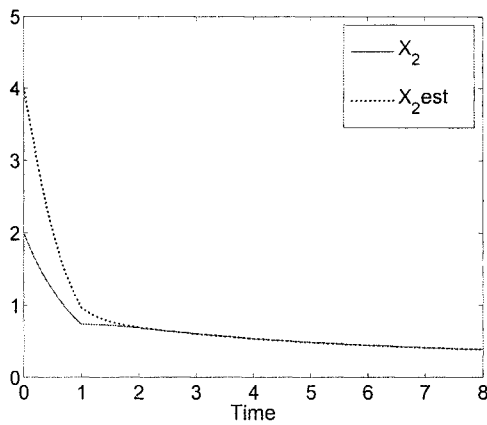


Figure 5-2: Estimation of x_2 where $\theta_c = 5$ for Case 5.3

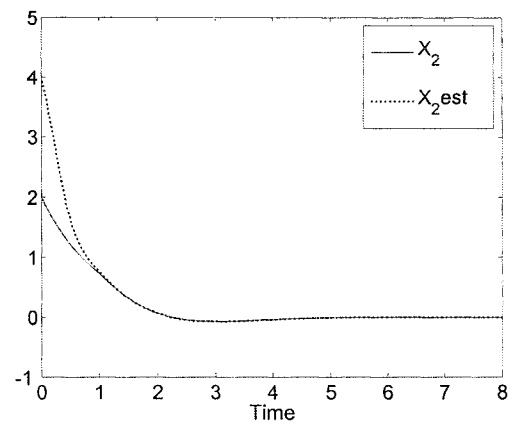


Figure 5-5: Estimation of x_2 where $\theta_c = -5$ for Case 5.4

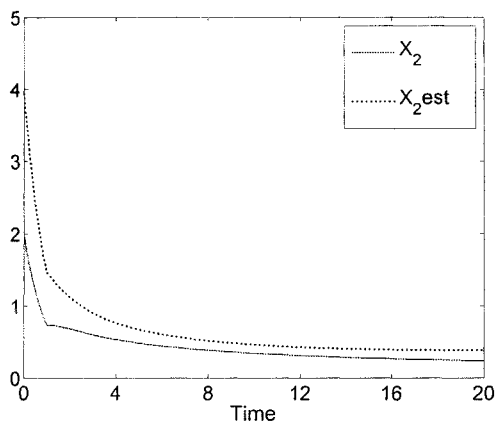


Figure 5-3: Failure in estimation of x_2 at the limit $\theta_c = -0.2$ for Case 5.3

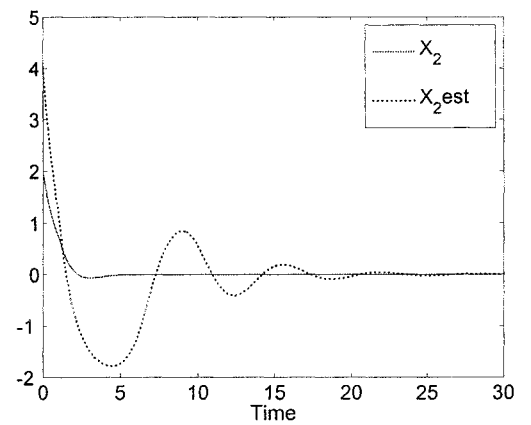


Figure 5-6: Degraded estimation of x_2 at the limit $\theta_c = 0.76$ for Case 5.4

Observer 1 - Case 5.5 In this case, for successful estimation, it is required that we choose $\theta_c > \frac{2\alpha_{\max}c_2}{\beta_0} = \bar{\theta}_0$. However, for the sake of this example, we will not determine the value of c_2 to find the range of θ_c . We will, however, show the values of θ_c at which the simulated estimation performances are no longer successful.

It should be noted here that when $\alpha(u, y) > 0$, the system (5.6) is unstable. Hence, in order to clearly illustrate the convergence performance of the observer, very low initial state values have been chosen. The fixed simulation parameter values used for Case 5.5 are shown in Table 5.2.

$x_1(0) = 0.01$	$\hat{x}_1(0) = 0.01$
$x_2(0) = 0.01$	$\hat{x}_2(0) = 1$

Table 5.2: Observer 1 - Case 5.5 parameter values

Figure 5-7 and Figure 5-8 show the observer performance with a choice of $\theta_c = 4$ and $\theta_c = 7$, respectively. From these, it is clear that a larger magnitude of θ_c results in a faster convergence performance. The range of θ_c is demonstrated in Figure 5-9 where a choice of $\theta_c = 2.5$ results in a failure of convergence.

Observer 1 - Case 5.6 Here, for successful estimation, it is required that we choose $\theta_c < \frac{-2\alpha_{\max}c_2}{\beta_1} = \bar{\theta}_1$. Again in this case, we will show examples of values of θ_c at which the simulation estimation performances are successful and when they are not. The fixed simulation parameter values used for Case 5.6 are shown in Table 5.3.

$x_1(0) = 0.01$	$\hat{x}_1(0) = 0.01$
$x_2(0) = 0.01$	$\hat{x}_2(0) = 2$

Table 5.3: Observer 1 - Case 5.6 parameter values

Figure 5-10 and Figure 5-11 show the observer performance with a choice of $\theta_c = -3$ and $\theta_c = -7$, respectively. Clearly, a larger magnitude of θ_c results in a faster convergence performance. Again, we demonstrate the range of θ_c , where in this case a choice of $\theta_c = -1.83$ results in a failure in convergence as shown in Figure 5-12.

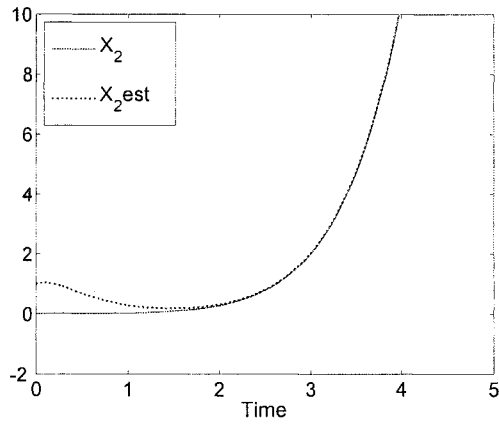


Figure 5-7: Estimation of x_2 where $\theta_c = 4$ for Case 5.5

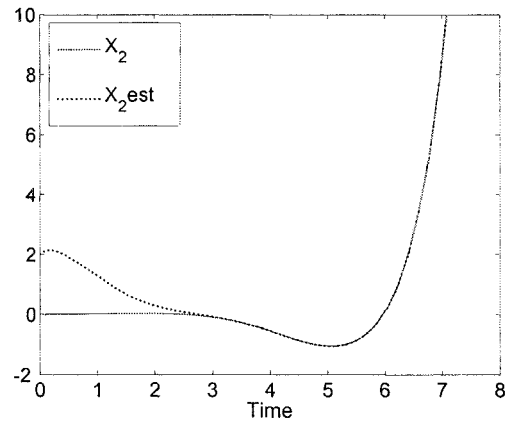


Figure 5-10: Estimation of x_2 where $\theta_c = -3$ for Case 5.6

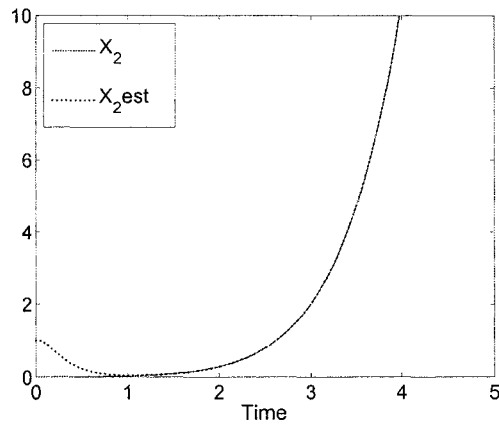


Figure 5-8: Estimation of x_2 where $\theta_c = 7$ for Case 5.5

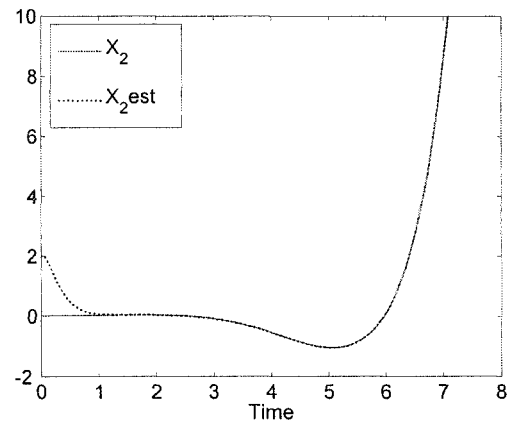


Figure 5-11: Estimation of x_2 where $\theta_c = -7$ for Case 5.6

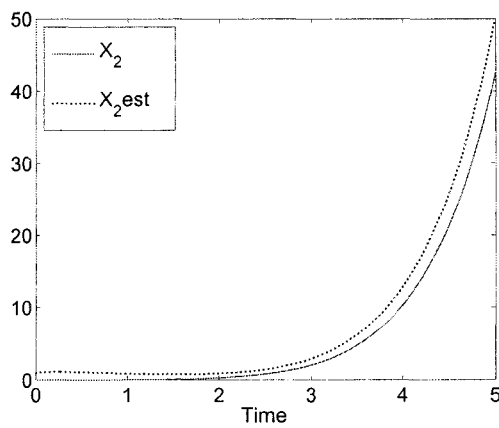


Figure 5-9: Failure in estimation of x_2 at the limit $\theta_c = 2.5$ for Case 5.5

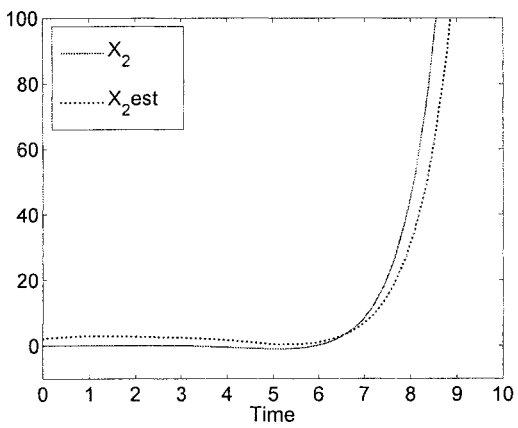


Figure 5-12: Failure in estimation of x_2 at the limit $\theta_c = -1.83$ for Case 5.6

5.2.2 Concluding remarks 1

An exponential observer design methodology has been given for a sub-class of state-affine systems. The design is facilitated by expressing the system under observation in the EJOOC form and uses a constant tuning parameter θ_c . Consequently, the construction of such an observer is simple and straightforward. It has been shown in theory and in simulation that the observer is capable of exponentially estimating the state variables of the sub-class of single-output state-affine systems considered. It is shown that the observer can be tuned using only a single tuning parameter θ_c , and that convergence is achieved more quickly when using a larger magnitude of which. However, as with any constant-gain observer, there must be a trade-off between the level of acceptable transient peaks, and an acceptable time period for convergence.

A major drawback of this observer is that its tuning parameter is constant and may not always be suitable where $\alpha(u, y) > 0$. In this case, it has been shown that θ_c must be either greater than $\bar{\theta}_0 = \frac{2\alpha_{\max}C_2}{\beta_0}$ or less than $\bar{\theta}_1 = \frac{-2\alpha_{\max}C_2}{\beta_1}$ depending on whether $\beta(u, y) > 0$ or $\beta(u, y) < 0$, respectively. Indeed, if $\alpha(u, y)$ takes on large values over a finite interval, the values of $\bar{\theta}_0$ and $\bar{\theta}_1$ might be too conservative, as illustrated in Figure 5-13. Note that for $t \geq t_1$, $\alpha(u(t), y(t))$ is fairly small. Consequently, for $t \geq t_1$, low magnitudes of $\bar{\theta}_0$ and $\bar{\theta}_1$ might just suffice. Hence, it is important to design an observer whose tuning parameter follows the variations of $\alpha(u, y)$. This is the main purpose of the next section.

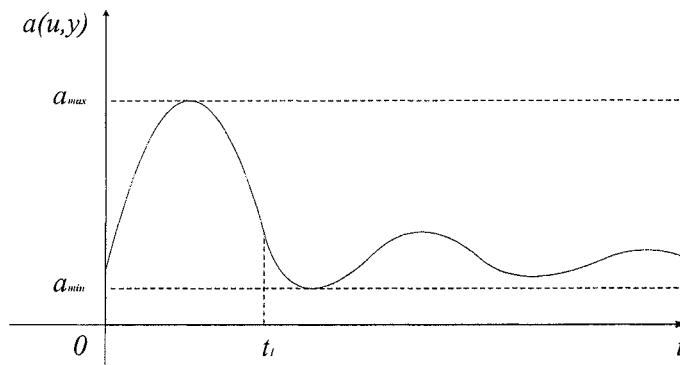


Figure 5-13: Profile of a varying $\alpha(u(t), y(t))$ illustrating large values over a finite time period and low values thereafter

5.3 Observer 2 - Adaptive observer design for a sub-class of systems in EJOc form

In the previous observer design, the tuning parameter θ_c is chosen constant and depends upon the upper and lower bounds of the system parameters $\alpha(u, y)$ and $\beta(u, y)$. Consequently, as mentioned above, certain cases may arise where $\alpha(u, y)$ varies significantly over time, and the constant-gain observer may not be suitable for that case. In addition, the presence of measurement noise may cause $\alpha(u, y)$ to vary significantly. One solution to this problem is to make the parameter θ_c vary with respect to $\alpha(u, y)$.

Indeed, consider again the above system (5.1) where $\Delta = \Omega = \text{diag} \begin{bmatrix} 1 & 2 & \dots & n \end{bmatrix}$.

The observer is now defined as

$$\dot{\hat{z}} = \Psi_{\alpha\beta}(u, y)\hat{z} + g(u, y) + \hat{K}(u, y)(y - C\hat{z}) \quad (5.8)$$

where

- $\hat{K}(u, y) = \beta(u, y) D_{\theta_a}^{-1} K_0 + L_{\alpha\beta}(u, y)$, where
- $D_{\theta_a} = \text{diag} \begin{bmatrix} \frac{1}{\theta_a} & \frac{1}{\theta_a^2} & \dots & \frac{1}{\theta_a^n} \end{bmatrix}$ with $\dot{\theta}_a(t) = \alpha(u(t), y(t))\theta_a(t)$, and
- K_0 is a constant vector chosen such that the matrix $\bar{A} - K_0 C$ is stable.

Note that we have changed the notation of the tuning parameter θ_c to θ_a to symbolise its adaptive nature.

We then state the following:

Theorem 5.2. *Assume that system (5.1) satisfies Assumptions A5.1)-A5.3). Then, the system (5.8) is an exponential observer for system (5.1).*

Proof of Theorem 5.2:

Following the same line of proof as in Theorem 5.1, we have

$$\begin{aligned}
\dot{e} &= (J_{\alpha\beta} - \beta D_{\theta_a}^{-1} K_0 C) e \\
&= (\alpha\Omega + \beta\bar{A} - \beta D_{\theta_a}^{-1} K_0 C) e \\
&= \alpha\Omega e + \beta (\bar{A} - D_{\theta_a}^{-1} K_0 C) e
\end{aligned}$$

where $e = z - \hat{z}$. The arguments of the various matrices have been dropped for the sake of convenience.

At this stage, it is important to remark that if $\alpha = 0$ and $K_0 = [C_n^1, C_n^2, \dots, C_n^n]^T$ where $C_n^p = \frac{n!}{(n-p)!p!}$, then the eigenvalues of the matrix $\Gamma = \beta (\bar{A} - D_{\theta_a}^{-1} K_0 C)$ are equal to $-\beta\theta_a$. Hence, the sign of the product $\beta\theta_a$ will be of crucial importance for the stability of the above error dynamics. Also note that by varying θ_a , the poles of the observer will be varied. The dynamics of θ_a will be chosen such that the influence of the first term, $\alpha\Omega e$, of the error dynamics is eliminated.

Indeed, let $\varepsilon = D_{\theta_a} e$. Then,

$$\begin{aligned}
\dot{\varepsilon} &= D_{\theta_a} \dot{e} + \dot{D}_{\theta_a} e \\
&= \alpha D_{\theta_a} \Omega e + \beta D_{\theta_a} (\bar{A} - D_{\theta_a}^{-1} K_0 C) e + \dot{D}_{\theta_a} e \\
&= \alpha D_{\theta_a} \Omega D_{\theta_a}^{-1} \varepsilon + \beta D_{\theta_a} (\bar{A} - D_{\theta_a}^{-1} K_0 C) D_{\theta_a}^{-1} \varepsilon + \dot{D}_{\theta_a} D_{\theta_a}^{-1} \varepsilon \\
&= \alpha D_{\theta_a} \Omega D_{\theta_a}^{-1} \varepsilon + \beta D_{\theta_a} \bar{A} D_{\theta_a}^{-1} \varepsilon - \beta D_{\theta_a} D_{\theta_a}^{-1} K_0 C D_{\theta_a}^{-1} \varepsilon + \dot{D}_{\theta_a} D_{\theta_a}^{-1} \varepsilon.
\end{aligned} \tag{5.9}$$

Since Ω and D_{θ_a} are diagonal matrices, it is easily shown that $D_{\theta_a} \Omega D_{\theta_a}^{-1} = \Omega$. It can also be shown that $D_{\theta_a} \bar{A} D_{\theta_a}^{-1} = \theta_a \bar{A}$, $C D_{\theta_a}^{-1} = \theta_a C$, and $\dot{D}_{\theta_a} D_{\theta_a}^{-1} = -\frac{\dot{\theta}_a}{\theta_a} \Omega$. Consequently, we can simplify (5.9) to

$$\begin{aligned}
\dot{\varepsilon} &= \alpha\Omega\varepsilon + \beta\theta_a (\bar{A} - K_0 C) \varepsilon - \frac{\dot{\theta}_a}{\theta_a} \Omega\varepsilon \\
&= \left(\alpha - \frac{\dot{\theta}_a}{\theta_a} \right) \Omega\varepsilon + \beta\theta_a (\bar{A} - K_0 C) \varepsilon.
\end{aligned} \tag{5.10}$$

Since $\dot{\theta}_a = \alpha\theta_a$, we have

$$\dot{\varepsilon} = \beta\theta_a (\bar{A} - K_0 C) \varepsilon. \tag{5.11}$$

Now, since the matrix $(\bar{A} - K_0C)$ is stable, there exists a symmetric positive definite matrix P such that

$$(\bar{A} - K_0C)^T P + P(\bar{A} - K_0C) = -I_n.$$

Defining the candidate Lyapunov function $V(\varepsilon) = \varepsilon^T P \varepsilon$, we obtain

$$\begin{aligned} \dot{V} &= 2\varepsilon^T P \dot{\varepsilon} \\ &= 2\varepsilon^T P [\beta\theta_a (\bar{A} - K_0C) \varepsilon] = -\beta\theta_a \varepsilon^T \varepsilon. \end{aligned}$$

It is clear that if the product $\beta\theta_a > 0$ for all $t \geq 0$, then $\dot{V} < 0$. It is therefore necessary to show when this is the case.

Note that

$$\frac{\dot{\theta}_a(t)}{\theta_a(t)} = \frac{d}{dt} \ln(\theta_a(t)) = \alpha(u(t), y(t)).$$

Therefore, by integrating the above equality, we obtain

$$\ln \theta_a(t) - \ln \theta_a(t_0) = \int_{t_0}^t \alpha(u(\tau), y(\tau)) d\tau$$

or equivalently

$$\ln \left(\frac{\theta_a(t)}{\theta_a(t_0)} \right) = \int_{t_0}^t \alpha(u(\tau), y(\tau)) d\tau.$$

Hence,

$$\theta_a(t) = \theta_a(t_0) \exp \left(\int_{t_0}^t \alpha(u(\tau), y(\tau)) d\tau \right). \quad (5.12)$$

Therefore, the sign of $\theta_a(t)$ is determined by the sign of $\theta_a(t_0)$ since the exponential term is always positive.

Hence, to ensure that $\beta(u(t), y(t))\theta_a(t)$ is positive for all $t \geq 0$, we choose $\theta_a(t_0)$ as follows:

- If $\beta(u(t), y(t)) > 0$ for all $t \geq 0$, then we choose $\theta_a(t_0) > 0$.
- If $\beta(u(t), y(t)) < 0$ for all $t \geq 0$, then we choose $\theta_a(t_0) < 0$.

Remark 5.1

Note that if $\theta_a(t_0) > 0$ and $\alpha(u(t), y(t)) > 0$ for all $t \geq 0$, then $\theta_a(t)$ will grow indefinitely. Also, if $\theta_a(t_0) < 0$ and $\alpha(u(t), y(t)) > 0$ for all $t \geq 0$, then $|\theta_a(t)|$ will grow indefinitely. In practice, $|\theta_a(t)|$ cannot be chosen excessively high since this will result in an amplification of noise. Similarly, if $\theta_a(t_0) > 0$ and $\alpha(u(t), y(t)) < 0$ for all $t \geq 0$, then $\theta_a(t)$ will tend to 0 as $t \rightarrow +\infty$, which may not always be desirable as far as tuning is concerned. This is also true if $\theta_a(t_0) < 0$ and $\alpha(u(t), y(t)) < 0$ for all $t \geq 0$. Consequently, it is important to place bounds on the maximum and minimum allowable values of $\theta_a(t)$. More precisely, the additional constraint on $\theta_a(t)$ is placed as follows:

- If $|\theta_a(t)| \geq |\theta_{\max}|$, then $\theta_a(t) = \theta_{\max}$.
- If $|\theta_a(t)| \leq |\theta_{\min}|$, then $\theta_a(t) = \theta_{\min}$.

The choice of the two threshold values θ_{\min} and θ_{\max} depends on the application that is being considered. The upper and lower bounds can be calculated as in the previous section related to the constant tuning parameter observer. For example, when $\beta > 0$, we would choose

$$\theta_{\max} > \frac{2\alpha_1\bar{c}_2}{\beta_0}.$$

Indeed, when $\theta = \theta_{\max}$, we would have, from equation (5.10),

$$\dot{\varepsilon} = \alpha\Omega\varepsilon + \beta\theta_{\max}(\bar{A} - K_0C)\varepsilon.$$

Choosing again the Lyapunov function $V = \varepsilon^T P\varepsilon$, we would have, after some computation,

$$\begin{aligned} \dot{V} &= 2\alpha\varepsilon^T P\Omega\varepsilon - \beta\theta_{\max}\varepsilon^T\varepsilon \\ &\leq 2|\alpha|\left|\varepsilon^T P\Omega\varepsilon\right| - \beta\theta_{\max}\varepsilon^T\varepsilon \\ &\leq 2|\alpha|\bar{c}_2\varepsilon^T\varepsilon - \beta\theta_{\max}\varepsilon^T\varepsilon \end{aligned}$$

for some $\bar{c}_2 > 0$.

That is,

$$\dot{V} \leq (2|\alpha|\bar{c}_2 - \beta\theta_{\max}) \varepsilon^T \varepsilon \leq (2\alpha_1\bar{c}_2 - \beta_0\theta_{\max}) \varepsilon^T \varepsilon.$$

Therefore, we choose θ_{\max} as

$$\theta_{\max} > \frac{2\alpha_1\bar{c}_2}{\beta_0}.$$

It can also be verified that θ_{\min} can be simply chosen as $\theta_{\min} > 0$.

Note that the arguments of the functions were dropped for simplicity.

This completes the proof of Theorem 5.2. □

5.3.1 Example 5.2

We now give a simulation example to illustrate the performance of the adaptive-gain observer. Consider the 2nd-order system expressed in the EJO form as

$$\begin{bmatrix} \dot{x}_1 \\ \dot{x}_2 \end{bmatrix} = \begin{bmatrix} \alpha(u, y) & \beta(u, y) \\ 0 & 2\alpha(u, y) \end{bmatrix} \begin{bmatrix} x_1 \\ x_2 \end{bmatrix} + \begin{bmatrix} \alpha(u, y) & 0 \\ 0 & 0 \end{bmatrix} \begin{bmatrix} x_1 \\ x_2 \end{bmatrix} + \begin{bmatrix} 0 \\ x_1 u \end{bmatrix} \quad (5.13)$$

$$y = x_1$$

where u is a step input, $\Delta = \Omega = \text{diag} \begin{bmatrix} 1 & 2 \end{bmatrix}$, $L_{\alpha\beta}(u, y) = \begin{bmatrix} \alpha(u, y) & 0 \end{bmatrix}^T$, $|\alpha| = \frac{1}{2}$, and $\beta(u, y) = \left| \frac{1}{x_1^2+1} \right|$. Note that in this system, $\alpha(u, y)$ is chosen such that its sign is constant throughout in order to clearly illustrate the performance in each of the following cases:

- Case 5.7: $\alpha(u, y) = -\frac{1}{2}$; $\beta(u, y) = \frac{1}{x_1^2+1}$.
- Case 5.8: $\alpha(u, y) = -\frac{1}{2}$; $\beta(u, y) = -\frac{1}{x_1^2+1}$.
- Case 5.9: $\alpha(u, y) = \frac{1}{2}$; $\beta(u, y) = \frac{1}{x_1^2+1}$.
- Case 5.10: $\alpha(u, y) = \frac{1}{2}$; $\beta(u, y) = -\frac{1}{x_1^2+1}$.

For each case considered, the observer gain is given by

$$\widehat{K} = \begin{bmatrix} \psi_1 & \psi_2 \end{bmatrix}^T = \beta(u, y) D_{\theta_a}^{-1} K_0 + L_{\alpha\beta}(u, y)$$

with K_0 chosen as

$$K_0 = \begin{bmatrix} 2 & 1 \end{bmatrix}^T$$

with $\dot{\theta}_a = \alpha(u, y) \theta_a$.

Simulation results

Observer 2 - Case 5.7 The results obtained are similar to those given by Observer 1 where the constant θ_c was used (see Figure 5-1) and are not repeated here. Instead, we show a comparison between the gains of Observers 1 and 2 that achieve the same convergence performance. The fixed simulation parameter values used for Case 5.7 are shown in Table 5.4.

$x_1(0) = 1$	$\widehat{x}_1(0) = 1$
$x_2(0) = 2$	$\widehat{x}_2(0) = 4$

Table 5.4: Observer 2 - Case 5.7 and Case 5.8 parameter values

Figures 5-14 and 5-15 show the profiles of ψ_1 and ψ_2 , respectively, of the adaptive Observer 2 where $\theta_a(0) = 4$ with lower bound $\theta_{\min} = 0.04$, and of Observer 1 with constant tuning parameter $\theta_c = 1$. Figure 5-16 shows the behaviour of the adaptive tuning parameter. From these results, it is clear that the use of the adaptive tuning parameter θ_a gives a gain profile converging to a much smaller magnitude than when using the constant tuning parameter θ_c .

Observer 2 - Case 5.8 The fixed simulation parameter values used here are shown in Table 5.4. The results obtained are similar to those given by Observer 1 where constant θ_c was used (see Figure 5-4) and are not repeated here. As in the previous case, we show a comparison between the gains of Observers 1 and 2 that achieve the same convergence performance.

Figures 5-17 and 5-18 show the profiles of ψ_1 and ψ_2 , respectively, when using Observer 2 with adaptive tuning parameter $\theta_a(0) = -1.5$ with lower bound $\theta_{\min} = -0.015$, and when using Observer 1 with the constant tuning parameter $\theta_c = -1$. Figure 5-19 shows the behaviour of the adaptive tuning parameter. Once again, it is clear that the use of the adaptive tuning parameter θ_a gives a gain profile converging to a much smaller magnitude than when using the constant tuning parameter θ_c .

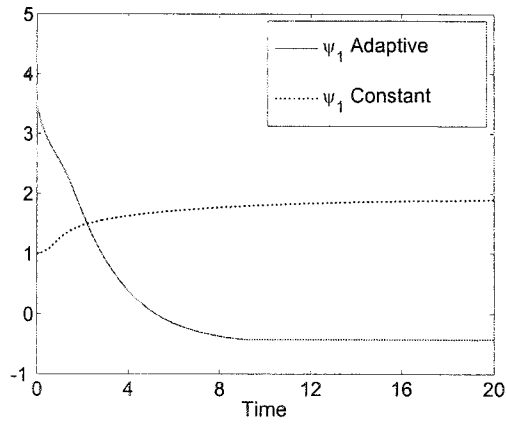


Figure 5-14: Comparison of ψ_1 for constant θ_c and adaptive θ_α for Case 5.7

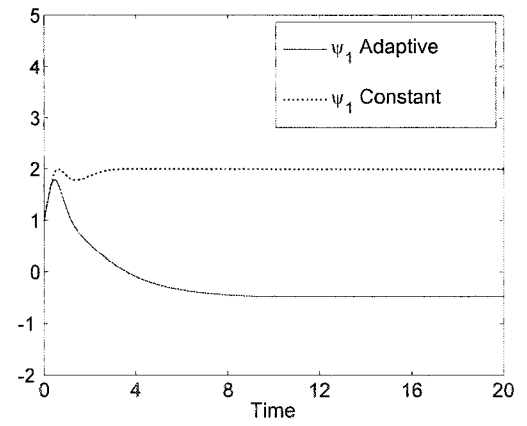


Figure 5-17: Comparison of ψ_1 for constant θ_c and adaptive θ_α for Case 5.8

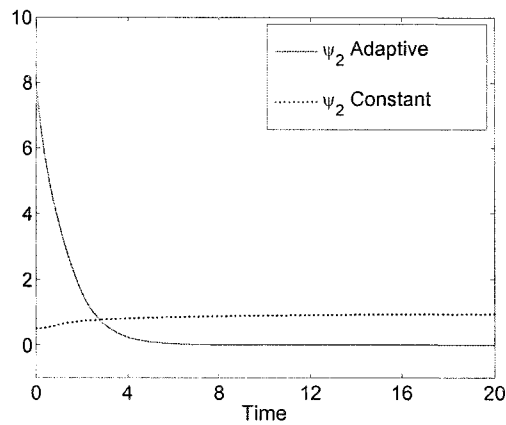


Figure 5-15: Comparison of ψ_2 for constant θ_c and adaptive θ_α for Case 5.7

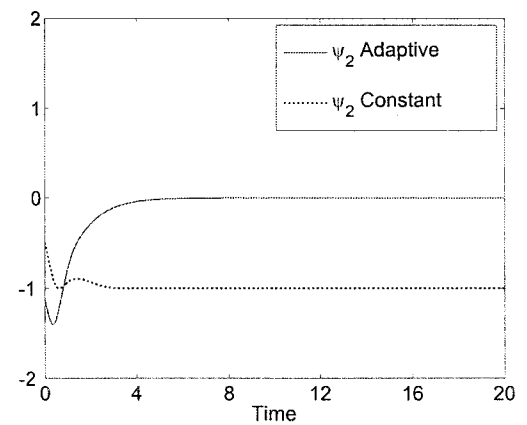


Figure 5-18: Comparison of ψ_2 for constant θ_c and adaptive θ_α for Case 5.8

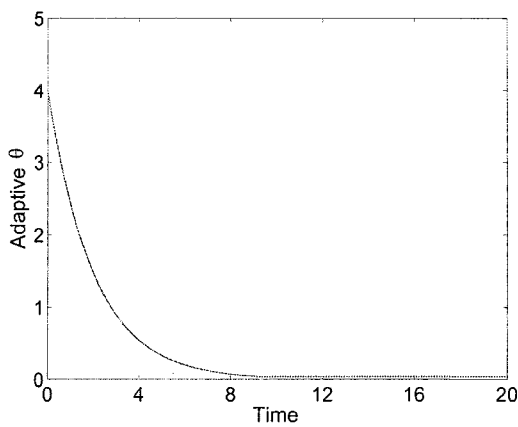


Figure 5-16: Profile of adaptive tuning parameter for Case 5.7

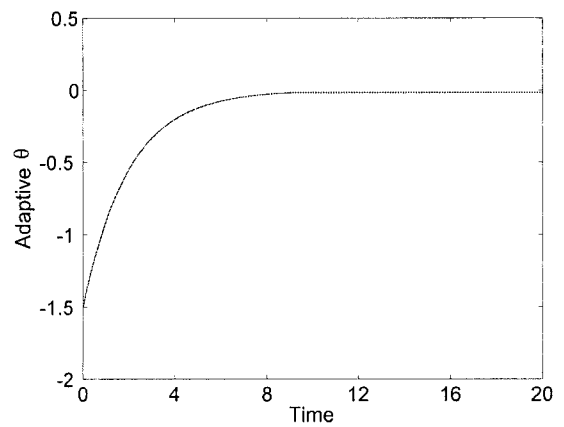


Figure 5-19: Profile of adaptive tuning parameter for Case 5.8

Observer 2 - Case 5.9 When $\alpha(u, y) > 0$, the system (5.13) is unstable. Hence, to clearly illustrate the convergence performance of the observer, very low initial state values have been chosen. The fixed simulation parameter values used for Case 5.9 are shown in Table 5.5.

$x_1(0) = 0.01$	$\hat{x}_1(0) = 0.01$
$x_2(0) = 0.01$	$\hat{x}_2(0) = 1$

Table 5.5: Observer 2 - Case 5.9 parameter values

Here, the varying tuning parameter θ_a increases in magnitude. To compare with Observer 1, there are two main options for setting the initial value $\theta_a(0)$. The first is to set $\theta_a(0) = \theta_{\max} = \theta_c$, which will give a virtually identical performance as Observer 1. The second option is to set $|\theta_a(0)| < \theta_{\max} = \theta_c$, which will result in a slightly slower convergence performance, but with a much less harsh initial value of gain. Here, the second option is chosen. Figure 5-20 shows the convergence performance of the adaptive tuning parameter observer with a choice of $\theta_a(0) = 3$ with upper bound $\theta_{\max} = 4$. Figures 5-21 and 5-22 show the profiles of ψ_1 and ψ_2 , respectively, when considering Observer 2 with the adaptive tuning parameter θ_a and when considering Observer 1 with the constant tuning parameter $\theta_c = 4$. Figure 5-23 shows the profile of the adaptive tuning parameter.

As expected, the estimation convergence time of Observer 2 is slower than when using a constant $\theta_c > \theta_a(0)$, as given previously. However, the adaptive technique allows for a much gentler initial effort in the observer gain, which can be useful where a high initial effort is undesirable.

Observer 2 - Case 5.10 The fixed simulation parameter values used for Case 5.10 are shown in Table 5.6.

$x_1(0) = 0.01$	$\hat{x}_1(0) = 0.01$
$x_2(0) = 0.01$	$\hat{x}_2(0) = 2$

Table 5.6: Observer 2 - Case 5.10 parameter values

As in the previous case, we set $|\theta_a(0)| < \theta_{\max} = \theta_c$. Figure 5-24 shows the convergence performance of the adaptive tuning parameter observer with a choice of $\theta_a(0) = -2$ with upper bound $\theta_{\max} = -3$. Figures 5-25 and 5-26 show the profiles of ψ_1 and ψ_2 , respectively, when using Observer 2 with the adaptive tuning parameter θ_a and when using Observer 1 with the constant tuning parameter $\theta_c = -3$. Figure 5-27 shows the profile of the adaptive tuning parameter.

As expected, the estimation convergence time of Observer 2 is slower than when using a constant $|\theta_c| > |\theta_a(0)|$. However, again we note that the adaptive technique allows for a much gentler initial effort in the observer gain, which can be useful where a high magnitude initial effort is undesirable.

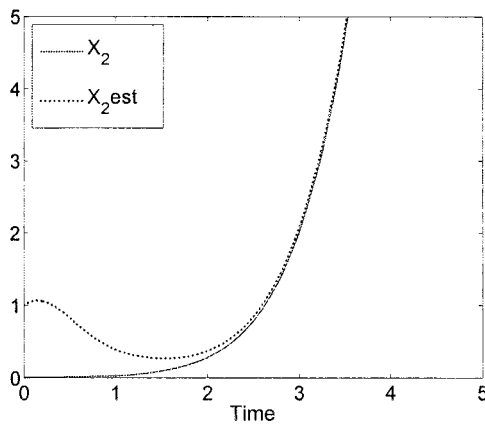


Figure 5-20: Adaptive estimation of x_2 for Case 5.9

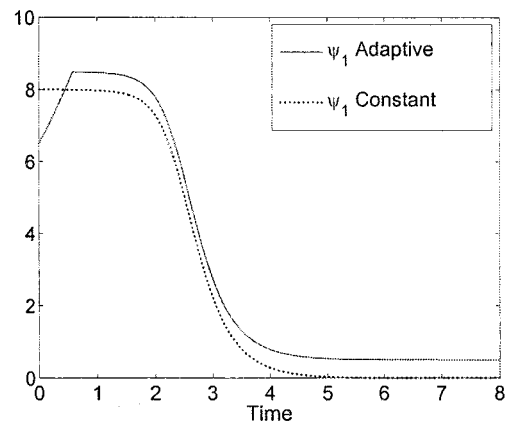


Figure 5-21: Comparison of ψ_1 for constant θ_c and adaptive θ_a for Case 5.9

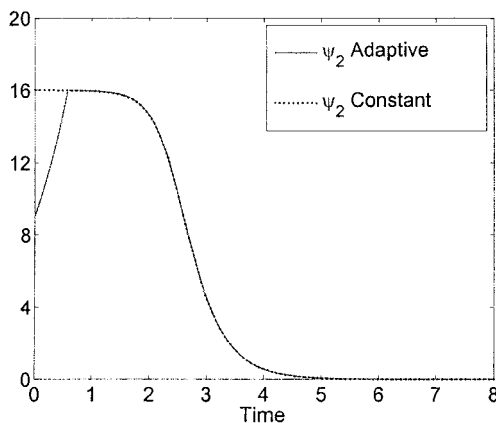


Figure 5-22: Comparison of ψ_2 for constant θ_c and adaptive θ_a for Case 5.9

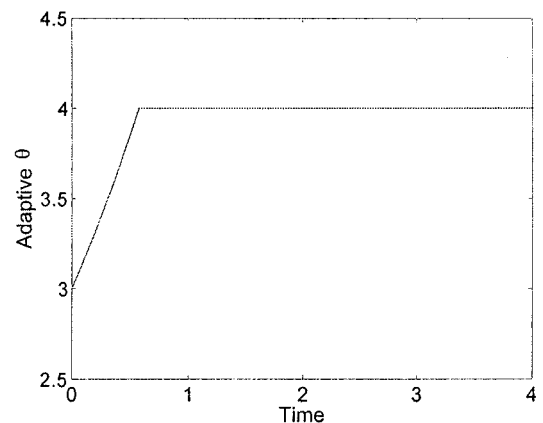


Figure 5-23: Profile of adaptive tuning parameter for Case 5.9

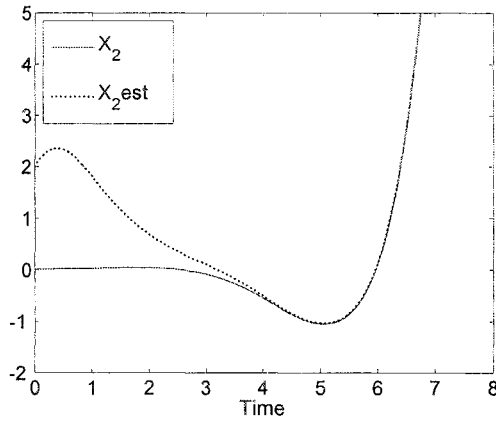


Figure 5-24: Adaptive estimation of x_2 for Case 5.10

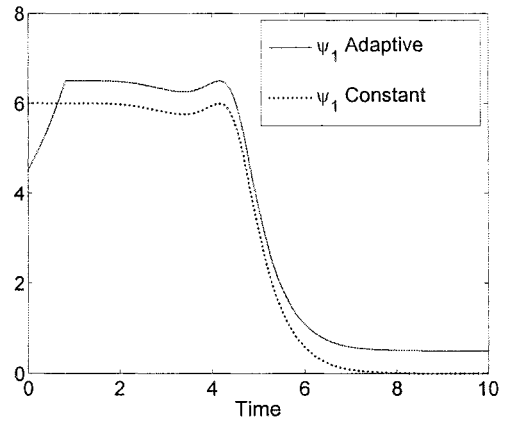


Figure 5-25: Comparison of ψ_1 for constant θ_c and adaptive θ_a for Case 5.10

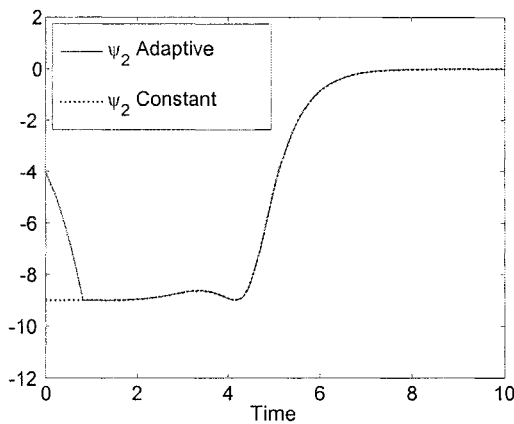


Figure 5-26: Comparison of ψ_2 for constant θ_c and adaptive θ_a for Case 5.10

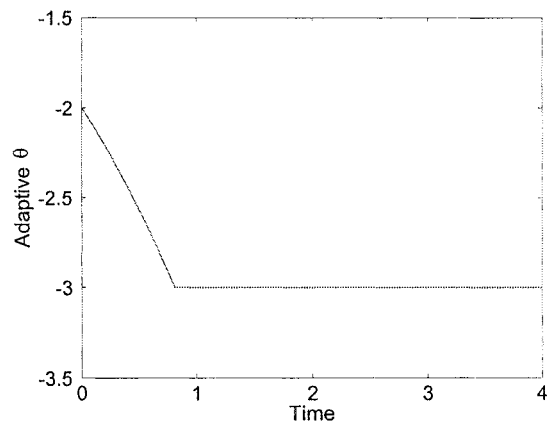


Figure 5-27: Profile of adaptive tuning parameter for Case 5.10

5.3.2 Concluding remarks 2

An exponential observer design methodology has been given for a sub-class of state-affine systems. As with the constant tuning parameter Observer 1, the design is facilitated by expressing the system under observation in the EJOC form. However, the main difference is that the current observer uses an adaptive tuning parameter θ_a in its gain. Indeed, the adaptive tuning parameter behaves in accordance with the magnitude and sign of $\alpha(u, y)$ and is lower and upper bounded by the limits θ_{\min} and θ_{\max} , respectively. The reason for the use of these bounds is twofold. Firstly, θ_{\min} is set in place for $\alpha(u, y) < 0$ where the tuning parameter θ_a tends to the specified θ_{\min} as $t \rightarrow \infty$. The use of θ_{\min} provides an additional

degree of freedom in tuning the observer with regards to speeds of convergence. Secondly, θ_{\max} is used to cater for $\alpha(u, y) > 0$ where the tuning parameter θ_a tends to the specified θ_{\max} as $t \rightarrow \infty$. The use of θ_{\max} ensures that an increasing magnitude can be limited as desired. In the former case, where θ_a decreases in magnitude, an initial value $\theta_a(0)$ of high enough magnitude can be selected such that convergence is quickly achieved. Thereafter, θ_a can be fixed at a constant low magnitude. This can be particularly useful when considering measurement noise since a lower amplification or even attenuation of noise can occur. In the latter case, where θ_a increases in magnitude, the tuning parameter can be allowed to ramp up to a desired value rather than be initialised at that value. Hence, estimation performances can be improved in systems where constantly high magnitudes would otherwise result in larger transients in the estimation profile. The increasing gain of the adaptive observer would provide an estimation containing lower magnitudes of transients, although with a longer convergence time. Therefore, a trade-off between acceptable transients and convergence times must be made for a given system.

Finally, the example given here considers a constant $\alpha(u, y)$. However, it must be emphasised that this adaptive-gain observer is particularly useful when considering a system where the magnitude and sign of $\alpha(u, y)$ does change. Indeed, for the case of $\alpha(u, y)$ with varying magnitude and polarity, the adaptive tuning parameter varies with the changes in $\alpha(u, y)$ and operates between both the upper and lower bounds. If either bound is reached, then the tuning parameter remains constant at that value until the sign of $\alpha(u, y)$ changes. In effect, unlike when using Observer 1, an efficient gain is given that is capable of guaranteeing exponentially stable error dynamics, without remaining unnecessarily high. Consequently, the adaptive Observer 2 will be particularly useful when considering measurement noise.

5.4 Observer 3 - Observer design for a sub-class of single-output state-affine systems partially transformable into EJOC form

The previous system (5.1) is already in the EJOC form. As stated earlier, it is not easy to characterise nonlinear systems that can be transformed into this form. However, it was shown in Chapter 3 that some classes of systems can be transformed into a partial EJOC form. As a matter of fact, some classes of state-affine systems can be transformed into the partial form. In this section, we shall consider this particular class of state-affine systems and indeed their transformation into the EJOC form. In effect, consider the single-output state-affine systems described by (2.3).

We assume the following:

A5.4) There exists a set of admissible inputs \mathcal{U} such that for all $u \in \mathcal{U}$, the matrix

$$\Upsilon(u, y) = \begin{bmatrix} H(u, y) \\ H(u, y) F(u, y) \\ \vdots \\ H(u, y) F^{n-1}(u, y) \end{bmatrix} \quad (5.14)$$

is of full rank for all $y \in \mathbb{R}$.

A5.5) The function $g(u, y)$ and the entries of the matrix $F(u, y)$ are smooth and bounded.

Comment 5.1

Since the matrix $\Upsilon(u, y)$ is non-singular for every $u \in \mathcal{U}$ and $y \in \mathbb{R}$, according to the result presented in Chapter 3, there exists a similarity matrix $M_{\alpha\beta}(u, y)$, for some given functions $\alpha(u, y)$ and $\beta(u, y)$, such that

$$M_{\alpha\beta}(u, y)F(u, y)M_{\alpha\beta}^{-1}(u, y) = \Psi_{\alpha\beta}(u, y) = J_{\alpha\beta}(u, y) + L_{\alpha\beta}(u, y)C$$

$$H(u, y)M_{\alpha\beta}^{-1}(u, y) = C$$

where $J_{\alpha\beta}(u, y) = \alpha(u, y)I_n + \beta(u, y)\bar{A}$.

We must note that since the functions $\alpha(u, y)$ and $\beta(u, y)$ are arbitrary, we are free to choose them as we wish, as long as $\beta(u, y) \neq 0$ for all u and y . As mentioned in Chapter 4, we generally choose these functions such that the norm of the term $\dot{M}_{\alpha\beta}(u, y)M_{\alpha\beta}^{-1}(u, y)$ is as small as possible. Also, we have shown that the case where $\alpha(u, y) > 0$ for all u and y does induce some difficulties in designing the gain of the observer. Consequently, it is always desirable to choose $\alpha(u, y) \leq 0$ for all u and y . Hence, we shall present here the observer design procedure for the particular choice where $\beta(u, y) > 0$ and $\alpha(u, y) \leq 0$. Obviously, the design procedure can be applied for other choices of $\alpha(u, y)$ and $\beta(u, y) \neq 0$.

In effect, consider the system given by

$$\dot{\hat{x}} = F(u, y)\hat{x} + g(u, y) + K_{\alpha\beta}(u, y)(y - H(u, y)\hat{x}) \quad (5.15)$$

where

- $K_{\alpha\beta}(u, y) = M_{\alpha\beta}^{-1}(u, y)(\beta(u, y)D_{\theta_c}^{-1}K_0 + L_{\alpha\beta}(u, y))$, where
- $D_{\theta_c} = \text{diag} \left[\frac{1}{\theta_c} \quad \frac{1}{\theta_c^2} \quad \dots \quad \frac{1}{\theta_c^n} \right]$ with $\theta_c > 0$,
- $M_{\alpha\beta}(u, y)$ is given as in (3.26) with $\beta(u, y) > 0$ and $\alpha(u, y) \leq 0$, $L_{\alpha\beta}(u, y)$ is as in (3.23) and C is of the form given in (5.1), and
- K_0 is a constant vector chosen such that the matrix $(\bar{A} - K_0C)$ is Hurwitz where \bar{A} is the constant matrix (5.4).

Note that θ_c represents a constant tuning parameter.

We now make an additional assumption:

A5.6) We assume that there exists an integer $p > 0$ and a real $c_0 > 0$ such that

$$\left\| D_{\theta_c} \dot{M}_{\alpha\beta}(u, y) M_{\alpha\beta}^{-1}(u, y) D_{\theta_c}^{-1} \right\| \leq \frac{c_0}{\theta_c^p}.$$

The main result of this section can be summarised in the following theorem:

Theorem 5.3. *Assume that system (2.3) satisfies Assumptions A5.3)-A5.6). Then, there exists $\theta_0 > 0$ such that for all $\theta_c > \theta_0$, the system (5.15) is an exponential observer for system (2.3).*

Proof of Theorem 5.3:

Defining the estimation error as $e = x - \hat{x}$, we have

$$\dot{e} = Fe - M_{\alpha\beta}^{-1}[\beta D_{\theta_c}^{-1} K_0 + L_{\alpha\beta}]He.$$

Consider a transformation on the error as $\bar{e} = M_{\alpha\beta}(u, y)e$. Then,

$$\begin{aligned} \dot{\bar{e}} &= M_{\alpha\beta} \dot{e} + \dot{M}_{\alpha\beta} e \\ &= M_{\alpha\beta} F M_{\alpha\beta}^{-1} \bar{e} - (\beta D_{\theta_c}^{-1} K_0 + L_{\alpha\beta}) H M_{\alpha\beta}^{-1} \bar{e} + \dot{M}_{\alpha\beta} M_{\alpha\beta}^{-1} \bar{e} \\ &= (J_{\alpha\beta} + L_{\alpha\beta} C) \bar{e} - (\beta D_{\theta_c}^{-1} K_0 + L_{\alpha\beta}) C \bar{e} + \dot{M}_{\alpha\beta} M_{\alpha\beta}^{-1} \bar{e} \\ &= J_{\alpha\beta} \bar{e} - \beta D_{\theta_c}^{-1} K_0 C \bar{e} + \dot{M}_{\alpha\beta} M_{\alpha\beta}^{-1} \bar{e} \\ &= \alpha \bar{e} + \beta (\bar{A} - D_{\theta_c}^{-1} K_0 C) \bar{e} + \dot{M}_{\alpha\beta} M_{\alpha\beta}^{-1} \bar{e}. \end{aligned}$$

Now, let $\varepsilon = D_{\theta_c} \bar{e}$. Then, using the observations made previously, we have

$$\dot{\varepsilon} = \alpha I_n \varepsilon + \beta \theta_c (\bar{A} - K_0 C) \varepsilon + D_{\theta_c} \dot{M}_{\alpha\beta} M_{\alpha\beta}^{-1} D_{\theta_c}^{-1} \varepsilon.$$

Now, since the matrix $(\bar{A} - K_0 C)$ is stable, there exists a symmetric positive definite matrix P such that

$$(\bar{A} - K_0 C)^T P + P(\bar{A} - K_0 C) = -I_n.$$

Consider the following candidate Lyapunov function $V(\varepsilon) = \varepsilon^T P \varepsilon$. Then,

$$\dot{V} = 2\varepsilon^T P \dot{\varepsilon}$$

$$\begin{aligned}
&= 2\alpha\varepsilon^T P\varepsilon + 2\beta\theta_c\varepsilon^T P(\bar{A} - K_0C)\varepsilon + 2\varepsilon^T PD_{\theta_c}\dot{M}_{\alpha\beta}M_{\alpha\beta}^{-1}D_{\theta_c}^{-1}\varepsilon \\
&= 2\alpha\varepsilon^T P\varepsilon - \beta\theta_c\varepsilon^T\varepsilon + 2\varepsilon^T PD_{\theta_c}\dot{M}_{\alpha\beta}M_{\alpha\beta}^{-1}D_{\theta_c}^{-1}\varepsilon.
\end{aligned}$$

Using the inequality

$$\left\| \varepsilon^T PD_{\theta_c}\dot{M}_{\alpha\beta}M_{\alpha\beta}^{-1}D_{\theta_c}^{-1}\varepsilon \right\| \leq \|\varepsilon\|^2 \|P\| \left\| D_{\theta_c}\dot{M}_{\alpha\beta}M_{\alpha\beta}^{-1}D_{\theta_c}^{-1} \right\|$$

we have

$$\dot{V} \leq 2\alpha\varepsilon^T P\varepsilon - \beta\theta_c\varepsilon^T\varepsilon + 2\|\varepsilon\|^2 \|P\| \left\| D_{\theta_c}\dot{M}_{\alpha\beta}M_{\alpha\beta}^{-1}D_{\theta_c}^{-1} \right\|.$$

Using Assumption A5.6), we have

$$\begin{aligned}
\dot{V} &\leq 2\alpha\varepsilon^T P\varepsilon - \beta\theta_c\|\varepsilon\|^2 + 2c_0\|P\|\|\varepsilon\|^2 \frac{1}{\theta_c^p} \\
&\leq 2\alpha\varepsilon^T P\varepsilon - \left(\beta\theta_c - 2c_0\|P\| \frac{1}{\theta_c^p} \right) \|\varepsilon\|^2.
\end{aligned}$$

Now, since $\alpha(u, y) \leq 0$, we require

$$\begin{aligned}
\beta\theta_c - 2c_0\|P\| \frac{1}{\theta_c^p} &> 0 \\
\theta_c &> \frac{2c_0\|P\| \frac{1}{\theta_c^p}}{\beta} \\
\theta_c^{p+1} &> \frac{2c_0\|P\|}{\beta} \\
\theta_c &> \sqrt[p+1]{\frac{2c_0\|P\|}{\beta}}.
\end{aligned}$$

Therefore, it is clear that choosing $\theta_c > \sqrt[p+1]{\frac{2c_0\|P\|}{\beta}} = \theta_0$, where the product $\theta_c\beta > 0$, yields $\dot{V} < 0$. Note that the arguments of the various matrices have been dropped for convenience.

This completes the proof of Theorem 5.3. □

Remark 5.2

1) The main advantage of the above observer is that the gain

$$K_{\alpha\beta}(u, y) = M_{\alpha\beta}^{-1}(u, y) (\beta(u, y)D_{\theta_c}^{-1}K_0 + L_{\alpha\beta}(u, y))$$

is designed in a systematic way. Unlike the extended Kalman filter or observer, it does not require any additional dynamical equations such as matrix Riccati equations to

update its gain. Therefore, there is less computational effort to update its gain.

- 2) In the special case where $M_{\alpha\beta}(u, y)$ and $L_{\alpha\beta}(u, y)$ are constant, the observer amounts to the classical Luenberger observer.
- 3) The dependence of the gain on u and y provides a certain degree of adaptiveness to the gain of the observer.
- 4) The Assumption A5.6) is quite restrictive since it is not easy to characterise systems for which $\left\| D_{\theta_c} \dot{M}_{\alpha\beta}(u, y) M_{\alpha\beta}^{-1}(u, y) D_{\theta_c}^{-1} \right\| \leq \frac{c_0}{\theta_c^p}$. However, it can be shown that if $M_{\alpha\beta}(u, y)$ is lower triangular, then such an assumption is obeyed.
- 5) One can also attempt to design an observer with an adaptive tuning parameter θ_a , as in Section 5.3 for the class of state-affine systems (2.3). However, this would not be an easy task since the tuning parameter θ_a has to take into account the residual term $\dot{M}_{\alpha\beta}(u, y) M_{\alpha\beta}^{-1}(u, y) \bar{e}$ induced by the transformation matrix $M_{\alpha\beta}(u, y)$.

5.4.1 Example 5.3

We now give a simulation example to illustrate the performance of the observer. Consider the 2nd-order system

$$\begin{cases} \dot{x}_1 = -x_1 + \frac{1}{x_1^2+1}x_2 \\ \dot{x}_2 = -x_2 + ux_1 \\ y = x_1 \end{cases} \quad (5.16)$$

where u is a step input. Notice that the system (5.16) is of the form (2.3) where

$$F(u, y) = \begin{bmatrix} -1 & \frac{1}{x_1^2+1} \\ 0 & -1 \end{bmatrix}, g(u, y) = \begin{bmatrix} 0 \\ ux_1 \end{bmatrix}$$

and

$$H(u, y) = \begin{bmatrix} 1 & 0 \end{bmatrix} = C.$$

It is clear that the above system is already in the EIOC form with $\alpha(u, y) = -1$ and $\beta(u, y) = \frac{1}{x_1^2+1}$. These are functions that are dictated by the system. However, to show the flexibility of the observer design, we shall choose $\alpha(u, y) = -1$ and $\beta(u, y) = 1$ and find the corresponding transformation matrix $M_{\alpha\beta}(u, y)$.

By applying the algorithm given in Chapter 3, one can show that

$$M_{\alpha\beta}(u, y) = \begin{bmatrix} 1 & 0 \\ 0 & \frac{1}{x_1^2+1} \end{bmatrix}.$$

It can readily be verified that

$$M_{\alpha\beta}(u, y)F(u, y)M_{\alpha\beta}^{-1}(u, y) = \begin{bmatrix} -1 & 1 \\ 0 & -1 \end{bmatrix}$$

$$\text{and } H(u, y)M_{\alpha\beta}^{-1}(u, y) = \begin{bmatrix} 1 & 0 \end{bmatrix} = C.$$

Consequently, the observer for system (5.16) is given by

$$\begin{cases} \dot{\hat{x}}_1 = -\hat{x}_1 + \frac{1}{x_1^2+1}\hat{x}_2 + \psi_1(y - \hat{x}_1) \\ \dot{\hat{x}}_2 = -\hat{x}_2 + ux_1 + \psi_2(y - \hat{x}_1) \end{cases}$$

where

$$K_{\alpha\beta}(u, y) = \begin{bmatrix} \psi_1 \\ \psi_2 \end{bmatrix} = M_{\alpha\beta}^{-1}(u, y) (\beta(u, y)D_{\theta_c}^{-1}K_0 + L_{\alpha\beta}(u, y))$$

with

$$K_0 = \begin{bmatrix} k_1 & k_2 \end{bmatrix}^T = \begin{bmatrix} 2 & 1 \end{bmatrix}^T.$$

More precisely, we have

$$\psi_1 = 2\theta_c$$

$$\psi_2 = \theta_c^2 (1 + x_1^2).$$

Simulation results

Here, we show the observer performance where $\alpha(u, y)$ and $\beta(u, y)$ are fixed and where θ_c is the constant tuning parameter. The parameter values used in this example are given in Table 5.7.

$x_1(0) = 1$	$\hat{x}_1(0) = 1$
$x_2(0) = 2$	$\hat{x}_2(0) = 4$

Table 5.7: Parameter values used for the comparison of Observers 1, 2 and 3

Figure 5-28 and Figure 5-29 demonstrate the effect of the tuning parameter θ_c , showing the observer performance where $\theta_c = 0.9$ and $\theta_c = 3$, respectively. Clearly, a larger magnitude of θ_c results in a faster convergence.

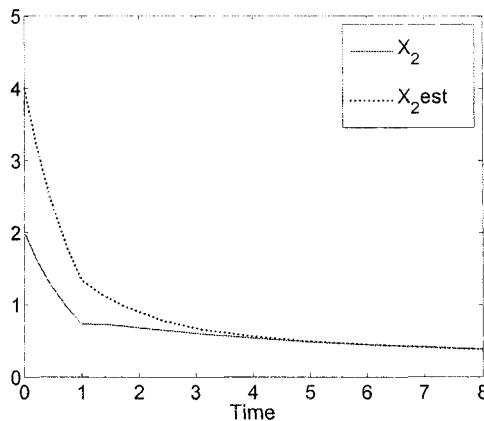


Figure 5-28: Estimation of x_2 where $\theta_c = 0.9$

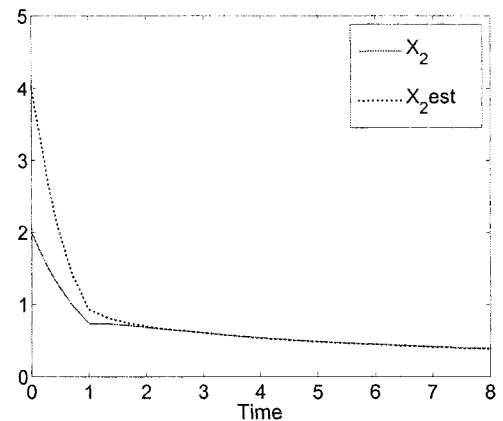


Figure 5-29: Estimation of x_2 where $\theta_c = 3$

We now give a comparison between the gain of Observers 1, 2 and 3 where $\alpha(u, y) < 0$ and $\beta(u, y) > 0$. More precisely, for Observer 1 we consider Case 5.3; for Observer 2 we consider Case 5.7; and for Observer 3 we choose $\alpha(u, y) = -1$ and $\beta(u, y) = 1$. The performances given by each observer are as shown in Figure 5-28.

Figures 5-30 and 5-31 show the profiles of ψ_1 and ψ_2 , respectively, with:

- Constant tuning parameter $\theta_c = 0.9$ (using the transformation method).
- Adaptive tuning parameter θ_a where $\theta_a(0) = 4$ with lower bound $\theta_{\min} = 0.04$, for the non-transformed case.
- Constant tuning parameter $\theta_c = 1$ for the non-transformed case.

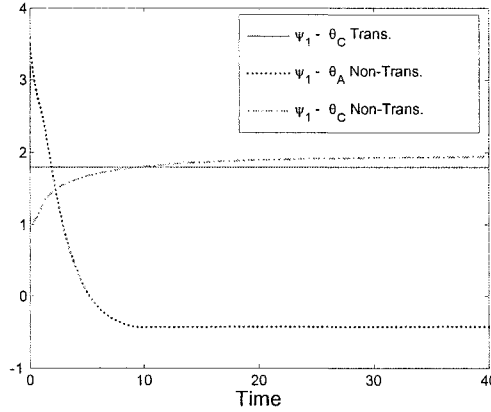


Figure 5-30: ψ_1 for constant θ_c using the transformation method and constant θ_c and adaptive θ_a for systems already in EJOC form

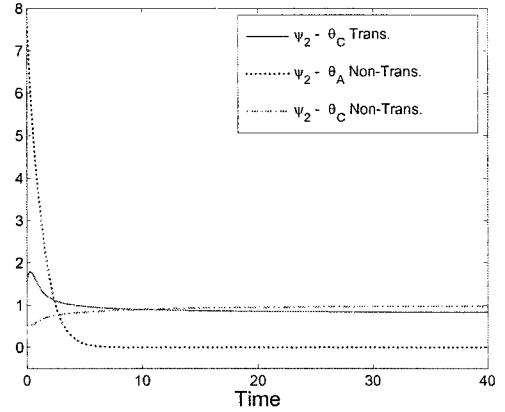


Figure 5-31: ψ_2 for constant θ_c using the transformation method and constant θ_c and adaptive θ_a for systems already in EJOC form

5.4.2 Concluding remarks 3

An exponential observer design methodology has been given for a sub-class of state-affine systems that can be transformed into the EJOC form.

As in the case of Observer 1, Observer 3 also uses a single constant tuning parameter θ_c , and convergence is achieved more quickly when using larger magnitudes of which. The example given here considers a constant $\alpha(u, y)$ (before transformation). However, in some cases, as shown in Chapter 8, the current observer can prove to be particularly useful when considering a system where the magnitude and sign of $\alpha(u, y)$ does change. Indeed, the tuning of the observer can be achieved by setting $\alpha(u, y)$ and $\beta(u, y)$ constant and selecting the tuning parameter θ_c appropriately. Hence, the parameters $\alpha(u, y)$ and $\beta(u, y)$ can be chosen rather than be dictated by the system. Consequently, we have additional degrees of freedom in tuning the observer, such that excessively high values of θ_c are not always required.

5.5 Observer 4 - Adaptive observer design for a sub-class of systems in EJOC form in the case of partially known parameters

We now consider the case where only a partial knowledge of the system parameters is available. Consider the system

$$\begin{cases} \dot{z} = (\Psi_{\alpha\beta}(u, y) + \Delta\Psi_{\alpha\beta}(u, y))z + g(u, y) \\ y = Cz \end{cases} \quad (5.17)$$

where $\Psi_{\alpha\beta}(u, y)$ and $g(u, y)$ are given as in (5.1) with $\Delta = \Omega = \text{diag} \begin{bmatrix} 1 & 2 & \dots & n \end{bmatrix}$ and where $\Delta\Psi_{\alpha\beta}(u, y)$ contains the unknown portion of the system parameters. Then, consider the observer

$$\dot{\hat{z}} = (\Psi_{\alpha\beta}(u, y) + \Delta\bar{\Psi}_{\alpha\beta}(u, y))\hat{z} + g(u, y) + \hat{K}(u, y)(y - C\hat{z}) \quad (5.18)$$

where $\Delta\bar{\Psi}_{\alpha\beta}(u, y)$ is an approximation of the unknown $\Delta\Psi_{\alpha\beta}(u, y)$ and

- $\hat{K}(u, y) = \beta(u, y)D_{\theta_a}^{-1}K_0 + L_{\alpha\beta}(u, y)$, where
- $D_{\theta_a} = \text{diag} \begin{bmatrix} \frac{1}{\theta_a} & \frac{1}{\theta_a^2} & \dots & \frac{1}{\theta_a^n} \end{bmatrix}$ with $\dot{\theta}(t) = \alpha(u, y)\theta_a(t)$, and
- K_0 is a constant vector chosen such that the matrix $\bar{A} - K_0C$ is stable.

The error dynamics are given as

$$\dot{\varepsilon} = \beta\theta_a(\bar{A} - K_0C)\varepsilon + D_{\theta_a}\Delta\Psi_{\alpha\beta}z - D_{\theta_a}\Delta\bar{\Psi}_{\alpha\beta}\hat{z}.$$

Then, following the same lines of proof as given in Section 5.3, we define the candidate Lyapunov function $V(\varepsilon) = \varepsilon^T P \varepsilon$, and obtain

$$\dot{V} = 2\varepsilon^T P \dot{\varepsilon}$$

$$\begin{aligned}
\dot{V} &= 2\varepsilon^T P[\beta\theta_a (\bar{A} - K_0 C) \varepsilon] + 2\varepsilon^T P D_{\theta_a} \Delta \Psi_{\alpha\beta} z - 2\varepsilon^T P D_{\theta_a} \Delta \bar{\Psi}_{\alpha\beta} \hat{z} \\
&= -\beta\theta_a \varepsilon^T \varepsilon + 2\varepsilon^T P D_{\theta_a} \Delta \Psi_{\alpha\beta} z - 2\varepsilon^T P D_{\theta_a} \Delta \bar{\Psi}_{\alpha\beta} \hat{z}.
\end{aligned}$$

We then propose the hypothesis:

Hypothesis 5.1. For $\|\Delta \Psi_{\alpha\beta} z - \bar{\Psi}_{\alpha\beta} \hat{z}\| \leq k \|z - \hat{z}\|$, where k is a constant, the system (5.18) is an asymptotic observer for system (5.17).

As with Observer 2, we use the two threshold values θ_{\min} and θ_{\max} . Hence, under Hypothesis 5.1, the necessary values of each of these bounds can be derived following a similar proof as given in Section 5.3.

5.5.1 Concluding remarks 4

An asymptotic observer design methodology has been given for a sub-class of state-affine systems with parameter uncertainty. As in the case of Observers 1 and 2, the design is for systems already in the EJOC form. It is shown in theory under Hypothesis 5.1 that the observer is capable of asymptotically estimating the states of the sub-class of state-affine systems considered, where only a partial knowledge of the parameters are assumed. The observer gain uses an adaptive tuning parameter θ_a whose dynamics are of the form described in Section 5.3. Indeed, the discussions of magnitudes of θ_a and constant and varying $\alpha(u, y)$ given in Section 5.3, are also applicable here.

5.6 Summary

Here, we have given four observer design strategies. The first two designs use a constant tuning parameter and an adaptive tuning parameter, respectively, and are facilitated by expressing the systems under observation as a sub-class of systems in the Extended Jordan Observable Canonical (EJOC) form. The third observer design methodology is facilitated

by a partial transformation of the system under observation into a sub-class of systems in the EJOE form. Finally, the fourth observer is designed for the case of uncertain system parameters and uses an adaptive gain. The design methodology follows the same lines as those of the previous adaptive observer, and estimations converge to within a bounded error.

The construction of all of the observer designs proposed is simple and straightforward, as is their implementation. For the case of known parameter values, it has been shown in theory and in simulation that Observers 1-3 are capable of exponentially estimating the state variables of the single-output systems considered. It has also been shown that these observers can be tuned using only a single tuning parameter and that convergence is achieved more quickly when using larger magnitudes of which. The profiles of the observer gains give a good indication of relative performances if measurement noise is to be considered. In fact, the stability of each of these observers is dependent upon the magnitude and sign of the entry appearing in the main diagonal of the extended Jordan block. As a result, the distinct advantage of using Observer 2 is the obtention of desirable performances due to using more efficient or gentler ramping gains.

The performance of Observer 4 is illustrated in a simulation example in Chapter 8 for the estimation of biomass concentration in a bioreactor, where not all system parameters are fully known.

Chapter 6

A Control Design Strategy for a Class of Linear Time-Delay Systems

So far in this work, we have considered the design of controllers and observers for systems assuming that no delays are present. However, as mentioned in Chapter 1, time-delays are natural occurrences in many physical, industrial and engineering systems, and their presence can be attributed to a number of factors. Sources include limited capabilities of information processing units, the location of measuring devices and transmission of system data, and the dynamics present in the transportation of materials in pipes and vessels in industrial processes. The stability analysis and control of time-delay systems (TDSs) are generally much more problematic than those of the delay-free case. Hence, the structural features of TDSs result in the need for non-standard analytical approaches. Consequently, the study of time-delay systems is indeed a current and hot topic of research.

In this chapter, we shall propose a control design methodology for a class of single-input single-output (SISO) linear time-delay systems expressed in the well-known Brunovskii controllable form. This work makes use of a new stability criteria that guarantees asymptotic stability at least in the sense of Krasovskii and is given in two main sections. The first pro-

poses a state feedback control design for linear time-delay systems under the assumption of a full-state measurement. The second section uses the result obtained in the first section in combination with a modification of a result on an observer design for linear time-delay systems [70] and proposes a separation principle for the same class of linear time-delay systems. The class of systems considered are SISO linear time-invariant (LTI) delay systems of the form shown below:

$$\begin{cases} \dot{x}(t) = Ax(t - \tau_1) + \check{A}x(t) + Bu(t); & t \geq 0 \\ y(t) = Cx(t - \tau_2) \end{cases} \quad (6.1)$$

where $x \in \mathbb{R}^n$, $u \in \mathbb{R}$, $y \in \mathbb{R}$, \check{A} is of some special form, which will be described later, and it is assumed that the system (6.1) is controllable and observable. The state delay is denoted by τ_1 and the output delay is denoted by τ_2 and are assumed to be known.

We firstly consider the case where the elements of the matrix \check{A} are all zero such that system (6.1) is given as

$$\begin{cases} \dot{x}(t) = Ax(t - \tau_1) + Bu(t); & t \geq 0 \\ y(t) = Cx(t - \tau_2) \end{cases} \quad (6.2)$$

where the initial condition $x(t) = g(t)$, $-\tau_1 \leq t \leq 0$ where $g(t)$ is a continuous function on the interval $[-\tau_1, 0]$.

6.1 A control design for a class of linear time-delay systems

In this section, we propose a full-state feedback control for the following system:

$$\dot{x}(t) = A_c x(t - \tau) + B_c u(t); \quad t \geq 0 \quad (6.3)$$

where the system matrices A_c and B_c are in the Brunovskii controllable canonical form:

$$A_c = \begin{bmatrix} 0 & 1 & 0 & \cdots & 0 \\ 0 & 0 & 1 & \ddots & \vdots \\ \vdots & \vdots & \ddots & \ddots & 0 \\ 0 & 0 & \cdots & 0 & 1 \\ a_1 & a_2 & \cdots & \cdots & a_n \end{bmatrix} \quad \text{and } B_c = \begin{bmatrix} 0 \\ 0 \\ \vdots \\ 0 \\ 1 \end{bmatrix}, \quad (6.4)$$

a full knowledge of the state vector x is assumed, and τ denotes the time-delay.

A systematic construction of the controller will be given such that the system under control is asymptotically stable.

The primary concern is to stabilise the system by using a control law of the form shown below:

$$u(x(t)) = Lx(t - \tau). \quad (6.5)$$

Under such a control law, the closed-loop system is given by

$$\dot{x}(t) = (A_c + B_c L) x(t - \tau). \quad (6.6)$$

The main difficulty in the design lies in the choice of control gain L such that the closed-loop system (6.6) is asymptotically stable in some sense. In the non-delayed case, the design of a state feedback controller is straightforward. However, there is no general approach, using linear techniques, for the design of a linear state feedback controller for the system considered (6.3) whenever $\tau \neq 0$. Indeed, this is still an open problem.

By taking the Laplace transform of system (6.6), the characteristic equation can be derived as

$$p(s) = \det [sI - (A_c + B_c L) e^{-s\tau}]. \quad (6.7)$$

The characteristic polynomial (6.7) is said to be asymptotically stable if all of the zeros of $p(s) = 0$ are situated in the left-half of the complex plane. However, the presence of the

exponential term $e^{-s\tau}$ means that the characteristic equation (6.7) has an infinite number of roots and therefore it is difficult to determine, explicitly, all the roots of the equation. In effect, the characteristic polynomial (6.7) is called a quasi-polynomial. It is then very difficult to explicitly determine all of the solutions or roots of $p(s)$ in order to prove stability. It is because of this difficulty that several approaches to controller design for time-delay systems have been introduced such as spectral decomposition theory, finite spectrum assignment technique, and delay-independent approaches. Consequently, several less restrictive definitions of asymptotic stability have been derived in the literature such as γ -stability (see e.g. [75]) and asymptotic stability in the sense of Krasovskii. For control and observer design purposes, asymptotic stability in the sense of Krasovskii is most commonly used and is defined as follows (see [76] and [77]):

Definition 6.1. *The characteristic equation (6.7) is said to be asymptotically stable in the sense of Krasovskii if all the solutions of $p(s) = 0$ are situated in the semi-plane $\{s : \text{Re}(s) \leq -\alpha; \alpha > 0\}$.*

The shaded region of Figure 6-1 depicts the Krasovskii stability region. The constant α is referred to as the stability margin of the characteristic equation. It is shown in [76] and [77] that a sufficient condition for asymptotic stability of (6.6) is that its associated characteristic equation is stable in the sense of Krasovskii.

In order to give a constructive and systematic design of a controller gain such that the closed-loop system is asymptotically stable, we use a new definition of asymptotic stability, which was recently introduced in [70]. The new stability criteria is called (α, r) -stability and is stronger than stability in the Krasovskii sense. It is defined as follows:

Definition 6.2. *The characteristic equation (6.7) is said to be (α, r) -stable if all the solutions of $p(s) = 0$ are situated in the semi-plane $\{s : \text{Re}(s) \leq -\alpha; \alpha > 0\} \cap \{s : |s| \geq r > 0\}$.*

The (α, r) -stability region is depicted by the shaded region in Figure 6-2. We shall say that an LTI system is (α, r) -stable if its corresponding characteristic equation is stable in the sense of Definition 6.2. It can easily be seen that, in general, (α, r) -stability is stronger than Krasovskii stability. More precisely, if a system is (α, r) -stable then it is stable in the Krasovskii sense for similar values of α ; since the Krasovskii stability region is included in the (α, r) -stability region.

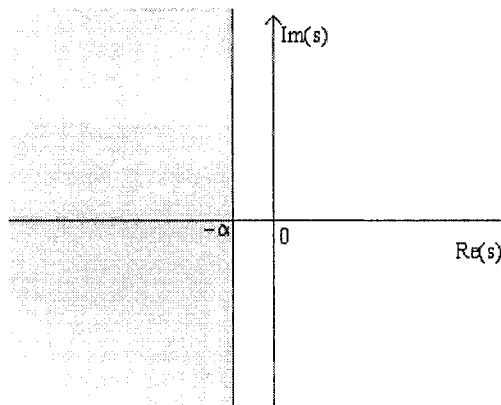


Figure 6-1: Krasovskii stability region

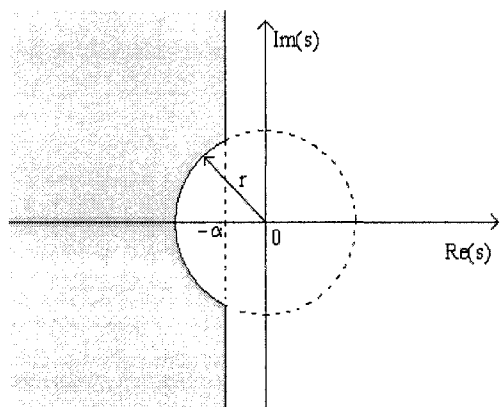


Figure 6-2: (α, r) -stability region

6.1.1 Control gain design

We now give a constructive and systematic design of a gain L for the controller (6.5) such that the characteristic equation of its closed-loop dynamics is asymptotically stable in the sense of Definition 6.2. This will automatically guarantee that the closed-loop system is stable in the Krasovskii sense, which will, in turn, guarantee that the closed-loop system is

asymptotically stable.

Consider the control law given by equation (6.5) and define L as follows:

$$L(\theta_c, \alpha_c, \tau) = -L_0 - L_1(\theta_c, \alpha_c, \tau) \quad (6.8)$$

where

$$L_0 = \begin{bmatrix} a_1 & a_2 & \cdots & a_n \end{bmatrix} \text{ and} \quad (6.9)$$

$$L_1(\theta_c, \alpha_c, \tau) = \begin{bmatrix} \theta_c^n e^{-n\alpha_c\tau} C_n^n & \cdots & \theta_c^2 e^{-2\alpha_c\tau} C_n^2 & \theta_c e^{-\alpha_c\tau} C_n^1 \end{bmatrix} \quad (6.10)$$

where $\theta_c > 0$ denotes the controller gain tuning parameter, $\alpha_c > 0$ denotes a stability margin and $C_n^p = \frac{n!}{p!(n-p)!}$. Subscripts of c that are present from this point in this chapter denote design with respect to a controller.

Note that when the control law (6.5) is applied with L defined as in (6.8), the elements of the last row of A_c are essentially replaced with the elements of $L_1(\theta_c, \alpha_c, \tau)$; thus giving A_c a new set of poles or eigenvalues.

Applying the choice of gain (6.9) and (6.10) to (6.8) yields the control law

$$u(x(t)) = -L_0 x(t - \tau) - L_1(\theta_c, \alpha_c, \tau) x(t - \tau). \quad (6.11)$$

We can now state the following:

Theorem 6.1. *Let $r_c > 0$ be an arbitrary positive constant. Then, for all $\theta_c \in [0, r_c]$, the origin of the closed-loop system*

$$\dot{x}(t) = A_c x(t - \tau) + B_c u(x(t)) \quad (6.12)$$

where $u(x(t))$ is described by (6.11), is (α_c, r_c) -stable.

Proof of Theorem 6.1:

First notice that the matrix A_c can be decomposed as $A_c = \bar{A} + B_c L_0$, where

$$\bar{A} = \begin{bmatrix} 0 & 1 & 0 & \cdots & 0 \\ 0 & 0 & 1 & \ddots & \vdots \\ \vdots & \vdots & \ddots & \ddots & 0 \\ \vdots & 0 & \cdots & 0 & 1 \\ 0 & 0 & \cdots & \cdots & 0 \end{bmatrix}.$$

By applying the control law (6.11) to system (6.3), we obtain the following closed-loop system:

$$\dot{x}(t) = A_c x(t - \tau) - B_c L_0 x(t - \tau) - B_c L_1 x(t - \tau).$$

Since $A_c = \bar{A} + B_c L_0$, we have

$$\begin{aligned} \dot{x}(t) &= \bar{A}x(t - \tau) + B_c L_0 x(t - \tau) - B_c L_0 x(t - \tau) - B_c L_1 x(t - \tau) \\ &= (\bar{A} - B_c L_1) x(t - \tau). \end{aligned} \quad (6.13)$$

By taking the Laplace transform of (6.13) (with zero initial conditions), we obtain

$$sX(s) = (\bar{A} - B_c L_1) X(s) e^{-s\tau}.$$

Hence, the characteristic equation of system (6.13) is given as

$$\begin{aligned} p(s) &= \det (sI - (\bar{A} - B_c L_1) e^{-\tau s}) \\ &= \det M(s) \end{aligned} \quad (6.14)$$

where the characteristic matrix is

$$M(s) = sI - (\bar{A} - B_c L_1) e^{-\tau s}. \quad (6.15)$$

The aim is to obtain an expression of the characteristic equation of the form $(s + \theta_c e^{-(s+\alpha_c)\tau})^n$ from which we shall show the system (6.3) is (α_c, r_c) -stable. Note that

$$(\bar{A} - B_c L_1) e^{-\tau s} = \begin{bmatrix} 0 & e^{-\tau s} & 0 & \dots & 0 \\ \vdots & \ddots & e^{-\tau s} & \ddots & \vdots \\ \vdots & & \ddots & \ddots & 0 \\ 0 & \dots & \dots & 0 & e^{-\tau s} \\ -\frac{\theta_c^n C_n^n}{e^{n\alpha_c \tau} e^{\tau s}} & \dots & \dots & -\frac{\theta_c^2 C_n^2}{e^{2\alpha_c \tau} e^{\tau s}} & -\frac{\theta_c C_n^1}{e^{\alpha_c \tau} e^{\tau s}} \end{bmatrix}.$$

In order to clearly show the coefficients of the characteristic polynomial, we now perform a transformation upon the characteristic matrix $M(s)$.

We define the diagonal matrix Δ_s as

$$\Delta_s = \begin{bmatrix} e^{n\tau s} & 0 & \dots & 0 \\ 0 & e^{(n-1)\tau s} & \ddots & \vdots \\ \vdots & \ddots & \ddots & 0 \\ 0 & \dots & 0 & e^{\tau s} \end{bmatrix}.$$

Then, a pre-multiplication and post-multiplication of the characteristic matrix $M(s)$ by Δ_s and Δ_s^{-1} , respectively, gives

$$\begin{aligned} \Delta_s M(s) \Delta_s^{-1} &= \Delta_s [sI - (\bar{A} - B_c L_1) e^{-\tau s}] \Delta_s^{-1} \\ &= s \Delta_s I \Delta_s^{-1} - \Delta_s (\bar{A} - B_c L_1) e^{-\tau s} \Delta_s^{-1} \\ &= sI - (\Delta_s \bar{A} \Delta_s^{-1} - \Delta_s B_c L_1 \Delta_s^{-1}) e^{-\tau s}. \end{aligned}$$

It can be checked that

$$\Delta_s \bar{A} \Delta_s^{-1} = e^{\tau s} \bar{A} \quad \text{and} \quad \Delta_s B_c = B_c e^{\tau s}$$

so that

$$\Delta_s M(s) \Delta_s^{-1} = sI - (\bar{A} - B_c L_1 \Delta_s^{-1}).$$

Since the determinant of a product of matrices is equal to the product of the determinants of the matrices, and that the determinant of the inverse of a matrix is the reciprocal of its

determinant, we have

$$\begin{aligned} p(s) &= \det M(s) \\ &= \det(\Delta_s M(s) \Delta_s^{-1}). \end{aligned}$$

In effect,

$$\det(\Delta_s M(s) \Delta_s^{-1}) = \det(\Delta_s) \cdot \det(M(s)) \cdot \det(\Delta_s^{-1}).$$

On the other hand,

$$\begin{aligned} \det(\Delta_s \Delta_s^{-1}) &= \det(\Delta_s) \cdot \det(\Delta_s^{-1}) \\ &= \det(I) = 1. \end{aligned}$$

That is,

$$\det(\Delta_s^{-1}) = \frac{1}{\det(\Delta_s)}.$$

Therefore,

$$p(s) = \det(M(s)) = \det(\Delta_s M(s) \Delta_s^{-1}) = \det(sI - (\bar{A} - B_c L_1 \Delta_s^{-1})).$$

The special structure of the matrix $\bar{A} - B_c L_1 \Delta_s^{-1}$ is

$$\bar{A} - B_c L_1 \Delta_s^{-1} = \begin{bmatrix} 0 & 1 & 0 & \cdots & 0 \\ \vdots & \ddots & 1 & \ddots & \vdots \\ \vdots & & \ddots & \ddots & 0 \\ 0 & \cdots & \cdots & 0 & 1 \\ -C_n^n \theta_c^n e^{-n(s+\alpha_c)\tau} & \cdots & \cdots & -C_n^2 \theta_c^2 e^{-2(s+\alpha_c)\tau} & -C_n^1 \theta_c e^{-(s+\alpha_c)\tau} \end{bmatrix}$$

from which it is clear that

$$\begin{aligned} p(s) &= s^n + C_n^1 s^{n-1} [\theta_c e^{-(s+\alpha_c)\tau}] \\ &\quad + C_n^2 s^{n-2} [\theta_c^2 e^{-2(s+\alpha_c)\tau}] + \cdots + [C_n^n \theta_c^n e^{-n(s+\alpha_c)\tau}] \\ &= (s + \theta_c e^{-(s+\alpha_c)\tau})^n. \end{aligned} \tag{6.16}$$

Hence, the solutions of the equation

$$p(s) = (s + \theta_c e^{-(s+\alpha_c)\tau})^n = 0 \quad (6.17)$$

satisfy the following equality

$$s = -\theta_c e^{-(s+\alpha_c)\tau} = -\theta_c e^{-\alpha_c\tau} e^{-s\tau} \quad (6.18)$$

or equivalently

$$s e^{s\tau} = -\theta_c e^{-\alpha_c\tau}. \quad (6.19)$$

Note that $s = 0$ is not a solution of (6.18) or (6.19) since $\theta_c > 0$. The main problem from here lies in the fact that the solution s appears as both a factor and an exponent of e . Consequently, it is not easy to explicitly find all the solutions of equation (6.19). However, our main concern is to find the conditions under which all the solutions of (6.19) have negative real parts. Indeed, consider a solution s_0 of (6.17) with a magnitude $r > 0$ and an argument φ . That is, $s_0 = \mu + j\omega$ with $|s_0| = \sqrt{\mu^2 + \omega^2} = r$ and $\arg\{s_0\} = \varphi$. The solution s_0 can also be written as $s_0 = r e^{j\varphi}$. Hence, by replacing s_0 in (6.19), we have

$$\begin{aligned} s_0 e^{s_0\tau} &= r e^{j\varphi} e^{(\mu+j\omega)\tau} \\ &= r e^{j\varphi} e^{\mu\tau} e^{j\omega\tau} \\ &= r e^{\mu\tau} e^{j(\varphi+\omega\tau)} \\ &= -\theta_c e^{-\alpha_c\tau} + j0. \end{aligned}$$

Since $e^{j(\varphi+\omega\tau)} = \cos(\varphi + \omega\tau) + j \sin(\varphi + \omega\tau)$, we have

$$r e^{\mu\tau} \cos(\varphi + \omega\tau) = -\theta_c e^{-\alpha_c\tau} \quad (6.20)$$

and

$$r e^{\mu\tau} \sin(\varphi + \omega\tau) = 0. \quad (6.21)$$

Since $r \neq 0$ and $e^{\mu\tau} \neq 0$, we have, from equation (6.21), $\sin(\varphi + \omega\tau) = 0$, which implies that

$$\varphi + \omega\tau = k\pi; \quad k \in \mathbb{Z}. \quad (6.22)$$

On the other hand,

$$\cos(\varphi + \omega\tau) = \frac{-\theta_c e^{-\alpha_c \tau}}{r e^{\mu\tau}} < 0.$$

Since $\varphi + \omega\tau = k\pi$; $\cos(\varphi + \omega\tau) = \cos(k\pi)$ is negative if and only if k is odd. In which case $\cos(k\pi) = -1^k = -1$. Hence,

$$e^{\mu\tau} = \frac{\theta_c e^{-\alpha_c \tau}}{r}.$$

That is,

$$\mu\tau = \ln\left(\frac{\theta_c}{r}\right) + \ln e^{-\alpha_c \tau} = \ln\left(\frac{\theta_c}{r}\right) - \alpha_c \tau$$

or

$$\mu = -\alpha_c + \frac{1}{\tau} \ln\left(\frac{\theta_c}{r}\right). \quad (6.23)$$

Note that s_0 has to be the solution of (6.19). It can be verified that it also yields the above two conditions (6.22) and (6.23).

Since s_0 was chosen arbitrarily, this means that any other solution s of (6.19) with real part μ and imaginary part ω will have to satisfy (6.22) and (6.23).

We are now going to find conditions on θ_c , τ , and α_c under which the solution of (6.19) is (α_c, r_c) -stable for some $r_c > 0$.

For this, first of all, we need:

$$\frac{\pi}{2} < \varphi < \frac{3\pi}{2}.$$

This implies that

$$\frac{\pi}{2} < k\pi - \omega\tau < \frac{3\pi}{2}.$$

That is,

$$-k\pi + \frac{\pi}{2} < -\omega\tau < -k\pi + \frac{3\pi}{2}$$

or

$$k\pi - \frac{\pi}{2} > \omega\tau > k\pi - \frac{3\pi}{2}.$$

Hence,

$$\omega\tau < k\pi - \frac{\pi}{2}$$

or

$$\omega < \frac{1}{\tau} \left(k\pi - \frac{\pi}{2} \right).$$

The minimum upper bound on ω is satisfied by $k = 1$, where

$$\omega < \frac{1}{\tau} \frac{\pi}{2}.$$

Also,

$$\omega\tau > k\pi - \frac{3\pi}{2}$$

or

$$\omega > \frac{1}{\tau} \left(k\pi - \frac{3\pi}{2} \right).$$

Therefore, the maximum lower bound on ω is satisfied by $k = 1$, where

$$\omega > -\frac{1}{\tau} \frac{\pi}{2}.$$

Note that if $\tau \rightarrow +\infty$, then $\omega \rightarrow 0$. This means that the region of stability will eventually shrink; which is the penalty to be paid for large τ .

Next, if we choose $0 < \theta_c \leq r_c$, where r_c is an arbitrary positive constant, we show that the solution of (6.19) is (α_c, r_c) -stable.

Suppose $|s| = r \geq r_c$, then from (6.23), we have

$$\mu = -\alpha_c + \frac{1}{\tau} \ln \left(\frac{\theta_c}{r} \right) \leq -\alpha_c + \frac{1}{\tau} \ln \left(\frac{\theta_c}{r_c} \right).$$

Since $\theta_c \leq r_c$; $\ln \left(\frac{\theta_c}{r_c} \right) \leq 0$. Hence, $\mu \leq -\alpha_c$.

Next, we show that $\mu > 0$ if $r < r_c$. Indeed,

$$\mu = -\alpha_c + \frac{1}{\tau} \ln \left(\frac{\theta_c}{r} \right) > 0$$

implies that

$$\begin{aligned}\frac{1}{\tau} \ln \left(\frac{\theta_c}{r} \right) &> \alpha_c \\ \ln \left(\frac{\theta_c}{r} \right) &> \alpha_c \tau.\end{aligned}$$

That is,

$$\frac{\theta_c}{r} > e^{\alpha_c \tau}$$

or

$$r < \theta_c e^{-\alpha_c \tau}.$$

Since $\alpha_c \tau > 0$, we have $e^{-\alpha_c \tau} < 1$. Therefore,

$$r < \theta_c < r_c.$$

This completes the proof of Theorem 6.1. □

Remark 6.1

1. Note that in the non-delayed case ($\tau = 0$) all the poles of the closed-loop system (6.12) will be located at $-\theta_c$ in the left-half complex plane when controller (6.11) is applied with $\tau = 0$.
2. The above control design technique can be extended to the following class of systems:

$$\dot{x}(t) = A_c x(t - \tau) + \check{A}x(t) + B_c v(t); \quad t \geq 0 \tag{6.24}$$

where $x \in \mathbb{R}^n$, $v \in \mathbb{R}$ and \check{A} is of the special form $\check{A} = B_c K$ for some vector $K \in \mathbb{R}^n$.

Indeed, if we apply the preliminary control

$$v(t) = -Kx(t) + u(t) \tag{6.25}$$

to system (6.24), we obtain

$$\dot{x}(t) = A_c x(t - \tau) + B_c u(t); \quad t \geq 0$$

which is of the form described by system (6.3). Hence, the complete stabilising feedback for system (6.24) is given by

$$v(x(t)) = -Kx(t) + u(x(t))$$

where $u(x(t))$ is given by (6.11).

6.1.2 Example 6.1

In this subsection, we shall illustrate the previous design methodology through an academic example. Consider the following 2nd-order single-input system:

$$\dot{x}(t) = A_c x(t - 0.2) + B_c u(t) \quad (6.26)$$

where

$$x(t) = \begin{bmatrix} x_1(t) \\ x_2(t) \end{bmatrix}, \quad A_c = \begin{bmatrix} 0 & 1 \\ 1 & 2 \end{bmatrix} \quad \text{and} \quad B_c = \begin{bmatrix} 0 \\ 1 \end{bmatrix}.$$

The above system is of the form (6.3) with a time-delay $\tau = 0.2$ s. Consequently, by applying the previous design methodology, the control law that will stabilise the system at the origin is given by

$$u(x(t)) = -L_0 x(t - \tau) - L_1(\theta_c, \alpha_c, \tau) x(t - \tau)$$

where

$$L_0 = \begin{bmatrix} 1 & 2 \end{bmatrix}$$

and

$$\begin{aligned} L_1(\theta_c, \alpha_c, \tau) &= \begin{bmatrix} \theta_c^2 e^{-2\alpha_c \tau} & 2\theta_c e^{-\alpha_c \tau} \end{bmatrix} \\ &= \begin{bmatrix} \theta_c^2 e^{-0.4\alpha_c} & 2\theta_c e^{-0.2\alpha_c} \end{bmatrix} \end{aligned}$$

with $\alpha_c, \theta_c > 0$. Hence,

$$u(x(t)) = - (1 + \theta_c^2 e^{-0.4\alpha_c}) x_1(t - 0.2) - 2 (1 + \theta_c e^{-0.2\alpha_c}) x_2(t - 0.2).$$

The closed-loop system is given by

$$\dot{x}(t) = \tilde{A}x(t - 0.2)$$

$$\text{where } \tilde{A} = \begin{bmatrix} 0 & 1 \\ -\theta_c^2 e^{-0.4\alpha_c} & -2\theta_c e^{-0.2\alpha_c} \end{bmatrix}.$$

Simulation results

Several sets of simulations were carried out to show the behaviour of the closed-loop system. Here, we have chosen $\alpha_c = 0.1$ and $r_c = 3$ so that $0 < \theta_c \leq 3$. Figure 6-3 and Figure 6-4 show the profiles of x_1 and x_2 , respectively, when $\theta_c = 1$. It can be seen that the state variables converge to the origin as expected. Figures 6-5 and 6-6 show the profiles of x_1 and x_2 , respectively, when $\theta_c = 3$. Here, it can be seen that the convergence is much quicker.

In general, the use of higher values of θ_c (which implies larger values of r_c) results in a quicker convergence performance. This is because the poles are pushed further to the left in the left-half complex plane. Indeed, as one would expect in such a case, a larger control effort is needed to achieve this. This is confirmed in Figure 6-7, where it is clear that larger values of θ_c yields larger transient peaks. Therefore, there is a trade-off between the desired magnitude of r_c and the amplitude of acceptable transient peaks and control effort. This trade-off obviously depends on an individual system's operating parameters.

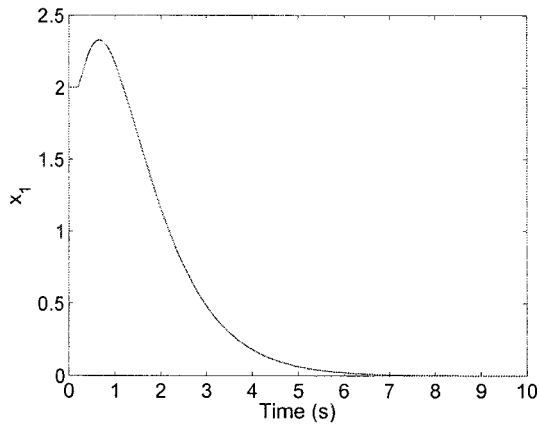


Figure 6-3: Profile of x_1 when $\theta_c = 1$

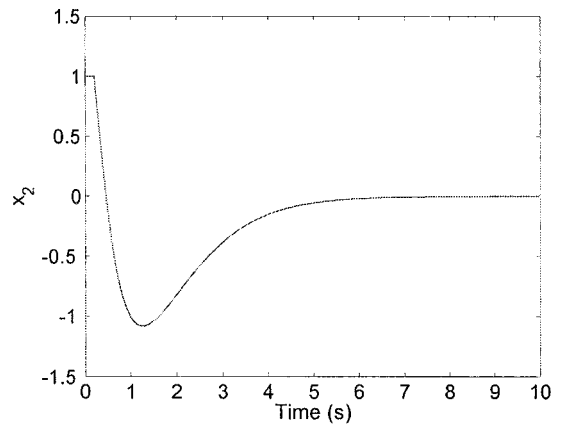


Figure 6-4: Profile of x_2 when $\theta_c = 1$

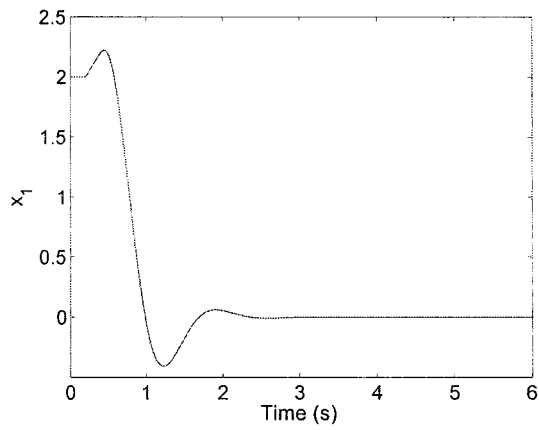


Figure 6-5: Profile of x_1 when $\theta_c = 3$

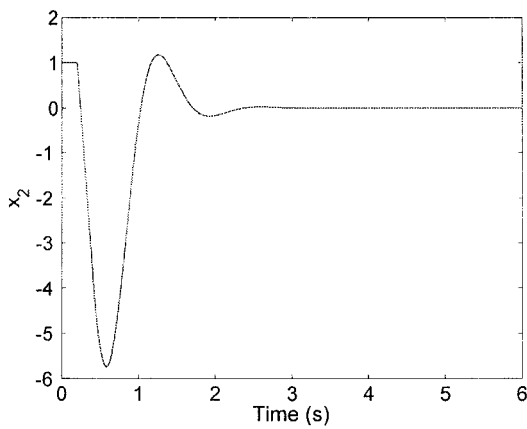


Figure 6-6: Profile of x_2 when $\theta_c = 3$

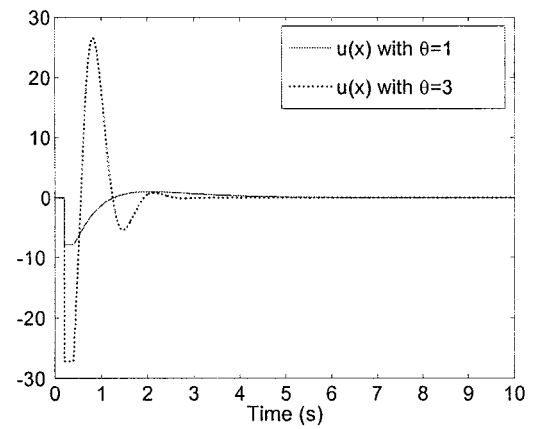


Figure 6-7: The control $u(x(t))$ when $\theta_c = 1$ and $\theta_c = 3$

6.1.3 Concluding remarks 5

To summarise, a controller for a class of single-input linear systems with known delay has been designed where the design is based on the specific choice of controller gain such that the closed-loop system is asymptotically stable in the sense of (α_c, r_c) -stability. The asymptotic stability of the resulting closed-loop system is stronger than Krasovskii stability. It is also easy to prove since (α_c, r_c) -stability is proven using polar form rather than cartesian. Furthermore, the system can be easily tuned via one parameter θ_c and it is shown that the use of higher values of θ_c results in a quicker convergence performance. However, in such a case, the larger control effort needed to achieve this can result in system behaviour containing larger transient peaks. Therefore, a trade-off is required between the desired convergence time and the amplitudes of acceptable transient peaks and control effort.

The stability of the closed-loop system is delay-dependent. In fact, the conditions on θ_c , τ , and α_c under which the closed-loop system is (α_c, r_c) -stable have been shown where larger values of τ results in a shrinking stability region.

Most work in control of time-delay systems use either the eigenstructure assignment or the Lyapunov-based methods. In addition, these methods rely on the definition of asymptotic stability employed. The present work is distinctive from other work in this area in that it exploits the features of the characteristic equation of the system to derive the controller gain. In fact, no *a priori* control design approach was set in advance; that is, the controller was designed based on first principles.

It should be noted that this work is applicable to the cases of delay in the state only and delay both in the state and the output, where the value of the output delay can be any value less than or equal to that of the state delay.

The main drawback of this work lies in the fact that a full-state measurement is assumed to be available on-line. This was assumed for the sake of the control design and is, of

course, often not the case in the real world where physical system constraints or the expense or indeed the non-existence of sensors to measure state variables restrict the availability of information on the system state vector. It is therefore important to consider a control strategy that incorporates some kind of estimation technique. Such a control strategy design is presented in the next section.

6.2 A separation principle for a class of linear time-delay systems

In this section, we develop the controller proposed in the previous section in conjunction with a result on an observer design for linear time-delay systems and propose a separation principle for a class of single-input single-output (SISO) linear time-delay systems of the following form:

$$\begin{cases} \dot{x}(t) = A_c x(t - \tau_1) + B_c u(t); & t \geq 0 \\ y(t) = C x(t - \tau_2) \end{cases} \quad (6.27)$$

where $x \in \mathbb{R}^n$, $u \in \mathbb{R}$, $y \in \mathbb{R}$, the pair (A_c, B_c) is in the Brunovskii controllable canonical form and

$$C = \begin{bmatrix} c_1 & c_2 & \cdots & \cdots & c_n \end{bmatrix}.$$

In addition, it is assumed that the system (6.27) is observable.

It should be emphasised that the separation principle presented here is applicable to the following case: $0 \leq \tau_2 \leq \tau_1$. For simplicity, it is assumed that any value $\tau_2 > 0$, is increased in the design such that $\tau_2 = \tau_1$. Consequently, any delay term used from this point onwards will be denoted as τ . The design for the class of systems considered is therefore not too restrictive.

The design of a linear state feedback controller and a linear full-state observer for non-delayed systems is fairly straightforward. In addition, the control of the system via the observer is also possible even though the two syntheses are done independently of each other. In effect, the stability of the combined system is guaranteed and it is found that there is a separation of the poles of the observer and the poles of the controlled system without the observer. This observer-based control strategy is the well-known separation principle. However, in the delayed case it is not at all clear that a separation principle can be established. This is mainly because there is no general approach for the design of a linear state feedback controller and a linear full-state observer for the system (6.27) whenever $\tau \neq 0$. In addition, there are several definitions of asymptotic stability for time-delay systems, which implies that the types of stability and convergence should be made precise when designing observers and controllers for such systems. In the separation principle proposed here, we will use the (α, r) -stability criteria previously described. More precisely, we will use the results of the time-delay control design given in the previous section and the results of [70] to establish a separation principle for the class of linear time-delay systems considered (6.27). However, before using the observer in [70], a preliminary transformation is required in order to make it compatible with the controller.

6.2.1 Preliminary results

Now, consider the following SISO linear time-delay system:

$$\begin{cases} \dot{z}(t) = A_o z(t - \tau) + B u(t); & t \geq 0 \\ y(t) = C_o z(t - \tau) \end{cases} \quad (6.28)$$

where $z \in \mathbb{R}^n$, $u \in \mathbb{R}$, $y \in \mathbb{R}$ and the pair (A_o, C_o) are in the Brunovskii observable form:

$$A_o = \begin{bmatrix} \bar{a}_1 & 1 & 0 & \cdots & 0 \\ \bar{a}_2 & 0 & \ddots & \ddots & \vdots \\ \vdots & \vdots & \ddots & \ddots & 0 \\ \vdots & \vdots & & \ddots & 1 \\ \bar{a}_n & 0 & \cdots & \cdots & 0 \end{bmatrix},$$

$$C_o = \begin{bmatrix} 1 & 0 & \cdots & \cdots & 0 \end{bmatrix}$$

and B is a constant n -dimensional column vector. The time-delay τ is assumed to be known and we have the initial condition $z(t) = h(t)$, $-\tau \leq t \leq 0$ where $h(t)$ is a continuous function on the interval $[-\tau, 0]$.

Consider the linear observer defined by

$$\dot{\hat{z}}(t) = A_o \hat{z}(t - \tau) + Bu(t) + K(y(t - \tau) - C_o \hat{z}(t - \tau)) \quad (6.29)$$

where

$$K = K_0 + K_1$$

with

$$K_0 = \begin{bmatrix} \bar{a}_1 & \bar{a}_2 & \cdots & \bar{a}_n \end{bmatrix}^T$$

and

$$K_1 = \begin{bmatrix} \theta_o e^{-\alpha_o \tau} C_n^1 & \theta_o^2 e^{-2\alpha_o \tau} C_n^2 & \cdots & \theta_o^n e^{-n\alpha_o \tau} C_n^n \end{bmatrix}^T$$

where $\theta_o > 0$ denotes the observer gain tuning parameter, $\alpha_o > 0$ denotes a stability margin and $C_n^p = \frac{n!}{p!(n-p)!}$. Subscripts of o that are present from this point in this chapter denote design with respect to an observer. Note that K_0 is the 1st column of A_o .

Theorem 6.2 [70]. *Let $r_o > 0$ be an arbitrary positive constant. Then, for all $\theta_o \in [0, r_o]$,*

the system described by (6.29) is an asymptotic observer for system (6.28).

More precisely, it is shown in [70] that the error dynamics of the observer are (α_o, r_o) -stable.

Now, assume that the pair (A_o, B) is also controllable. Then, there exists a similarity matrix P such that the system (6.28) can be transformed into the controllable form (6.3). Indeed, by setting $x(t) = Pz(t)$, we have

$$\begin{cases} \dot{x}(t) = A_c x(t - \tau) + B_c u(t) \\ y(t) = Cx(t - \tau) \end{cases} \quad (6.30)$$

where $PA_oP^{-1} = A_c$, $PB = B_c$ and $C_oP^{-1} = C$.

As a result, by setting $\hat{x}(t) = P\hat{z}(t)$, an observer for system (6.30) is given by

$$\dot{\hat{x}}(t) = A_c \hat{x}(t - \tau) + B_c u(t) + PK(y(t - \tau) - C\hat{x}(t - \tau)). \quad (6.31)$$

6.2.2 Observer-based control

In this section, we are going to study the stability of the following overall system:

$$\begin{cases} \dot{x}(t) = A_c x(t - \tau) + B_c u(\hat{x}(t)) \\ \dot{\hat{x}}(t) = A_c \hat{x}(t - \tau) + B_c u(\hat{x}(t)) + PK(y(t - \tau) - C\hat{x}(t - \tau)) \end{cases} \quad (6.32)$$

where $u(\hat{x}(t))$ is the estimated feedback control

$$u(\hat{x}(t)) = L\hat{x}(t - \tau) \quad (6.33)$$

where L is defined as in (6.8).

This is equivalent to studying the stability of

$$\begin{cases} \dot{x}(t) = [A_c + B_c L] x(t - \tau) - B_c L \varepsilon(t - \tau) \\ \dot{\varepsilon}(t) = [A_c - PKC] \varepsilon(t - \tau) \end{cases} \quad (6.34)$$

where $\varepsilon(t) = x(t) - \hat{x}(t)$.

Recall that the matrix A_c can be decomposed as $A_c = \bar{A} + B_c L_0$, where

$$\bar{A} = \begin{bmatrix} 0 & 1 & 0 & \cdots & 0 \\ 0 & 0 & 1 & \ddots & \vdots \\ \vdots & \vdots & \ddots & \ddots & 0 \\ \vdots & 0 & \cdots & 0 & 1 \\ 0 & 0 & \cdots & \cdots & 0 \end{bmatrix}. \quad (6.35)$$

Then, since $L = -L_0 - L_1$, we have $A_c + B_c L = \bar{A} - B_c L_1$. Similarly, the matrix A_o can be decomposed as $A_o = \bar{A} + K_0 C_o$. Since $A_c = P A_o P^{-1}$ and $C_o P^{-1} = C$, we have

$$\begin{aligned} A_c &= P A_o P^{-1} \\ &= P (\bar{A} + K_0 C_o) P^{-1} \\ &= \hat{A} + P K_0 C \end{aligned}$$

where $\hat{A} = P \bar{A} P^{-1}$. Therefore, $A_c - P K C = \hat{A} - P K_1 C$.

Consequently, system (6.34) can be written in matrix form as

$$\begin{bmatrix} \dot{x}(t) \\ \dot{\varepsilon}(t) \end{bmatrix} = \begin{bmatrix} \bar{A} - B_c L_1 & -B_c L \\ \mathbf{0}_{n \times n} & \hat{A} - P K_1 C \end{bmatrix} \begin{bmatrix} x(t - \tau) \\ \varepsilon(t - \tau) \end{bmatrix}. \quad (6.36)$$

We can now state the following:

Theorem 6.3. *Let $r_o > r_c > 0$ be arbitrary positive constants. Then, for all $\theta_o \in [0, r_o]$ and for all $\theta_c \in [0, r_c]$ such that $\theta_o > \theta_c$, the origin of the augmented system (6.34) is (α, r) -stable.*

Proof of Theorem 6.3:

Consider system (6.36). For simplicity, by setting

$$\xi(t) = \begin{bmatrix} x(t) \\ \varepsilon(t) \end{bmatrix} \text{ and } F = \begin{bmatrix} \bar{A} - B_c L_1 & -B_c L \\ \mathbf{0}_{n \times n} & \hat{A} - P K_1 C \end{bmatrix}$$

the system can be written as

$$\dot{\xi}(t) = F\xi(t - \tau). \quad (6.37)$$

The characteristic equation of (6.37) is given by

$$q(s) = \det(sI_{2n} - Fe^{-\tau s})$$

where I_{2n} is the $2n$ -dimensional identity matrix. It can be verified that

$$q(s) = \det(sI_n - e^{-\tau s}(\bar{A} - B_c L_1)) \times \det(sI_n - e^{-\tau s}(\hat{A} - PK_1 C)).$$

Recall that for any row vector $L = [l_1, l_2, \dots, l_n]$ and for any column vector

$K = \text{col}[k_1, k_2, \dots, k_n]$, we have

$$\begin{aligned} \eta_c(\lambda) &= \det(\lambda I_n - (\bar{A} - B_c L)) \\ &= \lambda^n + \lambda^{n-1} l_n + \dots + \lambda l_2 + l_1 \end{aligned}$$

and

$$\begin{aligned} \eta_o(\lambda) &= \det(\lambda I_n - (\bar{A} - KC_o)) \\ &= \lambda^n + k_1 \lambda^{n-1} + k_2 \lambda^{n-2} + \dots + k_n. \end{aligned}$$

In particular, if we choose $l_i = \rho^{n-(i-1)} C_n^{n-(i-1)}$ and $k_i = \sigma^i C_n^i$, then

$$\eta_c(\lambda) = (\lambda + \rho)^n \quad \text{and} \quad (6.38)$$

$$\eta_o(\lambda) = (\lambda + \sigma)^n. \quad (6.39)$$

Now, consider

$$\begin{aligned} p_c(s) &= \det(sI_n - e^{-\tau s}(\bar{A} - B_c L_1)) \\ &= \det\{e^{-\tau s} I_n (se^{\tau s} I_n - (\bar{A} - B_c L_1))\} \\ &= \det(e^{-\tau s} I_n) \det(se^{\tau s} I_n - (\bar{A} - B_c L_1)). \end{aligned}$$

By using the above observation, and with L_1 defined as previously (6.10), we obtain

$$\det(se^{\tau s} I_n - (\bar{A} - B_c L_1)) = (se^{\tau s} + \theta_c e^{-\alpha_c \tau})^n.$$

This can readily be seen by replacing λ by $se^{\tau s}$ and ρ by $\theta_c e^{-\alpha_c \tau}$ in (6.38). Hence,

$$\begin{aligned} p_c(s) &= e^{-s\tau n} (se^{\tau s} + \theta_c e^{-\alpha_c \tau})^n \\ &= (s + \theta_c e^{-(s+\alpha_c)\tau})^n. \end{aligned} \quad (6.40)$$

Now, with

$$M_o = \left(sI_n - e^{-\tau s} \left(\widehat{A} - PK_1C \right) \right)$$

consider

$$\begin{aligned} p_o(s) &= \det(M_o) \\ &= \det(P^{-1}M_oP) \\ &= \det \left(sI_n - e^{-\tau s} \left[P^{-1}\widehat{A}P - P^{-1}PK_1CP \right] \right) \\ &= \det \left(sI_n - e^{-\tau s} \left(\overline{A} - K_1C_o \right) \right). \end{aligned}$$

Using a similar reasoning as above, it can be shown that

$$p_o(s) = (s + \theta_o e^{-(s+\alpha_o)\tau})^n. \quad (6.41)$$

As a result,

$$\begin{aligned} q(s) &= p_c(s)p_o(s) \\ &= (s + \theta_c e^{-(s+\alpha_c)\tau})^n (s + \theta_o e^{-(s+\alpha_o)\tau})^n. \end{aligned}$$

The new compact form of the characteristic equation means that now all solutions can be accounted for, and it can be deduced from [70] and the previous section that obtaining a characteristic equation in such a form results in an (α, r) -stable system. Indeed, from this we can see that, as in the non-delayed case, the set of poles of the combined system (6.37) is the union of the control poles and the estimator poles. Hence, a separation principle is also verified in this case. The control poles satisfy

$$s + \theta_c e^{-(s+\alpha_c)\tau} = 0 \quad (6.42)$$

and the observer poles satisfy

$$s + \theta_o e^{-(s+\alpha_o)\tau} = 0. \quad (6.43)$$

Since the response of the observer should be quicker than that of the controller, we choose $\theta_o > \theta_c > 0$. It is shown in the previous section that if $0 < \theta_c \leq r_c$, where r_c is a positive number, then all complex numbers s which satisfy the equation (6.42) are given by $s = \mu_c + j\omega_c$ such that $\sqrt{\mu_c^2 + \omega_c^2} = r \geq r_c$ and where μ_c and ω_c satisfy $\mu_c = -\alpha_c + \frac{1}{\tau} \ln\left(\frac{\theta_c}{r}\right)$ and $\omega_c\tau + \varphi = k\pi$, where k is odd.

Note that $\mu_c \leq -\alpha_c$ since $\frac{\theta_c}{r} \leq 1$. As a result, the controlled system (without the observer) is (α_c, r_c) -stable. Consequently, the controlled system is also Krasovskii stable with stability margin α_c ; hence asymptotically stable.

Similarly, if θ_o is chosen such that $0 < \theta_o \leq r_o$ for some positive number r_o , then all complex numbers s which satisfy the equation (6.43) are given by $s = \mu_o + j\omega_o$ such that $\sqrt{\mu_o^2 + \omega_o^2} = \bar{r} \geq r_o$ and where μ_o and ω_o satisfy $\mu_o = -\alpha_o + \frac{1}{\tau} \ln\left(\frac{\theta_o}{\bar{r}}\right)$ and $\omega_o\tau + \varphi = k\pi$, where k is odd. As a result, the observer is (α_o, r_o) -stable.

This completes the proof of Theorem 6.3. □

Remark 6.2

In the same sense as the controller of the previous section, the above separation principle design technique can be extended to the following class of systems:

$$\begin{cases} \dot{x}(t) = A_c x(t - \tau_1) + \check{A}x(t) + B_c v(t); & t \geq 0 \\ y(t) = Cx(t - \tau_2) \end{cases} \quad (6.44)$$

where $x \in \mathbb{R}^n$, $v \in \mathbb{R}$, $y \in \mathbb{R}$ and \check{A} is of the special form $\check{A} = B_c L_d$ for some vector $L_d \in \mathbb{R}^n$. Indeed, if we apply the preliminary control

$$v(t) = -L_d x(t) + u(t) \quad (6.45)$$

to system (6.44), we obtain

$$\begin{cases} \dot{x}(t) = A_c x(t - \tau_1) + B_c u(t); & t \geq 0 \\ y(t) = Cx(t - \tau_2) \end{cases}$$

which is of the form described by system (6.27).

6.2.3 Example 6.2

Consider the simple mechanical system as shown in Figure 6-8, consisting of a mass m of 1kg and a delayed input force $u(t - \tau)$.

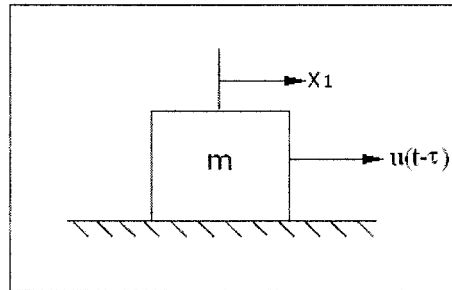


Figure 6-8: Simple mechanical system

From Newton's 2nd Law of Motion, it can easily be seen that

$$\ddot{y}(t) = u(t - \tau)$$

where y is the displacement. By setting $x_1(t) = y(t)$ and $x_2(t - \tau) = \dot{y}(t)$, we obtain the following system:

$$\begin{cases} \dot{x}_1(t) = x_2(t - \tau) \\ \dot{x}_2(t) = u(t) \\ y(t) = x_1(t) \end{cases} \quad (6.46)$$

where

$$\begin{bmatrix} \dot{x}_1(t) \\ \dot{x}_2(t) \end{bmatrix} = \begin{bmatrix} 0 & 1 \\ 0 & 0 \end{bmatrix} \begin{bmatrix} x_1(t - \tau) \\ x_2(t - \tau) \end{bmatrix} + \begin{bmatrix} 0 \\ 1 \end{bmatrix} u(t).$$

It is clear that system (6.46) is of the form (6.27) and is also in both controllable and ob-

servable form. Consequently, by using the controller design procedure previously given, we obtain

$$u(x(t)) = -\theta_c^2 e^{-2\alpha_c \tau} x_1(t - \tau) - 2\theta_c e^{-\alpha_c \tau} x_2(t - \tau). \quad (6.47)$$

By following the observer design procedure, we obtain

$$\dot{\hat{x}}(t) = A_o \hat{x}(t - \tau) + Bu(t) + K(y(t - \tau) - \hat{x}_1(t - \tau))$$

where $K = \text{col} \begin{bmatrix} 2\theta_o e^{-\alpha_o \tau} & \theta_o^2 e^{-2\alpha_o \tau} \end{bmatrix}$.

Where observer-based control is considered, we have the controller expressed in terms of the estimated state variables as

$$u(\hat{x}(t)) = -\theta_c^2 e^{-2\alpha_c \tau} \hat{x}_1(t - \tau) - 2\theta_c e^{-\alpha_c \tau} \hat{x}_2(t - \tau)$$

and the observer given as

$$\dot{\hat{x}}(t) = A_o \hat{x}(t - \tau) + Bu(\hat{x}(t)) + K(y(t - \tau) - \hat{x}_1(t - \tau)).$$

Simulation results

Simulations of the above observer and controller were carried out with the following numerical values: $\theta_o = 3$, $\theta_c = 2$, $\tau = 0.2$ and $\alpha_c = \alpha_o = 0.1$. This choice of gains is in line with the necessity to have the observer respond more quickly than the controller, such that reliable estimated state values are provided to the controller. The performance of the observer-based control strategy is compared to that, when a full knowledge of the state is assumed, as in the previous section. Figure 6-9 shows the convergence of x_1 to the origin when the feedback control (6.47) is applied to the system. Figure 6-10 shows the performance of the observer in open-loop when a step input is applied to the system. It can be seen that the estimate \hat{x}_2 (dotted line) of the non-measured variable converges to its real value x_2 (solid line) within 2.5 seconds. The convergence rate can be increased by choosing a larger value of θ_o . Figures 6-11 and 6-12 show the performance of the closed-loop system when it is controlled via the

observer. It is clear from these results that the observer-based closed-loop system has good convergence properties with regards to the stabilisation of the state variables to the origin.

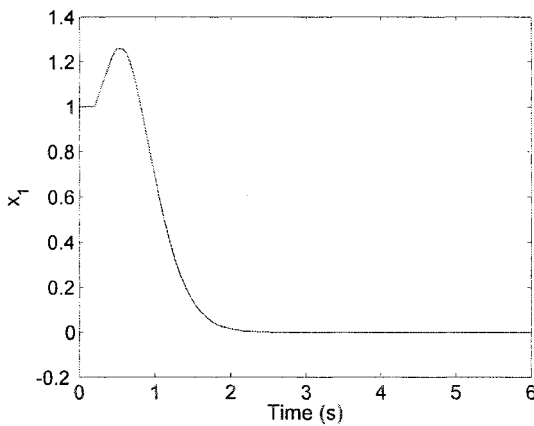


Figure 6-9: Profile of x_1 when $u(x(t))$ is applied

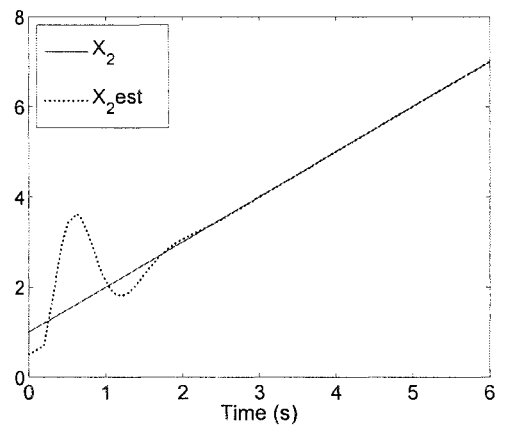


Figure 6-10: Estimation of x_2

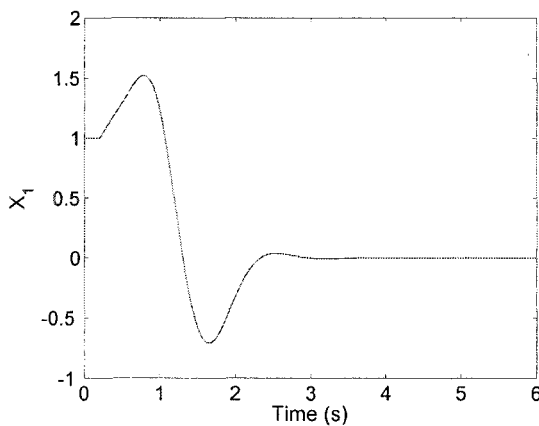


Figure 6-11: Profile of x_1 when $u(\hat{x}(t))$ is applied

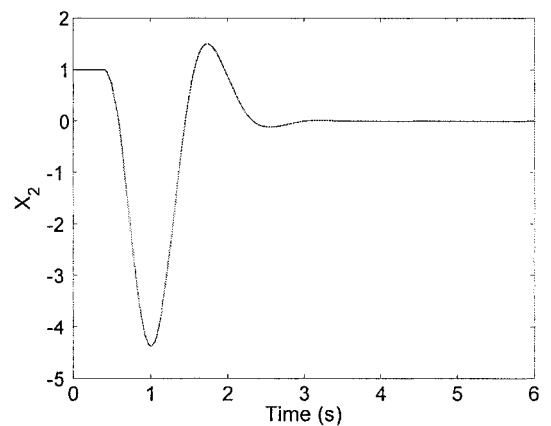


Figure 6-12: Profile of x_2 when $u(\hat{x}(t))$ is applied

6.2.4 Concluding remarks 6

To summarise, a separation principle for a class of linear time-delay systems has been established where the design is based on the specific choice of asymptotic stability criteria. Indeed, the criterion used is (α, r) -stability, which is stronger than stability in the Krasovskii sense. It is shown that there is a separation of the poles of the observer, and the poles of the closed-loop system without the observer - as in the non-delayed case. Furthermore, the design is based on first principles.

Simulations were conducted to demonstrate the good convergence performance of the controller, the open-loop observer, and the closed-loop system controlled via the observer. The magnitude of the observer gain tuning parameter θ_o was chosen to be greater than that of the controller gain tuning parameter θ_c in order to have the observer operate more rapidly than the controller. Indeed, the controller and observer can each be easily tuned using only one tuning parameter, where higher values of each result in quicker convergence performances. However, the same trade-off, with regards to transient peaks, as described for the controller in the previous section, applies here.

It should be noted that this work is delay-dependent in the sense that for larger values of τ , the performances of the controller, the open-loop observer, and the observer-based controller become poorer. Indeed, larger values of τ result in a shrinking of the (α_c, r_c) - and (α_o, r_o) -stability regions, as indicated in the previous section.

Finally, it should be emphasised that this work is not restricted to the consideration of a delay in the state alone. Indeed, it can deal with a delay in the state (τ_1) and a delay in the output (τ_2). The reason behind this is simple; when no delay is present in the output measurements, it is introduced and used in the controller and observer. In both the state-delayed case, and state- and output-delayed case, the values of delay used in the controller and observer must be equal to the state delay itself. Consequently, this work is applicable to the case $0 \leq \tau_2 \leq \tau_1$ since the output delay τ_2 can always be increased such that $\tau_2 = \tau_1$ and subsequently be used in the observer-based controller.

Chapter 7

Focus of Application: Biological

Wastewater Treatment and Progress in the Determination of Biomass

7.1 The need for clean water

The need for water to sustain humanity is phenomenal and comes in a variety of forms, which include direct consumption, bathing, cleaning, and is of course essential and vastly used in the production of food. The provision of clean, safe and reliable water supplies to homes, businesses and industries in the UK and other developed countries in the world is a service which is taken almost for granted in modern times. In the developing world, however, this basic human right is not yet fully available. It is estimated that 2.4 *billion* people in the world are without improved sanitation facilities, and in 2002 approximately 1.1 *billion* people were still using water from unimproved sources [78]. Inevitably, the risk of using untreated water leads to pollution and disease. The most frequent human diseases related to poor water supply and sanitation include diarrhoea, intestinal worms, trachoma, schistosomi-

asis, and cholera. The consequences of these resulting diseases are indeed terrible. Globally, according to the World Health Organisation (WHO) [79], around 2 *million* people die each year, most of which are children under the age of 5 and countless others suffer from poor health. Indeed, it is reported that 90% of wastewater in developing countries is untreated. In Latin America, 98% of domestic sewage is discharged directly into the nearest streams, and all of India's major rivers are similarly polluted [80].

Organisations such as UNICEF and WaterAid are continuing to help the countries of the world to engage these problems, with the ultimate goal, according to WHO [78], being the provision of water, sanitation and good hygiene for all by 2025.

According to the State Hydrological Institute in St. Petersburg, the total amount of water on Earth today is estimated at 1.4 *billion km³* [80]. The water making up the world's Oceans is too salty for consumption or irrigation and accounts for 97.5% of the total volume. The majority of the remaining 2.5% is locked up either in the polar ice caps or elsewhere as permanent snow [80]. Freshwater lakes and rivers, from which we obtain most of our water, contain only around 90,000 *km³* (0.26% of the 2.5% freshwater supply of the world). Sources of freshwater that are being tapped include those that have accumulated over millennia and are effectively non-renewable, so will consequently deplete. The renewable sources are actually unevenly distributed across the globe. In effect, the World Meteorological Organisation states a more realistic figure of readily available freshwater is 12,500 *km³*.

Today, the vast necessity of water, especially in the production of food, affirms the need to recycle water. Indeed, based upon a daily intake of 3000 *kcal* per person per day, it is reported that such a consumption represents a water depletion of 3500 *l* per person per day [28]. In addition, feeding humanity currently requires a consumptive water use of 6800 *km³/year*, where 1800 *km³/year* is in the form of irrigation. With around 70 *million* people added to the planet each year, humanity will require an additional 5600 *km³/year* by 2050 [28].

Hence, since the self-cleaning capabilities of water are finite, it is clear that improved efficient use of water must include efficient treatment of wastewater.

7.2 The development of clean water in the UK

The task of developing clean and safe water supplies in the UK has greatly tested the engineering skills and ingenuity of inventors for hundreds of years. Most of the 19th and 20th centuries saw the most significant changes in water supply and sewage disposal methods and the learning curves that evolved. Indeed, up until 1847, there was no central government supervision of water supplies, and typical disposal methods for wastewater comprised of returning it to waterways untreated, causing environmental pollution and risking public health. After a number of large-scale fatal outbreaks of Cholera in the UK, and consequently a number of reports [81] on the state of sanitation in towns in Britain, Parliament were persuaded to commence the task of overseeing water supply and sewage disposal, and began with the passing of the Public Health Act 1848. From the late 19th century, water supply and sewage disposal methods were developing well, but were treated as separate issues. In the 1960's, there was still a divide between water supply, sewage treatment, and the recreational use of water. However, the recognition of the increasing demand for water from limited sources and of the continuing disposal of sewage into waterways brought about the realisation that the issues could no longer be treated separately [82]. Consequently, water management in England and Wales was reorganised into ten Regional Water Authorities (RWA) through the passing of The Water Act 1973. The duties of each RWA include the supply of water and the disposal of sewage in such a way as to aid the recreational use of water. Recently, The Water Act 2003 made significant impacts upon water management and regulation in England and Wales, bringing in changes in abstraction licensing, water resources notices, regulation,

and water management [83]. Indeed, water should be acknowledged as a valuable resource and should be used wisely by all sectors of society. Hence, together with the phenomenal global demand for water, it is easy to appreciate the need for such organised use of water in order to prevent pollution in the environment and prevent disease in the consumption of recycled water. This awareness further affirms the need for contributions towards wastewater treatment solutions.

7.3 Biological wastewater treatment

The treatment of wastewater comprises the three main stages: collection, treatment, and disposal. Wastewater is collected from homes, businesses, industries (after a pre-treatment), and storm drains via an intricate network of sewers and is transported primarily by the force of gravity to wastewater treatment (WWT) plants. The WWT plants remove impurities from the wastewater stream so that the water can be safely returned to waterways for reuse. More specifically, WWT prevents pollution in waterways and prevents disease in consumers of recycled water. The impurities that are removed from the stream are either transported to landfill sites (grit, debris etc.) or undergo further treatment (sludge) so that they can be used in agricultural applications. Generally, WWT plants only accept direct wastewater from domestic dwellings. Industrial plants usually have to treat their own before returning it to waterways or to the domestic treatment system.

The main stages that are found in WWT plants are preliminary, primary, secondary, and tertiary treatment and are summarised below:

Preliminary Treatment - Screens and shreds large polluting bodies and removes grit.

Primary Treatment - Uses clarifiers to remove settled particles and floating oils.

Secondary Treatment - Biologically removes pollutants using bioreactors.

Tertiary Treatment - Removes pathogenic micro-organisms.

The secondary treatment stage is also known as biological treatment and is the application focussed upon in this research work. The type of biological treatment considered is the Activated Sludge Process (ASP), which is currently the most widely applied biological wastewater treatment method in the developed world for the treatment of domestic and industrial wastewaters [84]. The conventional ASP is comparable to one of the naturally occurring purification processes that takes place in lakes and rivers; the microbial aerobic oxidation of nutrients. In this process, bacteria and other free-living micro-organisms suspended in the water body utilise organic matter and oxygen for cell metabolism and growth. Similarly, in the ASP, an inoculum is introduced into a carefully controlled environment containing nutrient-rich wastewater capable of sustaining cell metabolism and growth of micro-organisms. The carefully controlled environment takes the form of treatment units called bioreactors. Figure 7-1 shows the general arrangement of secondary treatment in a conventional ASP configuration using the continuous flow reactor type. The conditions are adjusted such that micro-organisms are able to thrive and transform the impurities into more easily removable forms (additional micro-organisms and CO_2). The nutrient reactions involved in the biological treatment of wastewater can be classified into the removal of organic carbon, nitrogen, and phosphorus and can be aerobic, anaerobic, and anoxic, although aerobic is more widely used since it is more rapid. The conventional ASP biologically removes organic carbon by using heterotrophic micro-organisms growing aerobically or anoxically. In the aerobic case, typical methods involve treatment using aeration basins into which the wastewater is directed and supplied with air, or sometimes pure oxygen, from feed points along the bottom of the chamber. The type of nutrient reaction considered in this work is the aerobic removal of carbon.

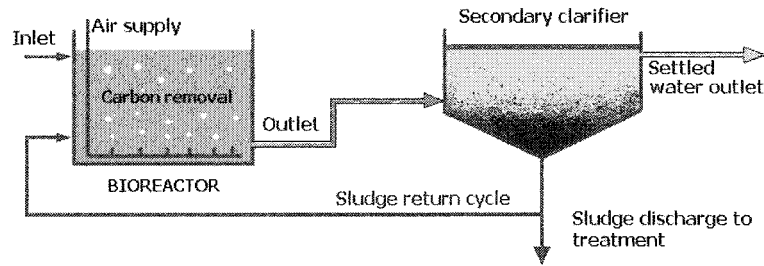


Figure 7-1: Arrangement of Secondary treatment in conventional Activated Sludge Processes

7.3.1 The aerobic bioprocess model considered

There are a number of types of bioreactors available in which biological treatment can take place. However, the most common types are stirred tank reactors taking the form of fedbatch and continuous stirred tank reactors (CSTR). The general reactor arrangement of the latter is illustrated in Figure 7-2, showing the reactor with one inflow and one outflow.

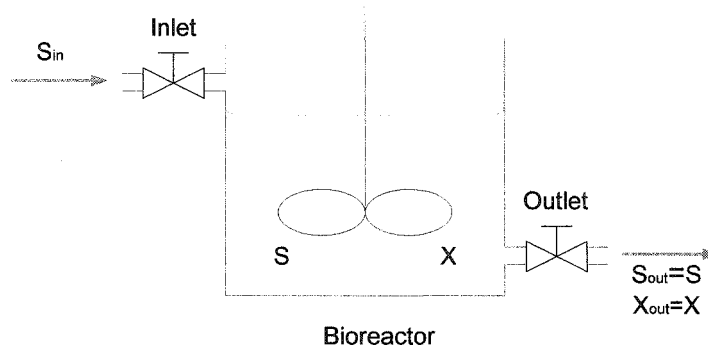


Figure 7-2: Continuous Stirred Tank Reactor arrangement

The bioprocesses can be described by the following microbial growth reaction:



where S : Substrate (organic content) concentration and X : Biomass (micro-organisms) concentration.

Upon making a number of assumptions about the process, the modelling of either type of reactor using mass balance equations enables the derivation of the following dynamical model, describing a wide class of bioprocesses:

$$\begin{cases} \dot{S}(t) = D(t)(S_{in}(t) - S(t)) - Y_s \mu(t) X(t) \\ \dot{X}(t) = \mu(t) X(t) - D(t) X(t) \end{cases} \quad (7.2)$$

where μ is the specific growth rate (SGR) of biomass; D is the dilution rate; S_{in} is the influent substrate concentration, and Y_s is the yield coefficient for substrate concentration. The descriptions of the SGR that are generally used in industrial WWT plants are usually of the form of the well-reputed Monod law:

$$\mu = \frac{\mu_{\max} S}{K_s + S} \quad (7.3)$$

or the Haldane law:

$$\mu = \frac{\mu_0 S}{K_s + S + \frac{S^2}{K_i}}$$

where μ_{\max} is the maximum specific growth rate, K_s is the saturation constant, K_i is the inhibition parameter, and

$$\mu_0 = \mu_{\max} \left(1 + 2\sqrt{\frac{K_s}{K_i}} \right).$$

The Haldane law is a development of the Monod law and is useful in situations where substrate inhibition is important (i.e. at very high concentrations).

For details of the modelling derivation, see Appendix B. It is, in fact, the microbial growth reaction (7.1) and the dynamical model (7.2) that are considered in this work, with the specific growth rate given by the Monod law (7.3).

Note that the model (7.2) is very widely used and accepted for the description of the bioprocess considered when dealing with control and estimation strategies (see e.g. [32], [44], [45], [85], [86]).

7.4 Main problems in the control of aerobic biological treatment

Here, we detail some difficulties faced in the control and monitoring of aerobic carbon removal processes and present a detailed account of work done that focus upon such difficulties.

7.4.1 Specific growth rate of biomass

The specific growth rate (SGR) of biomass is of special importance since it governs the actual dynamics of the bioreactor. Unfortunately, it is very difficult to measure directly. In general, the SGR is a nonlinear function of the state of the process and, consequently, the whole process is nonlinear.

Several dozen models for the SGR have been developed for very specific systems that require on-line measurement of all variables involved. In fact, biochemical experiments have clearly shown that the SGR varies with time and is influenced by many physio-chemical and biological factors, amongst which some important ones are: substrate concentration, biomass concentration, temperature, pH level, dissolved oxygen (DO) concentration, light intensity and various inhibitors of microbial growth. Some of the many models that have been derived can be seen in Appendix B.

7.4.2 Determination of biomass concentration

The maintenance of appropriate biomass levels is vital to the success of the ASP process and, therefore, knowledge of biomass concentration is essential if effective control is to be attained (see e.g. [32], [44], [47], [85]). However, there is currently a lack of reliable and inexpensive equipment to provide on-line measurements of the biomass concentration and

it is usual to use some indirect measurement techniques. Methods for the determination of biomass concentration are given next.

Measurement of biomass

The concentration of viable biomass present in wastewater treatment plants is not measured on-line. Instead, most full-scale UK operators make the assumption that the active micro-organisms are directly proportional to Mixed Liquor Suspended Solids (MLSS) concentration. Hence, they use readily available monitoring methods to measure the MLSS and use the simple proportional relation as an indicator of biomass concentration. The use of this measurement has a number of downfalls. Historically, measurement of MLSS has been conducted gravimetrically on grab samples and can mean a delay of up to 2 or 3 days before obtaining the result. Therefore, real-time monitoring and control cannot be implemented since operation would be on the basis of data which is no longer valid. However, monitoring equipment for the on-line measurement of MLSS are now available [87], but are as yet not used throughout the industry. In fact, they do not necessarily provide reliable values of MLSS since they use a related parameter to infer the MLSS value, usually using methods of optical absorption. The problems arise from the assumption of a constant relationship between the absorption and solids concentration. This assumption is not true, since it is affected by a number of factors such as particle size and possible chemical species that can absorb at the same wavelength [88].

Besides the efforts required in obtaining information on the MLSS, other problems can actually arise as a result of using this data. Since the MLSS measurement is a total measure of the dry weight of suspended matter, it is not actually possible to distinguish the type of activity of the different important classes of micro-organisms (heterotrophs and autotrophs). This is clear if one considers that the suspended matter is made up of both inorganic and

organic matter. Indeed, the inorganic matter contains no biological activity, and the organic matter contains a complex variety of organic material, some of which is responsible for the consumption and oxidation of organic components (heterotrophic and autotrophic micro-organisms), and some of which is not. In fact, using the value of MLSS would not indicate the relative abundance of the heterotrophic and autotrophic micro-organisms. Hence, two sludge samples with identical MLSS values can possess completely different levels of viable biomass concentrations [88].

This inaccurate method has spurred a number of efforts to develop monitoring equipment for the on-line measurement of biomass concentration. As a result, there are now emerging monitoring equipment designed for just this [87]. In a recent publication [89], the accuracy of on-line viable biomass measurements was investigated. The equipment under study was the Biomass Monitor (BM 214-M, Aber Instruments Ltd., Aberystwyth, UK) used for on-line viable biomass measurement of activated sludge from a brewery wastewater treatment plant. It was shown that there existed satisfactory correlations between the on-line measurements and off-line analysis. However, the on-line measurements had a very poor signal to noise ratio, and off-line filtering was necessary to provide satisfactory results. In addition, the cost of the monitor was around £8,500, which was actually the lowest priced monitor in the range.

Indeed, robust methods for the on-line monitoring of biomass concentrations are still not yet as established as those for the on-line monitoring of substrate concentration (see Appendix B), and alternative methods, such as estimation of biomass, remain very much an appealing solution, as detailed in the next section.

7.5 Estimation of biomass using observers - a comparative literature study

An approach that has received much attention in recent years for the determination of biomass concentration is observer-based estimation. Different types of state observers have been considered for application to a number of bioprocesses under various assumptions (see e.g. [32], [44], [47]). Cases considered include the problem of state estimation where it is assumed that the kinetic rates of reaction are known and where they are not known. To give an appreciation of the difficulties involved in such a problem, and indeed improvements that can be made in designing observer-based estimators for such systems, some well-known results are given in the following.

Known kinetic reaction rates For the case of known kinetic reaction rates, [32] and [44] consider a well-known standard form of observer. The approach is to consider a linearised tangent approximation of the resulting error dynamics around some desired equilibrium point. The problem from here is to choose appropriate values of matrix gain such that the resulting linear time-varying system has desirable stable properties. Two standard solutions are presented to do this. These are the design of an Extended Luenberger Observer (ELO) and an Extended Kalman Observer (EKO). The gains for the ELO are calculated such as to assign some pre-specified negative real values to the eigenvalues of the linearised time-varying error dynamics. In doing so, the error term will asymptotically converge to the equilibrium point. The updating of the gain of the EKO requires the computation of the solution of three dynamical equations. These solutions supply the two gain terms required. Simulation examples show the performance of both observers when applied to the simple microbial growth reaction (7.1) in a single tank reactor that is considered in this work. It is assumed that the

substrate concentration S is measured on-line and that the structure of the specific growth rate is known, as are all parameters involved in its description. The structures used to represent the specific growth rate are the Contois law and the Haldane law. Convergence when using either observer can be achieved in around 10 hours through appropriate assignment of eigenvalues and choice of initial conditions for the ELO and EKO, respectively. However, the gain terms involved are complex, especially considering the significant computational effort required to update the gain of the EKO. Also, the stability and convergence properties are only valid over a given operating point and it is difficult to guarantee stability over wide ranges of operation. Furthermore, there is no consideration of estimation in the presence of measurement noise.

Another work, which shows biomass estimation based upon a full knowledge of the process is found in [45]. The process considered is the growth reaction (7.1) and its description uses the Monod law to represent the specific growth rate. They show the performance of a high-gain exponential observer, originating from an idea established in [17], to estimate the biomass using on-line measurement of substrate concentration. An additive white noise is considered on the measurement of S with amplitudes equivalent to 10% of the measured value. As expected, due to the nature of high-gain observers, convergence is rapid at less than 3 hours. However, it is well-known that high-gain observers perform poorly in the presence of measurement noise. Hence, it is not surprising that the estimation result obtained contains noise with growing amplitudes of 15% of the noise-free simulation, after which point no further results are shown. Clearly, such observers are unsuitable when noisy measurements are to be considered.

From the foregoing results, it is clear that much more can be done to improve the state estimation for the class of systems considered, even with a fully known model. On the other hand, since the description of the kinetic rates of reaction are quite involved, it is also clear

that the assumption of a full knowledge of kinetic rates is quite severe. It is, therefore, important to consider biomass estimation based upon little or no knowledge of the specific growth rate. Work that has been done in this area includes the consideration of classical [32], asymptotic [32], [44], and adaptive observers [32].

Unknown kinetic reaction rate An approach presented in [32] and [44], involves the use of asymptotic observers where it is assumed that all knowledge of the kinetic rates is not available. The idea is to make a state partition of measured and unmeasured components and then perform a state transformation such that in the new description, the dynamics are independent of the reaction rates. From this point, an asymptotic observer is used to provide an estimate of the transformation variable and, in turn, together with on-line information of the measured components, derives an estimate of the unmeasured component. However, the speed of the convergence dynamics cannot be arbitrarily assigned, and are determined via the value of the dilution rate. Examples of an anaerobic digestion process can be found in [32] and [44] that illustrate the slow convergence dynamics of the asymptotic observers with convergence achieved at around 50 hours. This is not entirely unexpected due to the nature of the class of systems considered, which are detectable only. However, the application of such asymptotic observers to systems which are observable, such as the microbial growth reaction described by (7.1), would result in an estimation strategy to which arbitrarily fast convergence dynamics cannot be assigned, since the convergence speed would also be dictated by the process at hand. Also, performance in the presence of measurement noise is not considered.

In [47], an observer is proposed for the estimation of biomass concentration for the aerobic bioprocess (7.1) for batch and continuous modes of operation. The observer is synthesised under the assumption that the Oxygen Uptake Rate (OUR) is measured on-line. Ex-

pressions describing the biomass and biomass growth dynamics are derived, but are linear. Consequently, the method uses standard linear stability criteria in the selection of appropriate observer gain such that, in a noise-free case, the error dynamics are exponentially stable and Bounded Input Bounded Output (BIBO) stable in the case of noisy measurements of OUR. With respect to the measured value, the amplitude of noise considered on the measurements of OUR is 10%. The results show the performance of the observer when applied to the continuous process under steady-state operation. The estimation of the biomass concentration, in the absence of measurement noise, converges to within 13% of the simulated value in 20 hours and converges to the simulated value after 40 hours. In the presence of measurement noise, the estimation of the biomass concentration again converges to within 13% of the simulated value in 20 hours and to within 2% of the simulated value in 40 hours. The convergence performance is clearly slow, and it must also be emphasised that these results are obtained using linear error dynamics and are based upon convergence to a constant biomass concentration.

Another work considering the microbial growth reaction (7.1) with unknown kinetic rates can be found in [45]. The estimation strategy presented is based upon an idea given in [44]. The approach uses an asymptotic observer to estimate the biomass using on-line measurements of substrate concentration. A change of variables is made, resulting in a dynamical system independent of the kinetic rates. The asymptotic observer takes the form of the system with no correction term. The estimation of the transformation variable provided by the observer is then used in an algebraic manipulation to give a value of the biomass concentration. Simulation results show the performance when an additive white noise is considered on the measurements of S with amplitudes equivalent to 10% of the measured value. The estimation is shown with very low levels of noise ($< 1\%$ of simulated real value), but with an extremely slow convergence time. In fact, the performance is shown only for up to 30 hours,

in which time convergence is not attained since the dynamics of which are dictated only by the bioprocess.

Partially known kinetic reaction rates

Alternative approaches for state estimation in bioprocesses involve the consideration that the models of kinetic rates of reaction are known, but that the values of the parameters of which are poorly known.

In [32], the ELO is considered for the estimation of biomass for the simple microbial growth reaction (7.1) for poorly known parameters. It is assumed that the substrate concentration is available on-line and that the structure of the specific growth rate is given by the widely used Monod law. It is considered that the uncertainty lies in either the parameter μ_{\max} or the parameter K_s . A simulation example shows the performance when considering an error of 10% in K_s . A slow performance results when using low gains with convergence attained at around 60 hours, whilst the use of higher gains results in faster dynamics at the expense of considerable offsets. In fact, the work in [32] was given in order to illustrate the need to develop observers that can handle parameter uncertainties in such bioprocesses. As a result, the same authors have proposed some observer designs for such cases. In fact, they consider poorly known parameters as design parameters for state estimation. The idea is to calculate the poorly known parameter value that would satisfy a zero steady-state condition. Firstly, an ELO is used with appropriate choice of gains such that the error terms go to zero. The next step is to derive an expression for the badly known parameter. To do this, the time derivatives of the estimation errors are set to zero, such that the system operating conditions are of that in steady-state. An expression for the steady-state error is given and from this, an expression for the poorly known parameter is derived. The poorly known parameters considered are either the saturation constant \tilde{K}_s or maximum specific growth rate $\tilde{\mu}_{\max}$. In each

individual case, the value of \tilde{K}_s and $\tilde{\mu}_{\max}$ can be chosen such that the zero steady-state error for the estimation of X is guaranteed. The values of gain, and hence the rates of convergence, are heavily dependent upon the dilution rate D and yield coefficient Y_s if zero steady-state performance is to be attained. This is evident in the simulation examples, which show the performance of the observer when considering the microbial growth reaction (7.1). The simulation results show the biomass estimation \hat{X} profile converging to that of the simulated biomass X at around 90 hours, and the substrate estimation \hat{S} profile converging to a biased profile from that of the simulated substrate S . The performance is then shown for a square wave influent substrate concentration S_{in} , although the system is initialised in steady-state. Simulation results show convergence of the biomass at around 100 hours, although small offsets are apparent at later periods of time. As before, the substrate estimation converges to a biased value with a large offset. It is clear that such an approach is very slow and does not necessarily hold true for time-varying dilution rates.

From the foregoing results presented, there is still a clear need to develop a class of observers that can perform well with system parameter uncertainties, which are typically found in biochemical processes. As a result, further work has been done in this area by [32], who introduce adaptive state observers as one possible improvement. The approach considers the use of a model of the specific growth rate with known structure and known nominal parameter values, where only one poorly known parameter is considered per measured variable. The aim is to estimate both the state and the unknown portion of the poorly known parameters. Hence, the observers are described as being adaptive due to the nature of adapting to the estimations of the unknown portion of the poorly known parameters. The biological process considered is the microbial reaction (7.1) where it is assumed that measurements of substrate concentration S are available on-line. The observer contains an additional dynamical equation representing the dynamics of the estimated unknown portion of the parameter,

which is thus treated as an extra state. The idea is to obtain a linear time-varying form of the error dynamics with an input that asymptotically decreases to zero. To do this, an asymptotic observer is also used to give estimations of biomass, which are subsequently used in the adaptive observer. The reason for this is to have the term in the error dynamics that is associated with the uncertainties, asymptotically decrease to zero. Simulation results show the convergence performance of the state observer strategy with 10% positive error on μ_{\max} . Convergence of the biomass estimation is achieved around 60 hours. They also present the performance of the same observer when the inlet substrate concentration S_{in} is a square wave. The system is initialised in steady-state and convergence occurs around 40 hours. The estimation profile of the unknown portion $\Delta\mu_{\max}$ also converges to the constant value used in the process model in around 40 hours. The case where μ_{\max} is assumed to be known and where K_s is assumed to contain an error of 10% is also treated. Here, convergence is achieved at around 40 hours. However, in both cases, they state that the error dynamics are linear and time-varying, and claim that with the system matrix of which being bounded, the problem has been simplified to the case of appropriate choice of gains, and hence eigenvalues, such that the stability of the error dynamics can be ensured. This sole reliance upon eigenvalues is not sufficient to ensure the stability of such error dynamics, which are not LTI.

In each of the foregoing cases, there is no indication of what profile of dilution rate is considered, even though it is actually a component of the gains used. Furthermore, there is no consideration of measurement noise, which is a very important factor if the observer is to be robust for practical implementation. Indeed, it is well-known that although good estimation results may well be obtained using observers with high enough gains, the use of such observers can often lead to very poor performance in the presence of measurement noise.

Alternative approaches to the problem of biomass estimation for processes with partially

known kinetic rates include the consideration of error observers and interval observers [45], [46], [85]. Bounded error observers with constant and time-varying gains are proposed in [45] for application to the microbial reaction (7.1). It is assumed that the specific growth rate μ depends only upon the measured substrate concentration S and is not exactly known. It is also assumed that μ is known to exist between two bounds such that for a partially known μ , the error dynamics do not necessarily converge to zero, but to a bounded value. The performance of the constant-gain observer with gain $\theta = 1$ is very slow with convergence to within 5% of the simulated biomass profile not achieved until around 30 hours. It is also shown that using a higher constant gain $\theta = 3$ results in an offset of 21% of the simulated biomass profile. There is also no consideration of measurement noise. Time-varying gains are then considered to improve the performance. The idea is to assign a rapid initial convergence, which then reduces to a rate equivalent to $0.1h^{-1}$. In doing this, two gains are considered. The first is an exponentially decaying function, and the second takes the form of a sigmoidal decay, neither of which are derived as a result of the observer design methodology, but rather from a choice of known decreasing functions. Simulation results show that the best convergence performance is achieved when using the sigmoidal gain. However, although convergence to within 5% of the simulated biomass profile is achieved, there is no consideration of measurement noise. Furthermore, no indication is given as to what magnitude of error in μ is considered.

In a recent work [85], an interval observer is proposed for state observation in a bio-process containing uncertainties on the process parameters and/or in the inputs. It is assumed in the work that the kinetics model structure is known but is described using the uncertain process parameters. The process considered is described by the microbial growth (7.1) where it is assumed that the substrate concentration S is available from on-line measurements. The design is based upon the process at hand possessing the property of cooperativity, for which

interval observers can be constructed. In order to obtain a cooperative system, a system variable transformation upon the system considered is required, along with the choice of suitable gains, of which there are four. The error dynamics are considered to be linear, although they claim that the methodology can be applied to more complex systems, and lower and upper bounds on the initial value of the estimate of biomass deny any arbitrary choice. The first case considers a specific growth rate described by the Monod law and with an uncertainty in μ_{\max} with an error of $\pm 50\%$ of the nominal value. The interval observer provides estimates of the upper and lower bounds of the biomass concentration, the errors of which reduce to within 5% of the simulated value at 50 hours when using constant high gains. However, measurement noise is not considered.

A further case is considered where the uncertainty in the specific growth rate μ is in the form of an upper and lower bound described using the Monod law ($\mu_{\max} = 0.495h^{-1}$) and Haldane law ($\mu_{\max} = 0.16h^{-1}$, $K_s = 5g/l$, $K_i = 25g/l$), respectively. A nominal profile of the specific growth rate is given using the Monod law ($\mu_{\max} = 0.33$). A square wave of known inlet substrate concentration S_{in} is used and again it is assumed that the substrate concentration S is available from on-line measurements. Their results show the biomass estimation error reducing to within 2% of the simulated value around 60 hours. This is followed by consideration of uncertainty on the output measurements. More precisely, a Gaussian white noise is added to the measurements of S with amplitudes of 5% of the measured value. As in the previous case, a square wave of known influent substrate concentration S_{in} is used. With the gain set to half the value used in the previous noise-free case, the results show a worsened estimation performance with regards to the offset. The biomass estimation reduces to within 10% of the simulated value in 50 hours with no clear improvement thereafter. This interval observer has a performance equivalent to a simple interval observer proposed in [46], with the exception of a smoother estimation in the presence of measurement noise.

The observer in [46] produces an estimation profile containing noise with amplitudes of 10% of the estimation value, whilst the observer given in [85] provides an estimation profile containing noise with amplitudes of 5% of the estimation value. The use of Monod and Haldane as upper and lower bounds of the specific growth rate is a good idea. However, the values of substrate considered have a maximum value of 1.5g/l . Up until this concentration, the profile given by the Haldane model is less than that of the nominal value by only 10%.

7.6 Summary

From the foregoing literature study, it is clear that there is a need to develop a class of observers for the estimation of biomass concentration for processes described by the microbial reaction (7.1). In particular, there is a distinct lack of consideration with regards to measurement noise, and in those cases which do consider this factor, the results are either estimations containing an amplified version of the measurement noise considered (e.g. high-gain observers), or estimations with low levels of noise, but with extremely long convergence times (asymptotic observers), which in some cases are so slow that the convergence point is not even shown. There is also a distinct lack of consideration with regards to different possible parameter values, such as the varying influent characteristics, different concentration values of substrate and biomass, and different values of yield coefficient.

It is important to consider biomass estimation, both in the absence and in the presence of measurement noise, where the kinetic rates of reaction are known and where they are not fully known. In each case, it is important to have good performance with regards to response times, convergence, low levels of noise in the estimation, or a combination thereof. In addition, the estimation performance should also be considered for various possible parameter values.

The following chapter presents four observers, based on the design methodologies given in Chapter 5, for the estimation of biomass concentration in the absence and in the presence of measurement noise for a variety of operational conditions. Furthermore, we also consider estimation for known and partially known specific growth rates.

Chapter 8

Estimation of Biomass Concentration in a Bioreactor

As established from the beginning of this thesis, one focus of this project is upon estimation strategies for some classes of dynamical systems with application to wastewater treatment systems. In line with this, the work presented in this chapter applies the observer design strategies given in Chapter 5 for the estimation of biomass concentration in the bioprocess described by the microbial growth reaction (7.1) and represented by the model (7.2). In fact, the model (7.2) belongs to a class of single-output state-affine systems and has been used to represent the bioprocess (7.1) in many works (see e.g. [32], [44], [45], [47], [85], [86], [90]). The model of the specific growth rate considered is the well-reputed Monod law (7.3).

Two cases are considered. In the first case, we assume full knowledge of the specific growth rate, whereas in the second, we assume only a partial knowledge of the specific growth rate. In each case, we consider estimation both in the absence and in the presence of measurement noise where it is assumed that measurements of the substrate S are available on-line.

Firstly, we present estimation in the case of a full knowledge of specific growth rate

where the gains of Observers 1-3, along with their construction, are given. Secondly, simulation results showing the estimation performances achieved by each observer are presented together in order to provide a clear comparison between them. Finally, we give the adaptive observer along with simulation results for estimation in the case of a partial knowledge of specific growth rate.

8.1 Biomass estimation for known SGR - Observer 1

Consider the biological system described by (7.2). Assuming that the substrate concentration S is measured, and by setting the coordinates of the system as: $x_1 = S$, $x_2 = X$, and $u = D$, we obtain the following state-space representation of system (7.2):

$$\begin{cases} \dot{x}_1 = u(S_{in} - x_1) - Y_s \mu x_2 \\ \dot{x}_2 = (\mu - u) x_2 \\ y = x_1 \end{cases} \quad (8.1)$$

where we use the Monod law (7.3).

The above system can be expressed in the EJO form:

$$\begin{cases} \dot{x} = \Psi_{\alpha\beta}(u, y) x + g(u, y) \\ y = Cx \end{cases} \quad (8.2)$$

where

$$\Psi_{\alpha\beta}(u, y) = J_{\alpha\beta}(u, y) + L_{\alpha\beta}(u, y) C$$

with

$$J_{\alpha\beta}(u, y) = \begin{bmatrix} (\mu - u) & -Y_s \mu \\ 0 & (\mu - u) \end{bmatrix}, \quad L_{\alpha\beta}(u, y) = \begin{bmatrix} -(\mu - u) \\ 0 \end{bmatrix}, \quad C = \begin{bmatrix} 1 & 0 \end{bmatrix}$$

and

$$g(u, y) = \begin{bmatrix} u(S_{in} - x_1) \\ 0 \end{bmatrix}.$$

Here, $\alpha(u, y) = (\mu - u)$ and $\beta(u, y) = -Y_s\mu$.

Firstly, to show that the system is observable, we study the observability matrix, given by

$$\Upsilon(u, y) = \begin{bmatrix} C \\ CF(u, y) \end{bmatrix} = \begin{bmatrix} 1 & 0 \\ 0 & -Y_s\mu \end{bmatrix}. \quad (8.3)$$

It is clear that $\det[\Upsilon(u, y)] = -Y_s\mu$ and it is easily verified that this term is never zero. Firstly, the yield coefficient, Y_s , is a non-zero constant. Secondly, the only situation in which the term $\mu = \frac{\mu_{\max}y}{K_s+y}$ would be zero is if the washout equilibrium were reached. More precisely, the specific growth rate would be zero if all of the micro-organisms were dead. Since this is clearly not an operating range to be considered, the system (8.1) is observable. Moreover, Assumption A5.1) is satisfied in that there exists a set of admissible inputs such that the observability matrix (8.3) is of full rank for all $y \in \mathbb{R}$. In addition, by practical considerations, the functions $g(u, y)$, $\alpha(u, y)$, and $\beta(u, y)$ are all bounded. We can, therefore, using the results of Chapter 5 - Section 5.2, design an observer as follows:

$$\begin{cases} \dot{\hat{x}}_1 = u(S_{in} - x_1) - Y_s\mu\hat{x}_2 + \psi_1(x_1 - \hat{x}_1) \\ \dot{\hat{x}}_2 = (\mu - u)\hat{x}_2 + \psi_2(x_1 - \hat{x}_1) \end{cases}$$

where

$$\widehat{K}(u, y) = \begin{bmatrix} \psi_1 \\ \psi_2 \end{bmatrix} = \beta(u, y)D_{\theta_c}^{-1}K_0 + L_{\alpha\beta}(u, y)$$

with $K_0 = \begin{bmatrix} 2 & 1 \end{bmatrix}^T$. That is,

$$\begin{bmatrix} \psi_1 \\ \psi_2 \end{bmatrix} = \begin{bmatrix} -2Y_s\mu\theta_c - (\mu - u) \\ -Y_s\mu\theta_c^2 \end{bmatrix}$$

with $\theta_c < 0$, since $\beta(u, y) < 0$.

8.2 Adaptive biomass estimation for known SGR

- Observer 2

In this section, a new observer design for the estimation of biomass concentration, using the model (7.2), is presented. Such a model has been employed in [45] and [90] for the estimation of kinetic rates and biomass concentration using high-gain observers. As mentioned in Chapter 1, one of the main shortcomings of high-gain observers is that they have a tendency to amplify measurement noise. Consequently, there is a need to design either low-gain observers or adaptive observers in order to handle measurement noise. Therefore, we propose an observer for the estimation of biomass concentration with an adaptive tuning parameter.

Consider again the biological system (7.2) expressed in its state-space form described by (8.1).

With a slight modification, the resulting system can be expressed in the EJO form:

$$\begin{cases} \dot{x} = \Psi_{\alpha\beta}(u, y)x + g(u, y) \\ y = Cx \end{cases}$$

where

$$\Psi_{\alpha\beta}(u, y) = J_{\alpha\beta}(u, y) + L_{\alpha\beta}(u, y)C$$

with

$$J_{\alpha\beta}(u, y) = \begin{bmatrix} \frac{(\mu-u)}{2} & -Y_s\mu \\ 0 & (\mu-u) \end{bmatrix}, \quad L_{\alpha\beta}(u, y) = \begin{bmatrix} -\frac{(\mu-u)}{2} \\ 0 \end{bmatrix}$$

and C and $g(u, y)$ are as given for (8.2). Here, we have an EJOE form with new $\alpha(u, y) = \frac{(\mu-u)}{2}$ and the same $\beta(u, y) = -Y_s\mu$, with respect to those in (8.2).

Again, by practical considerations, the functions $g(u, y)$, $\alpha(u, y)$, and $\beta(u, y)$ are all bounded. In addition, $\beta(u, y) \neq 0$ for all u and y . We can, therefore, design an observer with an adaptive tuning parameter (given in Chapter 5 - Section 5.3) as follows:

$$\begin{cases} \dot{\hat{x}}_1 = u(S_{in} - x_1) - Y_s\mu\hat{x}_2 + \psi_1(x_1 - \hat{x}_1) \\ \dot{\hat{x}}_2 = (\mu - u)\hat{x}_2 + \psi_2(x_1 - \hat{x}_1) \end{cases} \quad (8.4)$$

where

$$\widehat{K}(u, y) = \begin{bmatrix} \psi_1 \\ \psi_2 \end{bmatrix} = \beta(u, y)D_{\theta_a}^{-1}K_0 + L_{\alpha\beta}(u, y)$$

with $K_0 = \begin{bmatrix} 2 & 1 \end{bmatrix}^T$. Indeed, K_0 is chosen such that the matrix $\bar{A} - K_0C$ is stable where

$$\bar{A} = \begin{bmatrix} 0 & 1 \\ 0 & 0 \end{bmatrix}.$$

The gain vector $\widehat{K}(u, y)$ is then given as

$$\widehat{K}(u, y) = \begin{bmatrix} \psi_1 \\ \psi_2 \end{bmatrix} = \begin{bmatrix} -2Y_s\mu\theta_a - \frac{(\mu-u)}{2} \\ -Y_s\mu\theta_a^2 \end{bmatrix}$$

with $\dot{\theta}_a = \frac{(\mu-u)}{2}\theta_a$ and with $\theta_a(t_0) < 0$, since $\beta(u, y) < 0$.

8.3 Biomass estimation for known SGR using the EJOC transformation method - Observer 3

The previous observer designs presented are for biomass concentration estimation based upon the model (7.2), which is already in EJOC form where the functions $\alpha(u, y)$ and $\beta(u, y)$ are more or less dictated by the system. Now, we consider the transformation of the bioprocess (7.2) into EJOC form, such that we can freely choose the values of $\alpha(u, y)$ and $\beta(u, y)$.

Consider again system (8.1) expressed in the EJOC form (8.2). This system contains functions $\alpha(u, y) = (\mu - u)$ and $\beta(u, y) = -Y_s\mu$. Here, we will use the algorithm given in Chapter 3 - Subsection 3.5.1 to transform the system (8.1) into an EJOC form, where we shall choose $\alpha(u, y) = -\frac{1}{2}$, $\beta(u, y) = 1$ and find the corresponding transformation matrix $M_{\alpha\beta}(u, y)$.

Indeed, it can be shown that

$$M_{\alpha\beta}(u, y) = \begin{bmatrix} 1 & 0 \\ (-\mu + u - \frac{1}{2}) & -Y_s\mu \end{bmatrix}$$

and it can be checked that

$$M_{\alpha\beta}(u, y)\Psi_{\alpha\beta}(u, y)M_{\alpha\beta}^{-1}(u, y) = \Psi_{(-\frac{1}{2}, 1)}(u, y).$$

Consequently, the observer for system (8.1) is given by

$$\begin{cases} \dot{\hat{x}}_1 = u(S_{in} - x_1) - Y_s\mu\hat{x}_2 + \psi_1(x_1 - \hat{x}_1) \\ \dot{\hat{x}}_2 = (\mu - u)\hat{x}_2 + \psi_2(x_1 - \hat{x}_1) \end{cases}$$

where

$$K_{\alpha\beta}(u, y) = \begin{bmatrix} \psi_1 \\ \psi_2 \end{bmatrix} = M_{\alpha\beta}^{-1}(u, y) (\beta(u, y) D_{\theta_c}^{-1} K_0 + L_{\alpha\beta}(u, y))$$

and $K_0 = \begin{bmatrix} 2 & 1 \end{bmatrix}$. That is,

$$\begin{aligned} \psi_1 &= 2\theta_c + 1 + \mu - u \\ \psi_2 &= \frac{(u - \mu - \frac{1}{2})(2\theta_c + 1 + \mu - u)}{\mu Y_s} - \frac{(\theta_c^2 + \frac{u}{2} - \frac{\mu}{2} - \frac{1}{4})}{\mu Y_s} \end{aligned}$$

where $\theta_c > 0$, since $\beta(u, y) > 0$.

8.4 Simulations for known specific growth rate

Here, we evaluate each observer in simulation under various operating conditions, showing the performances for four sets of nominal parameter values both in the absence and in the presence of measurement noise. The consideration of the different sets is concerned with the influence of different initial concentrations of substrate and biomass, and also the influence of the value of yield coefficient Y_s . For the sake of brevity, the results of Set 1 are presented here and the results of Sets 2-4 can be seen in Appendix A where it will be found that the results follow the same format as given in this section. The parameter values used are given in each case presented.

Equilisation basins are often used in conjunction with pumps and other flow control equipment in wastewater treatment systems to dampen the effects of harsh influent flow rate changes. The aim is to have a constant flow rate and dampened variations in influent pollutant concentrations. Therefore, we also show the performance of each observer under different influent conditions for each set of parameters considered. In fact, only some of these different influent characteristics are considered in the literature. Generally, either a

constant, a step or a square wave with time periods of the order of days are used to represent the dilution rate D .

In this work, three profiles of dilution rate are taken into account. Indeed, we show the performances of the observers when considering a constant dilution rate, a stepping dilution rate, and a typical influent flow rate profile of domestic wastewater treatment plants. The profiles of varying dilution rates used are based upon typical hourly variations found in domestic wastewater treatment plants [91], which can be seen in Figure 8-1. The daily profiles used for the stepping and typical dilution rates are given in Figures 8-2 and 8-3, respectively.

For each dilution rate considered in each set of parameters, we also consider a constant and varying influent substrate concentration S_{in} . Where a varying influent substrate concentration is considered, the daily profile used is as shown in Figure 8-4.

It is important to consider such a variety of scenarios, especially since the gains of each observer each contain the terms μ , Y_s , and D , and will more noticeably affect the performance in the presence of measurement noise. Indeed, as previously stated, one of the aims of this work is to also consider the performance of the proposed estimation strategies in the presence of measurement noise. To do this, a further set of simulations have been conducted where the output in these cases is of the form $y = S + \epsilon$ where ϵ is an additive noise. Amplitudes of ϵ considered are equal to 5% and 10% of the measured value S and are typically considered in the literature [47], [85].

The choice of parameter values used is based upon those typically found in the literature [32], [44], [45], [47], [85], and in WWT plants [91].

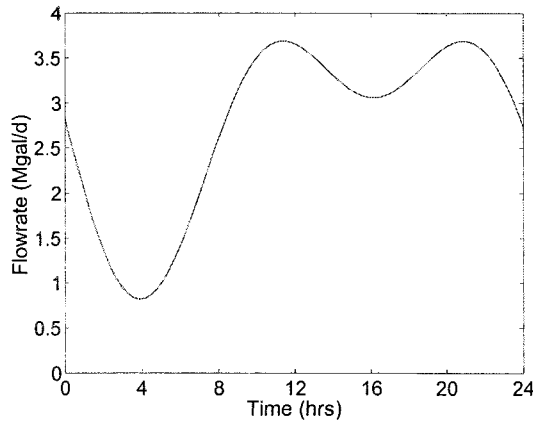


Figure 8-1: Typical hourly variations in domestic wastewater flow rates

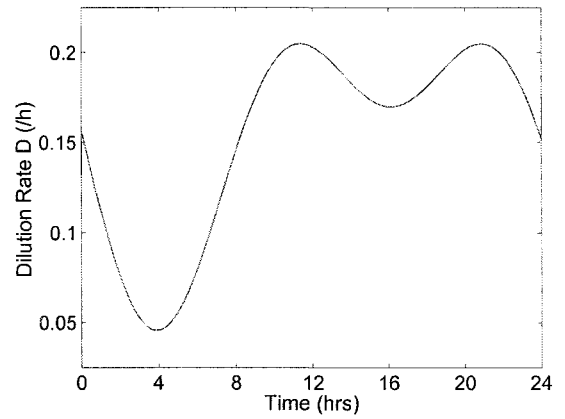


Figure 8-3: Varying dilution rate profile based upon typical hourly variations in domestic wastewater flow rates

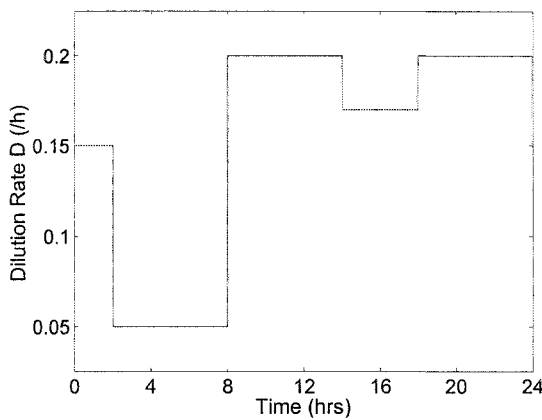


Figure 8-2: Stepping dilution rate profile based upon typical hourly variations in domestic wastewater flow rates

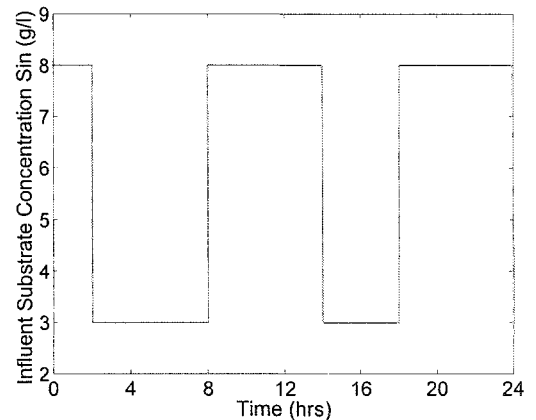


Figure 8-4: Stepping influent substrate concentration S_{in}

8.4.1 Estimation under clean measurement - Parameter Set 1

The parameter values used in Set 1 are given in Table 8.1.

$X(0) = 2.4g/l$	$K_s = 4g/l$
$\hat{X}(0) = 0g/l$	$Y_s = 3$
$S(0) = \hat{S}(0) = 0.8g/l$	$k_1 = 2$
$\mu_{max} = 0.3h^{-1}$	$k_2 = 1$

Table 8.1: Set 1 parameter values

The tuning parameters used for Observers 1-3 for estimation under clean measurement are summarised in Table 8.2. For Observer 3, a choice of $\alpha(u, y) = -\frac{1}{2}$ is used. Note CS_{in} : Constant S_{in} ; SS_{in} : Stepping S_{in} .

Figures 8-5 to 8-10 show the performance of Observer 1. It can be verified that these convergence performances can also easily be achieved when using either Observer 2 or Ob-

Observer		D Constant	D Stepping	D Typical
1	CS_{in}	$\theta_c = -3$	$\theta_c = -3$	$\theta_c = -3$
	SS_{in}	$\theta_c = -3$	$\theta_c = -3$	$\theta_c = -3$
2	CS_{in}	$\theta_a(0) = -3.7$	$\theta_a(0) = -3.7$	$\theta_a(0) = -3.7$
	SS_{in}	$\theta_a(0) = -3.3$	$\theta_a(0) = -3.3$	$\theta_a(0) = -3.3$
3	CS_{in}	$\theta_c\beta = 0.075$	$\theta_c\beta = 0.075$	$\theta_c\beta = 0.075$
	SS_{in}	$\theta_c\beta = 0.1$	$\theta_c\beta = 0.06$	$\theta_c\beta = 0.08$

Table 8.2: Observer tuning parameter values - Set 1

server 3. However, for the sake of brevity, those results are not shown here. Instead, to give an appreciation of the effort required of each observer gain, which results in the same performance, we show and compare the profiles of gain ψ_2 of each observer. These profiles are shown in Figures 8-11 to 8-16.

Observer 1 - Constant S_{in}

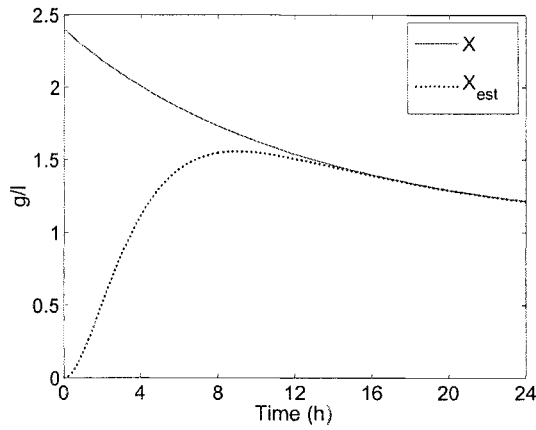


Figure 8-5: Performance of Observer 1 for parameter Set 1 with constant $S_{in} = 5g/l$ and constant $D = 0.1h^{-1}$

Observer 1 - Stepping S_{in}

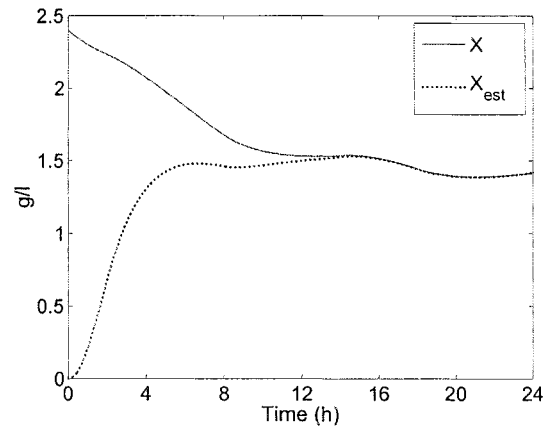


Figure 8-8: Performance of Observer 1 for parameter Set 1 with stepping S_{in} and constant $D = 0.1h^{-1}$

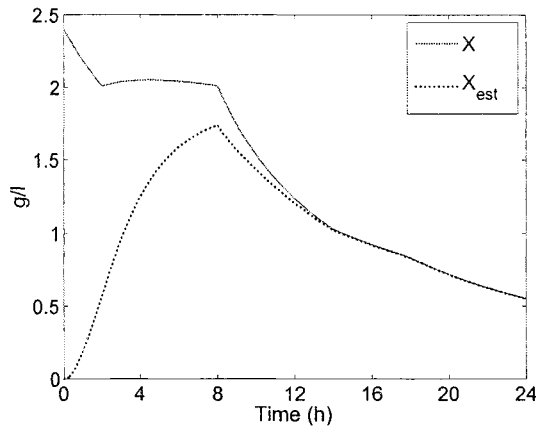


Figure 8-6: Performance of Observer 1 for parameter Set 1 with constant $S_{in} = 5g/l$ and stepping D

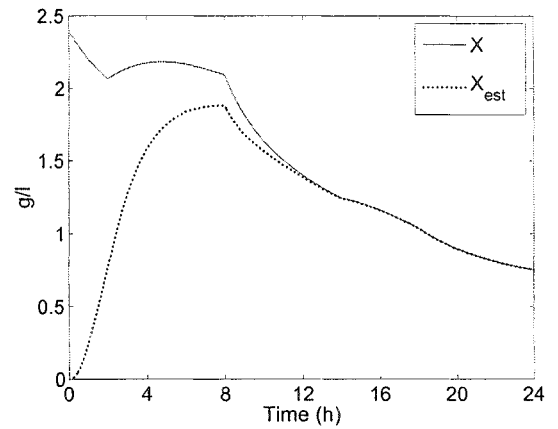


Figure 8-9: Performance of Observer 1 for parameter Set 1 with stepping S_{in} and stepping D

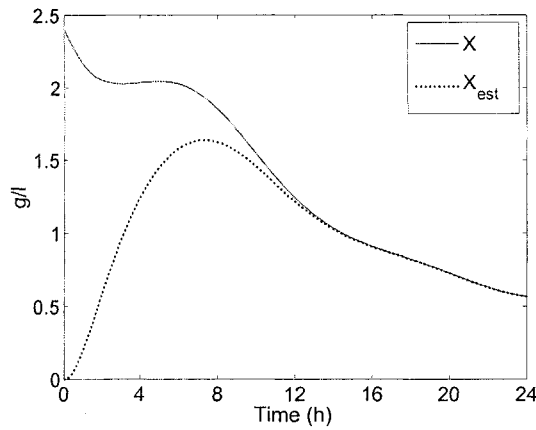


Figure 8-7: Performance of Observer 1 for parameter Set 1 with constant $S_{in} = 5g/l$ and typical D

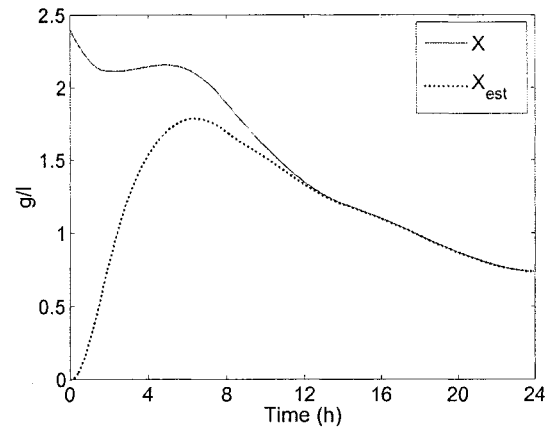


Figure 8-10: Performance of Observer 1 for parameter Set 1 with stepping S_{in} and typical D

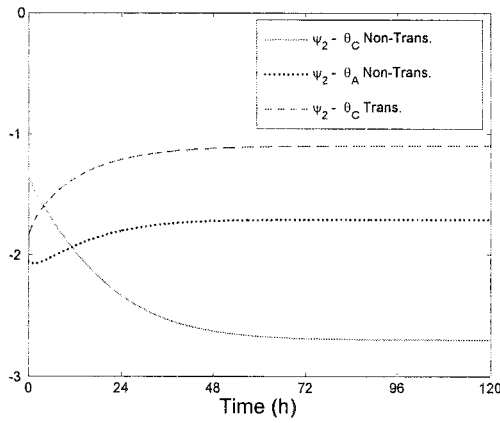


Figure 8-11: Profiles of ψ_2 of each observer for constant $S_{in} = 5g/l$ and constant $D = 0.1h^{-1}$

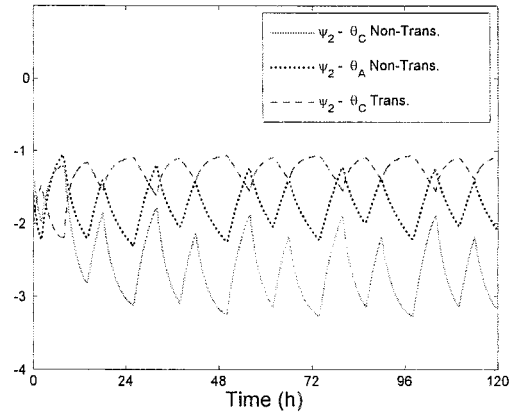


Figure 8-14: Profiles of ψ_2 of each observer for stepping S_{in} and constant $D = 0.1h^{-1}$

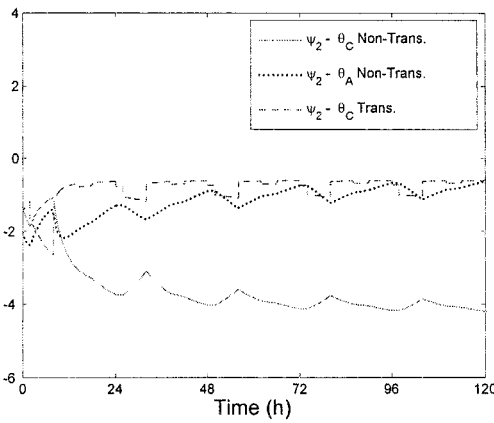


Figure 8-12: Profiles of ψ_2 of each observer for constant $S_{in} = 5g/l$ and stepping D

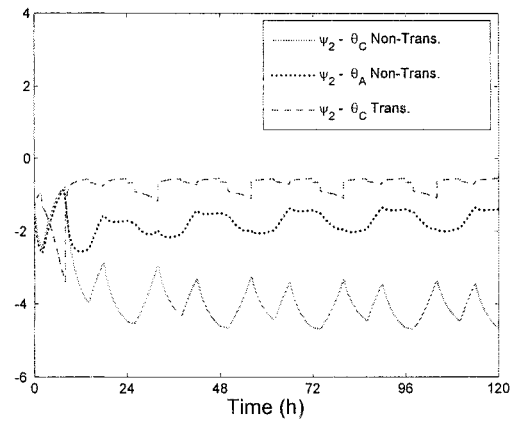


Figure 8-15: Profiles of ψ_2 of each observer for stepping S_{in} and stepping D

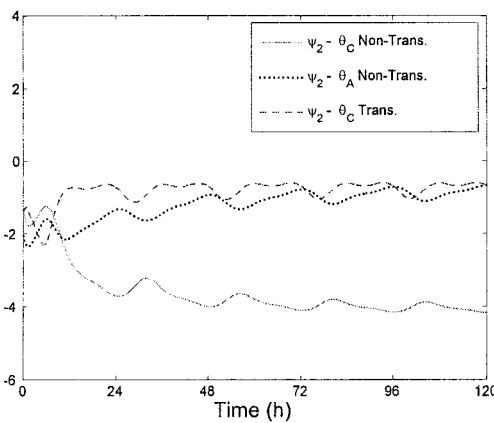


Figure 8-13: Profiles of ψ_2 of each observer for constant $S_{in} = 5g/l$ and typical D

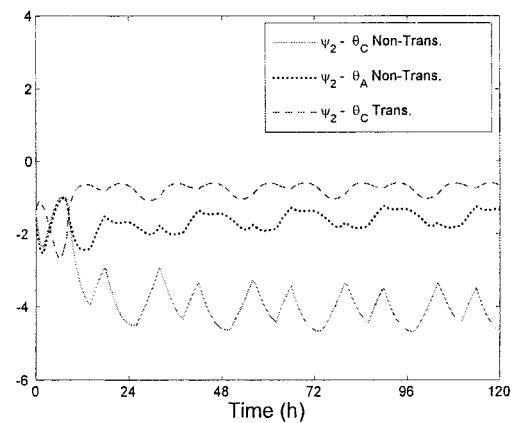


Figure 8-16: Profiles of ψ_2 of each observer for stepping S_{in} and typical D

Concluding remarks 7

The observers were tuned to give the same convergence performances in order to compare the gains of each. For parameter Sets 1 and 2, where the lower initial substrate concentration is considered, it is evident that the gain ψ_2 with the overall highest magnitudes are yielded by Observer 1. For the same parameter sets, the adaptive tuning parameter θ_a of Observer 2 varies accordingly with changes in magnitude and polarity of $\alpha(u, y)$ and often results in a decreasing gain ψ_2 of much lower magnitudes than those of Observer 1. However, for Sets 1 and 2 the gain ψ_2 is lowest when using Observer 3. This actually illustrates the main advantage of Observer 3, especially compared with Observer 1, in that a constant tuning parameter can be used that does not have to be excessively high to ensure stable error dynamics. This flexibility is due to the transformation of the system at hand into the EIOC form, providing additional degrees of freedom in tuning the observer. However, this advantage is only true for parameter Sets 1 and 2, since in Sets 3 and 4 it is seen that Observer 3 yields ψ_2 with the largest magnitudes. Indeed, it is shown in parameter Set 3, where the higher initial substrate concentration is considered with high yield coefficient, that the magnitude of gain ψ_2 is the lowest when using Observer 2. The results for parameter Set 4, where the higher initial substrate concentration is considered with low yield coefficient, show that gain ψ_2 is lowest when using Observers 1 or 2. Indeed, where the profiles of ψ_2 of Observers 1 and 2 are very similar, we have chosen a constant $\theta_a = \theta_c$. The reason for such a choice is due to the fact that the adaptive tuning parameter, in this case, would have otherwise grown in magnitude, and although we could have allowed θ_a to ramp up to the constant value, the same convergence time would not have been attained.

It is clear from the simulation results that very good performances are achieved when using any of the proposed Observers 1-3 for each set of parameters and different influent characteristics. It should be noted that in each case, a faster convergence performance can

be attained through choosing a larger magnitude of observer tuning parameter. However, the best overall performances, with regards to the use of efficient gains, are those of Observer 2. This discussion of gain magnitudes leads us on to the evaluation of the observers in the presence of measurement noise.

8.4.2 Estimation under noisy measurement - Parameter Set 1

The parameter values used in Set 1 are given in Table 8.1. For this set of values, we consider an additive noise ϵ with amplitudes equal to 5% of the measured value S . We also show the performances of Observers 2 and 3 for an additive noise ϵ with amplitudes equal to 10% of the measured value S .

The tuning parameter values used for Observers 1, 2, and 3 are shown in Table 8.3. Note, no limits were required in this case for the adaptive tuning parameter θ_a . Also note CS_{in} : Constant S_{in} ; SS_{in} : Stepping S_{in} .

Observer		D Constant	D Stepping	D Typical
1	CS_{in}	$\theta_c = -3$	$\theta_c = -3$	$\theta_c = -3$
	SS_{in}	$\theta_c = -3$	$\theta_c = -3$	$\theta_c = -3$
2	CS_{in}	$\theta_a(0) = -3.7$	$\theta_a(0) = -3.7$	$\theta_a(0) = -3.7$
	SS_{in}	$\theta_a(0) = -3.3$	$\theta_a(0) = -3.3$	$\theta_a(0) = -3.3$
3	CS_{in}	$\theta_c\beta = 0.075$	$\theta_c\beta = 0.075$	$\theta_c\beta = 0.075$
	SS_{in}	$\theta_c\beta = 0.1$	$\theta_c\beta = 0.06$	$\theta_c\beta = 0.08$

Table 8.3: Tuning parameter values under noisy measurement - Set 1

Constant S_{in} & constant D

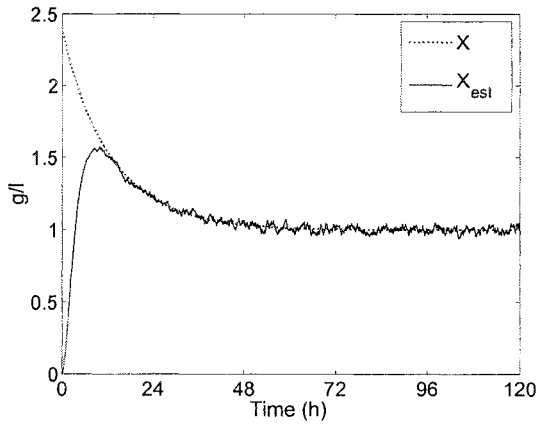


Figure 8-17: Performance of Observer 1 for 5% measurement noise

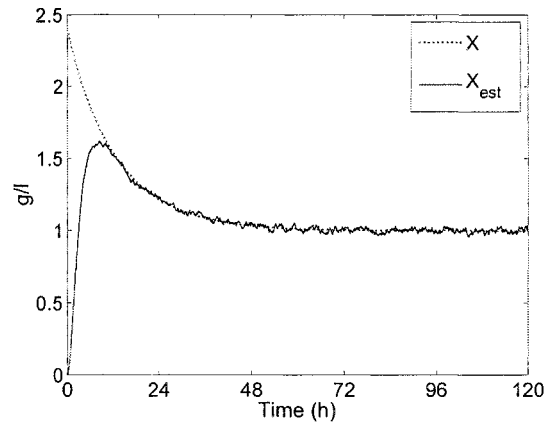


Figure 8-18: Performance of Observer 2 for 5% measurement noise

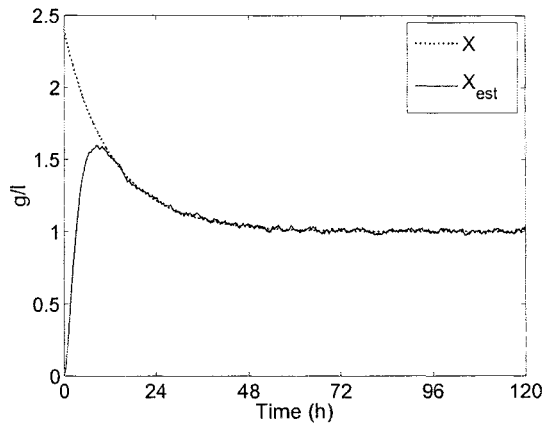


Figure 8-19: Performance of Observer 3 for 5% measurement noise

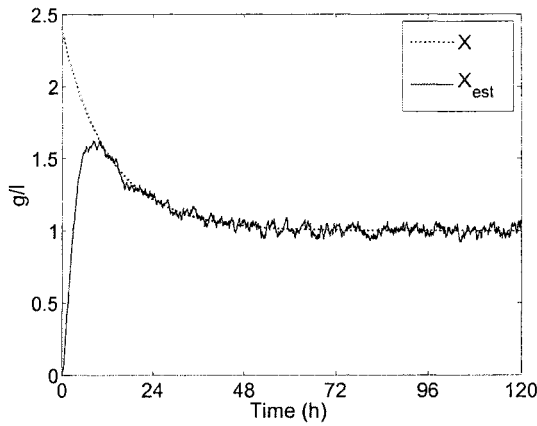


Figure 8-20: Performance of Observer 2 for 10% measurement noise

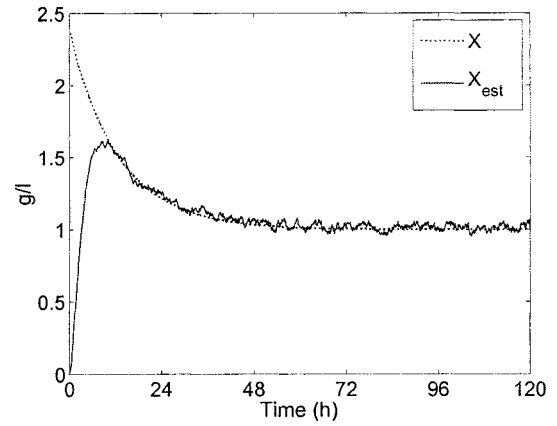


Figure 8-21: Performance of Observer 3 for 10% measurement noise

Constant S_{in} & stepping D

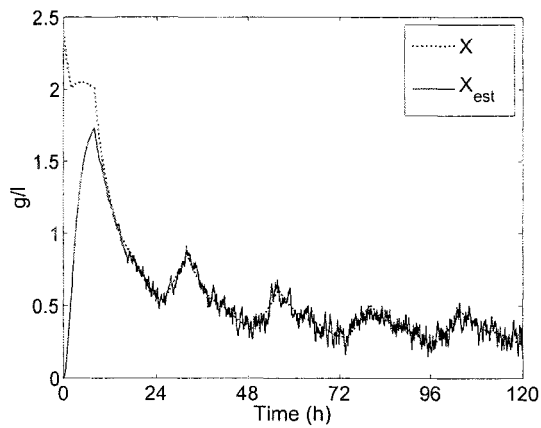


Figure 8-22: Performance of Observer 1 for 5% measurement noise

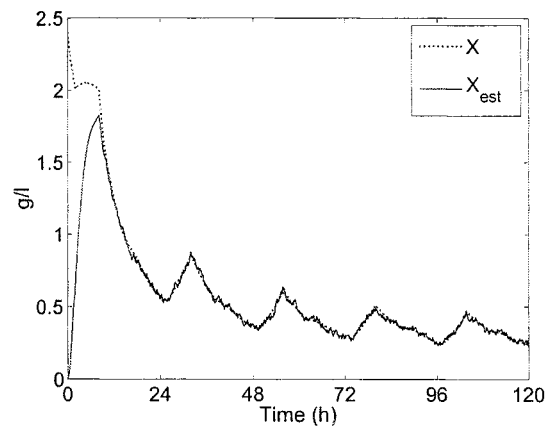


Figure 8-23: Performance of Observer 2 for 5% measurement noise

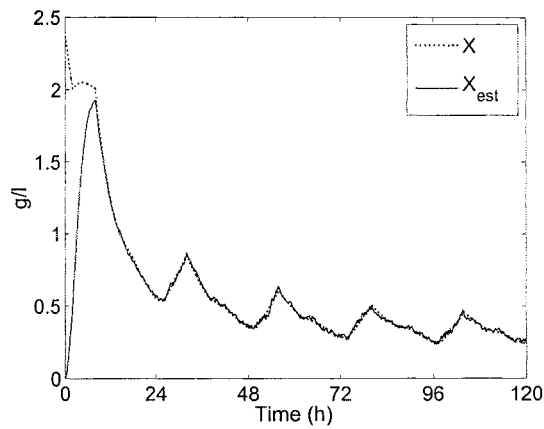


Figure 8-24: Performance of Observer 3 for 5% measurement noise

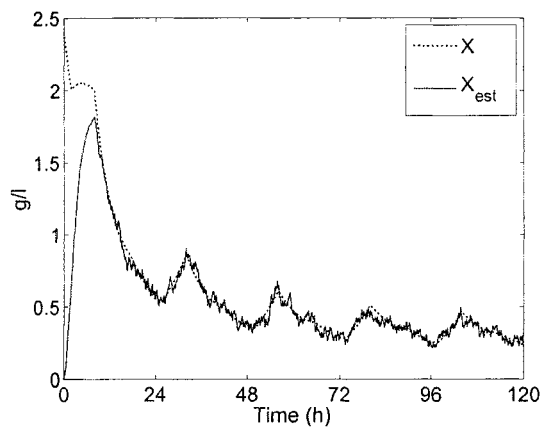


Figure 8-25: Performance of Observer 2 for 10% measurement noise

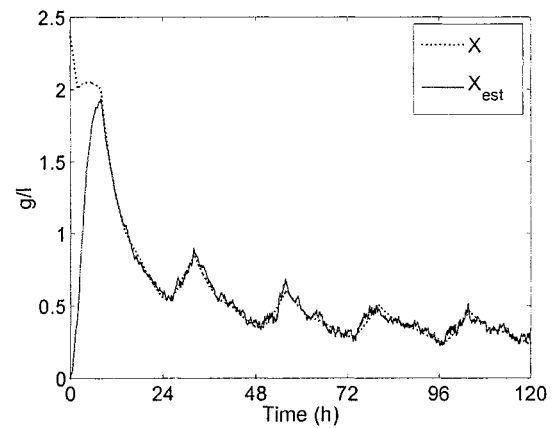


Figure 8-26: Performance of Observer 3 for 10% measurement noise

Constant S_{in} & typical D

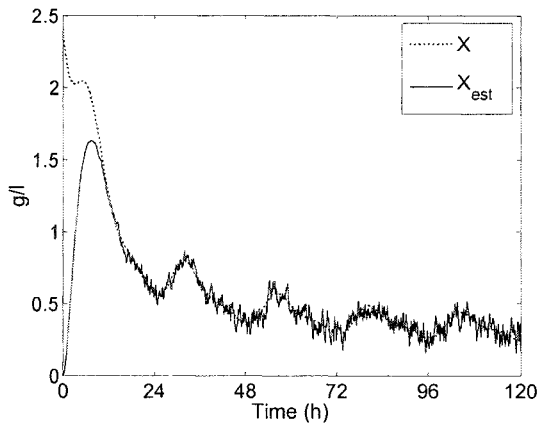


Figure 8-27: Performance of Observer 1 for 5% measurement noise

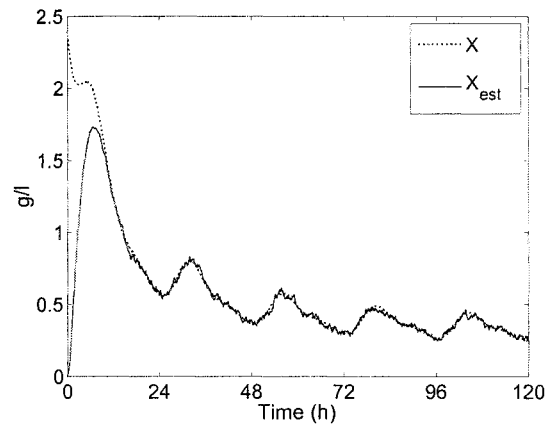


Figure 8-28: Performance of Observer 2 for 5% measurement noise

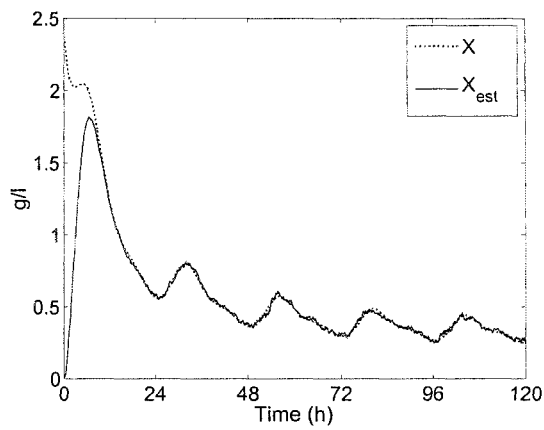


Figure 8-29: Performance of Observer 3 for 5% measurement noise

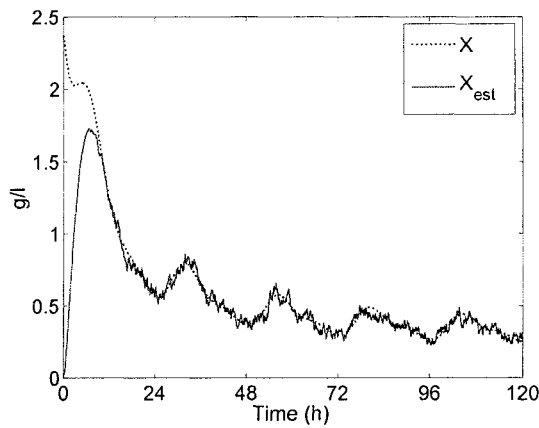


Figure 8-30: Performance of Observer 2 for 10% measurement noise

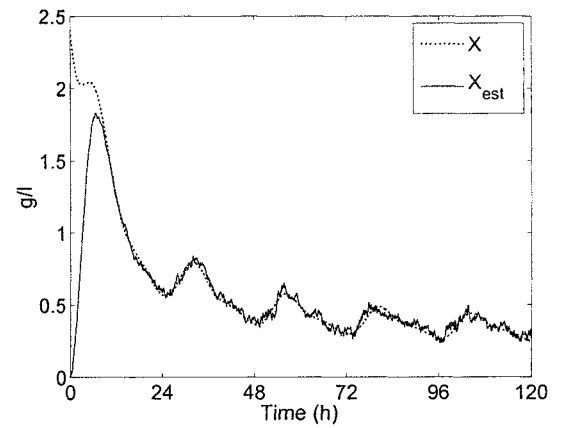


Figure 8-31: Performance of Observer 3 for 10% measurement noise

Stepping S_{in} & constant D

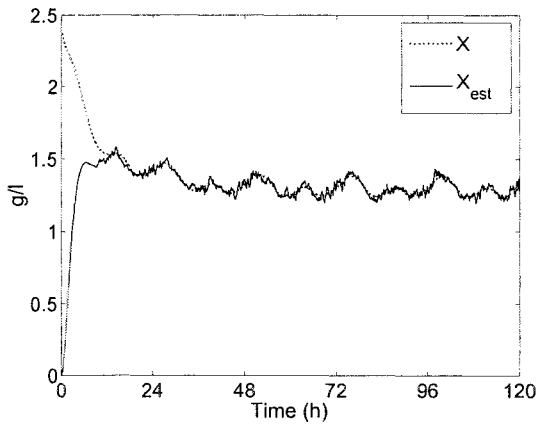


Figure 8-32: Performance of Observer 1 for 5% measurement noise

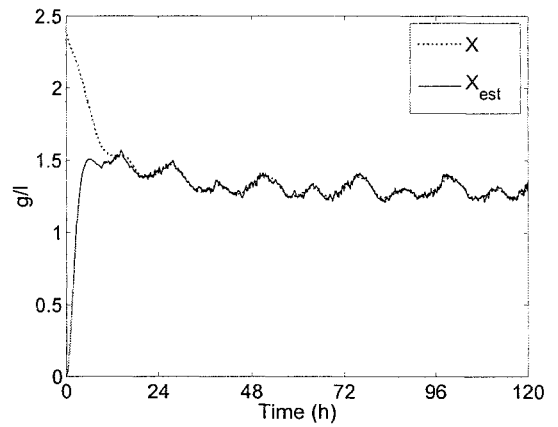


Figure 8-33: Performance of Observer 2 for 5% measurement noise

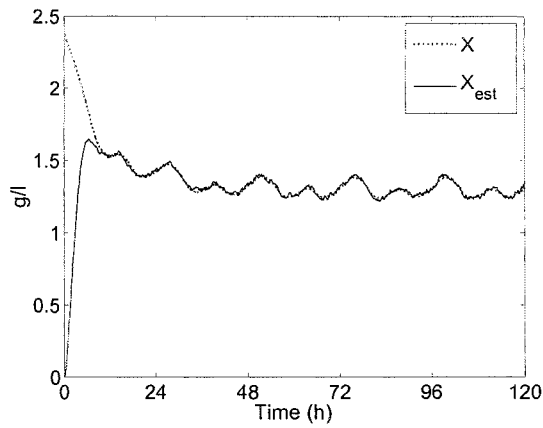


Figure 8-34: Performance of Observer 3 for 5% measurement noise

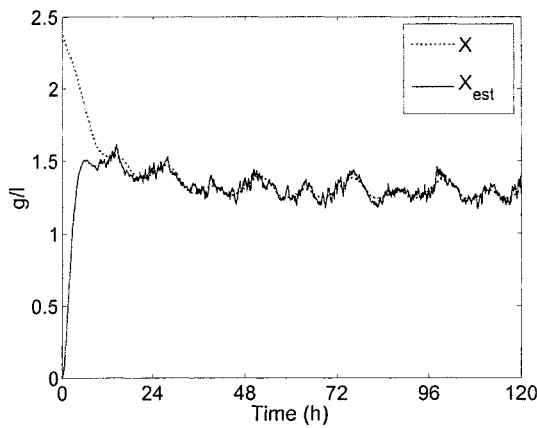


Figure 8-35: Performance of Observer 2 for 10% measurement noise

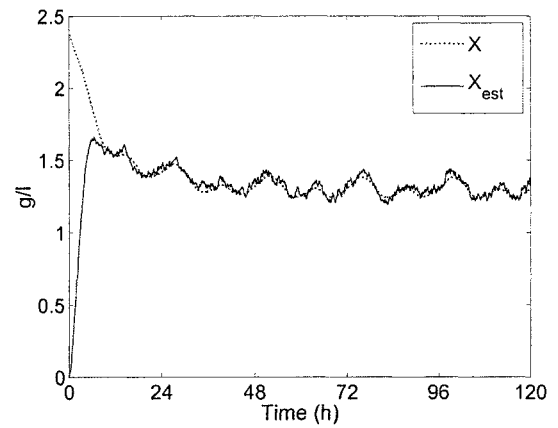


Figure 8-36: Performance of Observer 3 for 10% measurement noise

Stepping S_{in} & stepping D

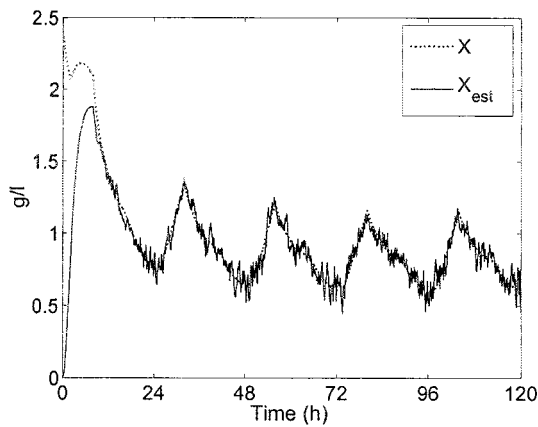


Figure 8-37: Performance of Observer 1 for 5% measurement noise

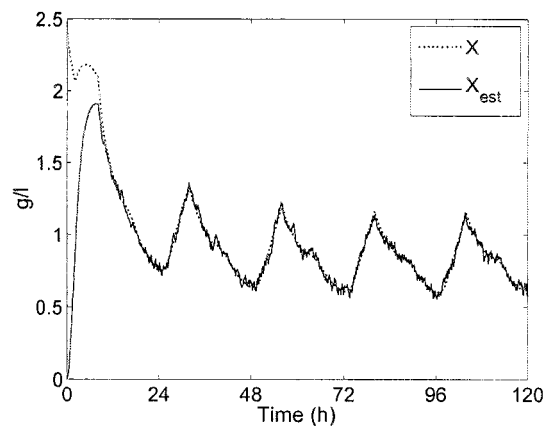


Figure 8-38: Performance of Observer 2 for 5% measurement noise

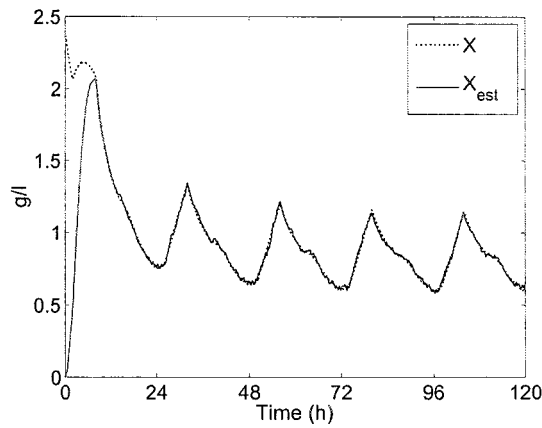


Figure 8-39: Performance of Observer 3 for 5% measurement noise

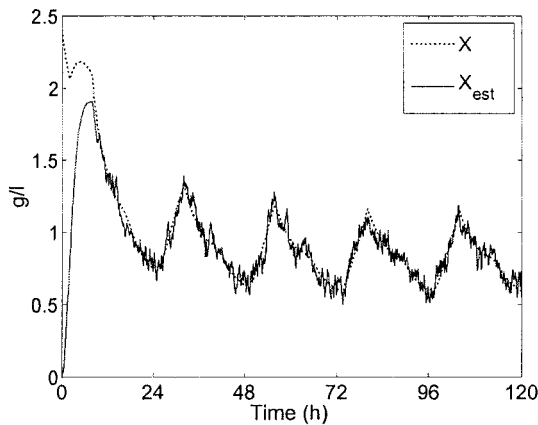


Figure 8-40: Performance of Observer 2 for 10% measurement noise

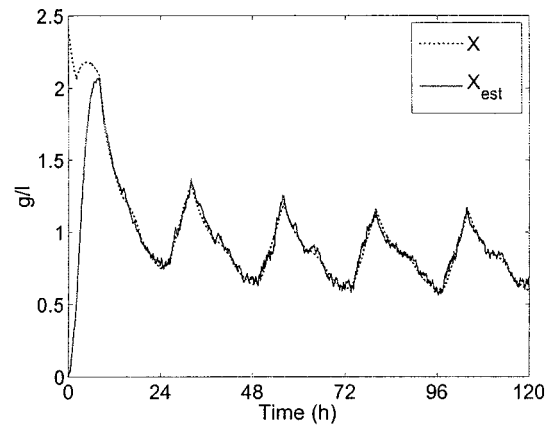


Figure 8-41: Performance of Observer 3 for 10% measurement noise

Stepping S_{in} & typical D

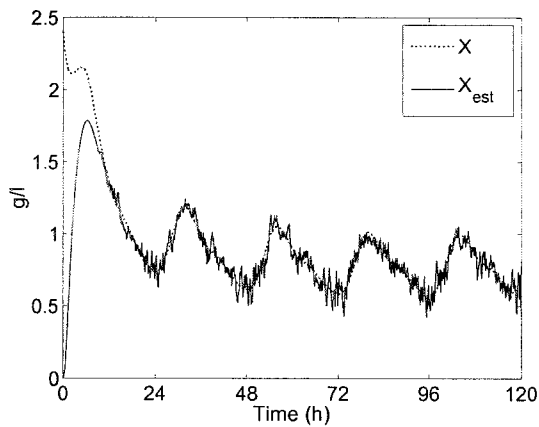


Figure 8-42: Performance of Observer 1 for 5% measurement noise

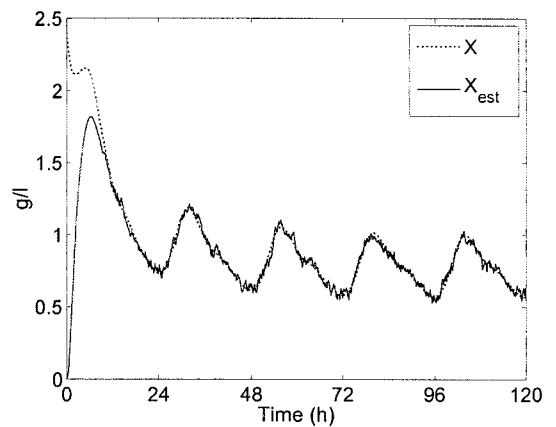


Figure 8-43: Performance of Observer 2 for 5% measurement noise

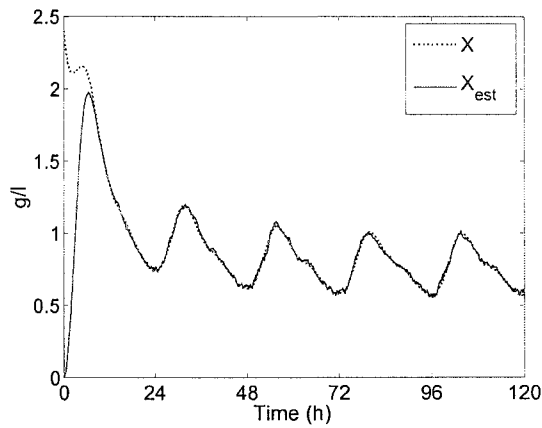


Figure 8-44: Performance of Observer 3 for 5% measurement noise

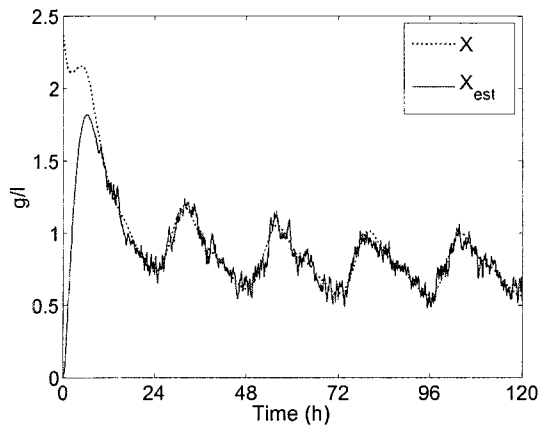


Figure 8-45: Performance of Observer 2 for 10% measurement noise

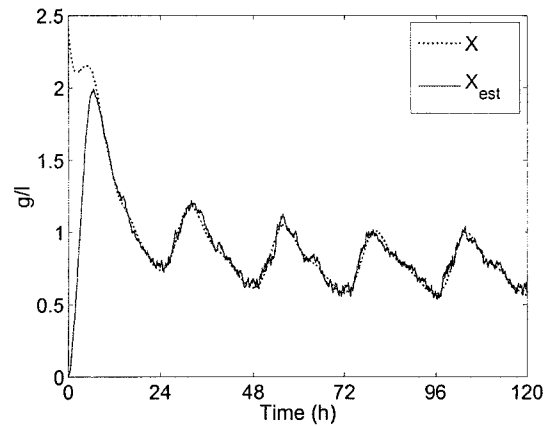


Figure 8-46: Performance of Observer 3 for 10% measurement noise

Concluding remarks 8

It is clear from the simulation results that very good performances are achieved for each set of parameters (see Appendix A) and different influent characteristics when using any of the proposed Observers 1-3 in the presence of measurement noise. When considering noise with amplitudes equal to 5% of that of the measured substrate concentration, the worst estimation performances are yielded under parameter Set 1 for the cases of stepping and typical dilution rates. Under this set, Observer 1 gives estimations containing noise with amplitudes of up to 30% of the simulated noise-free biomass profile for stepping and constant influent substrate concentrations, respectively. However, for similar convergence times, the best overall performances with regards to the presence of noise in the estimations are distinctly yielded from Observers 2 and 3. In fact, for the same parameter values and influent flow conditions under which Observer 1 yields the worst performances, those yielded from Observers 2 and 3 contain noise with amplitudes of less than 5% of the simulated real biomass concentration. This is not surprising when considering the profiles of their gains in the case of estimation under clean measurement. In most cases (see Sets 1, 3 and 4), these two observers provide estimations containing noise with amplitudes of less than 4% of the simulated noise-free biomass profile and in some cases less than 2%, whilst attaining convergence times of 12 hours. It seems that Observer 3 is particularly well-suited for parameter Sets 1 and 2, giving slightly better results than Observer 2. However, Observer 2 performs well for any of the parameter sets considered. It was, in fact, intended that the adaptive nature of this observer would improve the estimation performance when considering measurement noise. Indeed, Observer 2 out-performs Observer 3 in parameter Sets 3 and 4 where convergence times of the former estimation profiles are quicker by up to 8 hours and contain lower amplitudes of noise. It should also be noted that for parameter Sets 3 and 4, Observer 1 produces good estimation profiles containing noise with amplitudes of less than 5% of the simulated real

biomass concentration.

When considering measurement noise with amplitudes equal to 10% of that of the measured substrate concentration, the estimation profiles given by Observers 2 and 3 contain noise with amplitudes of less than 10% of the simulated noise-free biomass profile with convergence attained around 12 hours.

Since there are very few results in the literature that consider measurement noise in the estimation of biomass concentration, it is difficult to make accurate comparisons. However, it can be noted that recent biomass estimation results from leading researchers in this field [46] and [85] consider an additive noise with amplitudes of 5% of that of the measured value for partially known specific growth rates, and similar parameter values used herein. With regards to a percentage of the noise-free profiles, the resulting estimations contain noise with amplitudes of 10% [46] and 5% [85] and convergence to offsets is achieved in around 50 hours. In addition, it should be highlighted that performances of Observers 2 and 3 are better than those of constant high-gain observers, which tend to amplify measurement noise. For example, a high-gain observer is illustrated in [45] where an additive noise with average amplitudes of 10% of the measurement is considered. Although the convergence is achieved in less than 5 hours, the resulting biomass estimation contains noise of growing amplitudes up to 15% of the simulated biomass profile. In fact, performance is shown for 30 hours only at which point it seems the noise continues to grow.

We conclude that the adaptive tuning parameter observer gives the best overall performance for the various parameter values considered, where in some cases the noise has been attenuated by factors of up to five. It should also be noted that better performance with respect to noise can be attained through a compromise with convergence times. This is actually illustrated in the next section where we show the performance of Observer 4 where only a partial knowledge of the specific growth rate is assumed.

8.5 Adaptive biomass estimation for partially known specific growth rate - Observer 4

Here, we show the performance of Observer 4 for the case of biomass estimation with only a partial knowledge of the specific growth rate. It is assumed that the structure of the specific growth rate is known, but that not all parameters of the model used are perfectly known. The model used is the Monod law, where it is assumed that some nominal value of $\mu_{\max} = \hat{\mu}_{\max}$ is known so that we can decompose μ as follows:

$$\begin{aligned}\mu &= \frac{\hat{\mu}_{\max} S}{K_s + S} + \left[\frac{\mu_{\max} S}{K_s + S} - \frac{\hat{\mu}_{\max} S}{K_s + S} \right] \\ &= \mu_0 + \delta\mu\end{aligned}$$

where μ_0 is the known nominal part and $\delta\mu$ is unknown. Then, the system (7.2) is expressed as

$$\begin{cases} \dot{S} = D(S_{in} - S) - Y_s(\mu_0 + \delta\mu)X \\ \dot{X} = (\mu_0 + \delta\mu)X - DX \end{cases} \quad (8.5)$$

Using the same change of variables as before: $x_1 = S$, $x_2 = X$, and $u = D$, we obtain the following state-space representation of system (8.5):

$$\begin{cases} \dot{x}_1 = -Y_s(\mu_0 + \delta\mu)x_2 + u(S_{in} - x_1) \\ \dot{x}_2 = (\mu_0 + \delta\mu - u)x_2 \\ y = x_1 \end{cases} \quad (8.6)$$

The above system can be expressed as

$$\begin{cases} \dot{x} = (F(u, y) + \Delta F(u, y))x + g(u, y) \\ y = Cx \end{cases}$$

where

$$F(u, y) = J_{\alpha\beta}(u, y) + L_{\alpha\beta}(u, y)C$$

with

$$J_{\alpha\beta} = \begin{bmatrix} \frac{(\mu_0 - u)}{2} & -Y_s \mu_0 \\ 0 & (\mu_0 - u) \end{bmatrix}, \quad L_{\alpha\beta} = \begin{bmatrix} \frac{-(\mu_0 - u)}{2} \\ 0 \end{bmatrix}$$

and C and $g(u, y)$ are as given in (8.2). The unknown portions are given in

$$\Delta F(u, y) = \begin{bmatrix} 0 & -Y_s \delta\mu \\ 0 & \delta\mu \end{bmatrix}.$$

Here, $\alpha(u, y) = \frac{(\mu_0 - u)}{2}$ and $\beta(u, y) = -Y_s \mu_0$.

In such a case, using the result of Chapter 5 - Section 5.5, the observer of the above uncertain system is given by

$$\begin{cases} \dot{\hat{x}}_1 = -Y_s \mu_0 \hat{x}_2 - Y_s \bar{\mu}_0 \hat{x}_2 + u(S_{in} - x_1) + \psi_1(x_1 - \hat{x}_1) \\ \dot{\hat{x}}_2 = (\mu_0 - u) \hat{x}_2 + \bar{\mu}_0 \hat{x}_2 + \psi_2(x_1 - \hat{x}_1) \end{cases}$$

where $\bar{\mu}_0$ is an approximation of the unknown portion $\delta\mu$ and

$$\hat{K}(u, y) = \begin{bmatrix} \psi_1 \\ \psi_2 \end{bmatrix} = \begin{bmatrix} -2Y_s (\mu_0 + \bar{\mu}_0) \theta_a - \frac{((\mu_0 + \bar{\mu}_0) - u)}{2} \\ -Y_s (\mu_0 + \bar{\mu}_0) \theta_a^2 \end{bmatrix}$$

with

$$\dot{\theta}(t) = \frac{((\mu_0 + \bar{\mu}_0) - u)}{2} \theta_a(t); \quad \theta_a(t_0) < 0.$$

8.6 Simulations for partially known specific growth rate

We now show the performance of Observer 4 where we assume only a partial knowledge of the specific growth rate μ . More precisely, we assume the structure of μ is of the form given by the Monod law (7.3) and that the maximum specific growth rate parameter μ_{\max} is not perfectly known. In the model of the bioprocess, we use $\mu_{\max} = 0.3h^{-1}$, and assume that we know that μ_{\max} is somewhere around this value, but we don't know the exact value. However, from a knowledge of the bioprocess, we assume that we know μ_{\max} is at least $0.15h^{-1}$ and

at the most is $0.45h^{-1}$, i.e. $\pm 50\%$ of μ_{\max} . Therefore, for the negative unknown case, we use a nominal known value $\mu_{0\max}^- = 0.15h^{-1}$, and for the positive unknown case, we use a nominal known value $\mu_{0\max}^+ = 0.45h^{-1}$. We then make an estimate of what the unknown portions are. For the negative unknown case, we use an estimate of $\bar{\mu}_{0\max}^- = +0.06h^{-1}$, and for the positive unknown case, we use an estimate of $\bar{\mu}_{0\max}^+ = -0.06h^{-1}$. Therefore, in the observer we use values of $\pm 30\%$ of μ_{\max} .

Using Observer 4 for the positive error on μ_{\max} will give an estimation profile with a negative error with respect to the real biomass concentration. Similarly, using Observer 4 for the negative error on μ_{\max} will give an estimation profile with a positive error with respect to the real biomass concentration. In fact, if two observers of the form of Observer 4 are used, one with a positive and one with a negative error on μ_{\max} , then the uncertainty in the biomass estimation will have a definite bound. This is what is shown in the following simulation results. In fact, for the positive error on μ_{\max} , we use Observer 4 with a constant $\theta_a = \theta_c$, and for the negative error on μ_{\max} , we use an adaptive θ_a . The choice of $\theta_a = \theta_c$ is due to the fact that in the case of a positive error on μ_{\max} , we would have $\dot{\theta}_a > 0$. An increasing tuning parameter could be used with a maximum bound, but for illustration purposes it is not deemed necessary here.

For the sake of brevity, we do not consider all of the scenarios as in the known case. Instead, we present the performance of Observer 4 under parameter Sets 1 and 2 for constant, stepping, and typical dilution rates, and using a stepping influent substrate concentration, the profiles of which are as given in the previous section. We also consider estimation both in the absence and in the presence of measurement noise for amplitudes equal to 5% and 15% of the measured value of substrate concentration S .

8.6.1 Estimation under clean measurement - Parameter Set 1

The fixed system parameter values used are as given in Table 8.1. In all cases, the tuning parameter values used are given in Table 8.4.

	Positive unknown	Negative unknown
D Constant	$\theta_a(0) = -1.1, \theta_{\min} = -1.1$	$\theta_a(0) = -4, \theta_{\min} = -1.6$
D Stepping	$\theta_a(0) = -0.8, \theta_{\min} = -0.8$	$\theta_a(0) = -3, \theta_{\min} = -1$
D Typical	$\theta_a(0) = -0.8, \theta_{\min} = -0.8$	$\theta_a(0) = -3, \theta_{\min} = -1$

Table 8.4: Observer 4 tuning parameter values for the partially known case - Set 1

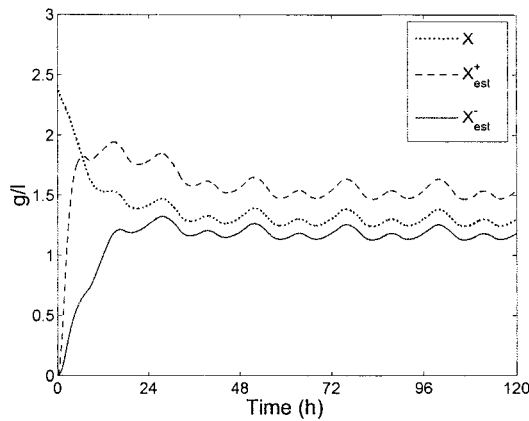


Figure 8-47: Biomass estimation for partially known μ with constant $D = 0.1h^{-1}$ under clean measurement

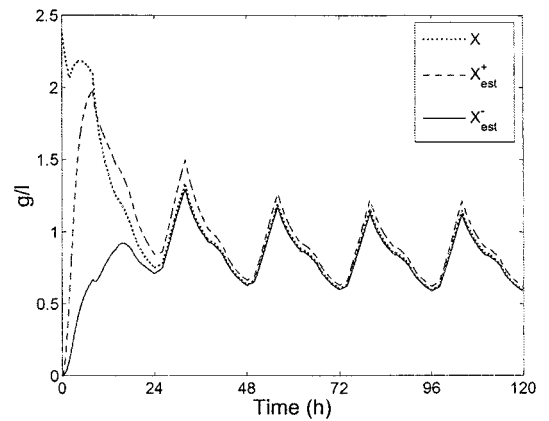


Figure 8-48: Biomass estimation for partially known μ with stepping D under clean measurement

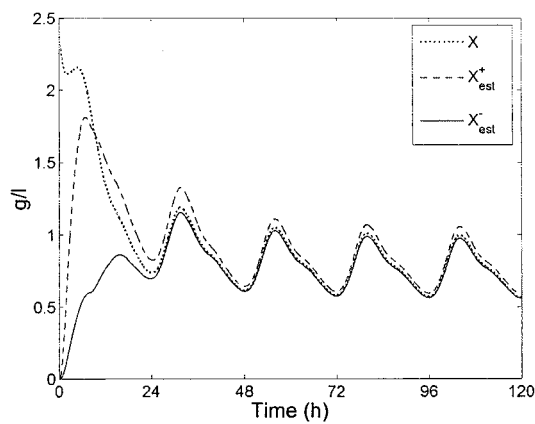


Figure 8-49: Biomass estimation for partially known μ with typical D under clean measurement

8.6.2 Estimation under noisy measurement - Parameter Set 1

The parameter values used are as given in Table 8.1, and the tuning parameter values used are given in Table 8.4.

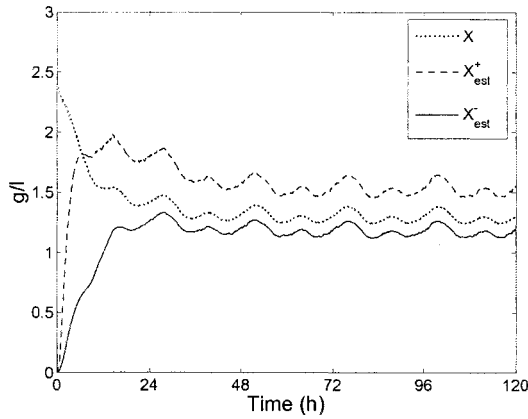


Figure 8-50: Biomass estimation for partially known μ with constant $D = 0.1 h^{-1}$ for 5% measurement noise

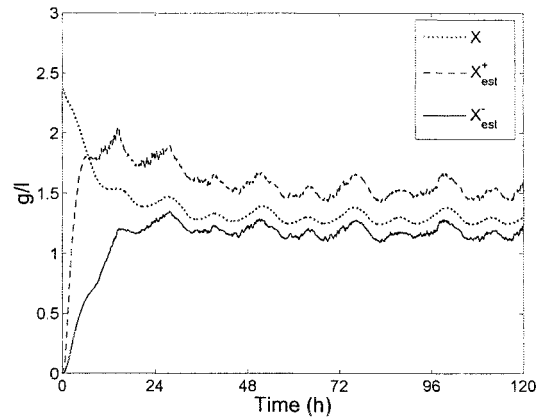


Figure 8-53: Biomass estimation for partially known μ with constant $D = 0.1 h^{-1}$ for 15% measurement noise

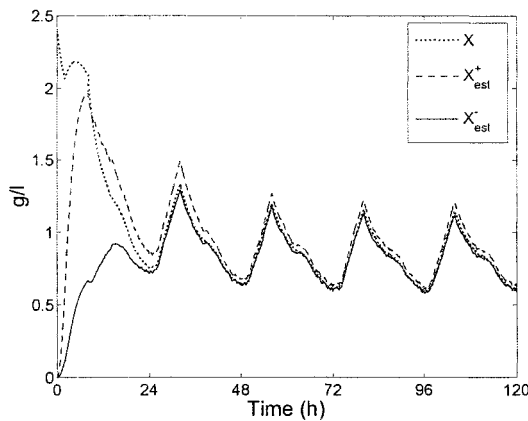


Figure 8-51: Biomass estimation for partially known μ with stepping D for 5% measurement noise

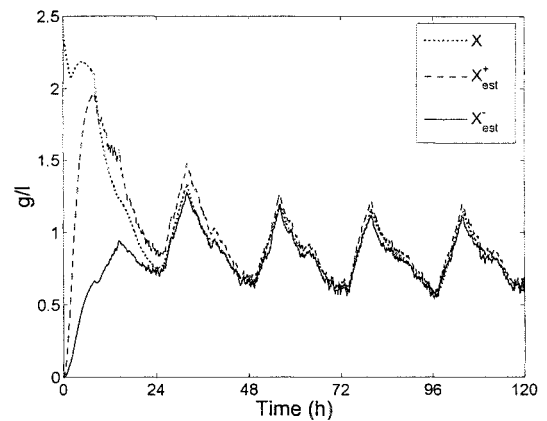


Figure 8-54: Biomass estimation for partially known μ with stepping D for 15% measurement noise

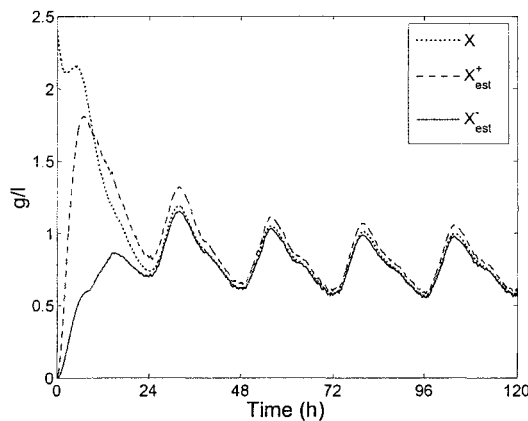


Figure 8-52: Biomass estimation for partially known μ with typical D for 5% measurement noise

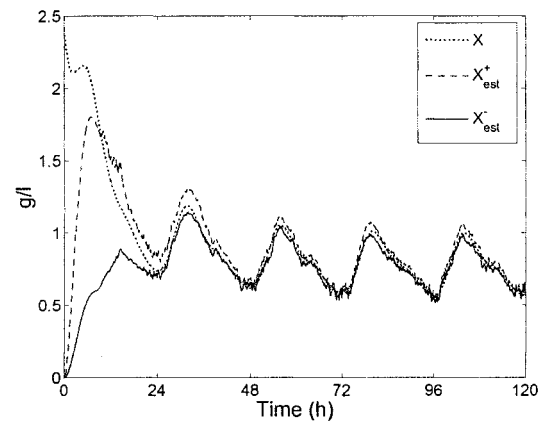


Figure 8-55: Biomass estimation for partially known μ with typical D for 15% measurement noise

The errors in the estimation profiles in the clean case are summarised in Table 8.5 with percentages given with respect to the magnitude of the real simulated biomass concentration.

	<i>D</i> Constant	<i>D</i> Stepping	<i>D</i> Typical
Positive error	17%	5%	5%
Negative error	8.5%	1.9%	1.9%

Table 8.5: Magnitudes of offsets as a percentage of the actual biomass value

The better performances are obtained for the more realistic influent dilution rate profiles. However, the positive estimation errors in each case are much bigger than the negative errors. The reason is due to the choice of higher values of θ_a where the observer uses the lower limit $\mu_0^- + \bar{\mu}_0^-$. This choice is made in order to attain similar convergence times of the real and estimated substrate concentration S , as those attained resulting in the negative estimation error. Consequently, a larger gain is experienced in the estimation of the biomass concentration, which yields larger offsets. Generally, a higher choice of θ_a results in a better estimation of S , and an estimation of X with larger offsets. Note that better results can be obtained if lower values of θ_a are considered such that the convergence of the measured and estimated values of substrate concentration S occurs at a later point in time.

The magnitudes of the noise present in the biomass estimation profiles when considering an additive noise with amplitudes equal to 5% of the measured value of substrate concentration S are summarised in Table 8.6. The magnitudes of the noise present in the biomass estimation profiles when considering an additive noise with amplitudes equal to 15% of the measured value of substrate concentration S are summarised in Table 8.7. The percentages are given with respect to the magnitude of the real simulated biomass concentration.

	<i>D</i> Constant	<i>D</i> Stepping	<i>D</i> Typical
Positive error on μ	< 1%	< 2%	< 2%
Negative error on μ	< 1%	< 2%	< 2%

Table 8.6: Noise present in the estimations for 5 percent measurement noise

	D Constant	D Stepping	D Typical
Positive error on μ	< 3%	< 7%	< 7%
Negative error on μ	< 3%	< 7%	< 7%

Table 8.7: Noise present in the estimations for 15 percent measurement noise

8.6.3 Concluding remarks 9

We have shown the performance of Observer 4 where we consider the parameter Sets 1 and 2 (see Appendix A) for the case of partially known parameters under constant, stepping, and typical dilution rates, all of which use a stepping influent substrate concentration. As for the case of a known specific growth rate, we consider estimation both in the absence and in the presence of measurement noise.

The partially known parameter considered is μ_{\max} where we assume an error of $\pm 30\%$ of μ_{\max} . The nominal, upper, and lower bounds used for the specific growth rate are given by the Monod law. Consequently, the differences between the nominal profile and the upper and lower profiles are $\pm 30\%$, respectively.

The smallest estimation errors occur under stepping and typical variations in dilution rate, at less than 2% of the simulated real biomass concentration and most other errors are under 5%. The biomass estimations reach their offset values within 26 hours where the observer is tuned according to convergence of the measured and estimated values of substrate concentration at 12 hours. Indeed, the tuning is far superior as compared to when using an ELO as highlighted in [32], which results in large offsets in S . It should be emphasised that although the worst offset was +17% of the simulated real biomass concentration, this can be improved through a reduction in magnitude of the tuning parameter. In doing so, the convergence of the measured and estimated values of substrate concentration S will occur at a later point in time. In addition, the biomass convergence time will be longer. Therefore, the performance attained is based upon the desired performance with respect to a trade-off

between offset magnitudes and convergence times.

This work compares well to prominent results for partially known specific growth rates [32], [45], [46], [85] with regards to magnitudes of the biomass estimation offset and the time taken to converge to the offset. In [45], an adaptive observer is proposed for biomass estimation with a bounded error in μ . However, the magnitude of the error considered is not stated, there is no consideration of measurement noise, and the convergence to the offset is twice as long as that of Observer 4. In fact, the adaptive nature of the tuning parameter θ_a of Observer 4 results in very good performances in the presence of measurement noise for amplitudes equal to 5% and 15% of the measured value. Indeed, the noise is attenuated by a factor of 5 and between 2.14-2.5 for constant and varying dilution rates, respectively, whilst convergence to offsets occurs at 26 hours. These performances also compare well with the foregoing results in the literature [46], [85], which consider measurement noise with amplitudes of 5% of the measured value. In those works, the noise is multiplied by a factor of 2 and 1, respectively, and convergence to offsets (with convergence errors of 10% of the simulated real biomass profile) is much slower, in the region of 50 hours. In fact, the use of lower gains in Observer 4 results in longer convergence times, but with smaller offsets and also better performance in the presence of measurement noise.

8.7 Biomass estimation for time-delayed bioprocesses

It can be shown that the work on LTI systems with delays, established in Chapter 6, can be applied to the bioprocess considered in this work. However, to do this, one would need to assume a constant specific growth rate. Since such an assumption is unrealistic, we have not pursued this here. In fact, the work on time-delay systems should be extended to the nonlinear case when considering systems such as the bioprocess in this work. However, the

extension of the time-delay work to the nonlinear case is beyond the scope of this thesis.

8.8 Summary of biomass estimation

The problem of biomass estimation for known and partially known specific growth rates of biomass has been tackled. The observers presented are based upon expressing or transforming the bioprocess at hand in, or into, an Extended Jordan Observable form. Hence, the observers are also applicable to other processes that can be expressed in this form or that can be transformed into which. In addition, the observers presented here are simple, and the design is facilitated by the particular expression of the system used. Consequently, one main advantage of the proposed observers lies in the simplicity of design. The structure of the gains results in observers that are easy to implement, especially when considering the well-known extended Kalman observer, which requires a large computational effort to update its gain. Moreover, application of the extended Kalman observer and the extended Luenberger observer (see [32] and [44]) to the bioprocess considered in this work is based upon methods of linearisation, for which stability and convergence is restricted to certain regions of operation.

The simulations carried out here demonstrate the good convergence performance of each observer when the single tuning parameter of each is chosen appropriately. Furthermore, the performances are illustrated in the presence of various influent flow characteristics and different parameter values, all combinations of which are not generally considered in the literature.

When considering either known or partially known specific growth rates, the choice of initial biomass concentration is not confined to any kind of interval as it is in [85]. Indeed, the initial value can be arbitrarily chosen. In addition, this work does not assume or rely

upon any initial or otherwise steady-state conditions as in some other results (see [32] and [47]).

The constant tuning parameter Observer 1 possesses good convergence performance under clean measurement when compared to any observer present in the literature. However, performance in the presence of measurement noise in some cases necessitated further development, which came in the form of the adaptive Observer 2.

Observer 2 demonstrates very good performance, both in the absence and in the presence of measurement noise. The observer uses an adaptive tuning parameter which varies according to changes in the system input and output. Consequently, it can use an efficient gain such that the observer is capable of fast convergence performances whilst attenuating measurement noise. Indeed, for a known specific growth rate, this observer provides the best overall biomass estimation performances.

The main advantage of Observer 3 lies in the fact that for some sets of parameter values, we have more control over the stability of the error dynamics in the sense that with the entries of the extended Jordan block held at constant low values and with appropriate polarity, we can choose a constant tuning parameter that does not have to be excessively high to ensure exponentially stable error dynamics.

Observer 4 uses an adaptive tuning parameter and demonstrates good performance for uncertainty in the specific growth rate, both in the absence and in the presence of measurement noise. As when using Observer 2, an efficient gain is used such that the observer is capable of fast convergence performances whilst attenuating measurement noise.

Chapter 9

Conclusions and Future Work

This chapter draws conclusions on the important results achieved in this work. A discussion of directions for future work is also given. Finally, a list of the publications generated as a result of this research is given.

9.1 Conclusions

The main focus of this work has been on the development of new methodologies for the design of observers and controllers for a class of nonlinear systems and time-delay systems, with the aim to apply the obtained results to the estimation of biomass concentration in a biological wastewater treatment reactor in theory and in simulation. Consequently, this project has generated several contributions to knowledge, introducing new methodologies for the design of observers and controllers for a class of state-affine systems and a class of linear time-delay systems. The reason for the interest in state-affine systems is mainly because the class of bioreactors considered falls into this category of systems. Consequently, the observer designs proposed for the state-affine case have been applied in theory and in simulation to biological wastewater treatment.

The designs were based on the concept of Jordan controllable and observable forms introduced in [35] for linear systems. Therefore, first and foremost, the concepts of the Jordan controllable and observable canonical forms were extended to the class of state-affine systems. The main motivation behind this is that the more general form helps in the design of observers and controllers for sub-classes of state-affine systems. It has been shown that there exist some classes of systems that are naturally of the so-called Extended Jordan Controllable and Observable Canonical (EJCC and EJOC, respectively) forms. It has also been shown that some classes of systems can be partially transformed into EJCC and EJOC forms and algorithms to do so have been given, herein. These canonical forms were used in this work to establish new controller and observer design methodologies for classes of state-affine systems. The designs established are summarised below.

- A controller for a class of control-affine and a sub-class of state-affine systems, which can be partially transformed into a class of the EJCC form.
- A constant tuning parameter observer for a sub-class of state-affine systems, which are already in a sub-class of the EJOC form.
- An adaptive tuning parameter observer for a sub-class of state-affine systems, which are already in a sub-class of the EJOC form. The robustness of this adaptive observer was shown under parameter uncertainty.
- A constant tuning parameter observer for a sub-class of state-affine systems, which was partially transformed into a sub-class of the EJOC form.

In the case of the controller design, it was shown that the use of the EJCC canonical form facilitates the design procedure and provides additional degrees of freedom in tuning the controller parameters. Moreover, the construction of the transformation matrix and the

expression of the system in the EJCC form provide components of the controller gain. In addition, only linear techniques are used for the controller design, which has been shown to compare well with an input-state linearising controller.

The first two observer designs were facilitated by expressing the systems under observation as a sub-class of systems in the EJOC form and use a constant and an adaptive tuning parameter, respectively. In order to show the flexibility of the approach, the third observer design methodology was given for systems that can be partially transformed into a sub-class of systems in the EJOC form. Similar to the foregoing controller, the construction of the transformation matrix provides components of the observer gain, as does the expression of the system in the EJOC form itself. The fourth observer is designed for the case of uncertain system parameters such that estimations given converge to within a bounded error. The design of each observer is based upon the use of linear techniques and consequently their construction is simple and straightforward. Implementation of the observers is also simple, with each having excellent convergence properties. It is shown that the observers can be tuned using only a single tuning parameter, and that convergence is achieved more quickly using larger magnitudes of which. In particular, the adaptive-gain observer has a number of advantages as compared to the case of using a constant tuning parameter, or any high-gain observer. Indeed, an efficient gain is given that is capable of guaranteeing exponentially stable error dynamics, without remaining unnecessarily high.

The foregoing work on controller and observer design is for systems that contain no delays. However, the problem of designing controllers and observer-based controllers for a class of linear time-delay systems (TDSs) has also been tackled in this work. Consequently, a full-state controller and a separation principle have been established for a class of SISO linear time-delay systems with known delays in the state and output. The designs are based on a new stability criterion and are derived from first principles.

The controller has been designed based on the specific choice of controller gain such that the closed-loop system is asymptotically stable in the sense of a recently introduced stability criterion called (α, r) -stability, which is stronger than stability in the Krasovskii sense. Furthermore, the system can be easily tuned via one parameter, higher magnitudes of which result in a quicker convergence performance. However, in such a case, the larger control effort needed to achieve this can result in system behaviour containing larger transient peaks. Therefore, a trade-off is required between the desired convergence time and the amplitudes of acceptable transient peaks and control effort.

This work on TDSs is distinctive from others in this area in that it exploits the features of the characteristic equation of the system to derive the controller gain. In fact, no *a priori* control design approach was set in advance; that is, the controller was designed based on first principles.

The time-delay controller synthesised in this project assumes that a full-state measurement is available. Since this is often not the case in practice, it is important to consider the possibility of establishing some kind of observer-based controller. Indeed, the possibility of combining the foregoing controller with a recent observer for the same class of TDSs was explored. As a result, a separation principle for the class of SISO linear TDSs considered has been established, based upon asymptotic stability in the sense of (α, r) -stability. In addition, the controller and observer are tuned individually, each using only one tuning parameter.

Both the controller and the observer-based controller strategy proposed are applicable to LTI systems with known delays in the state and output. In fact, they can be used where there is a delay in the state only or if there are delays both in the state and the output. In addition, the value of the delay in the output can be any value less than or equal to that of the state delay.

Finally, as previously mentioned, the application of interest in this research has been on

the biological treatment of wastewater. Difficulties in the control of such systems arise due to insufficient knowledge of the nonlinear specific growth rate of reaction and the lack of cheap and/or reliable monitoring equipment for the on-line measurement of biomass concentration. Consequently, one focus of this research has been upon the estimation of biomass concentration in a biological wastewater treatment bioreactor. The new observer design methodologies for the class of state-affine systems that have been established in this research have been applied in theory and in simulation to the estimation of biomass, both in the absence and in the presence of measurement noise. Two main cases have been considered. In the first case, we assumed a full knowledge of the specific growth rate of biomass, whereas in the second, we assumed only a partial knowledge of the latter.

In the case of a known specific growth rate, the observers were applied under a variety of influent flow characteristics and parameter values, both in the absence and in the presence of measurement noise. The performances attained compare very well with current results in the literature (see e.g. [45], [46], [47], [85]) with regards to convergence, time-response, and presence of noise in the estimation profiles. In fact, it was intended that the adaptive observer would improve the estimation performance when considering measurement noise. Indeed, the adaptive observer gives the best overall performance for the various parameter values considered.

In the case of a partially known specific growth rate, the robustness of the adaptive observer was shown where only $\pm 70\%$ of the maximum specific growth rate of reaction is used in the observer. Again, estimation under different influent characteristics is considered, both in the absence and in the presence of measurement noise. The smallest estimation errors shown are less than 2% of the simulated real biomass concentration and most are under 5%. It is also shown that noise is attenuated by factors of 5 and 2.14-2.5 for constant and varying dilution rates, respectively, and convergence to offsets occurs at 26 hours. These perfor-

mances compare well with the foregoing results in the literature [46], [85], which consider measurement noise with amplitudes of 5% of the measured value. In those works, the noise is multiplied by a factor of 2 and 1, respectively, and convergence to offsets, with convergence errors of the order of 10% of the simulated real biomass concentration, is much slower, in the region of 50 hours.

We can conclude that the most successful biomass estimations yielded from this research are those of the adaptive observer. Indeed, the adaptive nature of this observer can result in attenuation of noise with good convergence times, which might even be better than if a noisy direct measurement of biomass concentration were possible or affordable. Furthermore, the performances are illustrated in the presence of various influent flow characteristics and under different parameter values, all combinations thereof are not generally considered in the literature.

Although the aspect of time-delays in wastewater treatment processes was of interest in this work, we have not shown biomass estimation in the presence of delays. The reason for this is that the controller and observer-based controller given in this research would not be suitable for application to the bioprocess considered. This unsuitability originates from the need to assume a constant specific growth rate. However, such an assumption is unrealistic and, consequently, we have not pursued this here. In fact, the work on time-delay systems should be extended to the nonlinear case when considering systems such as the bioprocess in this work. However, the extension of the time-delay work to the nonlinear case is beyond the scope of this thesis.

9.2 Future work

One focus of this research has been to establish new methodologies for the design of observers and controllers for a class of state-affine systems. As a result, a controller design methodology and a number of observer design methodologies have been proposed based upon the EJCC and the EJOC forms, respectively. The operation and performances of the controller and observer designs have been illustrated separately. That is, no observer-based controller has been given. Consequently, based upon the foregoing designs, it would be interesting to investigate the possibility of establishing a separation principle for the class of state-affine systems considered in this work. Furthermore, the possibility of applying such an observer-based control strategy to a wastewater treatment bioreactor in simulation and in practice can also be explored.

As previously mentioned, the foregoing EJOC observer designs have been applied in theory and in simulation to the problem of biomass estimation. In particular, an adaptive-gain observer has been applied to the case of a partially known specific growth rate, and gives an estimation profile that is bounded to an interval. However, it would be interesting to investigate the possibility of establishing an estimation strategy for the estimation of the specific growth rate based upon the EJOC form.

Almost all systems contain time-delays, including many industrial processes such as biological wastewater treatment, which has been the application of interest in this research. Hence, in this work, interest has been placed upon observation and control of systems containing time-delays. As a result, a controller and a separation principle have been proposed and are applicable to LTI time-delay systems. However, if these results were to be applied to the bioprocess considered in this work, then one would have to assume a constant specific growth rate, such that the system under observation belongs to the latter class of systems. As

mentioned previously, this assumption is far too restrictive. Therefore, one area for future work would be on the extension of the time-delay controller and observer-based controller, established in this research, to the state-affine case.

Finally, all of the work in this research has been based upon SISO systems. Hence, one further suggestion would be to extend these results to the MIMO (Multi-Input Multi-Output) case.

9.3 Publications generated by this research

1. Tingey, D.; Busawon, K.; Danaher, S.; and Waterworth, G. "A control design for linear time-delay systems", *Proceedings of the 16th ICSE*, Coventry, 2003.
2. Tingey, D.; Busawon, K.; Danaher, S.; and Waterworth, G. "A control design for linear time-delay systems", *Systems Science*, vol. 29, no. 4, 2003.
3. Tingey, D.; Busawon, K.; Danaher, S.; and Waterworth, G. "A separation principle for a class of linear time-delay systems", *Proceedings of UKAC, Control 2004*, Bath, 2004.
4. Tingey, D.; Busawon, K.; Danaher, S.; and Waterworth, G. "An observer design for single-output state-affine systems with application to a bioprocess", *Proceedings of UKAC, Control 2004*, Bath, 2004.
5. Busawon, K.; Saif, M.; and Tingey, D. "Nonlinear control design using the extended Jordan controllable canonical form", *Journal of Measurement and Control*, vol. 1, no. 1, 2005.
6. Tingey, D.; Busawon, K.; and Saif, M. "Biomass concentration estimation using the extended Jordan observable form", *Proceedings of CCA05*, Toronto, Canada, 2005.

7. Busawon, K.; Tingey, D.; and Awami, A. "An adaptive observer design for a class of state-affine systems with application to a bioreactor", *Proceedings of the 18th ICSE*, Coventry, 2006.

Appendix A

Biomass Estimation Simulations

A.1 Estimation for known SGR - Parameter Set 2

Here, we show the simulation results for the estimation of biomass concentration for parameter Set 2 under different dilution rates D and influent substrate concentrations S_{in} . The parameter values used are given in Table A.1. The tuning parameters used for Observers 1-3 for estimation under clean measurement are summarised in Table A.2. For Observer 3, a choice of $\alpha(u, y) = -\frac{1}{2}$ is used. Note that where no maximum or minimum value is indicated for Observer 2, neither was required since good results were obtained without. Also, note that CS_{in} : Constant S_{in} ; SS_{in} : Stepping S_{in} .

$X(0) = 2.4g/l$	$K_s = 4g/l$
$\hat{X}(0) = 0g/l$	$Y_s = 10$
$S(0) = \hat{S}(0) = 0.8g/l$	$k_1 = 2$
$\mu_{max} = 0.3h^{-1}$	$k_2 = 1$

Table A.1: Set 2 parameter values

As in the results for estimation using parameter Set 1, for the clean measurement case, we show the estimation profile given by Observer 1. We then show the profiles of the gain ψ_2 of Observers 1-3 for the same estimation performance.

Observer		D Constant	D Stepping	D Typical
1	CS_{in}	$\theta_c = -3$	$\theta_c = -3$	$\theta_c = -3$
	SS_{in}	$\theta_c = -3$	$\theta_c = -3$	$\theta_c = -3$
2	CS_{in}	$\theta_a = \theta_{\max} = -3$	$\theta_a = \theta_{\max} = -3$	$\theta_a = \theta_{\max} = -3$
	SS_{in}	$\theta_a(0) = -3.6$	$\theta_a(0) = -3.6$	$\theta_a(0) = -3.6$
3	CS_{in}	$\theta_c\beta = 0.3$	$\theta_c\beta = 0.3$	$\theta_c\beta = 0.3$
	SS_{in}	$\theta_c\beta = 0.12$	$\theta_c\beta = 0.6$	$\theta_c\beta = 0.6$

Table A.2: Observer tuning parameter values under clean measurement - Set 2

For each observer, we also consider an additive noise ϵ with amplitude equal to 5% of the measured value S . We also consider an additive noise ϵ with amplitude equal to 10% of the measured value S and show the performance of Observer 2 for a stepping S_{in} and the performance of Observer 3 for both a constant and stepping S_{in} . Note that for this set of parameter values, it is shown through Figures A-7 to A-9 that the profile of the gain ψ_2 of the adaptive-gain observer is equivalent to that of the constant-gain observer for constant S_{in} where the tuning parameter is $\theta_a = \theta_c = -3$. The reason for such a choice is such that we obtain the same convergence time, and a ramping θ_a would not give this. Hence, for $\theta_a = \theta_c$ the performances, in the presence of measurement noise, yielded by Observers 1 and 2 are similar.

The tuning parameter values used for Observers 1-3 under measurement noise are summarised in Table A.3. Note that where no maximum or minimum value is indicated for Observer 2, neither was required since good performance was achieved without.

Observer		D Constant	D Stepping	D Typical
1	CS_{in}	$\theta_c = -1$	$\theta_c = -1$	$\theta_c = -1$
	SS_{in}	$\theta_c = -1$	$\theta_c = -1$	$\theta_c = -1$
2	CS_{in}	$\theta_a = \theta_{\max} = -1$	$\theta_a = \theta_{\max} = -1$	$\theta_a = \theta_{\max} = -1$
	SS_{in}	$\theta_a(0) = -3.6$	$\theta_a(0) = -3.6$	$\theta_a(0) = -3.6$
3	CS_{in}	$\theta_c\beta = 0.3$	$\theta_c\beta = 0.3$	$\theta_c\beta = 0.3$
	SS_{in}	$\theta_c\beta = 0.12$	$\theta_c\beta = 0.6$	$\theta_c\beta = 0.6$

Table A.3: Observer tuning parameter values under noisy measurement - Set 2

A.1.1 Estimation under clean measurement

Observer 1 - Constant S_{in}

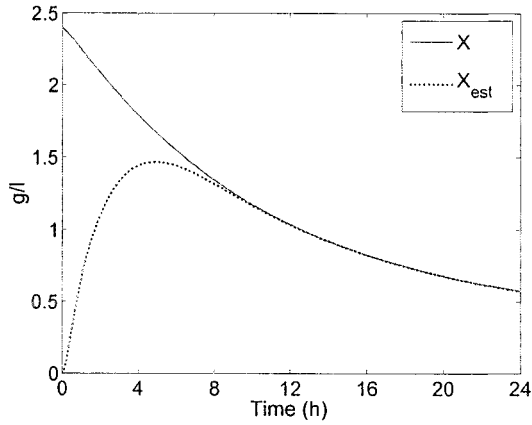


Figure A-1: Performance of Observer 1 for parameter Set 2 with constant $S_{in} = 5g/l$ and constant $D = 0.1h^{-1}$

Observer 1 - Stepping S_{in}

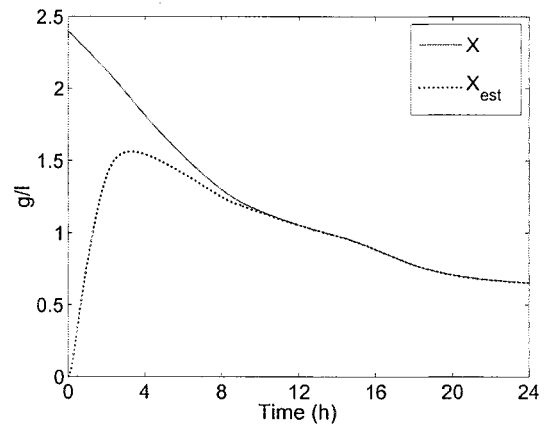


Figure A-4: Performance of Observer 1 for parameter Set 2 with stepping S_{in} and constant $D = 0.1h^{-1}$

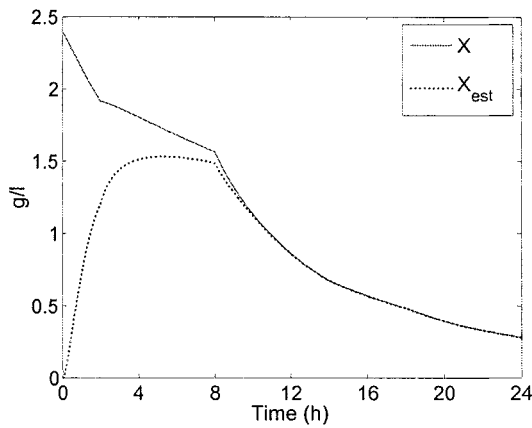


Figure A-2: Performance of Observer 1 for parameter Set 2 with constant $S_{in} = 5g/l$ and stepping D

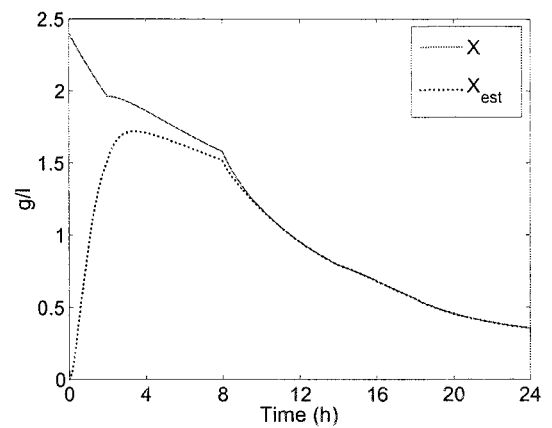


Figure A-5: Performance of Observer 1 for parameter Set 2 with stepping S_{in} and stepping D

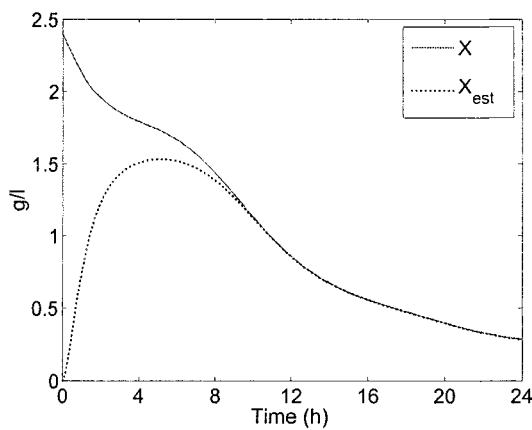


Figure A-3: Performance of Observer 1 for parameter Set 2 with constant $S_{in} = 5g/l$ and typical D

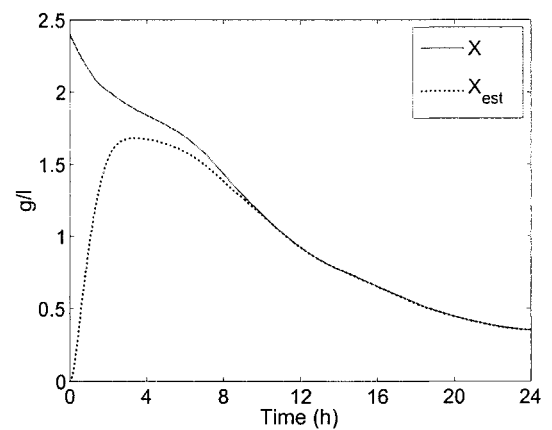


Figure A-6: Performance of Observer 1 for parameter Set 2 with stepping S_{in} and typical D

Gain of Observers 1, 2 & 3 - Constant S_{in} Gain of Observers 1, 2 & 3 - Stepping S_{in}

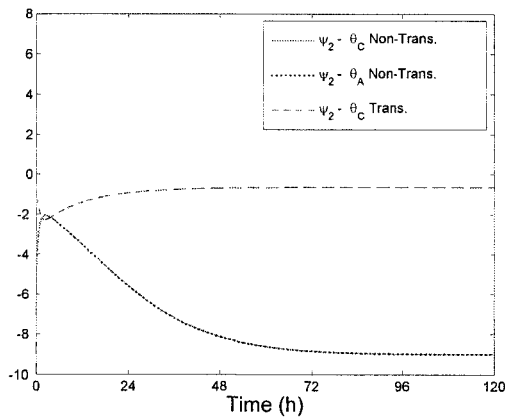


Figure A-7: Profiles of ψ_2 of each observer for constant $S_{in} = 5g/l$ and constant $D = 0.1h^{-1}$

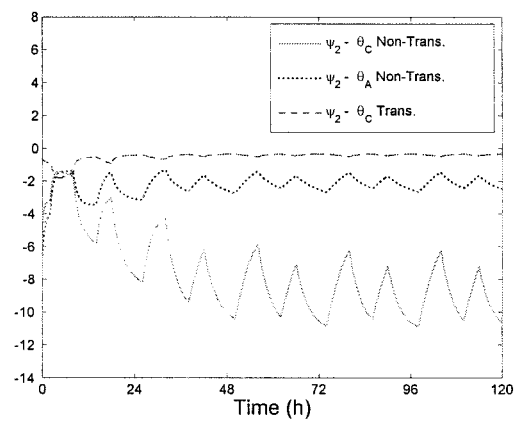


Figure A-10: Profiles of ψ_2 of each observer for stepping S_{in} and constant $D = 0.1h^{-1}$

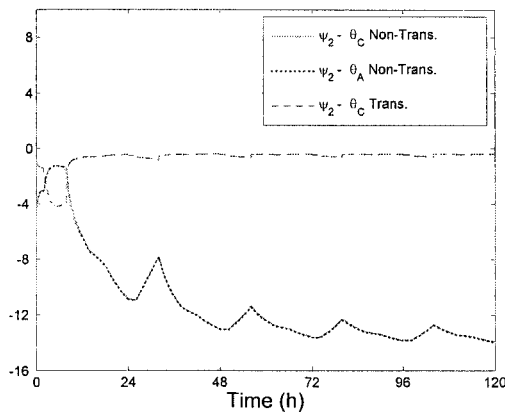


Figure A-8: Profiles of ψ_2 of each observer for constant $S_{in} = 5g/l$ and stepping D

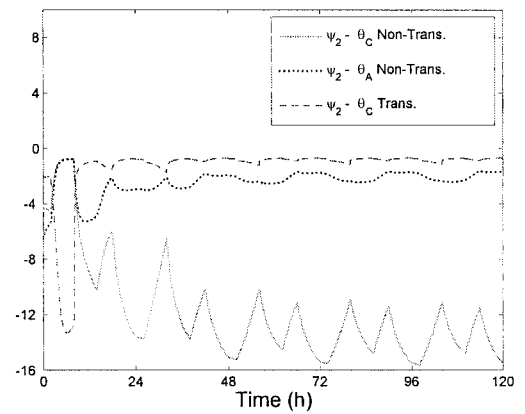


Figure A-11: Profiles of ψ_2 of each observer for stepping S_{in} and stepping D

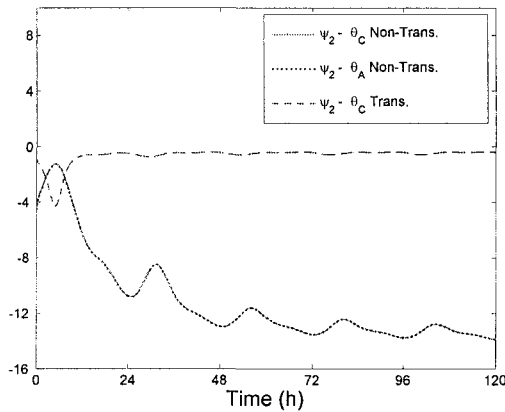


Figure A-9: Profiles of ψ_2 of each observer for constant $S_{in} = 5g/l$ and typical D

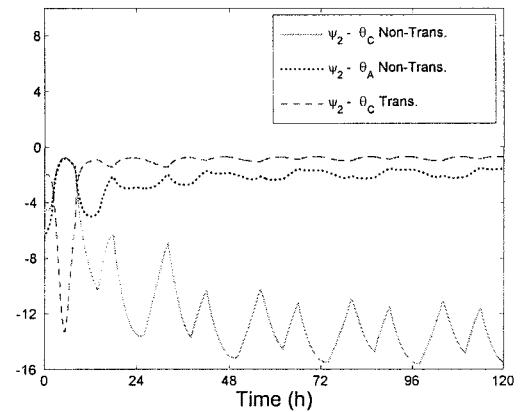


Figure A-12: Profiles of ψ_2 of each observer for stepping S_{in} and typical D

A.1.2 Estimation under 5% measurement noise

Constant S_{in} & constant D

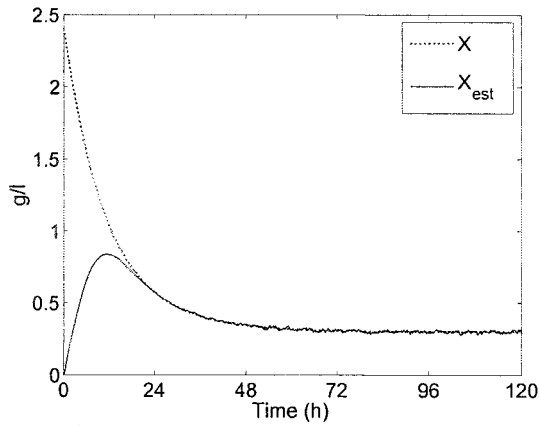


Figure A-13: Performance of Observers 1 and 2 for 5% measurement noise

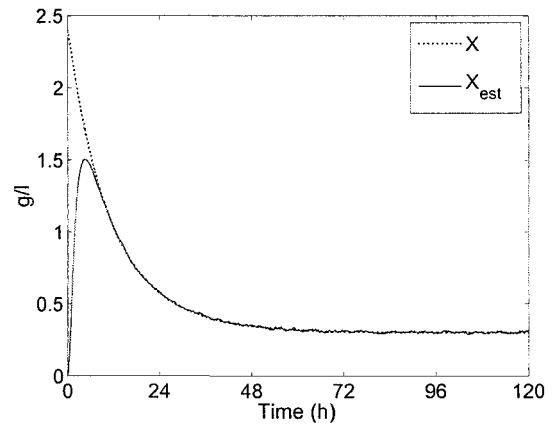


Figure A-14: Performance of Observer 3 for 5% measurement noise

Constant S_{in} & stepping D

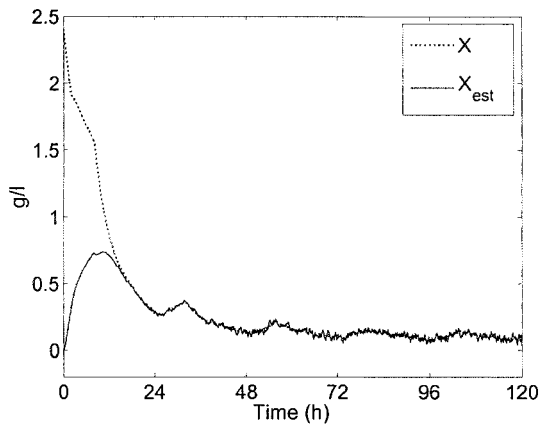


Figure A-15: Performance of Observers 1 and 2 for 5% measurement noise

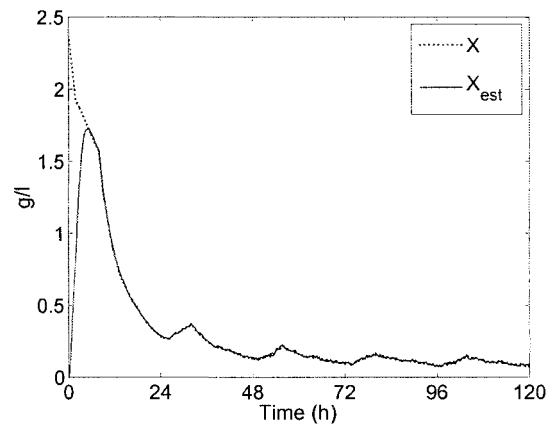


Figure A-16: Performance of Observer 3 for 5% measurement noise

Constant S_{in} & typical D

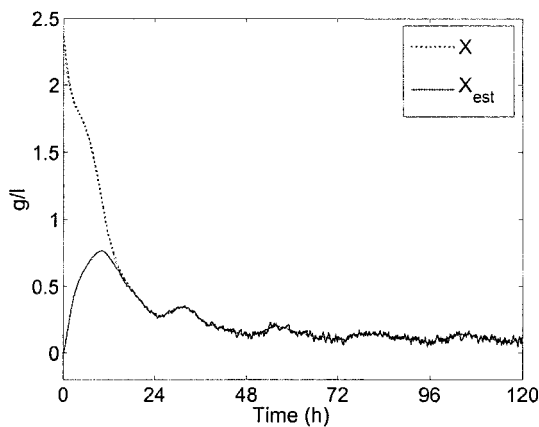


Figure A-17: Performance of Observers 1 and 2 for 5% measurement noise

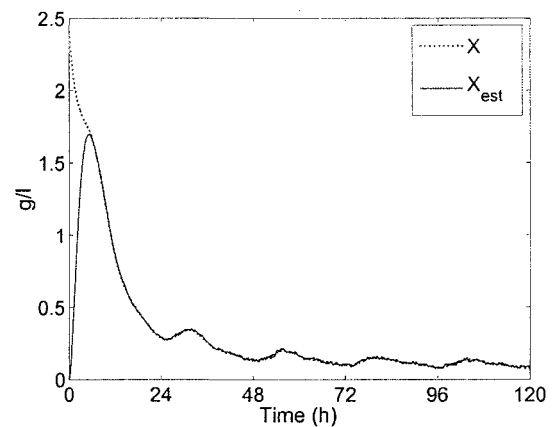


Figure A-18: Performance of Observer 3 for 5% measurement noise

Stepping S_{in} & constant D

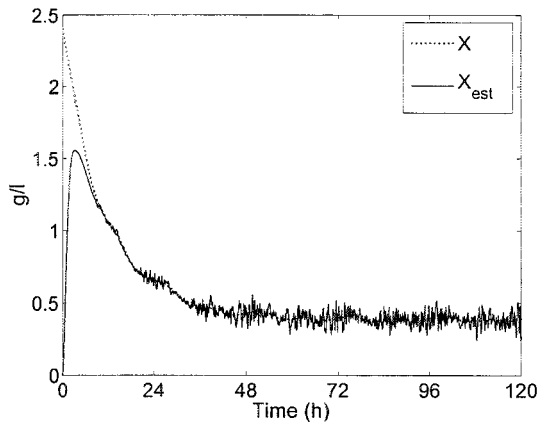


Figure A-19: Performance of Observer 1 for 5% measurement noise

Stepping S_{in} & stepping D

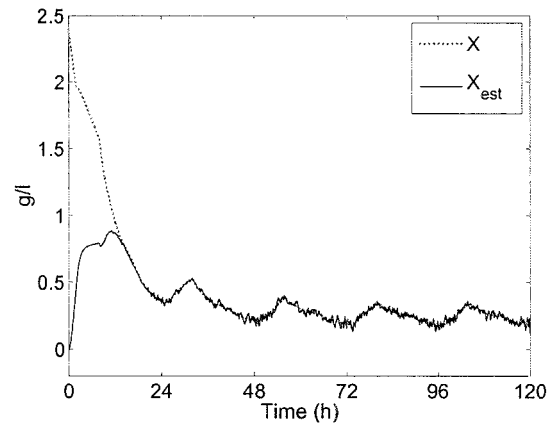


Figure A-22: Performance of Observer 1 for 5% measurement noise

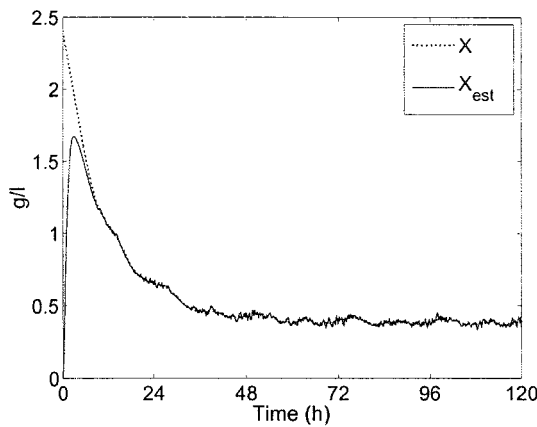


Figure A-20: Performance of Observer 2 for 5% measurement noise

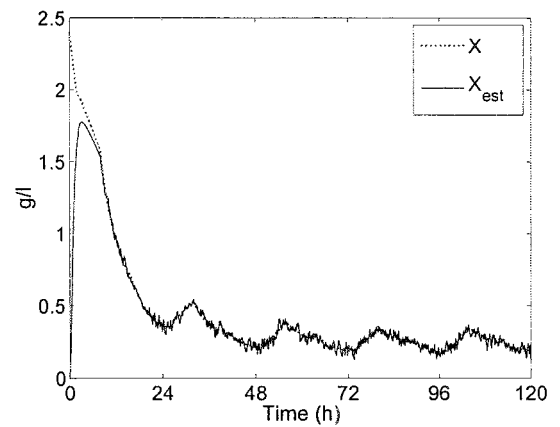


Figure A-23: Performance of Observer 2 for 5% measurement noise

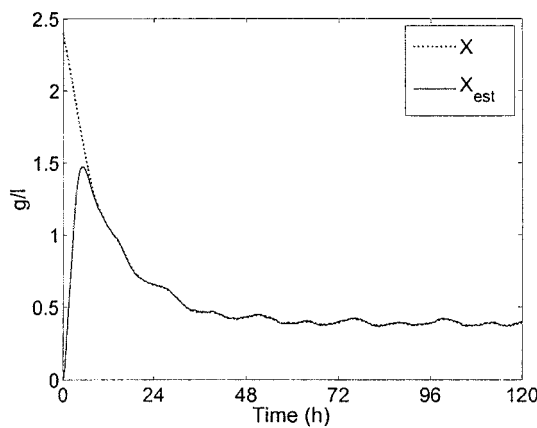


Figure A-21: Performance of Observer 3 for 5% measurement noise

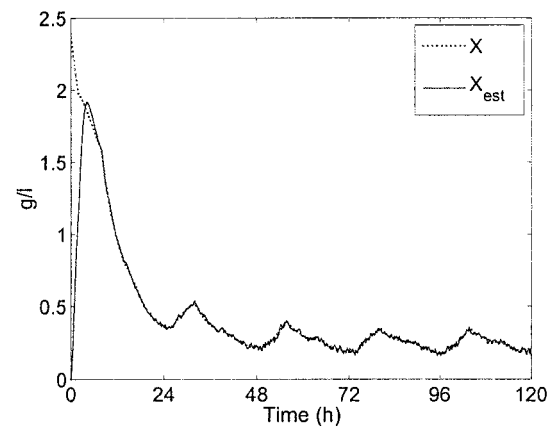


Figure A-24: Performance of Observer 3 for 5% measurement noise

Stepping S_{in} & typical D

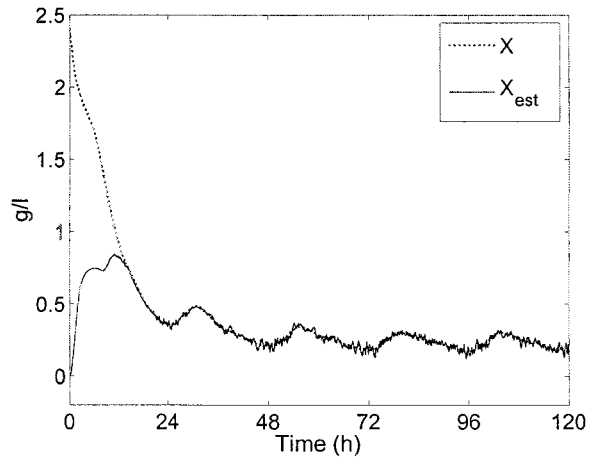


Figure A-25: Performance of Observer 1 for 5% measurement noise

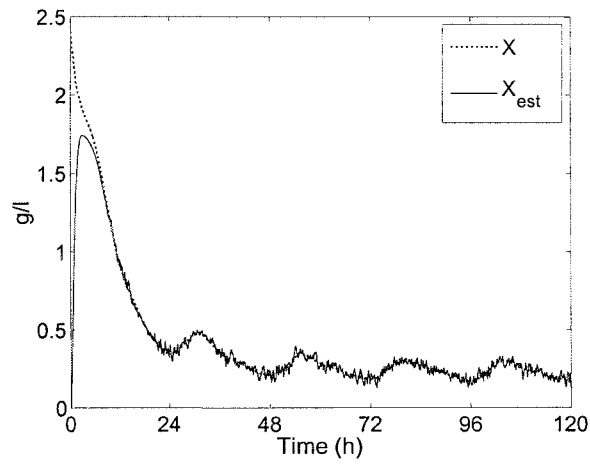


Figure A-26: Performance of Observer 2 for 5% measurement noise

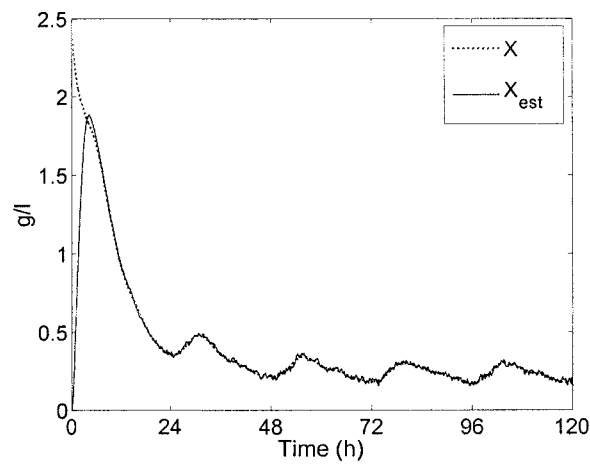


Figure A-27: Performance of Observer 3 for 5% measurement noise

A.1.3 Estimation under 10% measurement noise

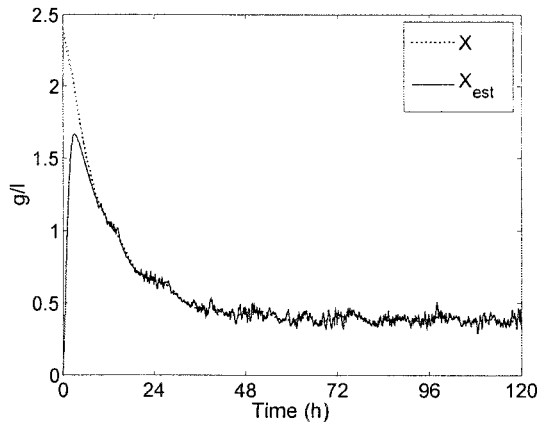


Figure A-28: Performance of Observer 2 for 10% measurement noise for stepping S_{in} and constant $D = 0.1h^{-1}$

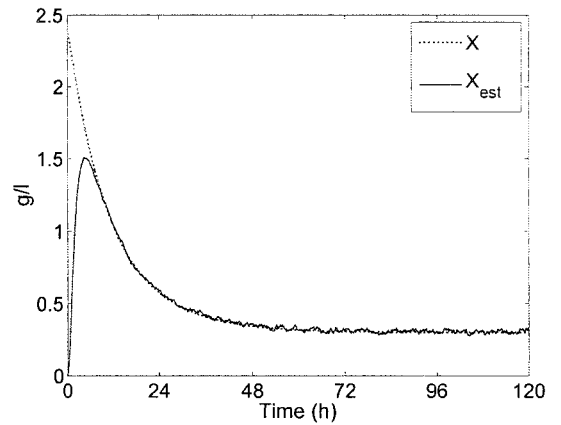


Figure A-31: Performance of Observer 3 for 10% measurement noise for constant $S_{in} = 5g/l$ and constant $D = 0.1h^{-1}$

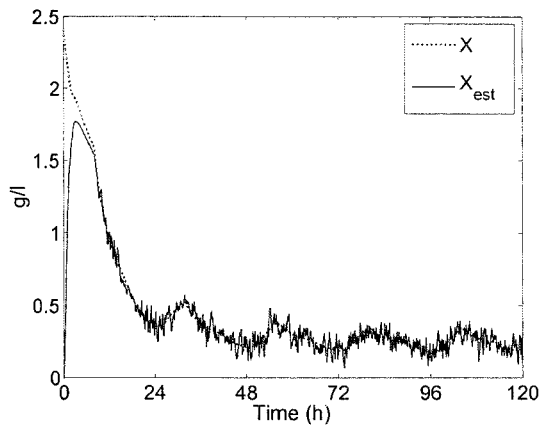


Figure A-29: Performance of Observer 2 for 10% measurement noise for stepping S_{in} and stepping D

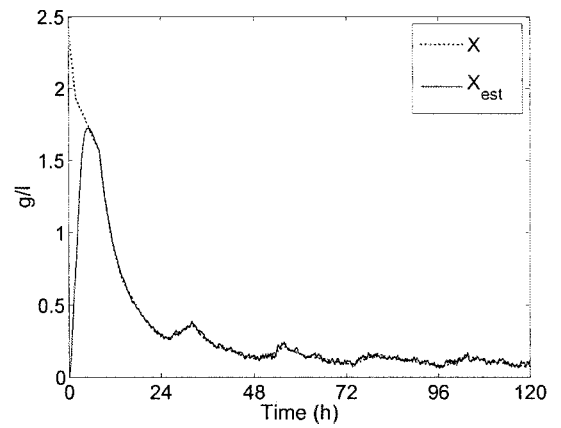


Figure A-32: Performance of Observer 3 for 10% measurement noise for constant $S_{in} = 5g/l$ and stepping D

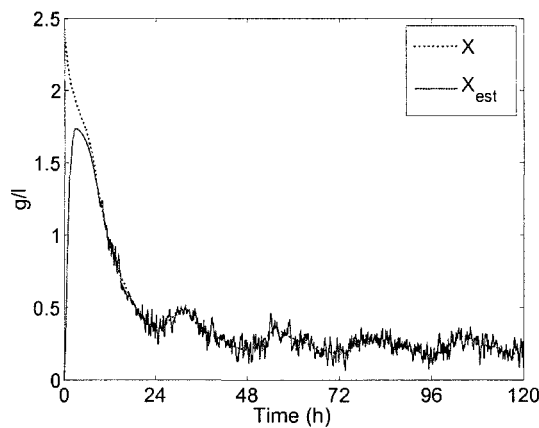


Figure A-30: Performance of Observer 2 for 10% measurement noise for stepping S_{in} and typical D

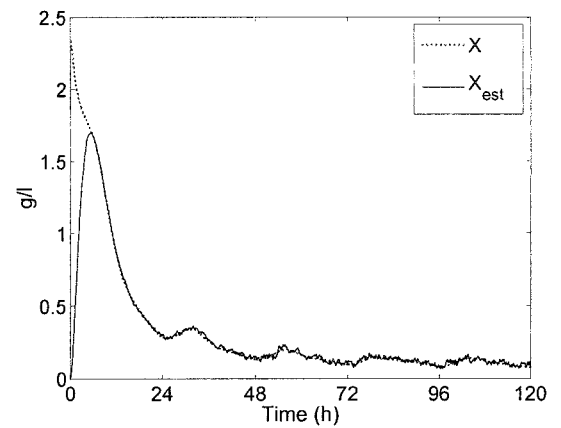


Figure A-33: Performance of Observer 3 for 10% measurement noise for constant $S_{in} = 5g/l$ and typical D

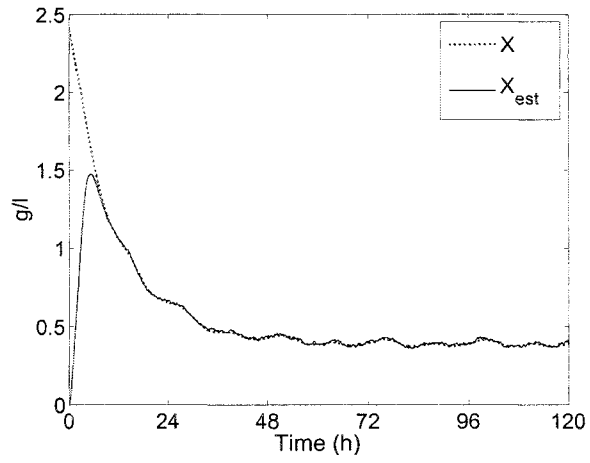


Figure A-34: Performance of Observer 3 for 10% measurement noise for stepping S_{in} and constant $D = 0.1h^{-1}$

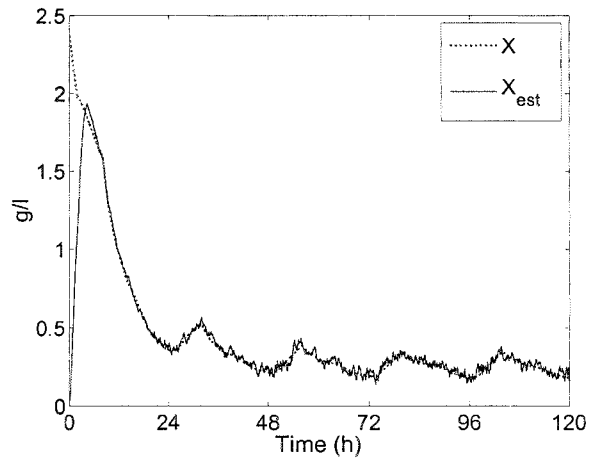


Figure A-35: Performance of Observer 3 for 10% measurement noise for stepping S_{in} and stepping D

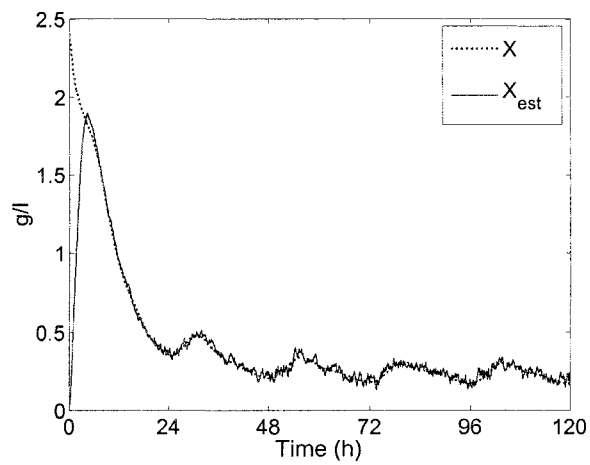


Figure A-36: Performance of Observer 3 for 10% measurement noise for stepping S_{in} and typical D

A.2 Estimation for known SGR - Parameter Set 3

Here, we show the simulation results for the estimation of biomass concentration for parameter Set 3 under different dilution rates D and influent substrate concentrations S_{in} . The parameter values used are given in Table A.4. The tuning parameters used for Observers 1-3 under clean measurement are summarised in Table A.5. For Observer 3, a choice of $\alpha(u, y) = -\frac{1}{2}$ is used. Note that where no maximum or minimum value is indicated for Observer 2, neither was required since good performance was achieved without. Also note CS_{in} : Constant S_{in} ; SS_{in} : Stepping S_{in} .

$X(0) = 0.5g/l$	$K_s = 4g/l$
$\hat{X}(0) = 0g/l$	$Y_s = 10$
$S(0) = \hat{S}(0) = 10g/l$	$k_1 = 2$
$\mu_{max} = 0.3h^{-1}$	$k_2 = 1$

Table A.4: Set 3 parameter values

Observer		D Constant	D Stepping	D Typical
1	CS_{in}	$\theta_c = -3$	$\theta_c = -3$	$\theta_c = -3$
	SS_{in}	$\theta_c = -3$	$\theta_c = -3$	$\theta_c = -3$
2	CS_{in}	$\theta_a(0) = -2.5$	$\theta_a(0) = -2.5$	$\theta_a(0) = -2.5$
	SS_{in}	$\theta_a(0) = -2.8$	$\theta_a(0) = -2.8$	$\theta_a(0) = -2.8$
3	CS_{in}	$\theta_c\beta = 4$	$\theta_c\beta = 4$	$\theta_c\beta = 4$
	SS_{in}	$\theta_c\beta = 5$	$\theta_c\beta = 5$	$\theta_c\beta = 5$

Table A.5: Observer tuning parameter values under clean measurement - Set 3

As in the results for estimation using parameter Set 1, for the clean measurement case, we show the estimation profile given by Observer 1. We then show the profiles of the gain ψ_2 of Observers 1-3 for the same estimation performance.

For each observer, we consider an additive noise ϵ with amplitudes equal to 5% of the measured value S . We also show the performances of Observers 2 and 3 for an additive noise ϵ with amplitudes equal to 10% of the measured value S .

The tuning parameter values used for Observers 1, 2, and 3 under noisy measurement are summarised in Table A.6. Note that where no maximum or minimum value is indicated for

Observer 2, neither was required since good performance was achieved without.

Observer		D Constant	D Stepping	D Typical
1	CS_{in}	$\theta_c = -0.7$	$\theta_c = -0.45$	$\theta_c = -0.45$
	SS_{in}	$\theta_c = -0.7$	$\theta_c = -0.45$	$\theta_c = -0.45$
2	CS_{in}	$\theta_a(0) = -0.7$	$\theta_a(0) = -0.7$	$\theta_a(0) = -0.7$
	SS_{in}	$\theta_a(0) = -0.7$	$\theta_a(0) = -0.7$	$\theta_a(0) = -0.7$
3	CS_{in}	$\theta_c\beta = 0.1$	$\theta_c\beta = 0.1$	$\theta_c\beta = 0.1$
	SS_{in}	$\theta_c\beta = 0.2$	$\theta_c\beta = 0.2$	$\theta_c\beta = 0.2$

Table A.6: Observer tuning parameter values under noisy measurement - Set 3

A.2.1 Estimation under clean measurement

Observer 1- Constant S_{in}

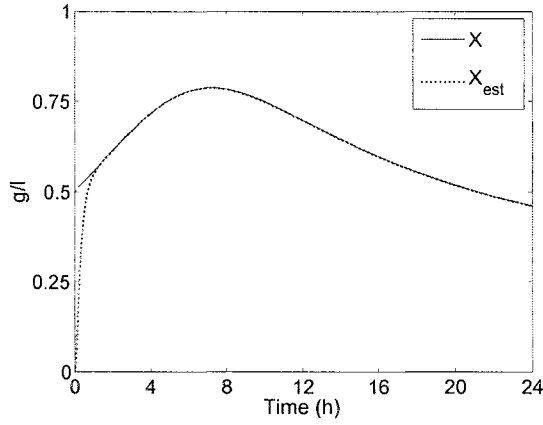


Figure A-37: Performance of Observer 1 for parameter Set 3 with constant $S_{in} = 5g/l$ and constant $D = 0.1h^{-1}$

Observer 1- Stepping S_{in}

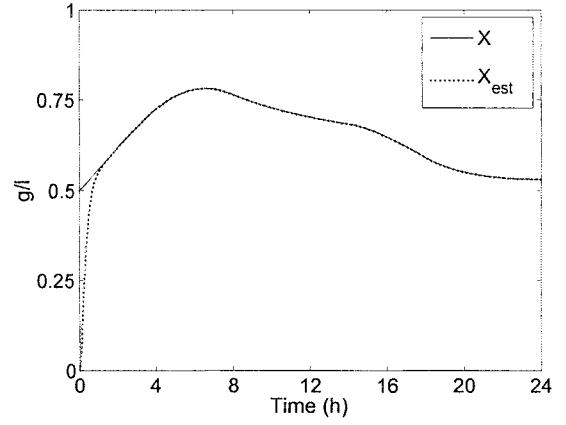


Figure A-40: Performance of Observer 1 for parameter Set 3 with stepping S_{in} and constant $D = 0.1h^{-1}$

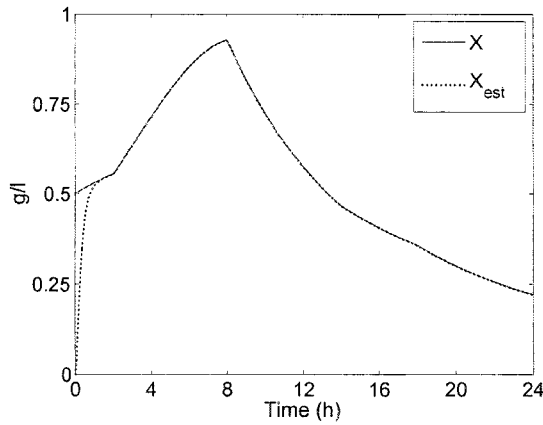


Figure A-38: Performance of Observer 1 for parameter Set 3 with constant $S_{in} = 5g/l$ and stepping D

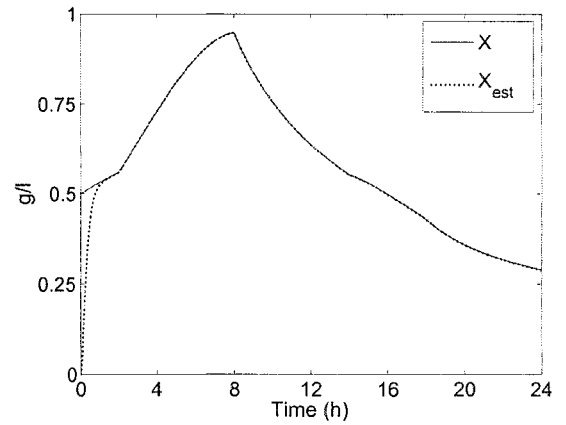


Figure A-41: Performance of Observer 1 for parameter Set 3 with stepping S_{in} and stepping D

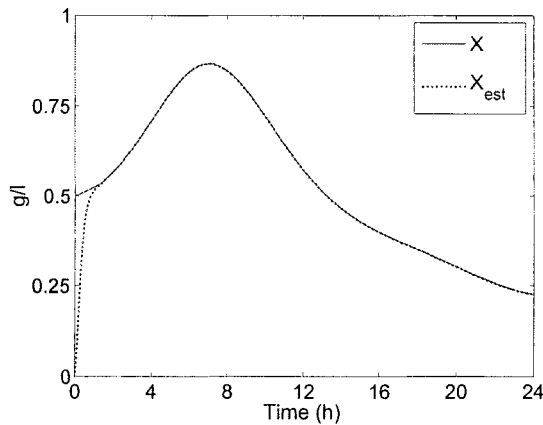


Figure A-39: Performance of Observer 1 for parameter Set 3 with constant $S_{in} = 5g/l$ and typical D

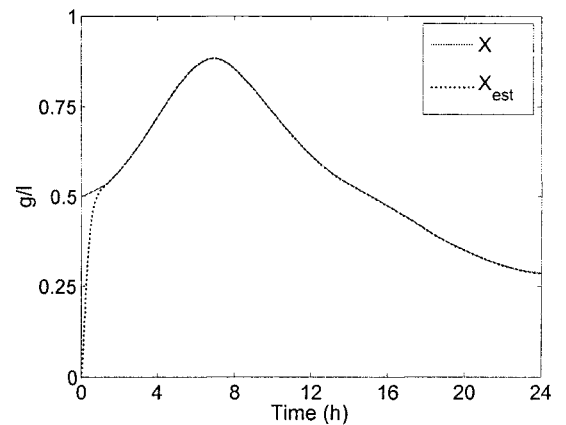


Figure A-42: Performance of Observer 1 for parameter Set 3 with stepping S_{in} and typical D

Gain of Observers 1, 2 & 3 - Constant S_{in} Gain of Observers 1, 2 & 3 - Stepping S_{in}

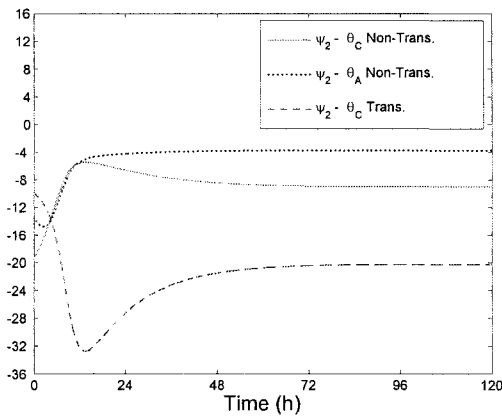


Figure A-43: Profiles of ψ_2 of each observer for constant $S_{in} = 5g/l$ and constant $D = 0.1h^{-1}$

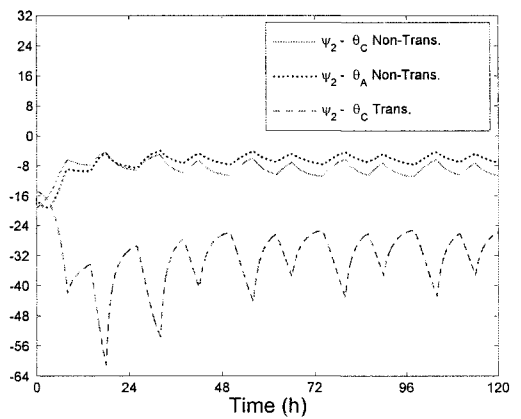


Figure A-46: Profiles of ψ_2 of each observer for stepping S_{in} and constant $D = 0.1h^{-1}$

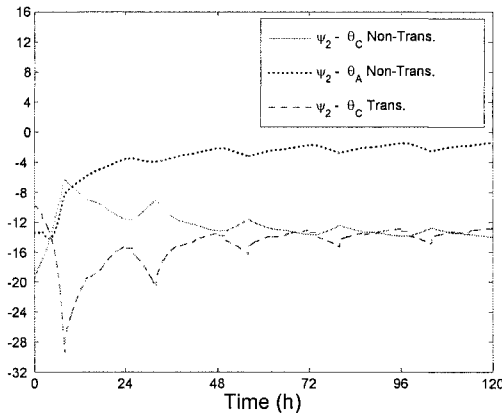


Figure A-44: Profiles of ψ_2 of each observer for constant $S_{in} = 5g/l$ and stepping D

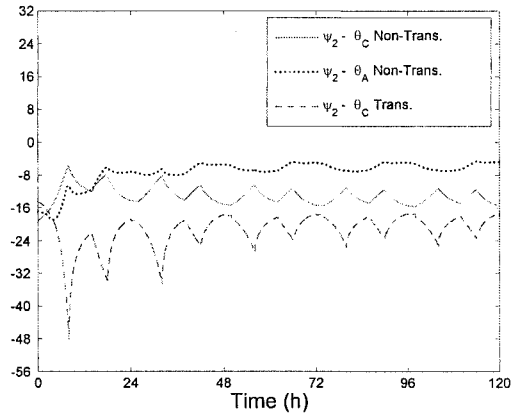


Figure A-47: Profiles of ψ_2 of each observer for stepping S_{in} and stepping D

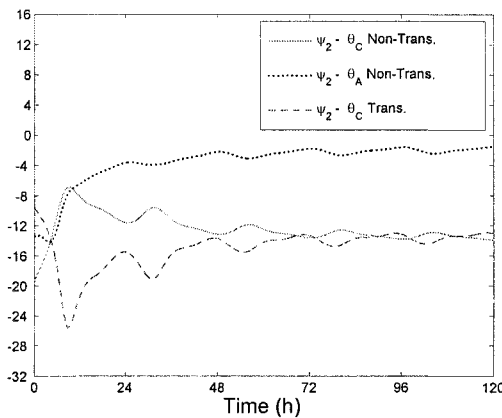


Figure A-45: Profiles of ψ_2 of each observer for constant $S_{in} = 5g/l$ and typical D

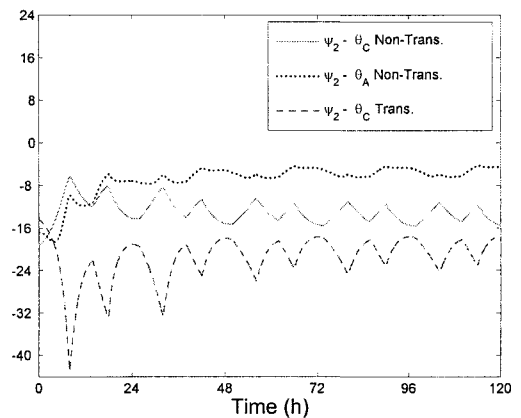


Figure A-48: Profiles of ψ_2 of each observer for stepping S_{in} and typical D

A.2.2 Estimation under 5% measurement noise

Constant S_{in} & constant D

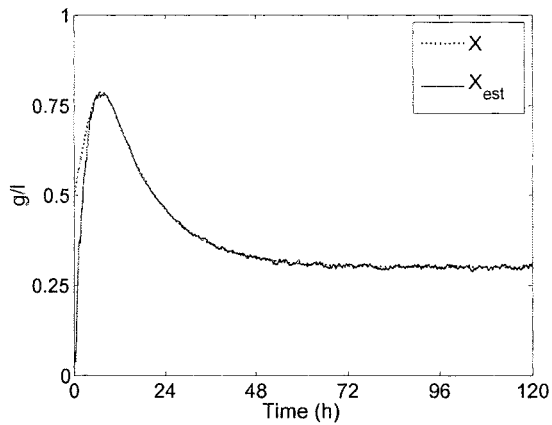


Figure A-49: Performance of Observer 1 for 5% measurement noise

Constant S_{in} & stepping D

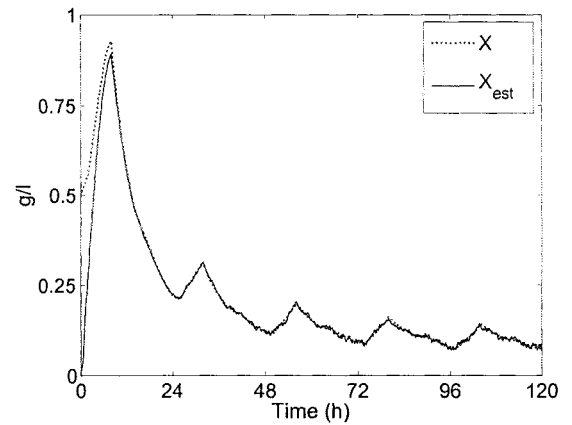


Figure A-52: Performance of Observer 1 for 5% measurement noise

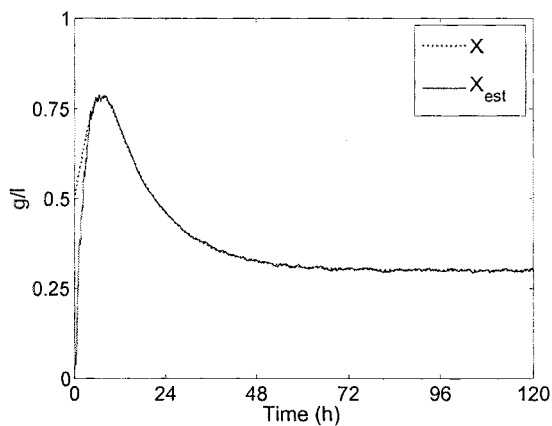


Figure A-50: Performance of Observer 2 for 5% measurement noise

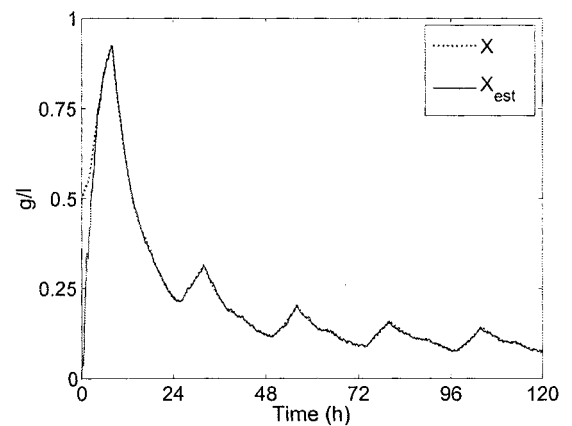


Figure A-53: Performance of Observer 2 for 5% measurement noise

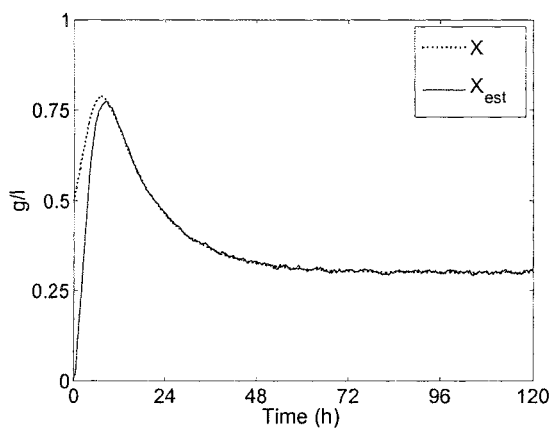


Figure A-51: Performance of Observer 3 for 5% measurement noise

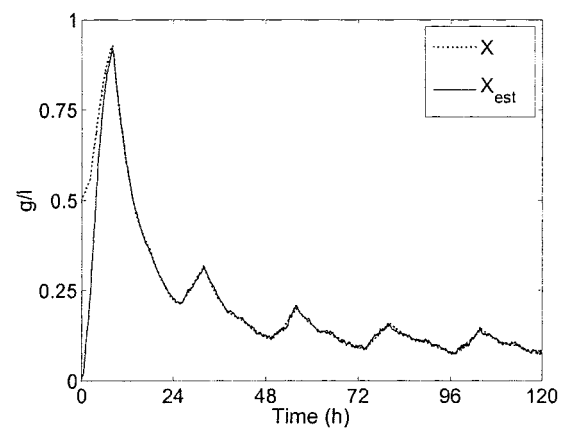


Figure A-54: Performance of Observer 3 for 5% measurement noise

Constant S_{in} & typical D

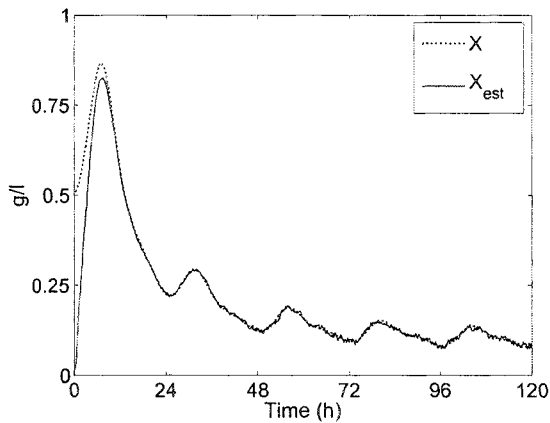


Figure A-55: Performance of Observer 1 for 5% measurement noise

Stepping S_{in} & constant D

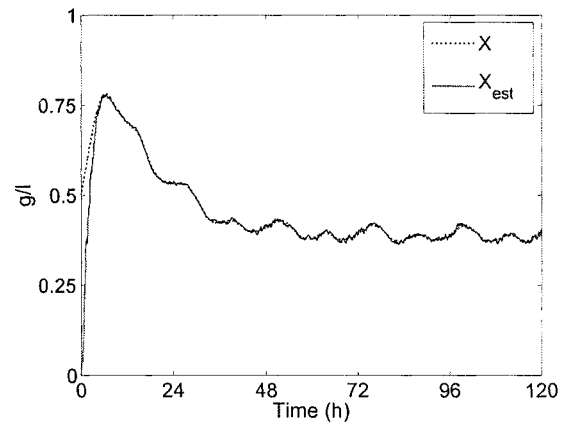


Figure A-58: Performance of Observer 1 for 5% measurement noise

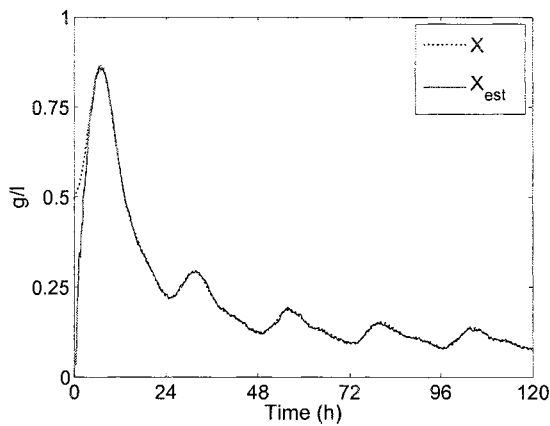


Figure A-56: Performance of Observer 2 for 5% measurement noise

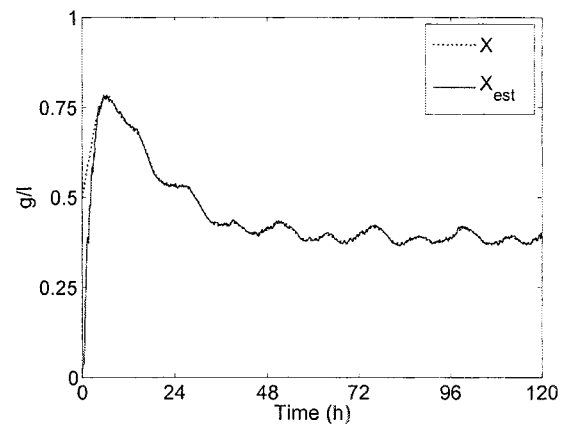


Figure A-59: Performance of Observer 2 for 5% measurement noise

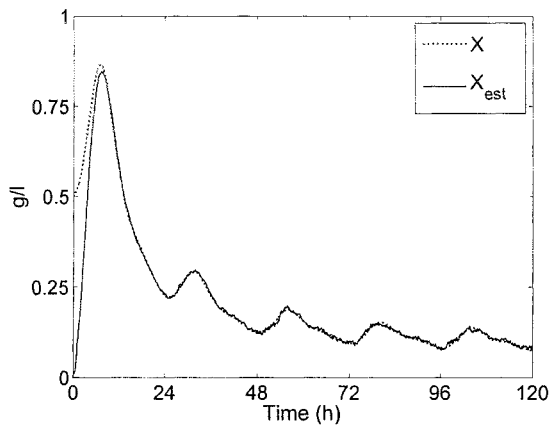


Figure A-57: Performance of Observer 3 for 5% measurement noise

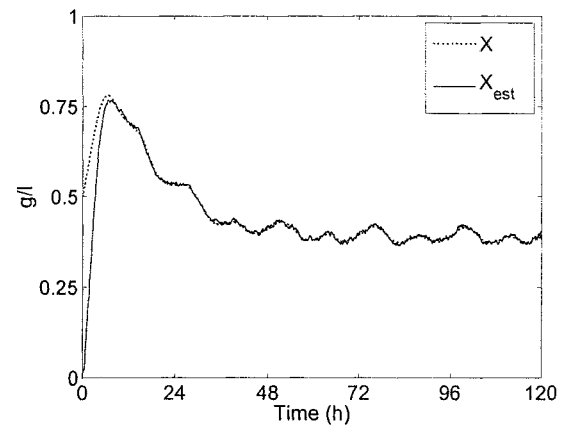


Figure A-60: Performance of Observer 3 for 5% measurement noise

Stepping S_{in} & stepping D

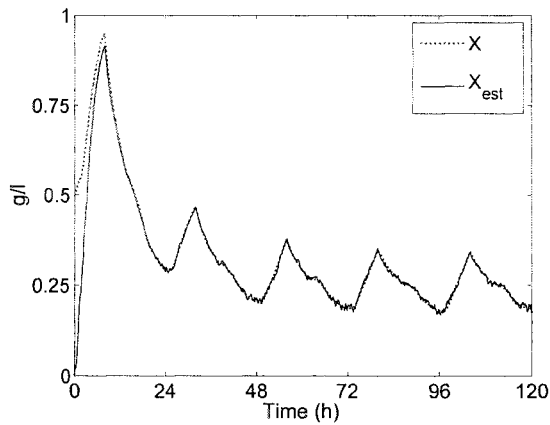


Figure A-61: Performance of Observer 1 for 5% measurement noise

Stepping S_{in} & typical D

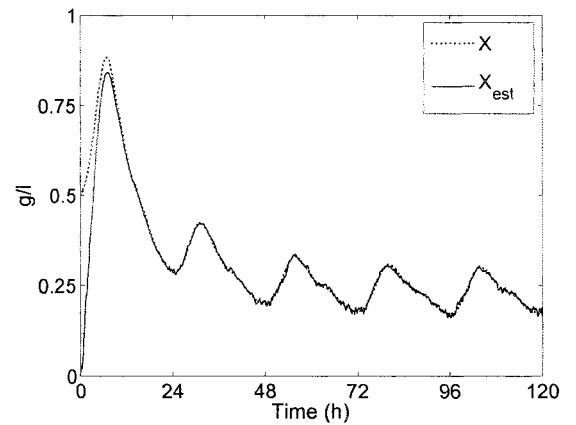


Figure A-64: Performance of Observer 1 for 5% measurement noise

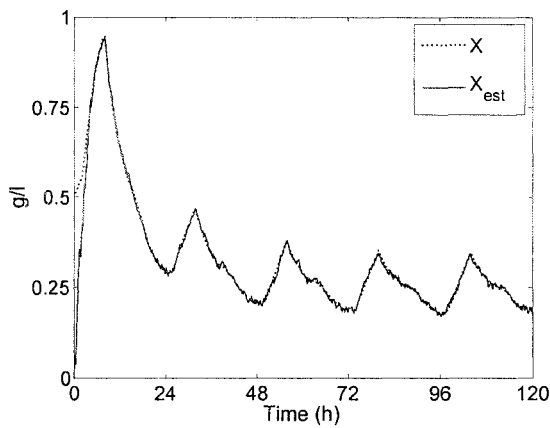


Figure A-62: Performance of Observer 2 for 5% measurement noise

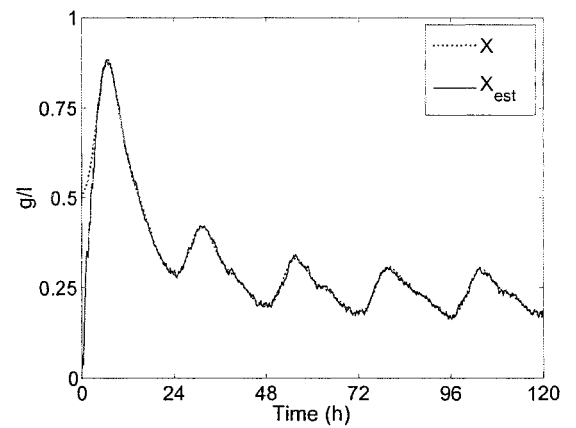


Figure A-65: Performance of Observer 2 for 5% measurement noise

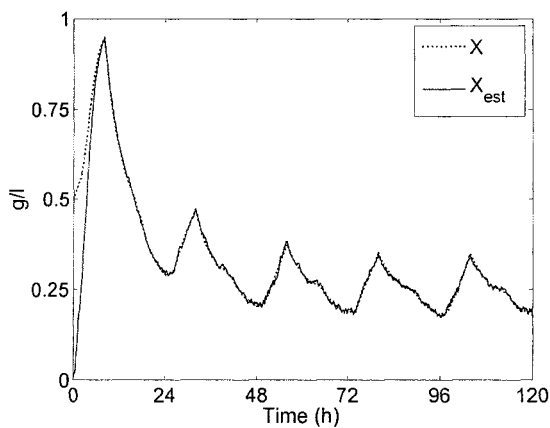


Figure A-63: Performance of Observer 3 for 5% measurement noise

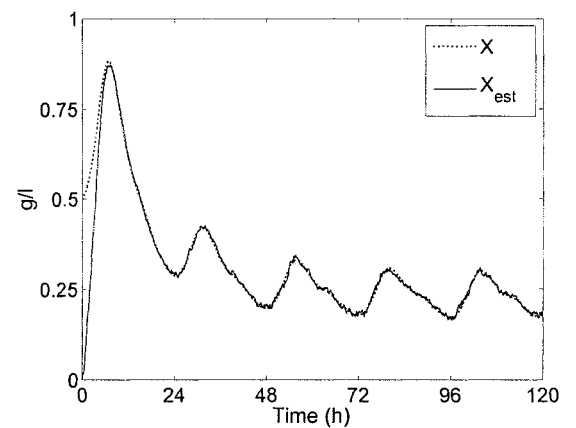


Figure A-66: Performance of Observer 3 for 5% measurement noise

A.2.3 Estimation under 10% measurement noise

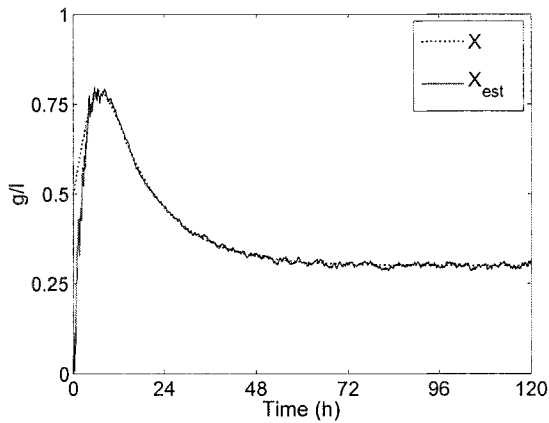


Figure A-67: Performance of Observer 2 for 10% measurement noise for constant $S_{in} = 5g/l$ and constant $D = 0.1h^{-1}$

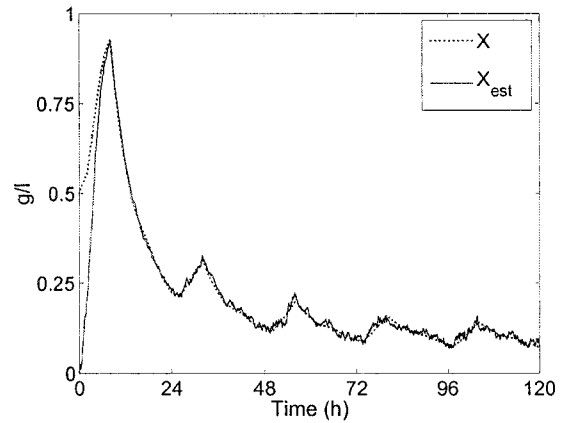


Figure A-70: Performance of Observer 3 for 10% measurement noise for constant $S_{in} = 5g/l$ and stepping D

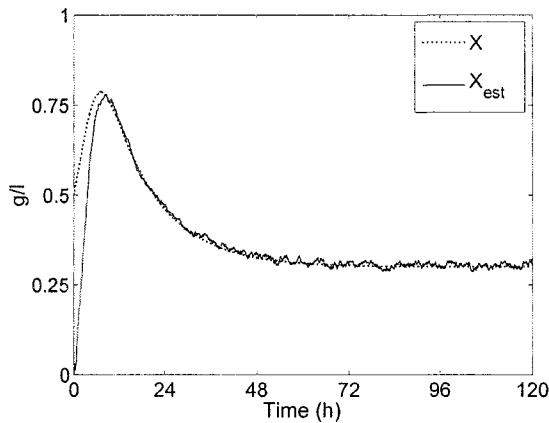


Figure A-68: Performance of Observer 3 for 10% measurement noise for constant $S_{in} = 5g/l$ and constant $D = 0.1h^{-1}$

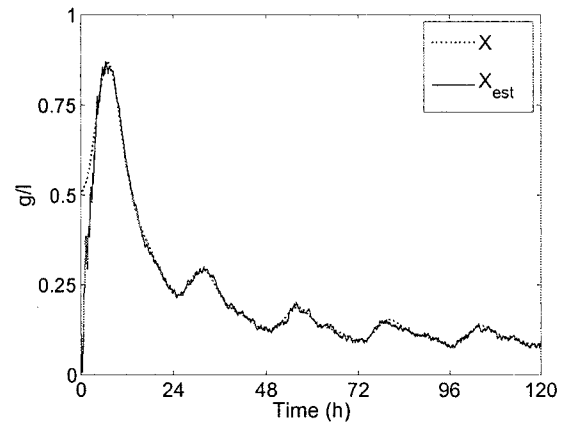


Figure A-71: Performance of Observer 2 for 10% measurement noise for constant $S_{in} = 5g/l$ and typical D

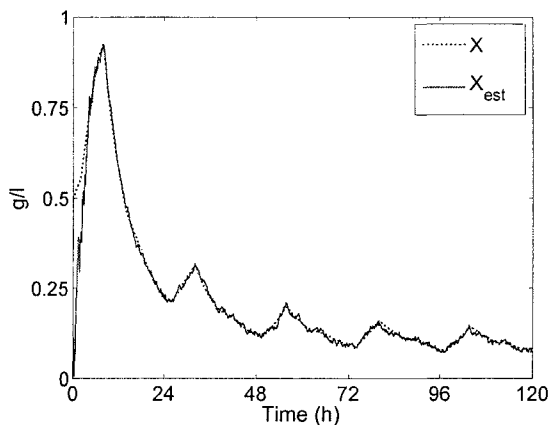


Figure A-69: Performance of Observer 2 for 10% measurement noise for constant $S_{in} = 5g/l$ and stepping D

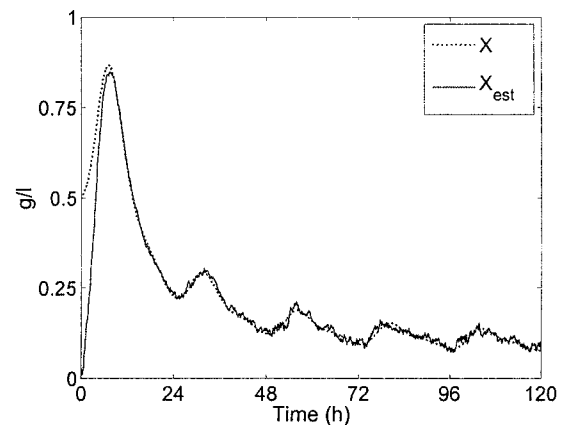


Figure A-72: Performance of Observer 3 for 10% measurement noise for constant $S_{in} = 5g/l$ and typical D

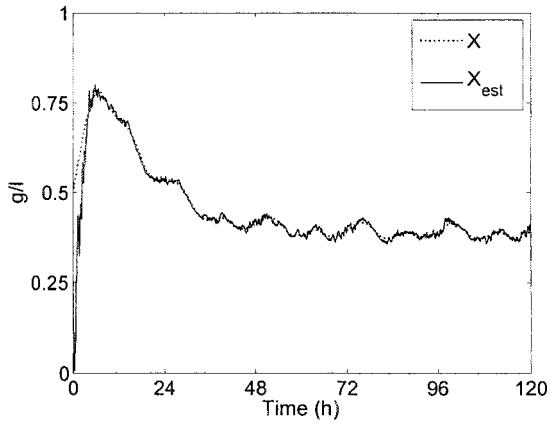


Figure A-73: Performance of Observer 2 for 10% measurement noise for stepping S_{in} and constant $D = 0.1h^{-1}$

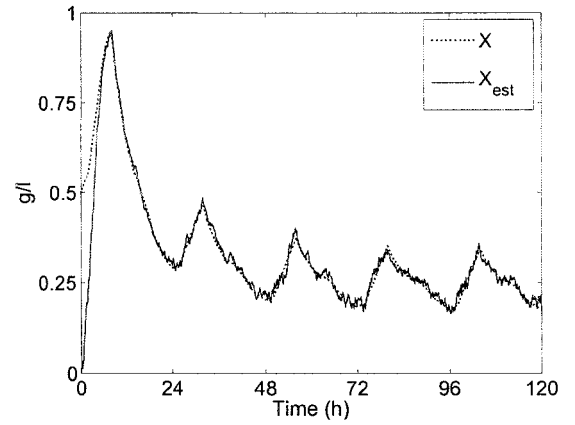


Figure A-76: Performance of Observer 3 for 10% measurement noise for stepping S_{in} and stepping D

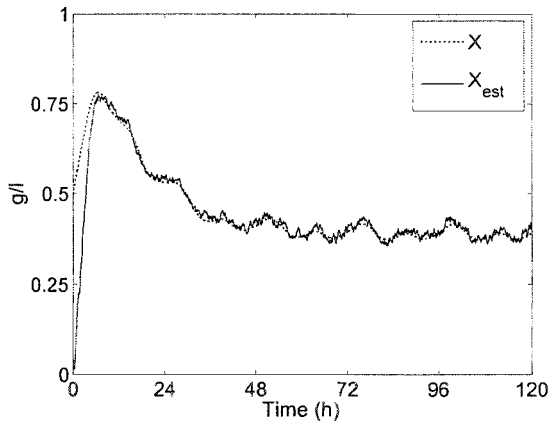


Figure A-74: Performance of Observer 3 for 10% measurement noise for stepping S_{in} and constant $D = 0.1h^{-1}$

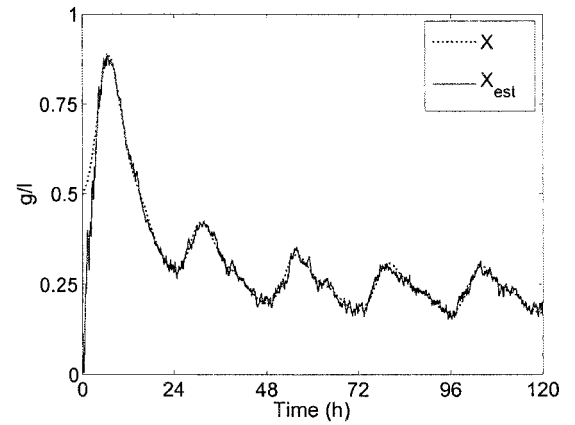


Figure A-77: Performance of Observer 2 for 10% measurement noise for stepping S_{in} and typical D

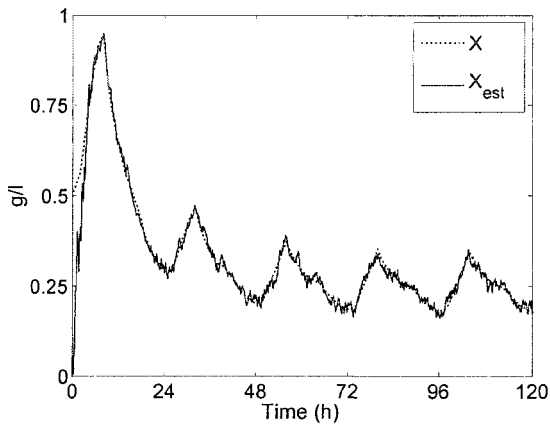


Figure A-75: Performance of Observer 2 for 10% measurement noise for stepping S_{in} and stepping D

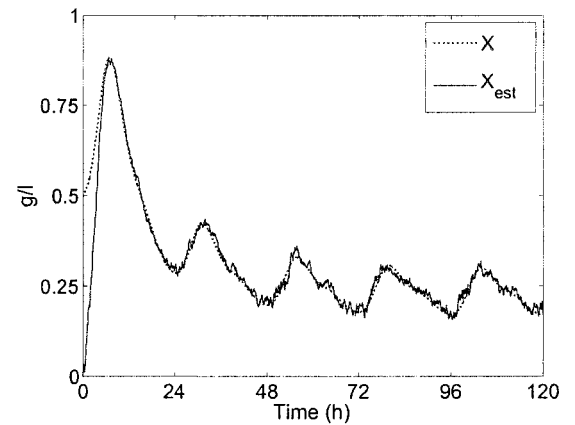


Figure A-78: Performance of Observer 3 for 10% measurement noise for stepping S_{in} and typical D

A.3 Estimation for known SGR - Parameter Set 4

Here, we show the simulation results for the estimation of biomass concentration for parameter Set 4 under different dilution rates D and influent substrate concentrations S_{in} . The parameter values used are given in Table A.7. The tuning parameters used for Observers 1-3 under clean measurement are summarised in Table A.8. For Observer 3, a choice of $\alpha(u, y) = -\frac{1}{2}$ is used. Note CS_{in} : Constant S_{in} ; SS_{in} : Stepping S_{in} .

$X(0) = 0.5g/l$	$K_s = 4g/l$
$\hat{X}(0) = 0g/l$	$Y_s = 3$
$S(0) = \hat{S}(0) = 10g/l$	$k_1 = 2$
$\mu_{max} = 0.3h^{-1}$	$k_2 = 1$

Table A.7: Set 4 parameter values

Observer		D Constant	D Stepping	D Typical
1	CS_{in}	$\theta_c = -3$	$\theta_c = -3$	$\theta_c = -3$
	SS_{in}	$\theta_c = -3$	$\theta_c = -3$	$\theta_c = -3$
2	CS_{in}	$\theta_a = \theta_{max} = -3$	$\theta_a = \theta_{max} = -3$	$\theta_a = \theta_{max} = -3$
	SS_{in}	$\theta_a = \theta_{max} = -3$	$\theta_a = \theta_{max} = -3$	$\theta_a = \theta_{max} = -3$
3	CS_{in}	$\theta_c\beta = 1$	$\theta_c\beta = 1$	$\theta_c\beta = 1$
	SS_{in}	$\theta_c\beta = 1$	$\theta_c\beta = 1$	$\theta_c\beta = 1$

Table A.8: Observer tuning parameter values under clean measurement - Set 4

As in the results for estimation using parameter Set 1, for the clean measurement case, we show the estimation profile given by Observer 1. We then show the profiles of the gain ψ_2 of Observers 1-3 for the same estimation performance.

For each observer, we consider an additive noise ϵ with amplitudes equal to 5% and 10% of the measured value S . The tuning parameter values used for Observers 1, 2, and 3 under noisy measurement are summarised in Table A.9.

Observer		D Constant	D Stepping	D Typical
1	CS_{in}	$\theta_c = -1.7$	$\theta_c = -1.3$	$\theta_c = -1.3$
	SS_{in}	$\theta_c = -1.7$	$\theta_c = -1.3$	$\theta_c = -1.3$
2	CS_{in}	$\theta_a = \theta_{\max} = -1.7$	$\theta_a = \theta_{\max} = -1.3$	$\theta_a = \theta_{\max} = -1.3$
	SS_{in}	$\theta_a = \theta_{\max} = -1.7$	$\theta_a = \theta_{\max} = -1.3$	$\theta_a = \theta_{\max} = -1.3$
3	CS_{in}	$\theta_c\beta = 0.05$	$\theta_c\beta = 0.05$	$\theta_c\beta = 0.05$
	SS_{in}	$\theta_c\beta = 0.05$	$\theta_c\beta = 0.05$	$\theta_c\beta = 0.05$

Table A.9: Observer tuning parameter values under noisy measurement - Set 4

A.3.1 Estimation under clean measurement

Observer 1 - Constant S_{in}

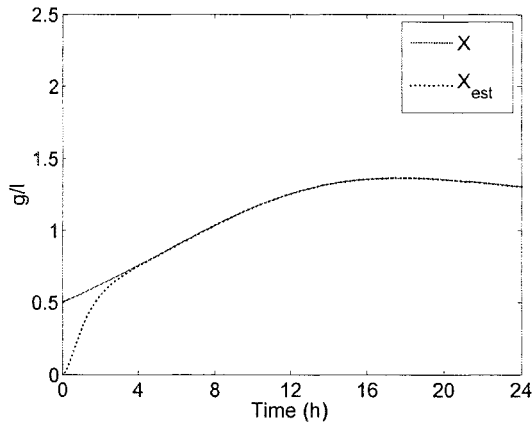


Figure A-79: Performance of Observer 1 for parameter Set 4 with constant $S_{in} = 5g/l$ and constant $D = 0.1h^{-1}$

Observer 1 - Stepping S_{in}

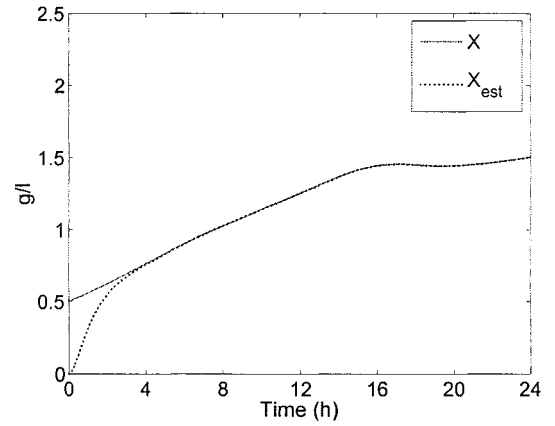


Figure A-82: Performance of Observer 1 for parameter Set 4 with stepping S_{in} and constant $D = 0.1h^{-1}$

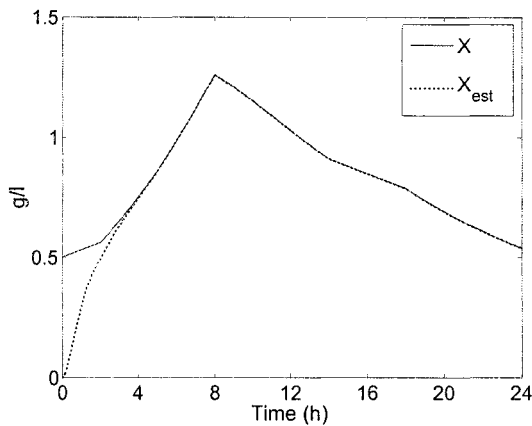


Figure A-80: Performance of Observer 1 for parameter Set 4 with constant $S_{in} = 5g/l$ and stepping D

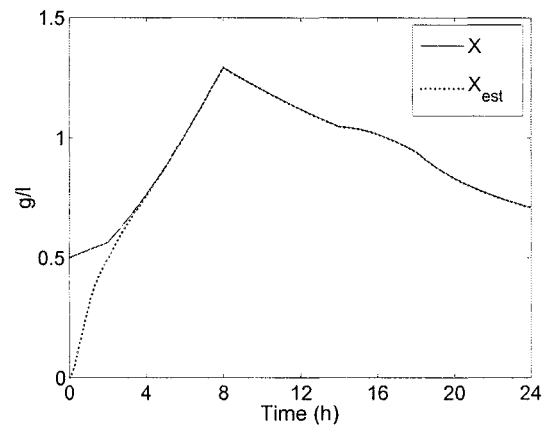


Figure A-83: Performance of Observer 1 for parameter Set 4 with stepping S_{in} and stepping D

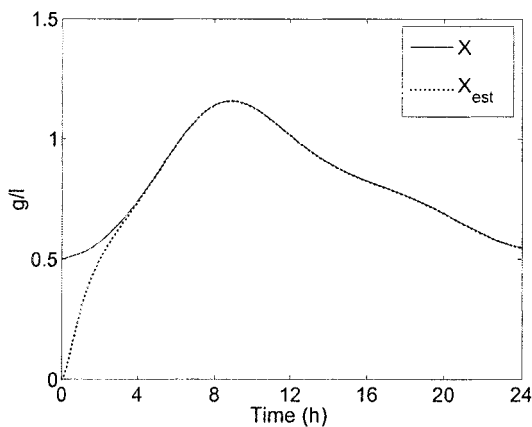


Figure A-81: Performance of Observer 1 for parameter Set 4 with constant $S_{in} = 5g/l$ and typical D

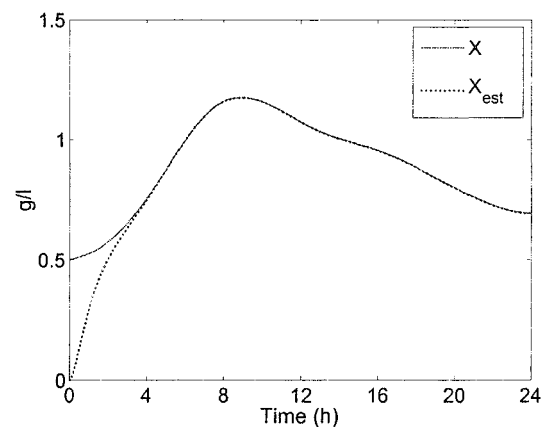


Figure A-84: Performance of Observer 1 for parameter Set 4 with stepping S_{in} and typical D

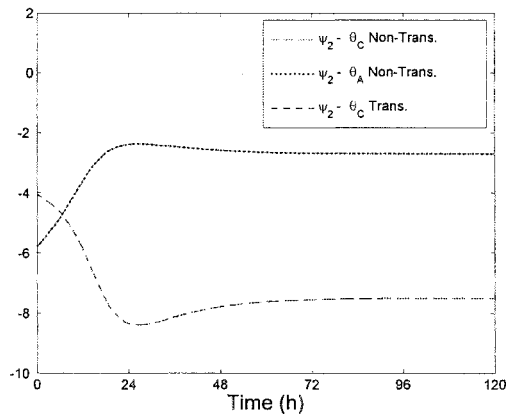


Figure A-85: Profiles of ψ_2 of each observer for constant $S_{in} = 5g/l$ and constant $D = 0.1h^{-1}$

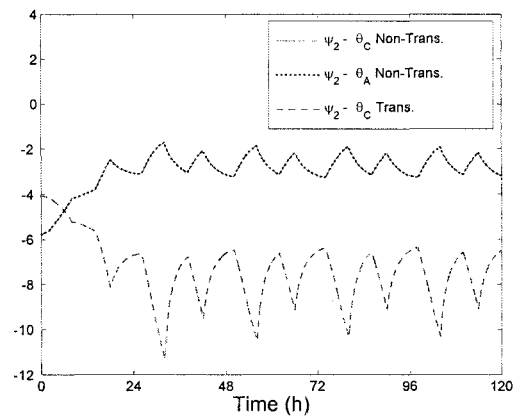


Figure A-88: Profiles of ψ_2 of each observer for stepping S_{in} and constant $D = 0.1h^{-1}$

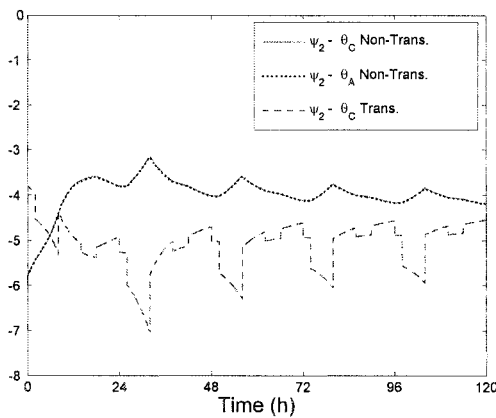


Figure A-86: Profiles of ψ_2 of each observer for constant $S_{in} = 5g/l$ and stepping D

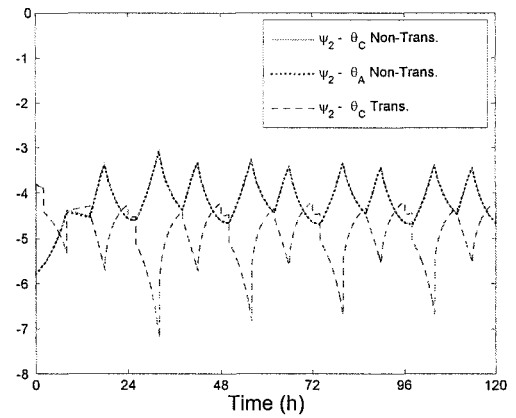


Figure A-89: Profiles of ψ_2 of each observer for stepping S_{in} and stepping D

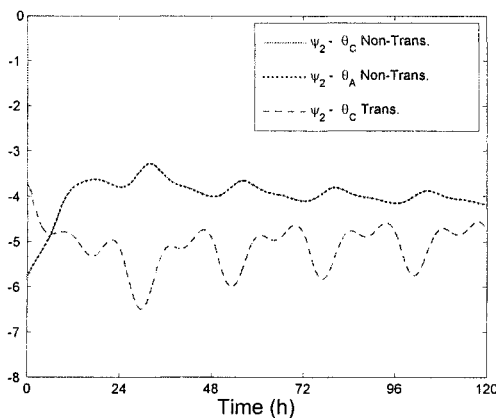


Figure A-87: Profiles of ψ_2 of each observer for constant $S_{in} = 5g/l$ and stepping D

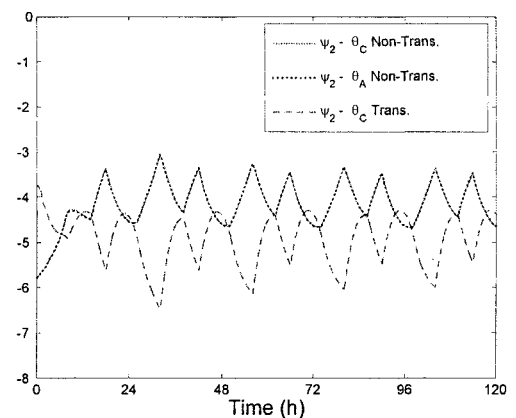


Figure A-90: Profiles of ψ_2 of each observer for stepping S_{in} and typical D

A.3.2 Estimation under 5% measurement noise

Constant S_{in} & constant D

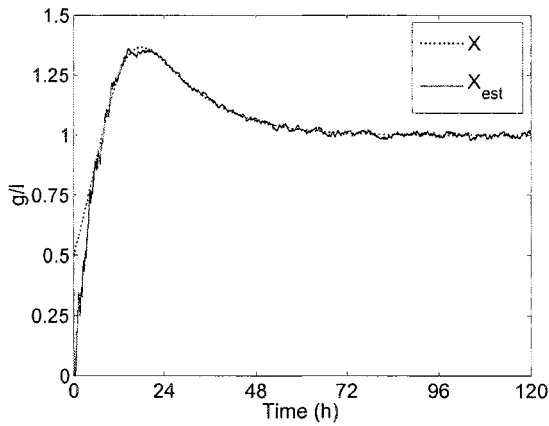


Figure A-91: Performance of Observers 1 and 2 for 5% measurement noise

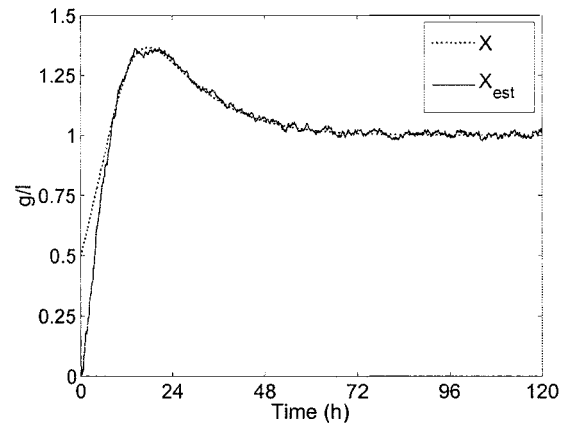


Figure A-92: Performance of Observer 3 for 5% measurement noise

Constant S_{in} & stepping D

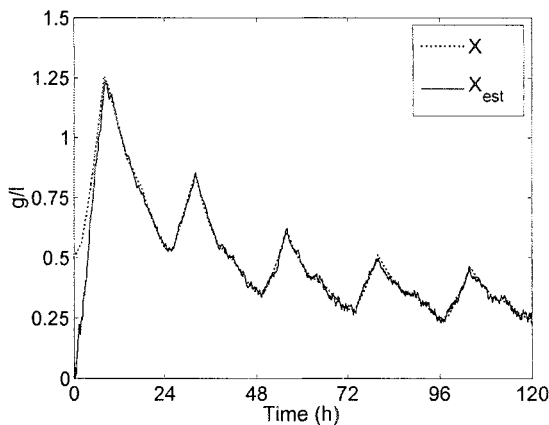


Figure A-93: Performance of Observers 1 and 2 for 5% measurement noise

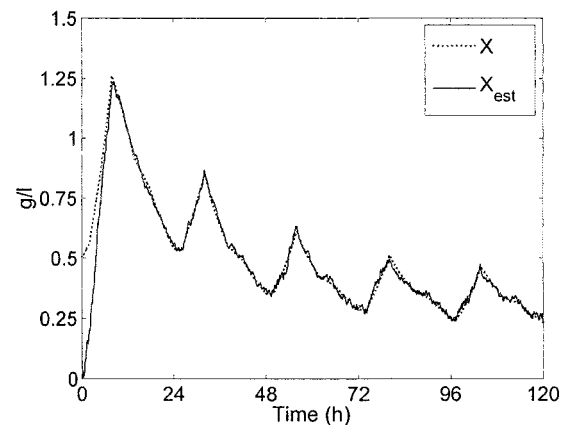


Figure A-94: Performance of Observer 3 for 5% measurement noise

Constant S_{in} & typical D

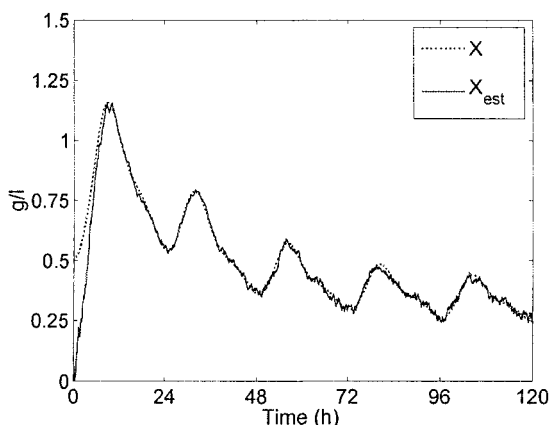


Figure A-95: Performance of Observers 1 and 2 for 5% measurement noise

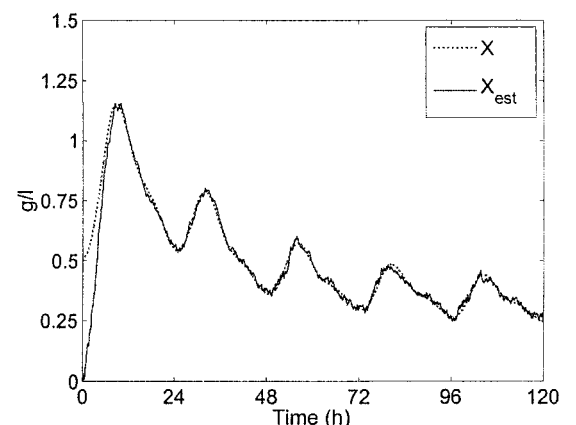


Figure A-96: Performance of Observer 3 for 5% measurement noise

Stepping S_{in} & constant D

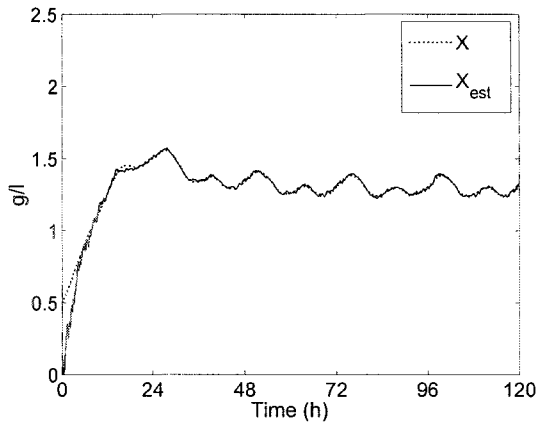


Figure A-97: Performance of Observers 1 and 2 for 5% measurement noise

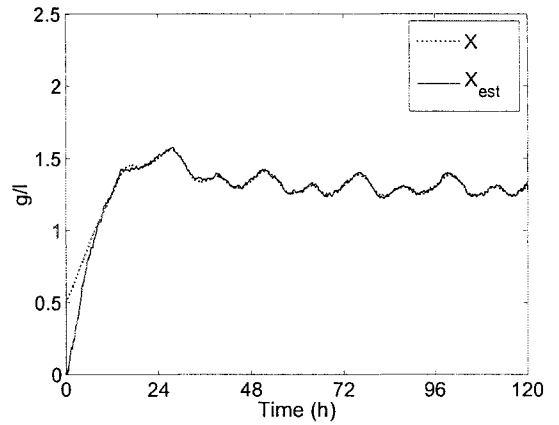


Figure A-98: Performance of Observer 3 for 5% measurement noise

Stepping S_{in} & stepping D

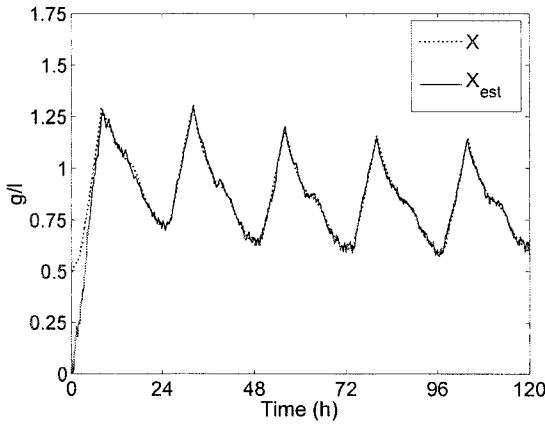


Figure A-99: Performance of Observers 1 and 2 for 5% measurement noise

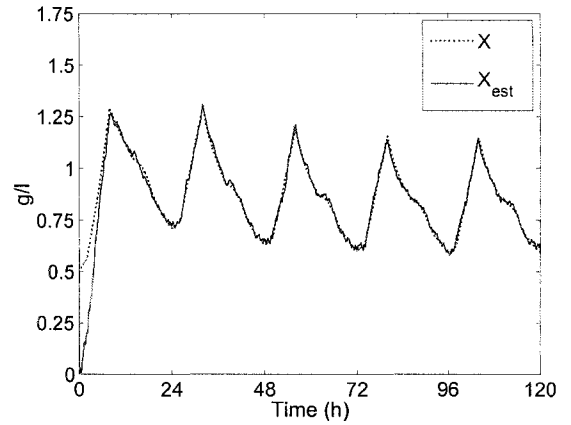


Figure A-100: Performance of Observer 3 for 5% measurement noise

Stepping S_{in} & typical D

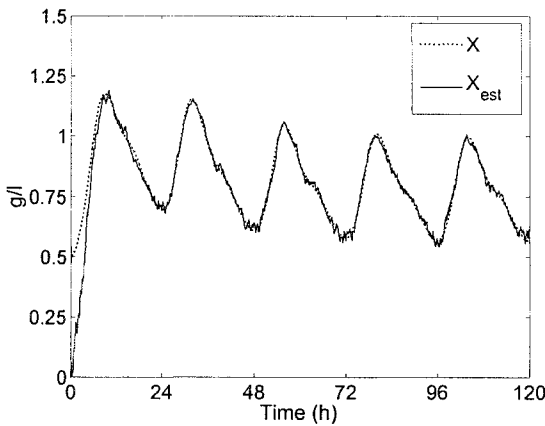


Figure A-101: Performance of Observers 1 and 2 for 5% measurement noise

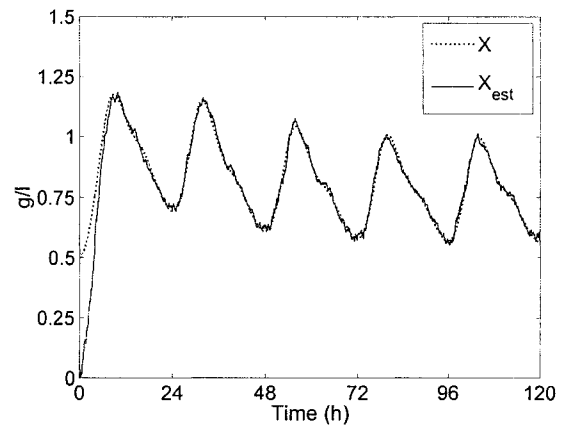


Figure A-102: Performance of Observer 3 for 5% measurement noise

A.3.3 Estimation under 10% measurement noise

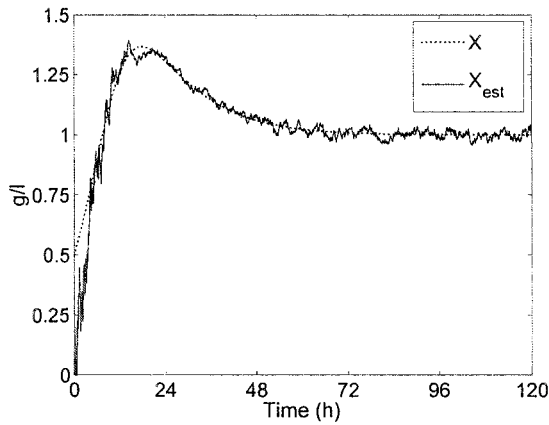


Figure A-103: Performance of Observers 1 and 2 for 10% measurement noise for constant $S_{in} = 5g/l$ and $D = 0.1h^{-1}$

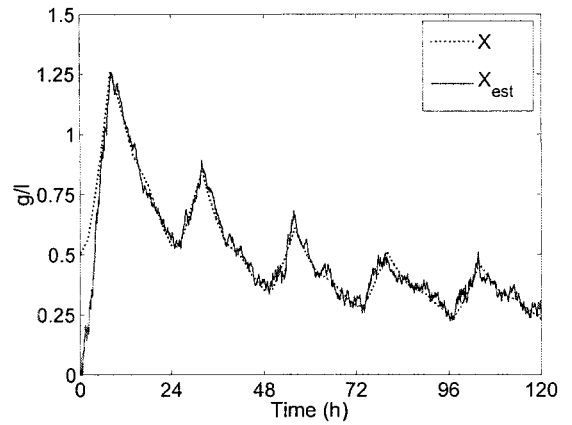


Figure A-106: Performance of Observer 3 for 10% measurement noise for constant $S_{in} = 5g/l$ and stepping D

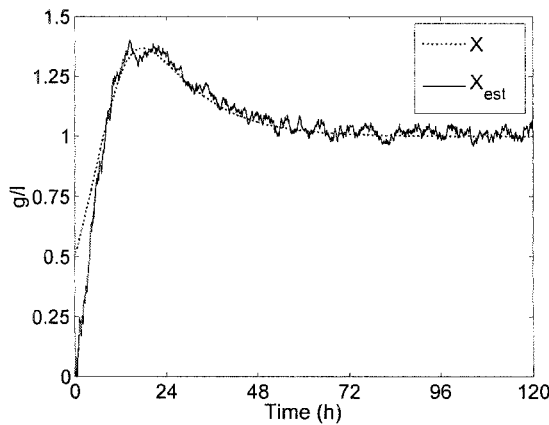


Figure A-104: Performance of Observer 3 for 10% measurement noise for constant $S_{in} = 5g/l$ and constant $D = 0.1h^{-1}$

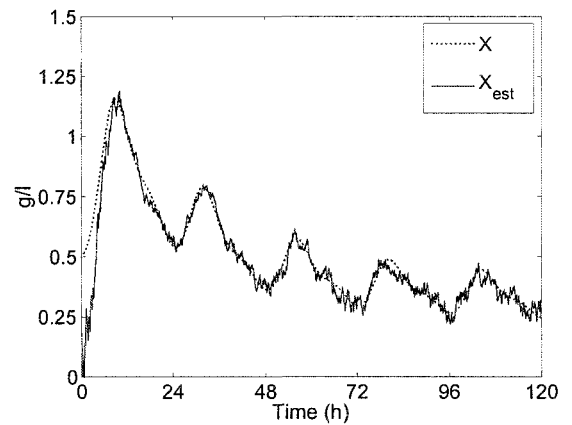


Figure A-107: Performance of Observers 1 and 2 for 10% measurement noise for constant $S_{in} = 5g/l$ and typical D

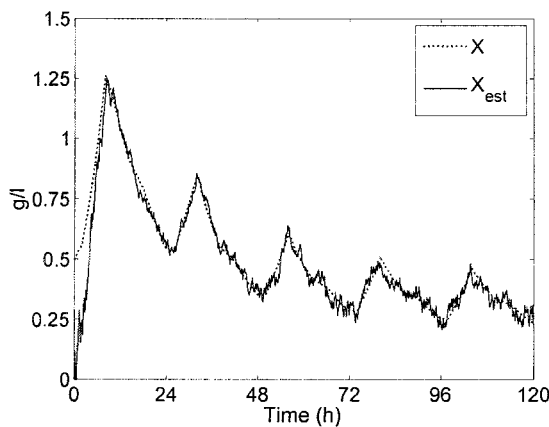


Figure A-105: Performance of Observers 1 and 2 for 10% measurement noise for constant $S_{in} = 5g/l$ and stepping D

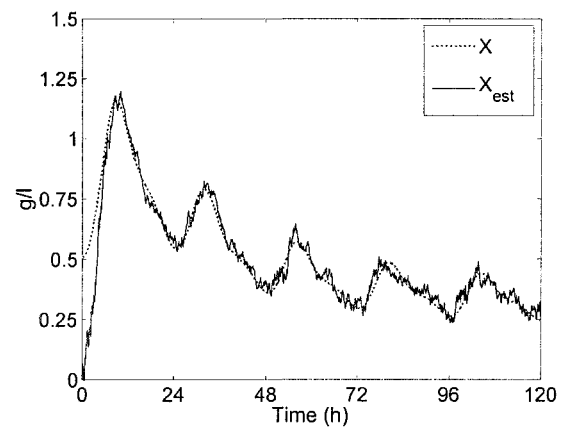


Figure A-108: Performance of Observer 3 for 10% measurement noise for constant $S_{in} = 5g/l$ and typical D

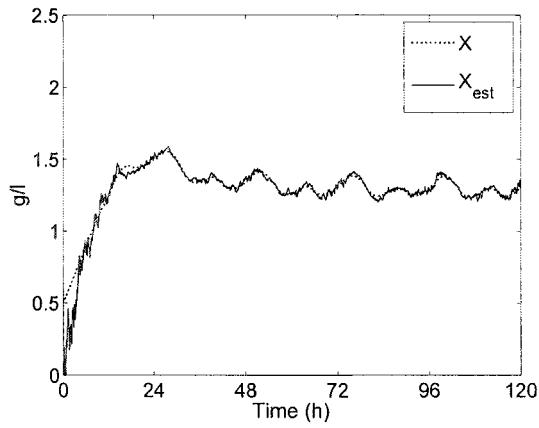


Figure A-109: Performance of Observers 1 and 2 for 10% measurement noise for stepping S_{in} and constant $D = 0.1h^{-1}$

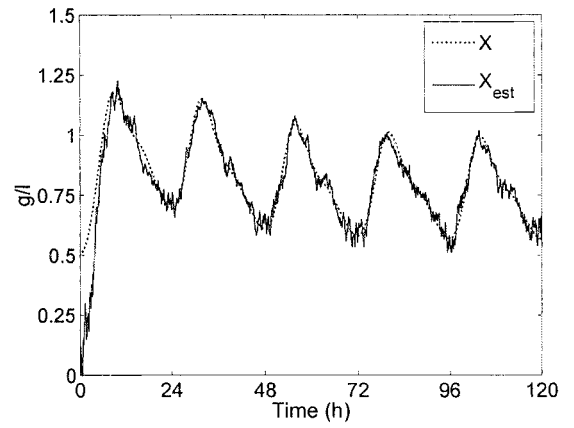


Figure A-111: Performance of Observers 1 and 2 for 10% measurement noise for stepping S_{in} and typical D

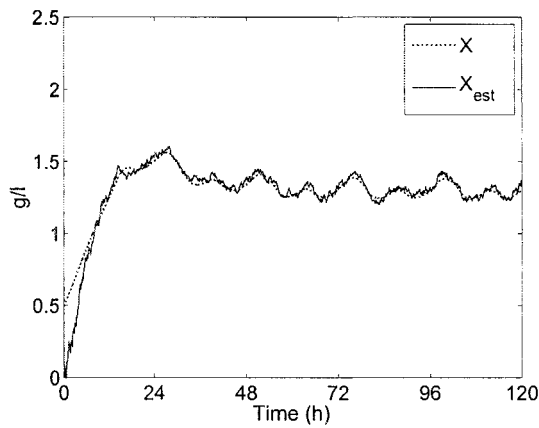


Figure A-110: Performance of Observer 3 for 10% measurement noise for stepping S_{in} and constant $D = 0.1h^{-1}$

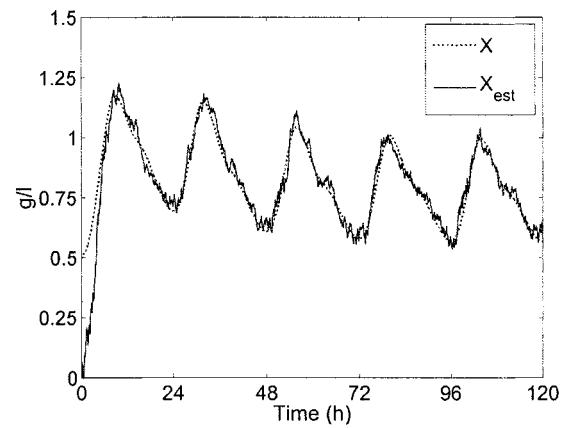


Figure A-112: Performance of Observer 3 for 10% measurement noise for stepping S_{in} and typical D

A.4 Estimation for partially known SGR - Parameter Set 2

Here, we show the performance of Observer 4 for the case of biomass estimation with only a partial knowledge of the specific growth rate using parameter Set 2. Constant, stepping, and typical dilution rates D , and a stepping influent substrate concentration S_{in} are used. Estimation is considered both in the absence and in the presence of measurement noise with amplitudes equal to 5% and 15% of the measured value of substrate concentration S . The parameter values used are as given in Table A.1. In all cases, the tuning parameter values used are given in Table A.10.

	Positive unknown	Negative unknown
D Constant	$\theta_a = \theta_{\min} = -0.35$	$\theta_a(0) = -1.5, \theta_{\min} = -0.5$
D Stepping	$\theta_a = \theta_{\min} = -0.25$	$\theta_a(0) = -1, \theta_{\min} = -0.35$
D Typical	$\theta_a = \theta_{\min} = -0.25$	$\theta_a(0) = -1, \theta_{\min} = -0.35$

Table A.10: Observer 4 tuning parameter values for the partially known case - Set 2

A.4.1 Estimation under clean measurement

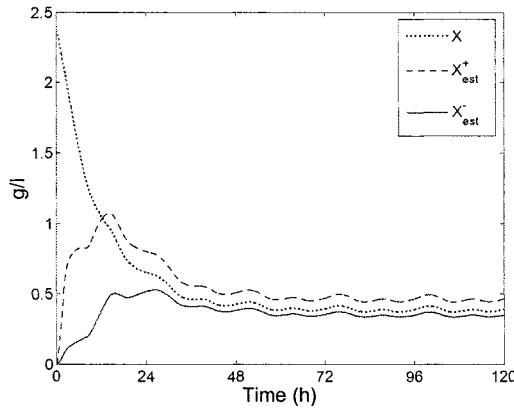


Figure A-113: Biomass estimation for partially known μ with constant $D = 0.1h^{-1}$ under clean measurement

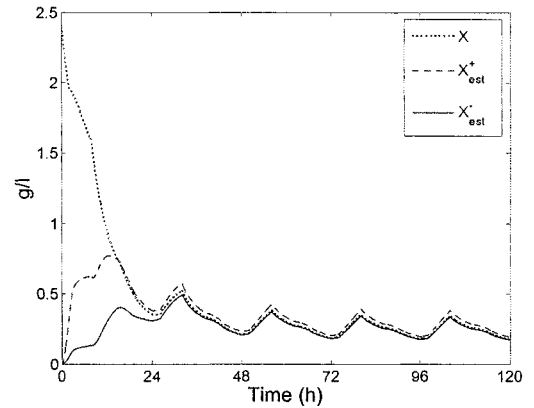


Figure A-114: Biomass estimation for partially known μ with stepping D under clean measurement

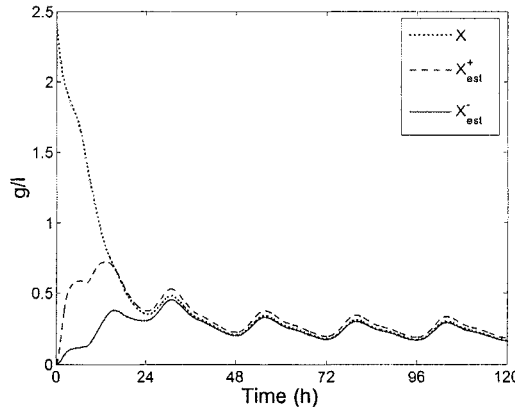


Figure A-115: Biomass estimation for partially known μ with typical D under clean measurement

A.4.2 Estimation under noisy measurement

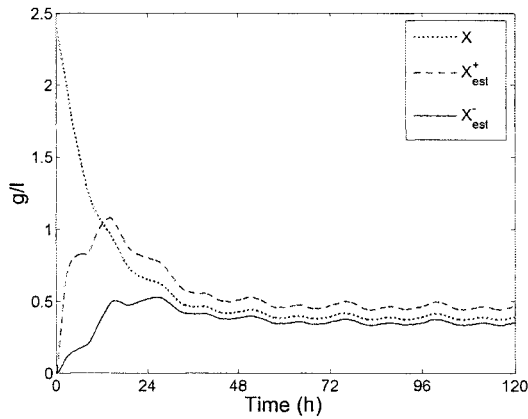


Figure A-116: Biomass estimation for partially known μ with constant $D = 0.1h^{-1}$ for 5% measurement noise

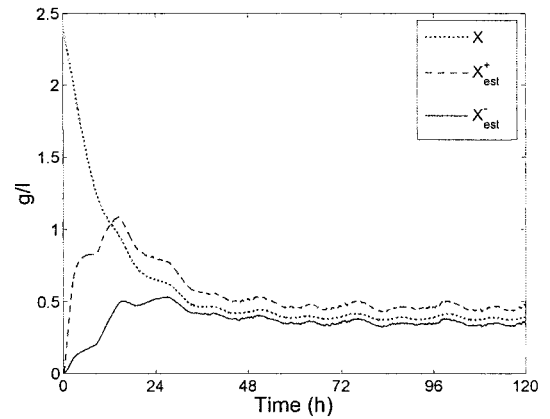


Figure A-119: Biomass estimation for partially known μ with constant $D = 0.1h^{-1}$ for 15% measurement noise

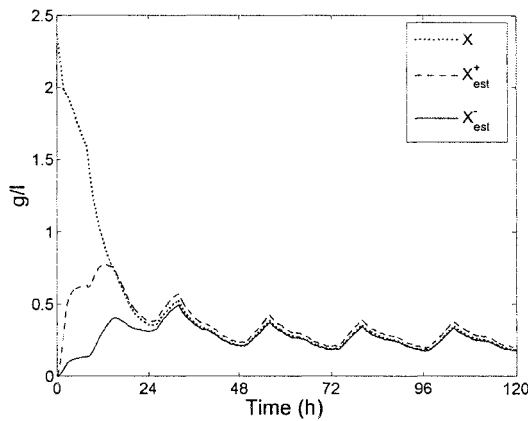


Figure A-117: Biomass estimation for partially known μ with stepping D for 5% measurement noise

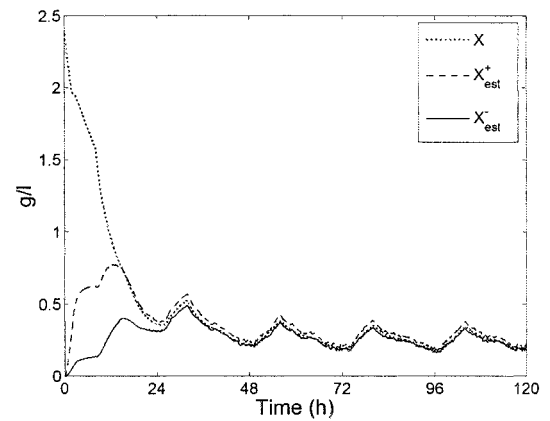


Figure A-120: Biomass estimation for partially known μ with stepping D for 15% measurement noise

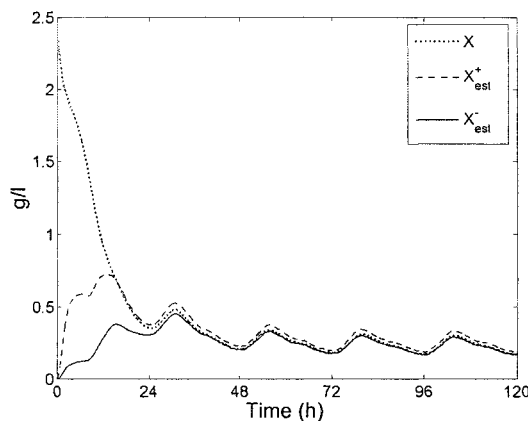


Figure A-118: Biomass estimation for partially known μ with typical D for 5% measurement noise

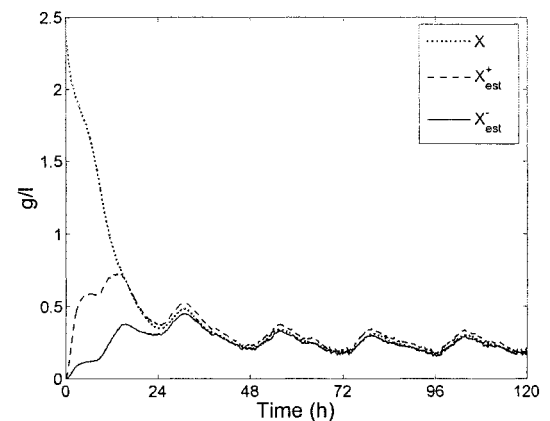


Figure A-121: Biomass estimation for partially known μ with typical D for 15% measurement noise

Appendix B

Bioprocess Background Information

B.1 Specific growth rate of biomass

The specific growth rate can be described using a multiplication of individual terms:

$$\mu(t) = \mu(S) \mu(X) \mu(S_o) \mu(pH) \mu(T) \dots$$

where S : substrate concentration; X : biomass concentration; S_o : dissolved oxygen concentration; pH : potential of hydrogen; and T : temperature. Some models that have been developed are now shown in the following subsections.

B.1.1 Influence of the substrate concentration

Michaelis-Menton law (1913) or Monod law:

$$\mu = \frac{\mu_{\max} S}{K_s + S}$$

where μ_{\max} is the maximum specific growth rate, and K_s is the Michaelis-Menton (or saturation) constant. The Michaelis-Menton constant is the value of substrate concentration at which the specific growth rate is equal to half its maximum value.

Tessier (1942):

$$\mu = \mu_{\max} \left(1 - e^{\frac{-S}{K_s}} \right).$$

Blackman:

$$\begin{aligned} \mu &= \frac{\mu_{\max}}{K_s} S && \text{if } S \leq K_s \\ &= \mu_{\max} && \text{if } S > K_s \end{aligned}$$

which is a combination of 1st-order kinetics for $S \leq K_s$, and zero-order kinetics for $S > K_s$.

Haldane

The Haldane law is a development of the Monod law and takes into account inhibition in enzyme-substrate reactions. The model takes the form:

$$\mu = \frac{\mu_0 S}{K_s + S + \frac{S^2}{K_i}}$$

where K_i is the inhibition parameter, and

$$\mu_0 = \mu_{\max} \left(1 + 2\sqrt{\frac{K_s}{K_i}} \right).$$

Haldane's model is useful in situations where substrate inhibition is important (at very high concentrations). The maximum specific growth rate occurs at

$$S = \sqrt{K_s K_i}.$$

B.1.2 Influence of the biomass concentration

Verhulst (1838), logistic model:

$$\mu(X) = \mu_{\max} (1 - aX)$$

where $a = \frac{1}{X_{\max}}$ is the inhibition constant.

Contois (1959):

$$\mu = \frac{\mu_{\max} S}{K_c X + S}.$$

This is clearly a function of S and X .

B.1.3 Influence of pH level

Microbial growth takes place only if temperature and pH are within ranges of admissible values. Few models for this pH dependency are presented up to now. One possibility is a bell-shaped function:

$$K_{pH} = K_{\max} \cdot \frac{1}{1 + 10^{pK_1 - pH} + 10^{pH - pK_2}}$$

where pK_1 and pK_2 are the low and the high pH with half of the maximum activity.

B.1.4 Influence of temperature

This is usually modelled by an Arrhenius-type law:

$$\mu(T) = a_1 e^{-\frac{E_1}{RT}} - a_2 e^{-\frac{E_2}{RT}} - b$$

where E_1 and E_2 are activation energies, R is the gas constant ($8.314 J.g.mol/K$), and a_1 , a_2 , and b are constants. This expression shows that the specific growth rate increases continuously with temperature until a maximum value T_{\max} (at which the cells die). This is often simplified to

$$\mu(T) = K_{T_1} \cdot 10^{-\alpha(T_1 - T_2)} \text{ or } K_{T_1} \cdot \theta^{-(T_1 - T_2)}$$

where θ is around 1.03 to 1.05 for most processes.

B.2 Bioprocess model derivation

The modelling method used can be found in [32]. The basis of the model derivation is the simple and well-known premise of conservation of mass and energy. For the system considered, the basis is simply what goes into the tank either remains there or exits at some point. The general mass balance equation, in this case, is expressed as:

$$\begin{aligned}
\text{Rate of change of mass in tank} &= \text{Rate of mass inlet} - \text{Rate of mass outlet} \\
&+ \text{Rate of mass produced} \\
&- \text{Rate of mass consumed.}
\end{aligned}$$

B.2.1 General model of component concentration

With the system expressed in terms of simple mass balance equations, expressions of the concentrations of interest can be derived and subsequently can provide a model of the bioreactor. The first step is to express the mass balance in terms of concentration and liquid medium volume, where mass m is expressed as

$$m = CV$$

where C denotes concentration, and V is the liquid medium volume in the tank. Throughout the modelling procedure, there are a number of assumptions made about the system. The first assumption made is that nutrient densities are equal and constant. The mass balance can then be written as

$$\frac{d(CV)}{dt} = C_{in}Q_{in} - C_{out}Q_{out} \pm V\phi$$

where C_{in} and C_{out} are the inlet and outlet component concentrations, respectively, Q_{in} and Q_{out} are the inlet and outlet volumetric flow rates, respectively, and ϕ denotes the conversion rate of C . The production rate is denoted by $+\phi$ and the consumption rate by $-\phi$.

The next assumption is that of perfect mixing, implying that the concentration considered, C , is homogeneous throughout the liquid medium. It is, therefore, assumed that the concentration at the bioreactor outlet is the same as that at any other point in the tank. A further assumption is made based upon a constant-volume tank. From basic modelling, the rate of change of liquid medium volume in the tank is given by

$$\frac{dV}{dt} = Q_{in} - Q_{out}.$$

For a constant-volume tank,

$$\frac{dV}{dt} = 0$$

which implies

$$Q_{in} = Q_{out}.$$

Following some simple manipulation, the mass balance equation can be simplified to

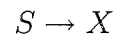
$$V \frac{dC}{dt} = Q_{in} (C_{in} - C) \pm V \phi$$

$$\dot{C} = D (C_{in} - C) \pm \phi$$

where $D = \frac{Q_{in}}{V}$ denotes the dilution rate.

B.2.2 Microbial growth reaction

Consider the following microbial growth reaction taking place in the bioreactor:



where S denotes the limiting substrate concentration and X denotes the biomass concentration. The first assumption in this instance, is that only the substrate S is present in the inlet.

The biomass model can be expressed as

$$\dot{X} = -DX \pm \phi_X$$

and the substrate model is given as

$$\dot{S} = D(S_{in} - S) \pm \phi_S.$$

With the transport dynamics expressions established, the final stage of the modelling process is to express the conversion dynamics, i.e. the concentration conversion rates ϕ_X and ϕ_S . In line with a widely accepted assumption, introduced by Monod in 1942, we consider that a reaction rate ρ is given as

$$\rho = \mu X$$

where the coefficient μ is the biomass' specific growth rate. For biomass, the conversion rate is equal to the reaction rate ρ :

$$\phi_X = \mu X \quad (\text{B.1})$$

and the conversion term for the substrate is given as

$$\phi_S = Y_s \rho = Y_s \mu X$$

where Y_s is a yield coefficient expressed as

$$Y_s = \frac{\text{one gram of substrate consumed}}{\text{biomass produced (g)}}.$$

In biochemical engineering, the yield coefficient Y is standardised with respect to the biomass X , and is expressed as

$$Y = \frac{\text{biomass produced (g)}}{\text{one gram of substrate consumed}}.$$

More specifically, it is the amount of biomass produced when one unit of substrate is consumed by the reaction. This standardisation corresponds to the form of the biomass conversion rate in (B.1).

The complete model of the bioreactor is then expressed as

$$\begin{cases} \dot{S}(t) = D(t) (S_{in}(t) - S(t)) - Y_s \mu(t) X(t) \\ \dot{X}(t) = \mu(t) X(t) - D(t) X(t) \end{cases}$$

where μ is the specific growth rate (SGR) of biomass; D is the dilution rate; S_{in} is the influent substrate concentration, and Y_s is the yield coefficient for substrate concentration.

B.3 Measurement of substrate concentration

In this work, the methods considered to provide estimations of the biomass concentration are observer-based and assume the on-line measurement of the substrate concentration is readily available. Therefore, it is important to establish that the on-line measurement of the substrate concentration is, in fact, viable. Indeed, there are a number of methods available for the determination of organic content in wastewater. These include standard analysis of global parameters such as Biological Oxygen Demand (BOD), Chemical Oxygen Demand (COD), and Total Organic Content (TOC). The determination of these parameters has, for many years, been performed via off-line laboratory-based analytical techniques, which can be time-consuming. Traditionally, the level of organic pollution is measured by a standard 5-day test called the BOD₅. First published in 1917, the technique determines the amount of dissolved oxygen required by heterotrophic bacteria to oxidise organic material in the 5-day period. To ensure a fair test is conducted, a small amount of micro-organism seed is initially added to each sample being tested. From the results, the concentration of organic pollution in the sample can be determined. An alternative test that has also been widely used is the COD test. The COD test is similar in function to the BOD test in that both provide an indirect measurement of the amount of organic compounds in water. The performance of the COD test involves the use of chemical reagents to fully oxidise organic material into carbon dioxide and water. The total quantity of oxygen required to do this is known as the chemical oxygen demand. From this, the organic content in the samples can be easily determined in a matter of hours. A test that provides results much quicker than BOD or COD, and which has become more common, is the TOC test. Although results can be achieved within minutes, this test measures only the organic content in the water and therefore no other substances that may contribute to the metabolism and reproduction of the micro-organisms (biomass)

are included [92]. From this, it is indicative that measurement of organic loading levels given by BOD and COD methods provide the most reliable values, and are, in fact, used by the RWAs in the UK.

In recent decades, much attention has been focussed upon the need to develop on-line monitoring techniques for the measurement of organic loading such that wastewater treatment processes can be monitored and controlled in real time [92]. There are a number of on-line TOC, COD, and BOD monitoring devices now available to do this [87]. It has been shown that on-line biosensor-based BOD monitors can give values of organic content that compare well with traditional methods within minutes [87], [93], [94], [95], [96].

It is clear that on-line measurement of the substrate concentration is, in fact, viable when considering observer-based estimation of biomass concentration.

Appendix C

Theoretical Concepts - Stability of Dynamical Systems

The very first concept considered when studying a dynamical system is the stability of its equilibrium point(s). The analysis and resulting determination of system stability is paramount in concluding whether the desired, correct and safe operation of a system will be attained, and what additional external stabilising influence is required. The stability of a system is concerned with its behaviour near its equilibrium point(s). This intuitive idea is actually very complex for nonlinear and time-delay systems in particular. Consequently, a large variety of definitions have been proposed. The main objective of the theory of stability is to be able to draw conclusions on the system behaviour without actually calculating its solution.

C.1 Stability of nonlinear systems

We are now going to present some of the definitions that are mainly used in the literature [6], most importantly: Lyapunov stability, asymptotic stability, uniform stability, and exponential

stability.

Consider the general autonomous nonlinear system

$$\dot{x} = f(t, x(t)), \quad t \geq 0, \quad x(0) = x_0 \quad (\text{C.1})$$

where $f : \mathbb{R}^n \times \mathbb{R}^+ \rightarrow \mathbb{R}^n$ is continuous. Since f is continuous, we are assuming that the above system has a unique solution corresponding to each initial condition. This is true, in particular, if f is a global Lipschitz function. Note that f is global Lipschitz if there exist finite positive constants T and k , such that

$$\|f(t, x) - f(t, y)\| \leq k \|x - y\|, \quad \forall x, y \in \mathbb{R}^n, \quad \forall t \in [0, T]. \quad (\text{C.2})$$

A function satisfying the Lipschitz condition (C.2) is said to be Lipschitz continuous, and is continuously differentiable.

Recall also that a state $x_e \in \mathbb{R}^n$ is an equilibrium point for system (C.1) if $f(t, x_e) = 0$, $\forall t \geq 0$. In what follows, we shall assume that x_e is an equilibrium point for system (C.1). We also denote by $x(t, t_0, x_0)$, the solution of (C.1) at time instant t corresponding to the initial condition $x_0 = x(t_0, t_0, x_0)$.

Definition C.1. *Lyapunov stability: The equilibrium point x_e of system (C.1) is stable or Lyapunov stable if for all $\varepsilon > 0$, there exists $\delta(\varepsilon, t_0) > 0$ such that*

$$\|x_0 - x_e\| < \delta(\varepsilon, t_0) \Rightarrow \|x(t, t_0, x_0) - x_e\| < \varepsilon, \quad \forall t \geq t_0.$$

On the other hand, the equilibrium point x_e is unstable if x_e is not Lyapunov stable.

Definition C.2. *Uniform stability: The equilibrium point x_e of system (C.1) is uniformly Lyapunov stable if for all $\varepsilon > 0$, there exists $\delta(\varepsilon) > 0$ such that*

$$\|x_0 - x_e\| < \delta(\varepsilon) \Rightarrow \|x(t, t_0, x_0) - x_e\| < \varepsilon, \quad \forall t \geq t_0.$$

Equivalently, when δ depends only on ε , the equilibrium point x_e is said to be *uniformly stable*.

Lyapunov stability does not guarantee that the solution $x(t, t_0, x_0)$ will converge to the equilibrium point x_e . It simply says that the solution will remain in some region around the equilibrium point as time passes, but will not necessarily ever approach it, so long as the initial condition was within a certain distance, δ , of the equilibrium point. A system with a limit cycle, in particular, is stable in the sense of Lyapunov.

As a result of such a bounded type of stability definition, the notions of attractivity, asymptotic stability, and exponential stability are defined.

Definition C.3. *Attractivity:* The equilibrium point x_e of system (C.1) is attractive or convergent if for each $t_0 \in \mathbb{R}^+$, there exists an $\eta(t_0) > 0$ such that

$$\|x_0 - x_e\| < \eta(t_0) \Rightarrow x(t_0 + t, t_0, x_0) \rightarrow x_e \text{ as } t \rightarrow \infty.$$

Definition C.4. *Uniform attractivity:* The equilibrium point x_e of system (C.1) is uniformly attractive if there exists a number $\eta > 0$ such that

$$\|x_0 - x_e\| < \eta, t_0 \geq 0 \Rightarrow x(t_0 + t, t_0, x_0) \rightarrow x_e \text{ as } t \rightarrow \infty, \text{ uniformly in } t_0 \text{ and } x_0.$$

By combining the above definitions, we obtain the important notion of asymptotic stability and uniform asymptotic stability.

Definition C.5. *Asymptotic stability:* The equilibrium point x_e of system (C.1) is asymptotically stable if it is stable and attractive. It is uniformly asymptotically stable if it is both uniformly stable and uniformly attractive.

In many practical situations, such as in the convergence of observers, exponential stability is preferred to asymptotic stability.

Definition C.6. *Exponential stability:* The equilibrium point x_e is exponentially stable if there exist constants $r, a, b > 0$ such that

$$\|x(t_0 + t, t_0, x_0) - x_e\| \leq a \|x_0 - x_e\| \exp(-bt), \forall t, t_0 \geq 0, \forall x_0 \in B_r$$

where B_r is a ball of radius r .

The above definitions are local in nature in the sense that they describe the behaviour of the system solution initialised near the equilibrium point. In other words, there is some region around the equilibrium point in which the initial condition vectors will lead to asymptotically or exponentially stable responses. This region is called the *zone of attraction* to the equilibrium point.

The following definitions are given in the sense of the global behaviour of system trajectories.

Definition C.7. *Global uniform asymptotic stability: The equilibrium point x_e is globally uniformly asymptotically stable if (i) it is uniformly stable, and (ii) for each pair of positive numbers M, ε with M arbitrarily large and ε arbitrarily small, there exists a finite time $T = T(M, \varepsilon)$ such that*

$$\|x_0 - x_e\| < M, t_0 \geq 0 \Rightarrow \|x(t_0 + t, t_0, x_0) - x_e\| < \varepsilon, \forall t \geq T(M, \varepsilon).$$

This definition says that the solution will converge to the equilibrium point and remain there as time passes (since $T(M, \varepsilon)$ is finite), in response to any initial condition (since M is arbitrarily large).

Definition C.8. *Global exponential stability: The equilibrium point x_e is globally exponentially stable if there exist constants $a, b > 0$ such that*

$$\|x(t_0 + t, t_0, x_0)\| \leq a \|x_0 - x_e\| \exp(-bt), \forall t, t_0 \geq 0, \forall x_0 \in \mathbb{R}^n.$$

It is worth noting that these kinds of definitions can only be satisfied for systems having a single equilibrium point at which the system can come to rest. This is the case of linear systems, where the origin is the unique equilibrium point.

In practice, the study of stability is done using Lyapunov's second, or direct, method. This consists of defining a Lyapunov function with appropriate properties; the existence of which will imply the type of desired stability. The second method allows the determination

of stability without having to solve the system equations (or find the eigenvalues in the linear case). Consequently, it is a useful method for nonlinear and time-varying systems where the solution of the state equations is very difficult to find in general. Recall that Lyapunov's first method comprises studying the stability of a nonlinear system in the vicinity of an equilibrium point by calculating the eigenvalues of a linearised model of the nonlinear system around the equilibrium point. This method is not considered here since the stability of linear systems is shown in the next section.

Note that we can always consider $x_e = 0$ since we can always bring the equilibrium point to the origin by a change of coordinates. In what follows, we shall effectively assume that such is the case.

Definition C.9. *Lyapunov function: A Lyapunov function for the system (C.1) is a real-valued function $V(x, t)$, which possesses the following properties:*

- i) $V(x, t)$ is of class C^1 such that $V(x_e, t) = 0$.*
- ii) $V(x, t)$ is positive definite. In other words, there exists a non-decreasing real continuous function α such that $\alpha(0) = 0$ and $0 < \alpha(\|x\|) \leq V(x, t)$, for all t and for all $x \neq 0$ with $\alpha(\|x\|) \rightarrow \infty$ as $\|x\| \rightarrow \infty$.*
- iii) $\dot{V}(x, t)$ is negative definite. In other words, there exists a non-decreasing real continuous function γ such that $\gamma(0) = 0$ and the time derivative $\dot{V}(x, t)$ of $V(x, t)$ along the trajectories of system (C.1) is such that: $\dot{V}(x, t) \leq -\gamma(\|x\|) < 0$ for all t and for all $x \neq 0$.*
- iv) There exists a non-decreasing real continuous function β such that $\beta(0) = 0$ and $V(x, t) \leq \beta(\|x\|)$ for all t .*

The following theorem shows that the existence of such a Lyapunov function is a necessary and sufficient condition for uniform asymptotic stability of system (C.1).

Theorem C.1. *The origin of system (C.1) is uniformly asymptotically stable if and only if system (C.1) admits a Lyapunov function.*

The properties on $V(x, t)$ can be weakened according to the type of stability desired. We therefore have the following corollary:

Corollary C.1. *The origin of system (C.1) is:*

a) *Stable if and only if system (C.1) admits a Lyapunov function which satisfies conditions i), ii) and the following condition: iii*) $\dot{V}(x, t) \leq 0$ for all t and for all x .*

b) *Uniformly stable if and only if system (C.1) admits a Lyapunov function which satisfies conditions i), ii), iii*) and iv).*

Corollary C.2. *For the autonomous system*

$$\dot{x} = f(x), \quad f(0) = 0 \quad (\text{C.3})$$

the asymptotic stability is guaranteed by the existence of a Lyapunov function $V(x)$ of class C^1 , such that:

1. $V(x_e) = 0$,
2. $V(x) > 0, \forall x \neq 0$,
3. $V(x) \rightarrow \infty$ as $\|x\| \rightarrow \infty$, and
4. $\dot{V}(x) < 0, \forall x \neq 0$.

C.2 Stability of linear time-invariant systems

In general, the Lyapunov direct method can also be applied to linear systems, whether they are time-varying or time-invariant. However, for time-invariant systems of the form

$$\dot{x} = Ax, \quad x \in \mathbb{R}^n \quad (\text{C.4})$$

the concept of positive and negative definite functions are readily defined in terms of quadratic functions involving positive and negative definite matrices, respectively. More precisely, the

quadratic form $V(x) = x^T P x$, where P is a Symmetric Positive Definite (SPD) matrix, is usually employed as a candidate Lyapunov function. Having chosen an SPD matrix P , the derivative of $V(x)$ with respect to time, along the trajectories of the system (C.4), is calculated to test for negative definiteness:

$$\begin{aligned}\dot{V}(x) &= x^T P \dot{x} + \dot{x}^T P x \\ &= x^T P A x + x^T A^T P x = x^T Q x\end{aligned}$$

where

$$P A + A^T P = Q. \quad (\text{C.5})$$

The equation (C.5) is called an *algebraic Lyapunov equation*. If the matrix Q turns out to be negative definite with the particular choice of P , then the origin of system (C.4) will be asymptotically stable.

Note that since the origin is the only (trivial) isolated equilibrium point of system (C.4), we generally speak of the asymptotic *stability of the system* rather than the asymptotic stability of the origin. It is also clear that asymptotic stability of the LTI system (C.4) also means global asymptotic stability of the latter since there is only one critical point.

Another interesting feature of the above LTI system is that its eigenvalues can also provide information regarding the stability of the system. Indeed, it is known that any matrix A can be transformed into the Jordan form by a change of coordinates. Let $z = Sx$ be a transformation such that $SAS^{-1} = J$, where J is in Jordan form. More precisely,

$$\dot{z} = S\dot{x} = SAS^{-1}z = Jz.$$

We know that the diagonal elements of J are the eigenvalues of A . In addition, $z(t) = e^{Jt}z(0) = \sum_{i=1}^r \sum_{j=1}^{m_i} p_{ij} t^{j-1} e^{\lambda_i t}$ where r is the number of distinct eigenvalues of A ; $\lambda_1, \dots, \lambda_r$; m_i is the multiplicity of the eigenvalues λ_i , and p_{ij} are interpolating polynomials. It is clear that $z(t) \rightarrow 0$ as $t \rightarrow \infty$ if the eigenvalues of A are all negative. This result is

summarised in the following theorem:

Theorem C.2. *The autonomous LTI system (C.4) is globally asymptotically stable if and only if all the eigenvalues of A have negative real parts; that is, all the eigenvalues of A lie in the left-half complex plane.*

C.3 Linear time-varying systems

The stability criteria which can be applied to the analysis of LTI systems does not necessarily apply to those with time-varying parameters. The stability analysis of such systems is more complicated than that of LTI systems. A commonly used stability analysis technique is the frozen coefficient method. More precisely, for the following time-varying system:

$$\dot{x}(t) = A(t) x(t), \quad x \in \mathbb{R}^n$$

the eigenvalues of the matrix $A(t)$ are calculated for each fixed time t_1, t_2, \dots and so on. If the eigenvalues are in the LHS of the s -plane, for all time, and if the coefficients and eigenvalues are not varying too rapidly, then the system is said to be stable. However, this is not strictly true for all time-varying systems and care must be taken when using such a technique. It is actually possible that some time-varying systems with negative real eigenvalues can be unstable (see [6]). It is also possible for some time-varying systems to have an eigenvalue in the RHS of the s -plane, and yet be stable under certain conditions. In such a case, further analysis of a different kind may be required.

C.4 Stability of linear time-delay systems

The stability analysis of time-delay systems (TDSs) is much more complex than that of the delay-free case. The behavioural characteristics and structural features of TDSs can require

non-standard analytical techniques for the determination of system stability.

Consider the LTI delayed system

$$\dot{x}(t) = Ax(t) + A_d x(t - \tau) \quad (\text{C.6})$$

and the functional

$$V(x_t) = x^T(t) Px(t) + \int_{-\tau}^0 x^T(t + \theta) Sx(t + \theta) d\theta \quad (\text{C.7})$$

where $\theta \in [-\tau, 0]$. Clearly, the functional (C.7) is an extension of the classical Lyapunov functions [67]. It is said that system (C.6) is asymptotically stable if there exist positive symmetric matrices P , S , and R satisfying the Riccati equation

$$A^T P + PA + PA_d S^{-1} A_d^T P + S + R = 0$$

or equivalently, the linear matrix inequality (LMI)

$$\begin{bmatrix} A^T P + PA + S & PA_d \\ A_d^T P & -S \end{bmatrix} < 0.$$

This is a Krasovskii-based method for the determination of stability of systems of the form (C.6). It is clear that the use of such stability criteria means that the design of observers and controllers for such systems is not straightforward.

Other methods include the consideration of rational approximations. The idea is basically to truncate the infinite series involved to an approximation and thus treat the infinite-dimensional system as a finite-dimensional one. However, this can lead to problems with regards to controller design for delayed systems. Indeed, for the case of a linear constant-delay system, a controller that can stabilise Pade approximations is not sufficient to ensure stable behaviour of the real system [67].

References

- [1] Brogan, W. L. "Modern control theory", Prentice Hall, New Jersey, 1991.
- [2] Luenberger, D. G. "Observing the state of a linear system", *IEEE Transactions on Military Electronics*, vol. 8, pp. 74-80, 1964.
- [3] Kalman, R. and Bucy, R. "New results in linear filtering and prediction theory", *Journal of Basic Engineering*, 82, Series D, pp. 35-40, 1960.
- [4] Brockett, R. W. "Lie theory and control systems defined on spheres", *SIAM Journal of Applied Mathematics*, vol. 25, no. 2, pp. 213-225, 1973.
- [5] Isidori, A. "Nonlinear control systems", Springer-Verlag, Berlin and Heidelberg, 1995.
- [6] Vidyasagar, M. "Nonlinear systems analysis", 2nd Ed., Prentice-Hall, Englewood Cliffs, New Jersey, 1993.
- [7] Fliess, M.; Lamnabhi, M.; and Lamnabhi-Lagarrigue, F. "An algebraic approach to nonlinear functional expansions", *IEEE Transactions on Circuits and Systems*, vol. 30, pp. 554-570, 1983.
- [8] LaSalle, J. P. "The stability of dynamical systems", *SIAM Regional Conference Series in Applied Mathematics*, Siam, vol. 25, 1976.

- [9] Sontag, E. D. "Remarks on stabilization and input-to-state stability", *Proceedings of the 28th IEEE Conference on Decision and Control*, New York, vol. 2, pp. 1376-1378, 1989.
- [10] Slotine, J.J.E. and Li, W. "Applied nonlinear control", Prentice Hall, New Jersey, 1991.
- [11] Van der Shaft, A. J. "Nonlinear dynamical control systems", Springer-Verlag, New York, 1990.
- [12] Krener, A. J. and Isidori, A. "Linearisation by output injection and nonlinear observers", *Systems and Control Letters*, vol. 3, pp. 47-52, 1983.
- [13] Astolfi, A.; Ortega, R.; and Sepulchre, R. "Passivity-based control of nonlinear systems", In "Control of complex systems", Astrom, K.; Albertos, P.; Blanke, M.; Isidori, A.; Schaufelberger, W.; and Sanz, R. (Eds.), Springer, London, 2000.
- [14] Kanellakopoulos, I.; Kokotovic, P. V.; and Morse, A. S. "A toolkit for nonlinear feedback design", *Systems and Control Letters*, vol. 18, no. 2, pp. 83-92, 1992.
- [15] Barbot, J. P. and Perruquetti, W. (Eds.) "Sliding mode control in engineering", Marcel Dekker, New York, 2002.
- [16] Gauthier, J. P.; Hammouri, H.; and Othman, S. "A simple observer for nonlinear systems: Application to bioreactors", *IEEE Transactions on Automatic Control*, vol. 36, no. 6, pp. 875-880, 1992.
- [17] Busawon, K. "Sur les observateurs des systemes non-lineaires et le principe de separation", Thesis (PhD), Lyon: l'Universite Claude Bernard, 1996.
- [18] Gustafsson, F. "Adaptive filtering and change detection", John Wiley and Sons Ltd, 2000.

- [19] Gauthier, J. P. and Bornard, G. "Observability for any $u(t)$ of a class of bilinear systems", *IEEE Transactions on Automatic Control*, vol. 26, pp. 922-926, 1981.
- [20] Jurdjevic, V. and Quinn, J. P. "Controllability and stability", *Journal of Differential Equations*, vol. 28, pp. 381-389, 1978.
- [21] Mammone, R. J. and Zeevi, Y. Y. (Eds.) "Neural networks: Theory and applications", Academic Press, London, 1991.
- [22] Zadeh, L.; Wang, P. Z.; and Loe, K. F. "Between mind and computer: Fuzzy engineering (Advances in fuzzy systems - applications and theory)", World Scientific Publishing, 1993.
- [23] Pratt, I. "Artificial intelligence", Basingstoke: Macmillan, 1994.
- [24] Quagliarella, D. (Ed.) "Genetic algorithms and evolution strategy in engineering and computer science: Recent advances and industrial applications", Chichester: Wiley, 1998.
- [25] Patton, R. J.; Frank, P. M.; and Clark, R. N. (Eds.) "Issues of fault diagnosis for dynamic systems", Springer-Verlag, London, 2000.
- [26] Moon, F. C. "Chaotic vibrations: An introduction for applied scientists and engineers", John Wiley and Sons, 2004.
- [27] Krasovskii, N. N. "Observation of a linear dynamical system and equations of retarded argument", *Differentsial'nye Uravneniya*, vol. 1, no. 12, pp. 1221-1225, 1965.
- [28] Swedish international development cooperation agency (Sida). "Let it reign: The new water paradigm for global food security", 2005. Available at: <http://www.mekonginfo.org/mrc>.

- [29] Krstić, M.; Kanallakopoulos, I.; and Kokotović, P. "Nonlinear and adaptive control design", Wiley-Interscience Publication, New York, 1995.
- [30] Tinias, J. "A theorem on global stabilization of nonlinear systems by linear feedback", *Systems and Control Letters*, vol. 17, pp. 357-362, 1991.
- [31] Van der Shaft, A. J. " L_2 -gain and passivity techniques in nonlinear control", *Lecture Notes in Control and Information Sciences*, vol. 218, Springer-Verlag, Berlin, 1996.
- [32] Vanrolleghem, P. and Dochain, D. (Eds.) "Dynamical modelling and estimation in wastewater treatment processes", Technomic Pub. Co., 2001.
- [33] Sabanovic, A.; Fridman, L. M.; and Spurgeon, S. (Eds.) "Variable structure systems: From principles to implementation", IEE, 2004.
- [34] Busawon, K.; Farza, M.; and Hammouri, H. "Observer design for a special class of nonlinear systems", *International Journal of Control*, vol. 71, pp. 405-418, 1998.
- [35] Busawon, K. "On Jordan observable and controllable canonical forms", *1st African Control Conference*, Cape Town, South Africa, 2003.
- [36] Zhou, K.; Doyle, J. C.; and Glover, K. "Robust and optimal control", Prentice Hall, New Jersey, 1996.
- [37] Hou, M.; Busawon, K.; and Saif, M. "Observer design based on triangular form generated by injective map", *IEEE Transactions on Automatic Control*, vol. 45, no. 7, pp. 1350-1355, 2000.
- [38] Besancon, G. and Hammouri, H. "On uniform observation of non-uniformly observable systems", *Systems and Control Letters*, vol. 29, no. 9, pp. 9-19, 1996.

- [39] Knapp T. D. and Budman H. M. "Robust control design of non-linear processes using empirical state affine models", *International Journal of Control*, vol. 73, no. 17, pp. 1525-1535, 2000.
- [40] Hammouri, H. and De Leon, M. J. "Observer synthesis for state affine systems", *Proceedings of the 29th IEEE Conference on Decision and Control*, 1990.
- [41] Tmar, Z.; Hammouri, H.; and Mechmeche, C. "Unknown input observer for state affine systems - a geometric existence condition", *IEEE International Conference on Industrial Technology*, vol. 3, pp. 1630-1635, 2004.
- [42] Nadri, M. and Hammouri, H. "Design of a continuous-discrete observer for state affine systems", *Applied Mathematics Letters*, vol. 16, pp. 967-974, 2003.
- [43] Bornard, G.; Couenne, N.; and Celle, F. "Regularly persistent observer for bilinear systems", *Proc. Colloque International en Automatique Non Lineaire*, Nante, 1988.
- [44] Bastin, G. and Dochain, D. "On-line estimation and adaptive control of bioreactors", vol. 1, Elsevier, Amsterdam, 1990.
- [45] Gouzé, J. L. and Lemesle, V. "A bounded error observer with adjustable rate for a class of bioreactor models", *Proceedings of the European Control Conference*, Portugal, 2001.
- [46] Gouzé, J. L.; Rapaport, A.; and Hadj-Sadok, M. Z. "Interval observers for uncertain biological systems", *Ecological Modelling*, vol. 133, pp. 45-56, 2000.
- [47] Lubenova, V. "On-line estimation of biomass concentration and non stationary parameters for aerobic bioprocesses", *Journal of Biotechnology*, vol. 46, pp. 197-207, 1996.

- [48] Boukas, E. K. and Liu, Z. K. "Delay-dependent stability analysis of singular linear continuous-time system", *IEE Proceedings of Control Theory and Applications*, vol. 150, pp. 325-330, 2003.
- [49] Nounou, H. N. and Mahmoud, M. S. "Variable structure adaptive control for a class of continuous time-delay systems", *IMA Journal of Mathematical Control and Information*, vol. 23, pp. 225-235, 2006.
- [50] Mirkin, B. M. and Gutman, P. "Output feedback model reference adaptive control for multi-input-multi-output plants with state delay", *Systems and Control Letters*, vol. 54, no. 10, pp. 961-972, 2005.
- [51] Jiao, X. and Shen, T. "Adaptive feedback control of nonlinear time-delay systems: The LaSalle-Razumikhin-based approach", *IEEE Transactions on Automatic Control*, vol. 50, no. 11, 2005.
- [52] Mahmoud, M. S. and Ismail, A. "Passivity and passification of time-delay systems", *Journal of Mathematical Analysis and Applications*, vol. 292, pp. 247-258, 2004.
- [53] Smith, O. J. M. "Closer control of loops with dead time", *Chemical Engineering Progress*, vol. 53, no. 5, pp. 217-219, 1957.
- [54] Niculescu, S. I. and Annaswamy, A. M. "An adaptive Smith-controller for time-delay systems with relative degree ≤ 2 ", *Systems and Control Letters*, pp. 347-358, 2003.
- [55] Lia, H.; Niculescu, S. I.; Dugard, L.; and Diona, J. M. "Robust guaranteed cost control of uncertain linear time-delay systems using dynamic output feedback", *Mathematics and Computers in Simulation*, vol. 45, pp. 349-358, 1998.

- [56] Oucheriah, S. "Exponential stabilization of linear delayed systems using sliding mode controllers", *IEEE Transactions on Circuits and Systems I: Fundamental Theory and Applications*, vol. 50, no. 6, 2003.
- [57] Gouaisbault, F.; Dambrine, M.; and Richard, J. P. "Sliding mode control of linear time-delay systems: A design via LMIs", *IMA Journal of Mathematical Control and Information*, vol. 19, pp. 83-94, 2002.
- [58] Orlov, Y.; Belkoura, L.; Richard, J. P.; and Dambrine, M. "Adaptive identification of linear time-delay systems", *International Journal of Robust Nonlinear Control*, vol. 13, pp. 857-872, 2003.
- [59] Fattouh, A.; Sename, A.; and Dion, J. M. "Robust observer design for time-delay systems: A Riccati equation approach", *Kybernetika*, vol. 35, no. 6, pp. 753-764, 1999.
- [60] Salamon, D. "Observers and duality between observation and state feedback for time-delay systems", *IEEE Transactions on Automatic Control*, vol. 25, no. 6, pp. 1187-1192, 1980.
- [61] Kharitonov, V. L. and Hinrichsen, D. "Exponential estimates for time-delay systems", *Systems and Control Letters*, vol. 53, no. 5, pp. 395-405, 2004.
- [62] Leyva-Ramos, J. and Pearson, A. E. "An asymptotic modal observer for linear autonomous time lag systems", *IEEE Transactions on Automatic Control*, vol. 40, pp. 1291-1294, 1995.
- [63] Kwon, O. M.; Park, J. H.; Lee, S. M.; and Won, S. C. "LMI optimization approach to observer-based controller design of uncertain time-delay systems via delayed feedback", *Journal of Optimization Theory and Applications*, vol. 128, no. 1, pp. 103-117, 2006.

- [64] Lee, J. W. and Chang, P. H. "Input/output linearisation using time-delay control and time-delay observer", *AACC*, 1998.
- [65] Lee, Y. Y. and Tsai, J. S. H. "Equivalent linear observer-based tracker for stochastic chaotic system with delays and disturbances", *IMA Journal of Mathematical Control and Information*, vol. 22, pp. 266-284, 2005.
- [66] Mahmoud, M. S. "Robust control and filtering for time-delay systems", Marcel Dekker Inc., New York, 2000.
- [67] Richard, J. P. "Time-delay systems: An overview of some recent advances and open problems", *Automatica*, vol. 39, pp. 1667-1694, 2003.
- [68] Pearson, A. E. and Fiagbedzi, Y. A. "An observer for time lag systems", *IEEE Transactions on Automatic Control*, vol. 34, no. 7, pp. 775-777, 1989.
- [69] Kharitonov, V. L. and Mondié, S. "Exponential estimates for neutral time-delay systems: An LMI Approach", *IEEE Transactions on Automatic Control*, vol. 50, no. 5, pp. 666-670, 2005.
- [70] Busawon, K.; Jones, R. W.; and Tham, M. T. "An observer for linear time-delay systems", *IASTED Control Conference on Modelling, Identification and Control*, 2003.
- [71] Boutayeb, M. "Observers design for linear time-delay systems", *Systems and Control Letters*, vol. 44, pp. 103-109, 2001.
- [72] Hou, M.; Zitek, P.; and Patton, R. J. "An observer design for linear time-delay systems", *IEEE Transactions on Automatic Control*, vol. 47, no. 1, 2002.
- [73] Chen, C. T. "Introduction to linear system theory", HRW series in Electrical Engineering, Electronics, and Systems, 1970.

- [74] Busawon, K. "Control design using Jordan controllable canonical form", *Proceedings of the 39th IEEE Conference on Decision and Control*, Sydney, Australia, pp. 3386-3392, 2000.
- [75] Kamen, E. W. "Linear systems with commensurate time-delays: Stability and stabilization independent of delay", *IEEE Transactions on Automatic Control*, vol. 27, no. 2, pp. 367-375, 1982.
- [76] Hewer, G. A. and Nazarov, G. J. "Observer theory for delayed differential equations", *International Journal of Control*, vol. 18, pp. 1-7, 1973.
- [77] O'Reilly, J. "Observers for linear systems", Mathematics in Science and Engineering series, Academic Press Inc., U. S., 1983.
- [78] World Health Organisation and United Nations Childrens Fund. "Global water supply and sanitation assessment 2000 report", Available at: <http://www.who.int/water_sanitation_health/monitoring/globalassess/en/>.
- [79] World Health Organisation. "Water supply, sanitation and hygiene development", Available at: <http://www.who.int/water_sanitation_health/hygiene/en/index.html>.
- [80] Black, M. "The no-nonsense guide to water", New Internationalist Publications Ltd., 2004.
- [81] Chadwick, E. "The Chadwick report on the sanitary condition of the labouring population with the local reports for England and Wales and other related papers", Irish University Press series of British Parliamentary Papers, 1837-42, printed 1971.
- [82] Twort, A. C.; Hoather, R. C.; and Law, F. M. "Water Supply", 2nd Ed., Arnold, 1985.

- [83] Environment Agency. "Water resources", Available at: <http://www.environment-agency.gov.uk/subjects/waterres/?lang=_e>.
- [84] Gray, N. F. "Activated sludge theory and practice", Oxford Science Publications, 1990.
- [85] Rapaport, A. and Dochain, D. "Interval observers for biochemical processes with uncertain kinetics and inputs", *Mathematical Biosciences*, vol. 193, pp. 235-253, 2005.
- [86] Wang, F. S.; Lee, W. C; and Chang, L. L. "On-line state estimation of biomass based on acid production in *Zymomonas mobilis* cultures", *Bioprocess Engineering*, vol. 18, pp. 329-333, 1998.
- [87] Water Online. "Water online newsletter", April 2006. Available at: <<http://www.wateronline.com>>.
- [88] Correspondence, Envitech, June 2006.
- [89] November, E. J.; Cenens, C. C.; and Van Impe, J. F. "Accuracy of on-line viable biomass measurement based on capacitance readings of activated sludge during batch and fed-batch process operation", *Water Intelligence Online, IWA Publishing*, 2002.
- [90] Farza, M.; Nadri, M.; and Hammouri, H. "Nonlinear observation of specific growth rate in aerobic fermentation processes", *Bioprocess Engineering*, vol. 23, pp. 359-366, 2000.
- [91] Metcalf and Eddy, Inc. Revised by Tchobanoglous, G. and Burton, F. L. "Wastewater engineering: Treatment, disposal, and reuse", London; New York: McGraw-Hill, 1991.
- [92] Bourgeois, W.; Burgess, J. E.; and Stuetz, R. M. "On-line monitoring of wastewater quality: A review", *Journal of Chemical Technology and Biotechnology*, vol. 76, pp. 337-348, 2001.

- [93] Liu, J.; Olsson, G.; and Mattiasson, B. "Short term BOD (BOD_{st}) as a parameter for on-line monitoring of biological treatment process Part 1: A novel design of BOD biosensor for easy renewal of bio-receptor", *Biosensors and Bioelectronics*, vol. 20, pp. 562-570, 2004.
- [94] Liu, J.; Olsson, G.; and Mattiasson, B. "Short term BOD (BOD_{st}) as a parameter for on-line monitoring of biological treatment process Part 2: Instrumentation of integrated flow injection analysis (FIA) system for BOD_{st} estimation", *Biosensors and Bioelectronics*, vol. 20, pp. 571-578, 2004.
- [95] O'Riordan, F. "Trial of STIP Biox 1010 BOD analyser at Middleton sewerage treatment plant Cork", Water Technology Ltd, Ireland, 2002. Available at: www.stip.de/english/Publications/middleton_pub.pdf.
- [96] Envitech company website. Available at: <http://www.envitech.co.uk>.

Bibliography

- [1] Arstein, Z. "Stabilization with relaxed controls", *Nonlinear Analysis*, vol. 7, pp. 1163-1173, 1983.
- [2] Sontag, E. D. "A Lyapunov-like characterization of asymptotic controllability", *SIAM Journal of Control and Optimisation*, vol. 21, pp. 462-471, 1983.
- [3] Lee, E. B. and Lu, W. "Coefficient assignability for linear systems with delays", *IEEE Transactions on Automatic Control*, vol. 29, no. 11, 1984.
- [4] Royce Technologies. "Dissolved oxygen control in wastewater treatment plants", *Applications Bulletin*, 1991.
- [5] Bachinger, T.; Martensson, P.; and Mandenius, C. F. "Estimation of biomass and specific growth rate in a recombinant *Escherichia coli* batch cultivation process using a chemical multisensor array", *Journal of Biotechnology*, vol. 60, pp. 55-66, 1998.
- [6] Kharitonov, V. L. "Robust stability analysis of time-delay systems: A survey", *Annual Reviews in Control*, vol. 23, pp. 185-196, 1999.
- [7] Mirkin, L. "On the extraction of dead-time controllers and estimators from delay-free parametrisations", *IEEE Transactions on Automatic Control*, vol. 48, no. 4, pp. 543-553, 2003.

- [8] Chen, W. and Saif, M. "An iterative learning observer for fault detection and accommodation in nonlinear time-delay systems", *International Journal of Robust Nonlinear Control*, vol. 16, pp. 1-19, 2006.
- [9] Roh, Y-H. "Robust stability of predictor-based control systems with delayed control", *International Journal of Systems Science*, vol. 33, no. 2, pp. 81-86, 2002.
- [10] DeSouza, C. E.; Palhares, R. E.; and Peres, P. L. D. "Robust H_∞ filtering for uncertain linear systems with multiple time-varying state delays: An LMI approach", *Proceedings of the 38th IEEE Conference on Decision and Control*, Phoenix, AZ, pp. 2023-2028, 1999.
- [11] Choi, H. H. and Chung, M. J. "Observer-based H_∞ controller design for state delayed linear systems", *Automatica*, vol. 32, no. 7, pp. 1073-1075, 1996.
- [12] Choi, H. H. and Chung, M. J. "Robust observer-based H_∞ controller design for linear uncertain time-delay systems", *Automatica*, vol. 33, no. 9, pp. 1749-1752, 1997.
- [13] Wang, Z.; Huang, B.; and Unbehauen, H. "Robust H_∞ observer design for uncertain time-delay systems: (I) the continuous case", *In IFAC 14th World Congress*, Beijing, China, pp. 231-236, 1999.
- [14] Richard, J. P. "Robust control of delay systems: A sliding mode control design via LMI", *Systems and Control Letters*, vol. 46, pp. 219-230, 2002.
- [15] Astrom, K. J.; Hang, C. C.; and Lim, B. C. "A new Smith predictor for controlling a process with an integrator and long dead time", *IEEE Transactions on Automatic Control*, vol. 39, pp. 343-345, 1994.

- [16] Freeman, R. A. and Kokotovic, P. V. "Global robustness of nonlinear systems to state measurement disturbances", *Proceedings of the 32nd IEEE Conference on Decision and Control*, Texas, pp. 1507-1512, 1993.
- [17] Couenne, N. "Synthese des observateurs de systemes affines an l'etat", Thesis (PhD), INPG, Grenoble, 1990.
- [18] Scragg, A. "Environmental biotechnology", Harlow: Longman, 1999.
- [19] Bolton, W. "Industrial control and instrumentation", Longman Scientific and Technical, 1991.
- [20] Carvalho, J. L. M. D. C. "Dynamical systems and automatic control", Prentice Hall, 1993.
- [21] Seal, A. M. "Practical process control", Arnold, 1998.
- [22] Ratledge, C. and Kristiansen, B. (Eds.) "Basic biotechnology", Cambridge, 2001.
- [23] Levine, W. S. (Ed.) "Control system fundamentals", CRC Press, 2001.
- [24] Paraskevopoulos, P. N. "Modern control engineering", Marcell Dekker, Inc., 2002.
- [25] Barty-King, H. "Water: The book: An illustrated history of water supply and wastewater in the United Kingdom", London: Quiller Press, 1992.
- [26] Dorf, R. C. and Bishop, R. H. "Modern control systems", Upper Saddle River: Prentice Hall, 2001.
- [27] Vanloon, G. W. and Duffy, S. J. "Environmental chemistry - a global perspective", Oxford, 2001.
- [28] Winkler, M. A. "Biological treatment of wastewater", Chichester: Horwood, 1981.

- [29] Mutambara, A. G. O. "Design and analysis of control systems", London: CRC Press, 1999.
- [30] Morris, R. J. "Cholera 1832: The social response to an epidemic", London: Croom Helm, 1976.
- [31] Leigh, J. R. "Essentials of nonlinear control theory", London: Peregrinus on behalf of the IEE, 1983.
- [32] Horn, R. A. and Johnson, C. R. "Matrix analysis", Cambridge: Cambridge University Press, 1985.
- [33] Clesceri, L. S.; Greenberg, A. E.; and Eaton, A. D. (Eds.) "Standard methods for the examination of water and wastewater", Washington, D. C.: American Public Health Association, 1992.
- [34] Schröder, D. "Intelligent observer and control design for nonlinear systems", Berlin; London: Springer, 2000.
- [35] Hammer, M. J. "Water and wastewater technology", New York; Chichester: Wiley, 1986.
- [36] D'Azzio, J. J. and Houppis, C. H. "Linear control system analysis and design: Conventional and modern", Tokyo; London: McGraw-Hill, 1975.
- [37] Crueger, W. and Crueger, A. "Biotechnology: A textbook of industrial microbiology", Sunderland, MA: Sinauer Associates, 1989.
- [38] Wang, S. S. "Further results on stability of $\dot{x}(t) = Ax(t) + Bx(t - \tau)$ ", *Systems and Control Letters*, vol. 19, pp. 165-168, 1992.

- [39] Zhang, J.; Knopse, C. R.; and Tsiotras, P. "Stability of time-delay systems: Equivalence between Lyapunov and scaled small-gain conditions", *IEEE Transactions on Automatic Control*, vol. 46, no. 3, pp. 482-486, 2001.
- [40] Yu, D. and Shields D. N. "A bilinear fault detection observer", *Automatica*, vol. 32, pp. 1597-1602, 1996.
- [41] Yu, D.; Shields, D. N.; and Daley, S. "A bilinear fault detection observer and its application to a hydraulic system", *International Journal of Control*, vol. 64, pp. 1023-1047, 1996.
- [42] Oliveira, R.; Ferreira, E.; and Feyo de Azevedo, S. "A study on the convergence of observer-based kinetics estimators in stirred tank reactors", *Journal of Process Control*, vol. 6, no. 6, pp. 367-371, 1996.
- [43] Busawon, K. and Saif, M. "A state observer for nonlinear systems", *IEEE Transactions on Automatic Control*, vol. 44, no. 11, pp. 2098-2103, 1999.
- [44] Olsson, G. and Newall, B. "Wastewater treatment systems: Modelling, diagnosis and control", IWA Publishing, 1999.
- [45] Busawon, K. and Kabore, P. "Disturbance attenuation using proportional integral observers", *International Journal of Control*, vol. 74, no. 6, pp. 618-627, 2001.
- [46] Busawon, K. and De Leon-Morales, J. "An observer design for uniformly observable non-linear systems", *International Journal of Control*, vol. 73, no. 15, pp. 1375-1381, 2000.
- [47] Busawon, K.; Farza, M.; and Hammouri, H. "A simple observer for a class of nonlinear systems", *Applied Mathematics Letters*, vol. 11, no. 3, pp. 27-31, 1998.

- [48] Farza, M.; Hammouri, H.; Othman, S.; and Busawon, K. "Nonlinear observers for parameter estimation in bioprocesses", *Chemical Engineering Sciences*, vol. 52, no. 23, pp. 4251-4267, 1997.
- [49] Hammouri, H. and Busawon, K. "A global stabilisation of a class of nonlinear systems by means of an observer", *Applied Mathematics Letters*, vol. 6, no. 1, pp. 31-34, 1993.
- [50] Busawon, K. and De Leon-Morales, J. "An improved high-gain observer for single-output uniformly observable systems", *Proceedings of the European Control Conference*, 1999.
- [51] Hou, M.; Busawon, K.; and Saif, M. "Nonlinear observer via triangular form", *Proceedings of the European Control Conference*, 1999.
- [52] Busawon, K.; Farza, M.; and Hammouri, H. "Observer's synthesis for a class of nonlinear systems with application to state and parameter estimation in bioreactors", *Proceedings of the 36th IEEE Conference on Decision and Control*, pp. 5060-5061, 1997.
- [53] Busawon, K.; Ellassoudi, A.; and Hammouri, H. "Dynamical output feedback stabilization of a class of nonlinear systems", *Proceedings of the 32nd IEEE Conference on Decision and Control*, Texas, pp. 1966-1971, 1993.
- [54] Farza, M.; Busawon, K.; and Hammouri, H. "Simple nonlinear observers for on-line estimation of kinetic rates in bioreactors", *Automatica*, vol. 34, no. 3, pp. 301-318, 1998.
- [55] Busawon, K. and Saif, M. "Stabilisation and control of nonlinear systems in strict feedback form", *IFAC World Congress*, Beijing, China, pp. 2077-2081, 1999.